



Ecole Nationale Supérieure des Télécommunications  
Département Traitement du Signal et des Images

# Récepteurs de Wiener Optimaux et Sous Optimaux à Rang Réduit pour le CDMA: Algorithmes et Performances.

Belkacem MOUHOUCHE

*Thèse présentée pour obtenir le grade de*

Docteur en Sciences

Soutenue le 06/12/2005 devant le jury composé de:

Geneviève Jourdain	Présidente
Dirk Slock	Rapporteurs
Thierry Chonavel	
Nicolas Ibrahim	Examineurs
Eric Moulines	
Karim Abed Meraim	Directeurs de thèse
Philippe Loubaton	

Paris - Décembre 2005



Ecole Nationale Supérieure des Télécommunications  
Département Traitement du Signal et des Images

Reduced-Rank Optimum and Suboptimum  
CDMA Wiener Receivers:  
Algorithms and Performances.

Belkacem MOUHOUCHE

*Submitted in partial fulfillment of the requirements for the degree of*

Doctor of Philosophy

Composition of the Jury

Geneviève Jourdain

Dirk Slock

Thierry Chonavel

Nicolas Ibrahim

Eric Moulines

Karim Abed Meraim

Philippe Loubaton

Paris - December 2005

# Contents

<b>Summary in French</b>	<b>13</b>
<b>Introduction</b>	<b>17</b>
<b>1 The UMTS-FDD Downlink</b>	<b>25</b>
1.1 Introduction . . . . .	25
1.2 From 2G to 3G . . . . .	26
1.3 Standardization of The UMTS . . . . .	27
1.3.1 3GPP . . . . .	27
1.4 Wideband CDMA FDD Downlink . . . . .	27
1.4.1 Physical channels . . . . .	28
1.4.2 Frames and Slots . . . . .	29
1.4.3 Spreading and Scrambling . . . . .	29
1.5 The Propagation Channel Model . . . . .	32
1.6 Downlink Received Signal Model . . . . .	34
1.7 Conclusions . . . . .	37
<b>2 Optimum and Suboptimum Reduced-Rank CDMA Wiener Receivers</b>	<b>39</b>
2.1 Introduction . . . . .	39
2.2 Reduced-Rank Methods . . . . .	40
2.2.1 Filter rank reduction . . . . .	42
2.2.2 The Krylov subspace $\mathcal{K}^D(\mathbf{R}, \tilde{\mathbf{c}})$ . . . . .	43
2.3 Reduced-rank techniques based on the Krylov subspace projection . . . . .	44
2.3.1 The Powers of R (POR) receiver . . . . .	45
2.3.2 The Multi-Stage Wiener Filter (MSWF) . . . . .	45
2.3.3 The Conjugate-Gradient Reduced-Rank Filter (CGRRF) . . . . .	47
2.3.4 Low-complexity approximate implementations . . . . .	50
2.4 Optimum Reduced-Rank CDMA Wiener Receivers . . . . .	51
2.5 Suboptimum Reduced-Rank CDMA Wiener Receivers . . . . .	54
2.5.1 Adaptive Chip Level MMSE Equalization . . . . .	55

2.6	Simulation Results . . . . .	58
2.6.1	Exact methods for available $\mathbf{R}_{xx}$ and $\mathbf{r}_{dx} = \mathbf{h}$ . . . . .	58
2.6.2	Exact method with adaptive estimation of $\mathbf{R}_{yy}$ and $\mathbf{r}_{yb}$ . . . . .	59
2.6.3	Approximate sample by sample methods . . . . .	62
2.6.4	Time-varying channels with exact methods . . . . .	62
2.6.5	Time-Varying Channels with approximate methods . . . . .	63
2.7	Conclusion . . . . .	64
<b>3</b>	<b>Blind Interference Cancellation for Multi-rate Long-Code CDMA</b>	<b>67</b>
3.1	Introduction . . . . .	67
3.2	Preliminaries . . . . .	68
3.3	Parallel Interference Cancellation . . . . .	70
3.3.1	Effective Spreading Codes and Virtual data symbols . . . . .	71
3.4	Equalization . . . . .	72
3.5	Improvement Through BPIC . . . . .	73
3.6	Simulation Results . . . . .	75
3.6.1	Comparison of Rake and Equalized PIC for Single Rate CDMA . . . . .	75
3.6.2	Comparison of Rake and Equalized PIC for Multi-Rate CDMA . . . . .	76
3.6.3	Comparison of Blind PIC with Known Codes PIC . . . . .	78
3.7	Conclusion . . . . .	79
<b>4</b>	<b>Asymptotic Performance of Reduced-Rank Wiener Receivers</b>	<b>83</b>
4.1	Introduction . . . . .	83
4.2	Asymptotic Analysis of Wiener receivers for i.i.d spread CDMA (Tse-Hanly)	84
4.3	Asymptotic Analysis of Reduced Rank Receivers for i.i.d spread CDMA (Honig-Xiao) . . . . .	88
4.4	New results of Loubaton-Hachem . . . . .	90
4.5	Conclusion . . . . .	96
<b>5</b>	<b>Asymptotic Performance of Reduced-Rank Equalization in CDMA Downlink</b>	<b>97</b>
5.1	Reduced-Rank Equalization for CDMA Downlink . . . . .	98
5.2	Asymptotic analysis of reduced-rank equalizers. . . . .	101
5.3	Simulation results . . . . .	108
5.3.1	Comparison of empirical and theoretical (asymptotic) BER . . . . .	108
5.3.2	Comparison of empirical and theoretical BER for very long delay spread channels . . . . .	109
5.3.3	Effect of the load factor $\alpha$ on the convergence rate . . . . .	110
5.3.4	Effect of the channel on the convergence rate . . . . .	110
5.4	Conclusion . . . . .	110

<b>6</b>	<b>Asymptotic Analysis of Space-Time Transmit Diversity with and without Equalization</b>	<b>113</b>
6.1	Introduction . . . . .	113
6.2	The Alamouti Space Time Block Code (STBC) . . . . .	114
6.3	CMDA System Model under STTD . . . . .	117
6.4	Asymptotic Performance of STTD . . . . .	119
6.4.1	The receivers . . . . .	120
6.4.2	Asymptotic analysis . . . . .	120
6.4.3	Discussion of the two theorems . . . . .	122
6.5	Simulation Results . . . . .	123
6.5.1	Comparison of empirical BER and asymptotic BER . . . . .	123
6.5.2	Gain of STTD for non-severe channels . . . . .	123
6.5.3	Gain of STTD for severe channels . . . . .	124
6.5.4	Effect of multipath channels on the performance of STTD . . . . .	126
6.6	Conclusion . . . . .	126
<b>7</b>	<b>Concluding remarks</b>	<b>129</b>
7.1	Equalizer and Blind Interference Cancellation based receivers . . . . .	129
7.1.1	Reduced-rank equalization algorithms . . . . .	129
7.1.2	Blind Interference Cancellation . . . . .	130
7.2	Asymptotic performance of CDMA receivers . . . . .	131
7.2.1	Asymptotic performance of reduced-rank Wiener receivers . . . . .	131
7.2.2	Asymptotic performance of reduced-rank equalization . . . . .	132
7.2.3	Asymptotic performance of Space Time Transmit Diversity . . . . .	132
<b>A</b>	<b>Appendix to chapter 2</b>	<b>135</b>
A.1	Proof of proposition 2.1 . . . . .	135
<b>B</b>	<b>Appendix to chapter 5</b>	<b>137</b>
B.1	Proof of Lemma 5.2 . . . . .	137
B.2	Proof of Lemma 5.3. . . . .	138
B.3	Proof of Lemma 5.4. . . . .	142
<b>C</b>	<b>Appendix to chapter 6</b>	<b>143</b>
C.1	Proof of Theorems 6.1 and 6.2 . . . . .	143
<b>D</b>	<b>Appendix to Chapter 3, Article Published in ISSSTA 2004 Proceedings</b>	<b>149</b>
D.1	Abstract . . . . .	150
D.2	Introduction . . . . .	150
D.3	Data model . . . . .	151

D.4	Review of the BIC algorithm [23]	152
D.5	BIC based on subspace decomposition and FWT projection	154
D.6	Discussion	155
D.6.1	Computational complexity	156
D.6.2	Blind channel estimation indeterminacy	156
D.6.3	Channel estimation	156
D.6.4	Further improvements	156
D.7	Computer simulations	156
D.8	Conclusions	157
<b>E</b>	<b>Appendix to Chapter 4, Article Published in Eusipco 2004 Proceedings</b>	<b>159</b>
E.1	Abstract	160
E.2	Introduction	160
E.3	A review of the main results of Loubaton-Hachem	162
E.4	The downlink CDMA model.	163
E.5	The reduced rank Wiener receivers.	164
E.6	Simulation results	166
E.7	Conclusion	168

# List of Figures

1.1	Physical channels and slot structure of UMTS-FDD. . . . .	29
1.2	Spreading and Modulation of UMTS-FDD physical channels. . . . .	30
1.3	OVSF spreading codes construction. . . . .	31
1.4	Multipath propagation and Multi Access Interference . . . . .	32
1.5	Simplified long-code CDMA model . . . . .	34
2.1	Multi-Stage Wiener Filter (rank $D = 4$ ). . . . .	46
2.2	The Conjugate-Gradient Reduced-Rank Filter (rank $D = 4$ ). . . . .	49
2.3	Suboptimum reduced-rank receiver structure. . . . .	54
2.4	BER performance of exact reduced rank equalization algorithms Vs the Rank for a CDMA system with $N = 32$ $K = 16$ users all fixed to 10 dB propagating through a Vehicular A channel and an equalizer of 20 taps. . . . .	59
2.5	BER performance of adaptive exact rank 4 reduced rank MSWF equalizer, Rake and MMSE vs time for a CDMA system with $N = 32$ $K = 20$ with an equalizer of 20 taps . . . . .	60
2.6	BER performance after convergence of adaptive reduced rank equalizer with different ranks vs SNR for a CDMA system with $N = 32$ $K = 20$ with an equalizer of 20 taps . . . . .	61
2.7	BER performance of adaptive approximate rank 4 reduced rank equalizer, Rake and RLS vs time for a CDMA system with $N = 32$ $K = 20$ for an equalizer of 20 taps . . . . .	62
2.8	BER performance of adaptive exact rank 3 reduced rank equalizer, Rake and MMSE vs time for a CDMA system with $N = 32$ $K = 15$ for an equalizer of 20 taps under time varying channels and a mobile speed of 80 Kmh . . . . .	63
2.9	BER performance of adaptive exact rank 3 reduced rank equalizer, Rake and SMI vs mobile speed for a CDMA system with $N = 32$ $K = 15$ for an equalizer of 20 taps. . . . .	64

2.10	BER performance of adaptive approximate rank 3 reduced rank equalizer, Rake and MMSE vs time for a CDMA system with $N = 32$ $K = 15$ for an equalizer of 20 taps under time varying channels and a mobile speed of 80 Km/h . . . . .	65
3.1	The proposed structure of the equalizer-based multi-rate PIC receiver. . . . .	74
3.2	BER comparison of equalized PIC, Rake-based PIC, Rake, equalization Vs SNR per user for a CDMA system with $N = 32$ and $K = 16$ . . . . .	77
3.3	BER comparison of equalized PIC, Rake-based PIC, Rake, equalization Vs SNR per user for a CDMA system with $N = 32$ and $K = 31$ . . . . .	77
3.4	BER comparison of equalized PIC, Rake-based PIC, Rake, equalization Vs SNR per user for a CDMA system with 28 multi-rate users and hard PIC decisions . . . . .	78
3.5	BER comparison of equalized PIC, Rake based PIC, Rake, equalization Vs SNR per user for a CDMA system with 28 multi-rate users and soft PIC decisions. . . . .	79
3.6	BER comparison of equalized PIC, Rake based PIC, Rake, equalization and multi-rate code-aware PIC Vs SNR per user for a CDMA system with 28 multi-rate users. . . . .	80
4.1	Simulated and Asymptotic SINR for reduced-rank and full-rank Wiener receiver for a half-loaded CDMA system with random spreading. . . . .	91
5.1	Comparison of empirical and asymptotic theoretical BER of a reduced-rank equalizer based receiver for a half loaded system and a Vehicular A channel. . . . .	109
5.2	Comparison of empirical and asymptotic theoretical BER of a reduced-rank equalizer based receiver for a half loaded system and a very long delay spread (Vehicular B) channel. . . . .	111
5.3	Influence of the load factor $\alpha$ on the convergence of the relative SINR of a reduced-rank equalizer-based receiver to the full-rank SINR . . . . .	111
5.4	Influence of the propagation channel on the convergence of the relative SINR of a reduced-rank equalizer-based receiver to the full-rank SINR . . . . .	112
6.1	A Communication system with 2 transmit antennas and one receive antenna employing the Alamouti Space-Time Code. . . . .	114
6.2	BER performance comparison for coherent QPSK of Alamouti scheme with other schemes. . . . .	116
6.3	Comparison of empirical and theoretical BER for a CDMA system employing Alamouti STBC with and without equalization. . . . .	124

6.4 The BER of the RAKE and equalizer-based receivers with and without transmit diversity for the Pedestrian A channel,  $\alpha = 0.5$  . . . . . 125

6.5 The BER of the RAKE and equalizer-based receivers with and without transmit diversity for a three equal path propagation channel,  $\alpha = 0.5$ . . . . . 125

6.6 BER of the RAKE and equalizer-based receivers with and without transmit diversity Vs the number of channel paths . . . . . 126

D.1 Code Detection Probability of Error vs. SNR for a 64 SF system. . . . . 157

D.2 BER vs.  $E_b/N_0$  for MMSE, single user and CD-PIC algorithm for  $N = 32$ ,  $K = 10$  system. . . . . 158

E.1 Influence of  $\alpha$  on the convergence of the SINR of a reduced-rank Optimum Wiener receiver to the full-rank SINR. . . . . 167

E.2 Influence of the propagation channel on the convergence of the optimum reduced-rank Wiener receiver SINR to the full-rank SINR. . . . . 167

E.3 Comparison of empirical and theoretical (asymptotic) BER of a reduced-rank Optimum Wiener receiver. . . . . 168

## List of abbreviations

---

BPSK	:	Binary Phase Shift Keying
CDMA	:	Code-Division Multiple Access
c.d.f	:	cumulative distribution function
CGA	:	Conjugate-Gradient Algorithm
CGRRF	:	Conjugate-Gradient Reduced-Rank Filter
CM	:	Constant Modulus
CMA	:	Constant Modulus Algorithm
FDD	:	Frequency-Division Duplex
FIR	:	Finite Impulse Response
FWT	:	Fast Walsh Transform
INR	:	Interference-to-Noise Ratio
ISI	:	Intersymbol Interference
MAI	:	Multiple-Access Interference
MSE	:	Mean-Squared Error
MSWF	:	Multi Stage Wiener Filter
MMSE	:	Minimum Mean-Squared Energy
MUI	:	MultiUser Interference
OFDM	:	Orthogonal Frequency-Division Multiplexing
p.d.f.	:	probability density function
PIC	:	Parallel Interference Canceller
QAM	:	Quadrature Amplitude Modulation
QPSK	:	Quadrature Phase Shift Keying
SIC	:	Successive Interference Canceller
SINR	:	Signal-to-Interference plus Noise Ratio
SMI	:	Sample matrix Inversion
SNR	:	Signal-to-Noise Ratio
STBC	:	Space Time Block Code
STTD	:	Space Time Transmit Diversity
SVD	:	Singular Value Decomposition
TDD	:	Time-Division Duplex
UMTS	:	Universal Mobile Telecommunications System
UTRA	:	UMTS Terrestrial Radio Access

# Notations

---

Some of the notations used throughout this work are defined below.

$\mathbb{C}$	: the set of complex numbers;
$(\cdot)^*$	: complex conjugate;
$(\cdot)^T$	: matrix transpose;
$(\cdot)^H$	: conjugate transpose;
$\overline{(\cdot)}$	: $((\cdot)^H)^T$ ;
$(\cdot)^\dagger$	: Moore-Penrose pseudoinverse;
$\Re\{\cdot\}, \Im\{\cdot\}$	: real, imaginary part of complex variable;
$ \cdot $	: absolute value;
$\ \cdot\ $	: Euclidian norm;
$\mathbb{E}\{\cdot\}$	: mathematical expectation;
$\delta_{mn}, \delta_k$	: Kronecker delta (= 1 for $m = n$ or $k = 0$ and 0 elsewhere);

$\mathbf{I}$	: identity matrix;
$\mathbf{I}_m$	: $m \times m$ identity matrix;
$\mathbf{0}$	: matrix with zero entries;
$\mathbf{A}_{i,j}$	: the $(i, j)$ th entry of matrix $\mathbf{A}$ ;
$\mathbf{A}_k$	: the $k$ th column of matrix $\mathbf{A}$ ;
$\text{span}\{\mathbf{A}\}$	: column span of matrix $\mathbf{A}$ ;
$\text{rank}\{\mathbf{A}\}$	: the dimension of $\text{span}\{\mathbf{A}\}$ ;
$\text{Trace}\{\mathbf{A}\}$	: trace of square matrix $\mathbf{A}$ ;

$\otimes$	: Kronecker product of matrices:
$\mathbf{A} \otimes \mathbf{B} \stackrel{\text{def}}{=} \begin{pmatrix} \mathbf{A}_{1,1}\mathbf{B} & \dots & \mathbf{A}_{1,k}\mathbf{B} & \dots \\ \vdots & & \ddots & \\ \mathbf{A}_{n,1}\mathbf{B} & & \mathbf{A}_{n,k}\mathbf{B} & \\ \vdots & & & \ddots \end{pmatrix};$	

$O(\cdot)$	: $b_n = O(a_n) \Leftrightarrow \exists N, \gamma_1 > 0, \gamma_2 > 0 : \gamma_2 a_n  \leq  b_n  \leq \gamma_1 a_n , \forall n > N.$
------------	--------------------------------------------------------------------------------------------------------------------------------------

Unless specified otherwise, the following semantic conventions are used:

- small Latin or Greek letters (like  $a$  or  $\alpha$ ) are used for scalar complex or real variables and integers;
- small Latin or Greek *boldface* letters (like  $\mathbf{a}$  or  $\boldsymbol{\alpha}$ ) are used for complex or real vectors;
- capital Latin or Greek boldface letters (like  $\mathbf{A}$ ) are used for complex or real matrices.

# Résumé en Français

---

Le contexte de la thèse est la détection en liaison descendante de l'UMTS-FDD. Cependant, la majorité des contributions restent valides dans un contexte de CDMA plus général. Le rapport est divisé en deux parties. Dans la première partie, nous présentons quelques algorithmes susceptibles d'améliorer la détection en liaison descendante tout en restant de complexité réduite. Dans la deuxième partie, nous discutons les performances asymptotiques de quelques récepteurs présentés dans la première partie et de quelques techniques plus générales.

Dans la liaison descendante de l'UMTS-FDD, nous avons un ensemble d'utilisateurs synchrones ayant des codes d'étalement orthogonaux (qui peuvent être de tailles différentes). Les symboles de ces utilisateurs sont étalés à l'aide de leurs codes respectifs. La somme des signaux résultants est alors brouillée (scramblée) avec un long code de scrambling pseudo aléatoire. Le signal chip résultant est mis en forme et transmis aux différents mobiles. Le canal de propagation est sélectif en fréquence à cause de sa nature multi trajets. L'orthogonalité des codes d'étalement n'est plus garantie à la réception. Le récepteur RAKE (récepteur en râteau) combine les différents échos de façon cohérente. Ce récepteur est optimal si l'on considère que l'Interférence Multi Utilisateurs (MAI) est un bruit blanc. Le MAI a une structure très différente d'un bruit blanc. Par conséquent, le récepteur RAKE est très limité pour les canaux sélectifs en fréquence. Plusieurs alternatives ont été proposées qui couvrent tout le spectre complexité/performance. Parmi ces alternatives, les récepteurs basés sur un égaliseur MMSE au rythme chip représentent un bon compromis entre la complexité et la performance.

Notre première contribution est d'adapter deux algorithmes de filtrage MMSE à complexité réduite au cas de l'égalisation pour le CDMA. Les deux algorithmes sont inspirés du Multi Stage Wiener Filter (MSWF) et du Conjugate Gradient Reduced Rank Filter (CGRRF) Ces algorithmes permettent de calculer des égaliseurs à rang-réduit. Dans un

filtre MMSE à rang réduit, on essaie d'adapter quelques coefficients du filtre seulement. Ceci induit une perte en performance mais le gain en complexité est considérable.

Une deuxième méthode pour s'affranchir de l'interférence est d'utiliser l'élimination d'interférence en parallèle (PIC). Dans un scénario de PIC, les symboles des interféreurs sont estimés et leur effet est retranché du signal reçu. Pour procéder au PIC, les codes des interféreurs (ou leurs estimés) doivent être disponible au récepteur. Le problème de l'UMTS-FDD réside dans le fait que les codes soient de facteurs différents. Ceci rend impossible leur estimation en utilisant une technique de moyennage. Dans ce contexte, nous proposons une technique qui combine l'égalisation avec le concept d'utilisateurs virtuels. Un utilisateur virtuel est un utilisateur dont le code est de la même longueur que l'utilisateur d'intérêt. Les simulations montrent que cela permet d'éliminer une grande partie de l'interférence.

Dans le cas du CDMA périodique (absence du code de scrambling), on peut profiter de la cyclo-stationnarité du signal reçu pour estimer les codes d'étalement. Dans l'appendice D, on donne un article qui traite ce cas. L'algorithme proposé dans ce cas est basé sur le sous-espace bruit en s'inspirant d'un article basé sur le sous-espace signal.

Dans la deuxième partie, on analyse les performances asymptotiques des récepteurs de Wiener optimaux et sous optimaux à rang réduit. La performance de la diversité à la transmission (STTD) est aussi étudiée avec l'égaliseur MMSE et le récepteur RAKE. Pour étudier les performances asymptotiques, on suppose que la matrice des codes d'étalement est aléatoire suivant une certaine distribution. On suppose aussi que le facteur d'étalement  $N$  et le nombre d'utilisateurs  $K$  tendent vers l'infini et que leur rapport reste fixe. On peut alors démontrer que les SINRs à la sortie des différents récepteurs tendent vers des valeurs déterministes indépendantes des codes d'étalement. L'interprétation de ces SINRs asymptotique permet une meilleure compréhension du comportement des différents récepteurs.

Le chapitre 4 résume les travaux précédents sur les performances asymptotiques des récepteurs de Wiener optimaux à rang réduit. Une partie de ces travaux (le travail de Loubaton-Hachem) a été utilisée dans un article publié dans Eusipco 2004. La conclusion principale de ce travail est de démontrer que la convergence du SINR à rang réduit vers le SINR à rang plein est localement exponentielle. Par conséquent, les performances atteintes en utilisant un filtre de rang 8 sont très proches de celles obtenues en utilisant un filtre de rang plein.

Les égaliseurs à rang réduit (les filtres de Wiener sous optimaux) sont étudiés dans le chapitre 5. Les conclusions restent les mêmes que dans le cas des filtres de Wiener opti-

maux. La convergence est très rapide et le rang requis pour atteindre des performances proches du rang plein reste modéré.

Une troisième technique pour améliorer la détection (autre que l'égalisation et le PIC) est la diversité à la transmission (STTD). Cette technique, originalement proposé par Alamouti en 1998, est devenu très populaire et a été retenu dans les standard 3GPP. Dans le chapitre 6, on étudie les performances asymptotiques du STTD combiné avec un récepteur RAKE ou un égaliseur MMSE. On conclue que l'égalisation permet de profiter de la diversité à la transmission.

Le chapitre 7 résume les conclusions et les perspectives futures de ce travail de thèse.

## Introduction:

---

Thesis Context, Overview and Contributions

# Introduction

---

In this summary, we give an overview of the problems discussed in this thesis along with the contributions. This is done in an informal way, the goal is to give a flavor of the way in which we approached the problems.

The present report is the result of a C.I.F.R.E thesis conducted at Wavecom and E.N.S.T. The context of the thesis is the detection in the downlink of UMTS-FDD. However, most of the contributions are valid for a general CDMA framework. The thesis is split into two parts. The first part concerns different algorithms that can be used to improve the detection while keeping reasonable complexity. The second part is about the performances of the receivers discussed in the first part and other more general receivers.

In the downlink of UMTS-FDD, we have a set of synchronous users with (possibly different length) orthogonal spreading codes. The sum of those users symbols spread by their spreading codes is scrambled with a long pseudo-random scrambling code. The resulting signal is pulse-shaped and transmitted through the propagation channel. In practical situations, propagation channels are highly frequency selective (because of the presence of many paths). This means that the orthogonality of the spreading codes is no more guaranteed at the receiver. The conventional receiver of CDMA, the RAKE receiver, coherently combines the echoes obtained from different paths. This is the optimal linear receiver if the Multi Access Interference (MAI) (i.e. the interference created due the non ideal property of the channel) is white. Of course, the MAI is far from white noise. Different receivers have been proposed ranging from non linear very complex ones to linear simple to implement ones. Recently, there has been an increasing interest in receivers that use an (MMSE) equalizer followed by descrambling and despreading. Equalizer based receivers represent a family that gives a good compromise between complexity and performance.

*Our first contribution lies in the equalizer based receiver domain. More precisely, we propose an adaptive way to calculate a reduced-rank equalizer that is applied to the received*

*signal to restore the orthogonality between the codes.* Reduced-rank means that the equalizer is different from the Wiener (MMSE) equalizer in that only some of the coefficients are optimized. This represents a loss in performance with respect to the full-rank (MMSE) equalizer. On the other hand, the computational complexity is reduced by a non negligible amount. The utility of reduced-rank filtering depend of course on a compromise between the complexity and the required performance.

Another way to enhance the performance is to use Parallel Interference Cancellation (PIC). In the PIC scenario, symbol estimates of different interferers are used to regenerate their effect and subtract it from the received signal. This allows a better detection of the user of interest provided that the interferers estimates are correct. The problem that arises in the UMTS-FDD Downlink is twofold: first, the interferers codes are not known to the receiver; second, they cannot be estimated by some averaging scheme because they are multi-rate (this means that the receiver sees a set of different spreading codes of different lengths modulated by random symbols). *In this context, we propose to combine MMSE equalization with a Blind PIC method that supposes the presence of virtual codes of the same rate. As will be shown, most of the time this allows to reject much of the interference.*

In the case of short-code (single-rate) CDMA, we can take advantage of the cyclostationarity of the received signal to design blind PIC algorithms. The code-detection is easier in this case. As the short-code CDMA is not part of this thesis, we only provide in Appendix D an article that treats this case. The algorithm proposed is based on the noise-subspace method as opposed to a previously proposed signal-subspace method.

The Second part of the thesis concerns the *Asymptotic Performance Analysis of CDMA receivers*. The asymptotic analysis (also called large-system analysis) means that we suppose that the spreading codes are random following a given distribution and find the limit of the output SINR associated with a given receiver when the spreading factor  $N$  and the number of users  $K$  both tend to infinity with fixed ratio. Studying the performance for finite values of the spreading factor is very difficult because the SINR of a given receiver depends in a complex manner on the spreading codes. To overcome the difficulty of interpreting the SINRs, we study the limit of the (random) SINRs in the asymptotic regime. Fortunately, the SINRs tend to deterministic limits independent of the spreading codes. The different parameters influencing the SINR can then be interpreted.

In chapter 4, we discuss the *performance of reduced-rank optimum Wiener receivers* for CDMA downlink under random spreading. This means that the receiver is supposed to know the channel and the interferers codes and uses an optimum reduced-rank linear receiver to detect the symbols of the user of interest. In this context, *we characterize*

*the convergence of a reduced-rank Wiener receiver SINR to the full-rank Wiener receiver SINR.* The convergence is shown to be *locally exponential*. This means that essentially, by using a reduced rank receiver of rank 8 we obtain the close to full-rank performance even for spreading factors tending to infinity.

Our next contribution, presented in chapter 5 concerns the *asymptotic performance of suboptimum receivers based on a MMSE equalizer (both full-rank and reduced-rank) followed by despreading*. Using the results of chapter 4, *we analyze the performance of full and reduced rank suboptimum receivers based on equalization*. We show that, similar to the optimum case, the convergence of reduced-rank SINR to the full-rank one is locally exponential.

A third way to improve the detection performance (besides equalization and PIC) is to use Space Time Block Codes (STBC). In the downlink, however, a lot of effort is being done to keep the mobile small and cheap. This limits the possibility of using multiple antennas at the receiver side. As proposed by Alamouti, Transmit Diversity can be used. Two transmit antennas are used with one receive antenna. In the flat fading case, The diversity provided by two transmit antennas and one receive antenna is the same as that provided by two receive antennas and one transmit antenna. In the multipath (frequency-selective) case, this no more valid.

In chapter 6, *we analyze the asymptotic performance of Space-Time Transmit Diversity with and without equalization*. We show that without equalization, the STTD performance can be worse than the performance without STTD. This means that the interference caused by using two transmit antennas is higher than the diversity provided. While, when using equalization, the benefit of diversity is restored.

Chapter 7 provides some conclusions and possible future research directions.

## Summary of thesis contributions

	Algorithm Development	Performance Analysis
Optimum Reduced-Rank CDMA Wiener Receivers	Thesis [20]	<b>Chapter 4, Appx E</b>
Suboptimum Reduced-Rank CDMA Wiener Receivers	<b>Chapter 2</b>	<b>Chapter 5</b>
Alamouti Space-Time Block-Code		<b>Chapter 6</b>
Parallel Interference Cancellation	<b>Chapter 3, Appx D</b>	

Table 1: Summary of Thesis Chapters

The presented study has resulted in the following contributions (The main Topics of the contributions are summarized in Table 1.):

- **Equalizer-based receivers for long-code CDMA** [1, 2]
  - Adaptation of two reduced-rank algorithms (SG-MSWF and ACGRRF), originally proposed for short-code CDMA detection, to the equalization in the downlink of long-code CDMA.
  - Proposing a pilot-based adaptation of the algorithms and proving the equivalence between an equalizer trained on a code-multiplexed pilot with chip-known adaptation.
- **Interference Cancellation for long-code multi-rate CDMA** [5, 8, 10, 13]
  - Proposing a new Blind PIC algorithm suitable for multi-rate CDMA systems by using the concept of single-rate virtual codes.
- **Interference Cancellation for short-code CDMA** [6]
  - Proposing a new (noise) subspace-based Blind PIC algorithms.

- **Asymptotic Performance of optimum Reduced-Rank Wiener receivers** [3, 7]
  - Characterization of the speed of convergence of the reduced-rank Wiener filter to the full-rank Wiener (MMSE) filter for a general filtering model.
  - Derivation of the asymptotic SINR performance of optimum reduced-rank CDMA receivers under multipath channels for isometric random-spreading.
- **Asymptotic Performance of suboptimum Reduced-Rank Wiener receivers** [4, 12]
  - Characterization of the speed of convergence of the reduced-rank suboptimum Wiener filter to the full-rank suboptimum Wiener filter for CDMA with frequency selective channels.
  - Derivation of the asymptotic SINR of reduced-rank equalizer-based receivers for the downlink of W-CDMA (multipath channel, orthogonal spreading and i.i.d scrambling)
- **Asymptotic Performance of Space-Time Transmit Diversity** [9]
  - Derivation of the asymptotic SINR of Space-Time Transmit Diversity for Downlink W-CDMA with RAKE-Reception.
  - Derivation of the asymptotic SINR of STTD for Downlink W-CDMA with MMSE-equalizer based receiver.



# Bibliography

- [1] B. Mouhouché, K. Abed-Meraim, N. Ibrahim and Ph. Loubaton, “Reduced-Rank Adaptive Chip level MMSE Equalization for the forward link of long-code DS-CDMA Systems,” *In Proc. International Symposium on Signal Processing Applications (ISSPA)*., Paris, France. October 2001.
- [2] B. Mouhouché, K. Abed-Meraim, N. Ibrahim and Ph. Loubaton, “Chip-Level MMSE Equalization in the Forward Link of UMTS-FDD: A Low Complexity Approach,” *In Proc. Vehicular Technology Conference (VTC-fall)*., Orlando, FL USA. October 2003.
- [3] B. Mouhouché, Ph. Loubaton, W. Hachem, K. Abed-Meraim and N. Ibrahim, “Analyse Asymptotique de certains filtres de Wiener à rang réduit,” *in Proc. GretsI 2003*, Paris, France. September 2003.
- [4] B. Mouhouché, Ph. Loubaton and W. Hachem, “Asymptotic Analysis of Chip Level MMSE Equalizers in the Downlink of CDMA Systems,” *In Proc. IEEE. Workshop on Signal Processing Advances for Wireless Communications (SPAWC)*. Lisboa, Portugal. July 2004.
- [5] B. Mouhouché, K. Abed-Meraim, N. Ibrahim and Ph. Loubaton, “Combined MMSE Equalization and Blind Parallel Interference Cancellation for Downlink Multirate CDMA Communications,” *In Proc. IEEE. Workshop on Signal Processing Advances for Wireless Communications (SPAWC)*. Lisboa, Portugal. July 2004.
- [6] B. Mouhouché, K. Abed-Meraim and S. Burykh, “Spreading Code Detection and Blind Interference Cancellation for DS/CDMA Downlink”, *IEEE International Symposium on Spread Spectrum Systems and Applications (ISSSTA)*). Sydney, Australia. August 2004.
- [7] B. Mouhouché, Ph. Loubaton, W. Hachem and N. Ibrahim, , “Asymptotic Analysis of Reduced Rank Downlink CDMA Wiener Receivers”, *In Proc. European Signal Processing Conference (EUSIPCO)*, Vienna, Austria, September 2004.

- [8] B. Mouhouche, K. Abed-Meraim and N. Ibrahim, "On the Effect Of Power and Channel Estimation in Equalized Blind PIC for Downlink Multirate CDMA Communications" ,” in *Proc. the 38th- Asilomar conference on Signals, Systems and Computers*, Pacific Grove, CA, USA. November 2004.
- [9] B. Mouhouche, Ph. Loubaton, K. Abed-Meraim and N. Ibrahim, , "On the Performance of Space Time Transmit Diversity for CDMA Downlink with and without equalization,” *In Proc. International Conference on Acoustics Speech and Signal Processing (ICASSP'05)*, Philadelphia, PA, USA. March 2005.
- [10] B. Mouhouche, K. Abed-Meraim, N. Ibrahim and Ph. Loubaton, "Procédé de Réception d'un signal CDMA á annulation d'interférence et récepteur correspondant,” *French National Patent N 03-10987*. Filed Sptember 2003.
- [11] B. Mouhouche, K. Abed-Meraim, N. Ibrahim and Ph. Loubaton, " Procédé de Détermination de codes d'étalement utilisés dans un Signal CDMA et dispositif de Communication Correspondant,” *French National Patent Pending* . Filed April 2004.
- [12] B. Mouhouche, Ph. Loubaton and W. Hachem, "Asymptotic Analysis of Chip Level MMSE Equalizers in the Donwlink of CDMA Systems,” *Submitted to IEEE Trans. On Signal Processing*. June 2005.
- [13] B. Mouhouche, K. Abed-Meraim and N. Ibrahim, " Combined MMSE Equalization and Partial Blind Interference Cancellation for W-CDMA ,” *Submitted to IEEE Communication Letters*. March 2005.

# Chapter 1

## The UMTS-FDD Downlink

---

### 1.1 Introduction

Mobile communication has become an important part of everyday's life since the introduction of the first cellular networks in the early 1980s. First Generation (1G) systems were based on analog technology and provided mainly voice communication to mobile users. Two major standards were used: Total Access Communication System (TACS) and Nordic Mobile Telephone (NMT). The need of a second generation (2G) was identified in Europe as early as 1982. The main goal of the second generation was to overcome the limited capacity of the 1G and to switch to the digital mode. The "Groupe Spécial Mobile" (GSM) committee was established to provide the technical specifications. Later, the GSM became the acronym for "Global System for Mobile communications". Other 2G standard were developed in parallel in other countries like Digital-AMPS/IS-136, Personal Digital Cellular (PDC) and cdmaOne/IS-95. The main novelty of the GSM was to provide other services additional to digital voice communication like text messaging and access to data networks.

Even before the GSM was launched, a new action started in Europe in the late 1980's to identify services and technologies for the Third Generation (3G) known as the Universal Mobile Telecommunications System (UMTS). The goal of the 3G is to provide services that require very high data rates like multimedia capabilities and internet access. In the late 90's, there has been a huge effort to harmonize the different candidate technologies of the 3G emerging in different parts in the world. Moreover, the success of 2G systems (One billion subscribers) has induced other activities aiming at a smooth transition from

the 2G to the 3G via a 2.5G<sup>1</sup> system such as the Enhanced Data rate for GSM Evolution (EDGE) that is able to provide some multimedia communications at a relatively high data rates.

## 1.2 From 2G to 3G

Instead of switching abruptly to 3G systems, most organizations believe in a smooth evolution of the 2G to 3G and slowly the 2G spectra will be reframed to provide extra 3G spectra [36]. This is supported by the big success of the 2G specially the GSM with more than one billion subscribers in 200 countries. Initially the bit rate per time slot for the GSM was 9.6 kbps (kilobits per second). 14.4 kbps per physical channel i.e. time slot was achieved by reducing the power of channel coding. In High Speed Circuit Switched Data (HSCSD) mode, several time slots per frame per user are allocated. The General Packet Radio Service (GPRS) uses packet-oriented connections with a bit rate up to 144 kbps per user. The last evolution is the Enhanced Data Rate for GSM Evolution (EDGE). EDGE is based on variable modulation schemes depending on the radio link quality. Thereby the system throughput is increased and the system can offer bit rates over 383 kbps per user. GPRS and EDGE can be considered 3G systems in a 2G network because they provide some interactive multimedia services that were not originally intended by the GSM.

The main requirements of the UMTS are [50]:

- full coverage and mobility for 144 Kbps (384 Kbps later) and limited coverage and mobility for 2 Mbps
- variable bit rates to offer bandwidth on demand and higher spectrum efficiency
- higher flexibility and multiplexing of new services with different qualities on a single connection (e.g. speech, video and packet data)
- asymmetric uplink and downlink traffic
- quality requirements for  $10^{-1}$  frame error rate and  $10^{-6}$  Bit Error Rate (BER)

Another requirement is, of course, the coexistence and compatibility with second generation systems during the transition period.

---

<sup>1</sup>The General Packet Radio Service (GPRS) is informally called the 2.5 G and the Enhanced Data Rate for GSM Evolution (EDGE) is called the 2.75G

## 1.3 Standardization of The UMTS

Different standardization processes shaping the 3G have been conducted in the world: European Telecommunications Standard Institute (ETSI) in Europe, Association of Radio Industries and Business (ARIB) in Japan, T1P1 in United States and Telecommunications Technologies Association (TTA) in South Korea. There are also efforts to harmonize these parallel works inside different forums. In Europe, the earlier program in the third generation technologies was initiated within the RACE I (Research of Advanced Communication technologies in Europe) in 1988. It was followed by the RACE II program within which two air interfaces have been evaluated: CDMA and TDMA in the COde DIVision Testbed (CODIT) and the Advanced TDMA (A-TDMA) projects respectively. Inside the Advanced Communications Technologies and Services (ACTS) program launched in 1995, the Future Radio Wideband Multiple Access System (FRAMES) project defined multiple access platform based on two modes: FMA1 and FMA2 based on WTDMA and WCDMA schemes respectively. These two modes were submitted to ETSI and ITU as UMTS and IMT-2000 air interfaces respectively. In 1998, strong support behind WCDMA led to the selection of WCDMA as an air interface for the UMTS Terrestrial Radio Access (UTRA) by the ETSI. Since then, the standardization task was transferred to the 3G Partnership Project (3GPP).

### 1.3.1 3GPP

The 3GPP was created to ensure a common specification on WCDMA and therefore an equipment compatibility. The main partners involved in this action are ARIB, ETSI, TTA, TTC and T1P1. The major goal is to define a unified platform of the standardization for the Universal Terrestrial Radio Access (UTRA). Recently the ChinaWireless Telecommunication Standard group (CWTS) and other market partners became members of the 3GPP. The 3GPP2 was created to support the merged work done in TR45.5 and TTA for cdma2000 direct-sequence (DS) and multi-carrier (MC). Other members are ARIB, TTC and CWTS. There was a general consensus on harmonized global 3G CDMA technologies with 3 modes: multi-carrier based on cdma2000, direct sequence spread based on UTRA FDD and TDD mode based on UTRA TDD.

## 1.4 Wideband CDMA FDD Downlink

In this section the main features and key parameters of the UTRA-WCDMA (FDD) are described without going into details but with some emphasis on the physical layer. For

more information the reader is referred to the web site of the 3GPP and ITU in addition to theses [36, 50].

### 1.4.1 Physical channels

The higher layers provide data to the transport channel. The transport channel maps these data to the physical layer. Most of the work in this thesis considers the physical layer, i.e. we consider a set of symbols that are transmitted without differentiating their origin in the higher layers. Basically, there are two generic classifications of physical channels: common and dedicated physical channels.

The Common Physical CHannel (CPCH) is shared by a set of active users in a cell. On the other hand, the Dedicated Physical CHannel (DPCH) is used to carry either user traffic information and is called dedicated Physical Data CHannel (DPDCH), or user control information and is named Dedicated Physical Control CHannel (DPCCH). The DPCCH used for control traffic contains pilot symbols for coherent detection, Transmission Power Control (TPC) symbols to increase or decrease the transmitted power and the Transport Format Combination Indicator (TFCI) to inform the receiver about the active Transport channels in the current frame.

#### The Common Pilot Channel (CPICH)

The Common Pilot Channel (CPICH) is an unmodulated code channel, which is scrambled with the cell specific scrambling code. The function of the CPICH is to aid the channel estimation at the terminal for the dedicated channel and to provide the channel estimation reference for the common channels when they are not associated with the dedicated channel. In an advanced receiver setting, the CPICH can be used to train a MMSE (full or reduced-rank) equalizer.

The CPICH can be seen as a user whose spreading factor is 256 and whose spreading code is all ones. Its transmitted symbols are always  $\frac{1+j}{\sqrt{2}}$ . Note that because the spreading code is all ones, the spreading factor can be considered any one between the smallest and the highest spreading factor present in the system. Another important remark is that the CPICH chip sequence is up to a constant factor equal to the scrambling code.

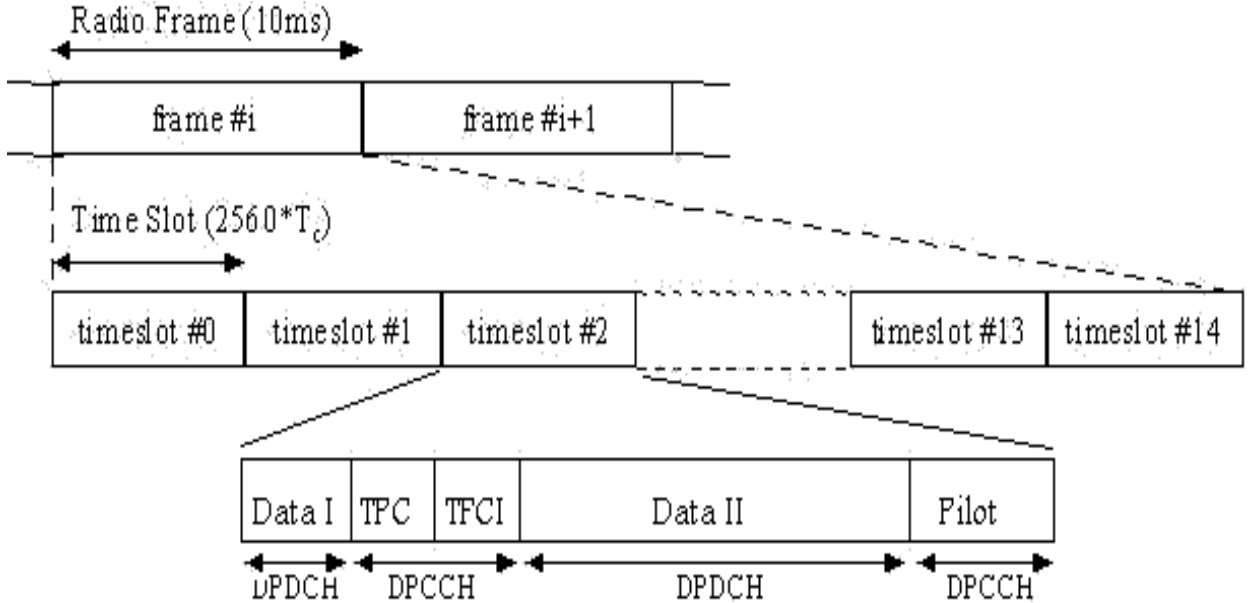


Figure 1.1: The slot structure of the physical channels of UMTS-FDD.

### 1.4.2 Frames and Slots

The Dedicated Physical CHannel (DPCH) forms a slot and is the result of a timemultiplexing of two dedicated subchannels, the data DPCH (DPDCH) and control DPCH (DPCCH), see Figure 1.1. In this thesis, we assume the use of the DPCH as transport channel. Each slot contains 2560 chips periods. The chip rate of UMTS is 3.84 Mchips/sec. This means that the chip period becomes 260.42 ns. The slot duration is 0.6667 ms. There are 15 slot in each frame that lasts for 10 ms. Frames are finally organized in superframes of 720 ms.

Table 11 of 3GPP specification TS 25.211 [14] gives the exact number of bits/field for every slot format, while Table 12 in the same document specifies the pilot symbol patterns. The DPDCH contains user data bits.

### 1.4.3 Spreading and Scrambling

Figure 1.2 illustrates the block diagram of spreading and modulation of the DPDCH/DPCCH. The modulation is QPSK where each pair of consecutive bits passes through a serial to parallel converter and get mapped to the Inphase (I) and Quadrature (Q) branches respectively. The two branches are then spread at the chip rate by the same real-valued channelization code. The I and Q sequences are treated as a single complex valued sequence that is scrambled by a complex-valued long scrambling code. The real

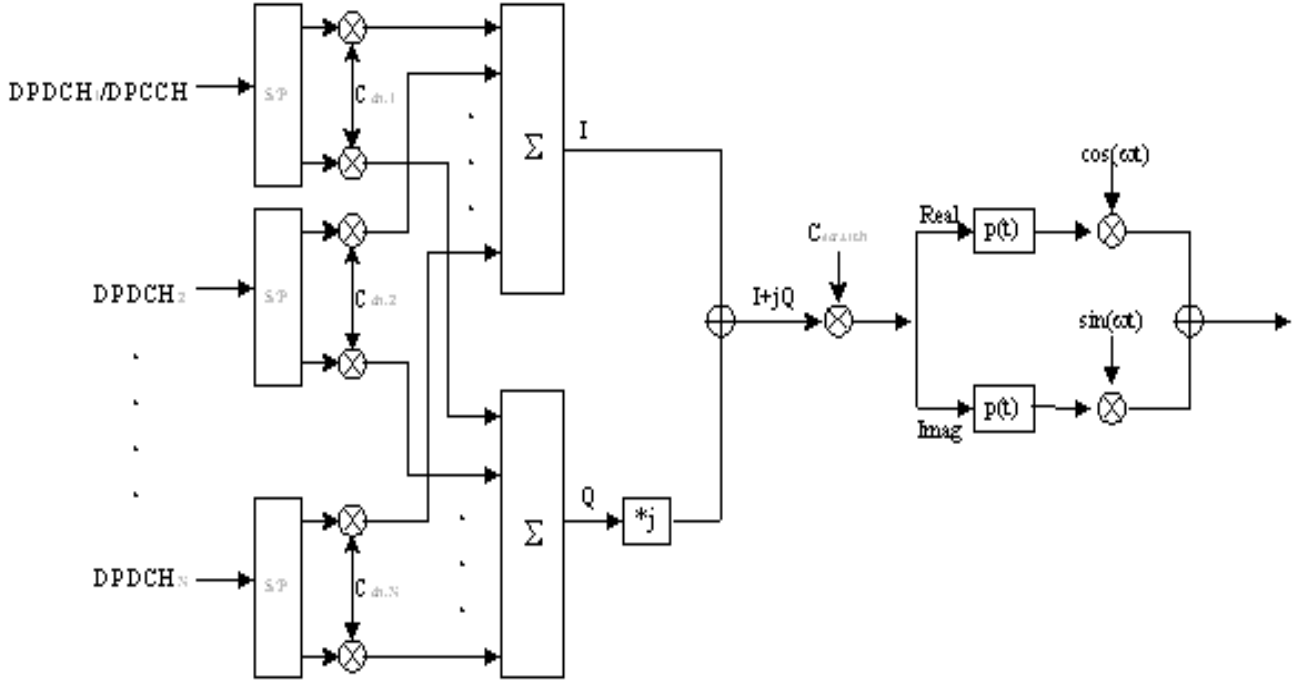


Figure 1.2: Spreading and Modulation of UMTS-FDD.

and imaginary parts are low pass filtered by a filter having a square root raised cosine impulse response with a roll-off factor of 0.22. The outputs are multiplied by the quadrature carriers  $\cos(\omega t)$  and  $\sin(\omega t)$  and added to yield the RF transmitted signal. The mechanisms used to spread and scramble the symbol sequence are detailed in the 3GPP specification TS 25.213 [15]. The spreading operation is necessary not only to widen the signal spectrum, but also to separate different users within a cell. The scrambling operation is needed to separate neighbor cells (base stations). A brief description of the spreading (channelization) and the scrambling codes is given below.

### Spreading (Channelization) Codes

Because of the synchronicity of user signals and of the common downlink radio channel, the spreading codes (or channelization codes) for the FDD downlink have been chosen to be orthonormal to each other, so that, in case of a channel equalizer receiver, codes are separable just by a simple correlation with the user of interest's channelization code. Mathematically, if  $\mathbf{c}_i = [c_i(0), \dots, c_i(N-1)]$  is the  $i^{\text{th}}$  user spreading code, orthonormality is expressed by

$$\mathbf{c}_i^T \mathbf{c}_j = \sum_{m=0}^{N-1} c_i(m)c_j(m) = \delta(i-j)$$

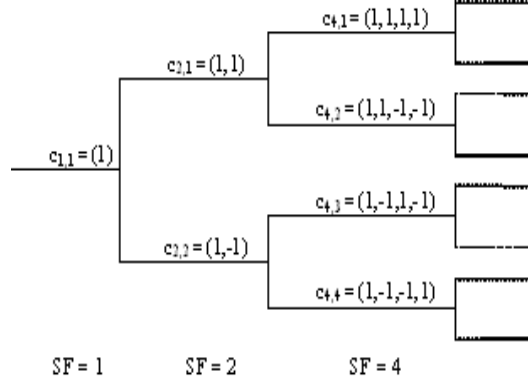


Figure 1.3: OVSF spreading Codes.

In this thesis, we will consider the spreading factor to be constant for all users (except in chapter 3 where the proposed methods are specific for multi-rate systems). The UMTS norm specifies that the system should support different data rates via Orthogonal Variable Spreading Factors (OVSF), see Fig 1.3. Codes are generated with the help of the Walsh-Hadamard matrices, that is, codes are the (real-valued) columns (or rows) of the square ( $N$  by  $N$ ) matrix  $\mathbf{W}_N$  such that

$$\mathbf{W}_N^H \mathbf{W}_N = \mathbf{I}_N,$$

where  $\mathbf{I}_N$  is the identity matrix of size  $N$ , the spreading factor. For example, for  $N = 4$  :

$$\mathbf{W}_4 = \begin{bmatrix} 1 & 1 & 1 & 1 \\ 1 & 1 & -1 & -1 \\ 1 & -1 & 1 & -1 \\ 1 & -1 & -1 & 1 \end{bmatrix}$$

and

$$\mathbf{W}_8 = \begin{bmatrix} \mathbf{W}_4 & \mathbf{W}_4 \\ \mathbf{W}_4 & -\mathbf{W}_4 \end{bmatrix}$$

the first row (or column) is usually used as pilot channel code . The spreading factor  $N$  can only be a power of 2, but the norm sets the possible values for  $N$  in the range  $[4, \dots, 512]$ . In case of different user data rates, codes are assigned from the OVSF tree in Figure 1.3 under the condition that two codes cannot be on same path towards the root of the tree.

### Scrambling codes

The scrambling stands for the multiplication of the chips resulting from the spreading operation by a quasi random QPSK scrambling code. Note that the scrambling does not

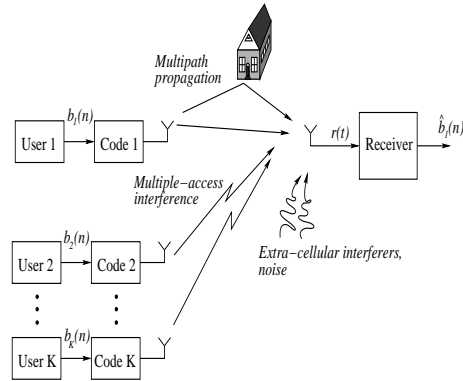


Figure 1.4: Multipath propagation and Multi Access Interference.

provide any additional “spreading” or spectrum widening since the multiplication is done chip-by-chip. The scrambling codes are frame periodic (38400 chips) and are segments of a Gold code of length  $2^{18} - 1$ . The polynomials that generate the real and imaginary parts of the code are  $X^{18} + X^7 + X^1$  and  $X^{18} + X^{10} + X^7 + X^5 + X^1$ . Along the Thesis we consider the scrambling sequence as a unit magnitude complex (QPSK) i.i.d. sequence, independent from the symbol sequence as well. In this case the chip sequence can be considered as white random signal; (chip rate i.i.d. sequence, hence stationary).

The scrambling code is often described as a long code because it is much longer than the symbol period. The cyclostationarity of the transmitted signal is destroyed by the scrambling code. Note that the presence of a long scrambling codes presents a real difficulty to apply much of the multiuser detection algorithms originally developed for periodic CDMA. It should be noted that UMTS TDD mode uses periodic (w.r.t. the symbol period) scrambling codes.

## 1.5 The Propagation Channel Model

Radio propagation from the base-station to the mobile unit is characterized by various undesired effects such as reflection, refraction and attenuation of the transmitted signal energy. Those effects result in what we call *multipath* propagation. More specifically, multipath stands for the composition of the originally transmitted signal plus duplicate images attenuated and shifted by a certain delay. The last path delay which represents the length of the channel is called the delay spread. Depending on the location of the mobile and its mobility we have many kinds of environments like: indoor, urban, pedestrian, vehicular, rural.

Figure 1.4 summarizes the undesired effects that the receiver has to face to detect a given

transmitted signal. The multipath propagation is the first undesired effect, it arises because of multiple replicas from neighboring buildings or hills for example. The second undesired effect is the Multi Access Interference (MAI). MAI is due to other users signal propagating through a non-ideal channel. The third undesired effect is the sum of noise and interference from other base stations. This is usually modelled as a white Gaussian noise.

The amplitude variation that the signal undergoes is known as *signal fading*. There are basically two types of fading : Large scale fading and Small scale fading. *Large scale fading* stands for the average signal attenuation caused by mobility over large areas. This includes the two main parameters that define a path: the propagation delay and the average power. Large scale fading varies very slowly with respect to the *Small Scale fading* which stands for the very rapid variation of the amplitude and the phase of a given path due to the superposition of a large number of undistinguishable multipath components impinging at the receiver antenna. This is usually modelled using the Jakes model [46].

Most of the thesis deals with slow-fading frequency selective multipath channels. The propagation channels is defined by a number of paths. Each path is defined by its corresponding delay and its average power. The propagation channel impulse response is given by:

$$h_p(t) = \sum_{q=0}^{P-1} \lambda_q \delta(t - \tau_q), \quad (1.1)$$

where  $\lambda_q$  and  $\tau_q$  are the complex gain and the delay associated with path  $q$ , and  $P$  is the total number of echoes.

The transmitted signal is passed through a pulse-shaping filter at the transmitter and at the receiver. The UMTS norm proposes to use the Root Raised Cosine (RRC)  $p(t)$  with a roll-off factor  $\alpha_{ro} = 0.22$ . The total channel (propagation and pulse-shaping ) is then given by:

$$h(t) = \sum_{q=0}^{P-1} \lambda_q p(t - \tau_q) \quad (1.2)$$

we usually deal with a chip-rate sampled version of this impulse response, the channel vector  $\mathbf{h}$  is given by:

$$\mathbf{h} = [h(0) \ h(T_c) \ \dots \ h(LT_c)]^T \quad (1.3)$$

where  $L$  is the delay-spread (in chip periods).

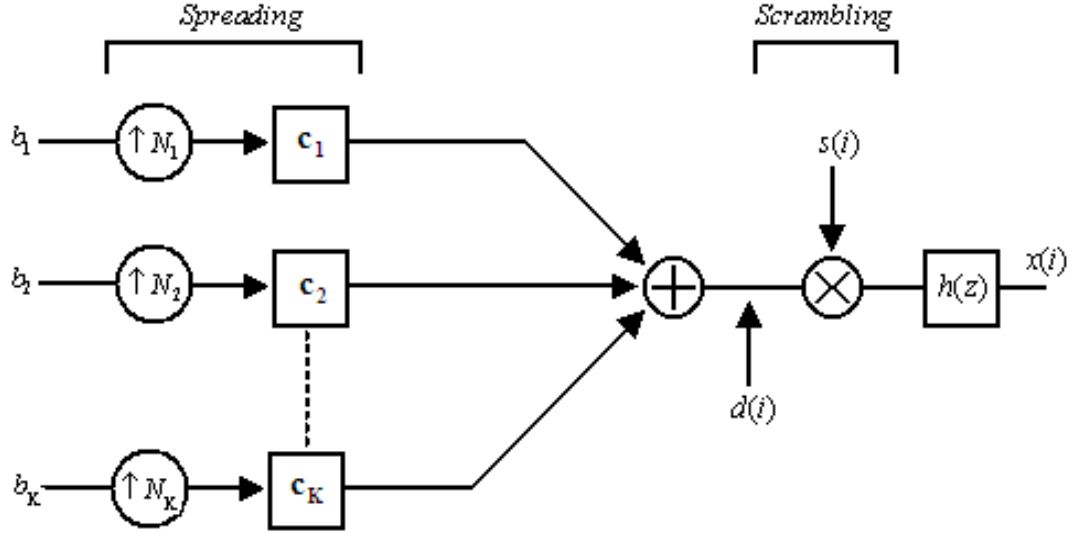


Figure 1.5: Simplified long-code CDMA model.

## 1.6 Downlink Received Signal Model

Figure 1.5 shows the model that will be used for the rest of the thesis. We consider a single base station transmitting the sum of  $K$  users chip signals given by:

$$d(i) = s(i) \sum_{k=1}^K \mu_k c_k(i \bmod N_k) b_k(\lfloor \frac{i}{N_k} \rfloor) \quad (1.4)$$

where  $s(i)$  is the base-station dependent QPSK (long) scrambling code,  $N_k$ ,  $b_k(\lfloor \frac{i}{N_k} \rfloor)$ ,  $\mu_k$  and  $c_k(i)$  are the spreading factor, the QPSK symbol sequence, the gain and the ( $N_k$ -periodic) spreading code of user  $k$ , respectively. (*mod* stands for the modulo and  $\lfloor \cdot \rfloor$  for the integer part).

Unless stated otherwise, we will assume that the scrambling sequence is a realization of an i.i.d sequence, and that users bits are independent zero mean QPSK signals. We will also assume that the index of the user of interest is 1 and, whenever needed, the index of the permanent pilot(CPICH) is 2.

The sum chip signal (1.4) is transmitted through a multipath channel whose impulse response is given by

$$h(t) = \sum_{q=0}^{P-1} \lambda_q p(t - \tau_q) \quad (1.5)$$

where  $p(t)$  is the total shaping filter (including the transmitter and the receiver matched filters),  $\lambda_q$  and  $\tau_q$  are the complex gain and the delay associated with path  $q$ , and  $P$  is the total number of resolvable paths.

The complex envelope of the received signal at the desired user terminal is then given by:

$$x(t) = \sum_i d(i)h(t - iT_c) + v(t) \quad (1.6)$$

where  $v(t)$  is a noise process (that we will assume to be white and Gaussian) and  $T_c$  is the chip period.

Chip-rate sampling of the received signal (1.6) results in:

$$x(i) = \sum_{l=0}^{L-1} h_l d(i-l) + v(i) \quad (1.7)$$

where  $h_l \triangleq h(t)|_{t=lT_c}$  is the  $l^{\text{th}}$  overall channel path sampled at chip rate,  $L$  is the number of channel coefficients and  $v(i)$  is a discrete white Gaussian noise resulting from the sampling of  $v(t)$ .

Let the spreading factor of the user of interest be  $N_1 = N$ . If we suppose that  $L < N$  then the received signal vector obtained by concatenating  $N$  samples of the received signal (1.7) can be written as <sup>2</sup>:

$$\mathbf{x}(m) = \mathbf{H}_0 \mathbf{d}(m) + \mathbf{H}_1 \mathbf{d}(m-1) + \mathbf{v}(m), \quad (1.8)$$

where

$$\mathbf{H}_0 = \begin{bmatrix} h_0 & 0 & & 0 \\ \vdots & h_0 & & \\ h_{L-1} & & & \\ & \ddots & \ddots & \\ 0 & & h_{L-1} & h_0 \end{bmatrix}, \quad (1.9)$$

$$\mathbf{H}_1 = \begin{bmatrix} & h_{L-1} & \dots & h_1 \\ & & \ddots & \vdots \\ 0 & & & h_{L-1} \end{bmatrix}, \quad (1.10)$$

$$\begin{aligned} \mathbf{x}(m) &= [x(mN), x(mN+1), \dots, x(mN+N-1)]^T, \\ \mathbf{d}(m) &= [d(mN), d(mN+1), \dots, d(mN+N-1)]^T \\ \text{and } \mathbf{v}(m) &= [v(mN), v(mN+1), \dots, v(mN+N-1)]^T. \end{aligned}$$

---

<sup>2</sup>Throughout the thesis, we will use the index  $i$  for chip-rate variables while index  $m$  will be used for symbol-rate variables.

For the majority of applications we usually use a model in which the spreading factors are all equal, i.e.  $N_k = N$ . We will use this model throughout the thesis except in chapter 3 where this model cannot be used.

In case of single SF system, the chip sequence  $\mathbf{d}(m)$  can be written as:

$$\mathbf{d}(m) = \mathbf{S}(m)\mathbf{C} \sqrt{\mathbf{P}} \mathbf{b}(m), \quad (1.11)$$

where  $\mathbf{S}(m)$  is a  $N \times N$  diagonal matrix whose diagonal entries are  $s(mN), \dots, s(mN + N)$ ,  $\mathbf{C} = [\mathbf{c}_1, \dots, \mathbf{c}_K]$  is the  $N \times K$  spreading code matrix,  $\sqrt{\mathbf{P}}$  is a  $K \times K$  diagonal matrix whose columns are  $\mu_1, \dots, \mu_K$  and  $\mathbf{b}(m) = [b_1(m), \dots, b_K(m)]^T$  is the  $K \times 1$  vector of transmitted symbols. The received signal can then be written as:

$$\mathbf{x}(m) = \mathbf{H}_0\mathbf{S}(m)\mathbf{C} \sqrt{\mathbf{P}} \mathbf{b}(m) + \mathbf{H}_1\mathbf{S}(m-1)\mathbf{C} \sqrt{\mathbf{P}} \mathbf{b}(m-1) + \mathbf{v}(m), \quad (1.12)$$

we usually group the overall code (scrambling and spreading) and the powers in a single matrix  $\mathbf{W}(m)$  given by:

$$\mathbf{W}(m) = \mathbf{S}(m) \mathbf{C} \sqrt{\mathbf{P}}, \quad (1.13)$$

finally we have the model:

$$\mathbf{x}(m) = \mathbf{H}_0\mathbf{W}(m)\mathbf{b}(m) + \mathbf{H}_1\mathbf{W}(m-1)\mathbf{b}(m-1) + \mathbf{v}(m). \quad (1.14)$$

Note that model (1.14) includes many other models. In fact, for short-code (periodic) CDMA, we have:

$$\mathbf{W}(m) = \mathbf{W}(m-1) = \mathbf{W}$$

Model 1.14 thus reduces to the general faded CDMA model with InterSymbol Interference (ISI)

$$\mathbf{x}(m) = \mathbf{H}_0\mathbf{W}\mathbf{b}(m) + \mathbf{H}_1\mathbf{W}\mathbf{b}(m-1) + \mathbf{v}(m), \quad (1.15)$$

If we further neglect the ISI term, we have the model:

$$\mathbf{x}(m) = \mathbf{H}_0\mathbf{W}\mathbf{b}(m) + \mathbf{v}(m), \quad (1.16)$$

which is the faded-CDMA model usually used in the literature.

In the case where the propagation channel is considered to be an Additive White Gaussian Noise (AWGN) channel, i.e.  $\mathbf{H}_0 = \mathbf{I}$ , we have the famous unfaded CDMA model:

$$\mathbf{x}(m) = \mathbf{W}\mathbf{b}(m) + \mathbf{v}(m). \quad (1.17)$$

The time index  $m$  can be removed in this case as it is irrelevant.

## 1.7 Conclusions

In this chapter, we discussed the different generation of communication systems. We highlighted the main steps of the standardization of Third Generation systems. We then briefly introduced the physical layer of the UMTS-FDD and the main requirements that should be fulfilled by third generation wireless communication systems. After this, we introduced the Downlink CDMA model that will be used throughout the thesis.

Part One:

---

Low Complexity Detection Algorithms for  
UMTS-FDD

# Chapter 2

## Optimum and Suboptimum Reduced-Rank CDMA Wiener Receivers

---

### 2.1 Introduction

Adaptive filtering has been used extensively in many signal processing applications like Interference Suppression [54], Multi-User Detection and equalization [42]. Depending on the application, an adaptive filter allows to estimate a set of parameters that are needed to estimate a given unknown information symbol. In short-code CDMA, for example, adaptive multiuser detection allows to estimate a set of filters. Those filters are used to estimate the transmitted symbols for each user. Adaptive techniques are useful where the statistics of the propagation media are not known and/or are time-varying. Numerous contributions have been made in the direction of improving the tradeoff between performance and complexity (see [37] and the references therein).

Recently, an elegant technique known as reduced-rank adaptive filtering has emerged and found its way in many signal processing applications. The basic idea behind reduced-rank filtering is to project the observation into a subspace  $\mathbb{S}^D$  of dimension  $D$  that is smaller than the total observation dimension  $N$  (the spreading factor in CDMA for example). A  $D$ -coefficients filter is then applied to the projected signal.

Different reduced-rank methods differ in the choice of the projection subspace  $\mathbb{S}^D$ . Principal Components (PC) method, for example, uses the subspace generated by the  $D$

eigenvectors corresponding to the  $D$  largest eigenvectors of the received signal covariance matrix  $\mathbf{R}$ . The Cross-Spectral method, on the other hand, chooses the  $D$  eigenvectors of  $\mathbf{R}$  that minimize the Mean Squared-Error (MSE). There is a third method, called Partial Despreading (PD) [66], in which the received signal is partially despread over consecutive segments of  $j$  chips, where  $j$  is a parameter. The partially despread vector has dimension  $D = \lceil N/j \rceil$  and is the input to the  $D$ -tap filter. Consequently,  $j = 1$  corresponds to the full-rank MMSE filter, and  $j = N$  corresponds to the matched filter (RAKE). For PD method,  $\mathbb{S}^D$  is spanned by non-overlapping segments of the channel vector  $\tilde{\mathbf{c}}$ , where each segment is of length  $j$ .

The Krylov subspace methods use the Krylov subspace associated to the observation covariance matrix  $\mathbf{R}$  and the data-observation cross correlation vector  $\tilde{\mathbf{c}}$ . The Krylov vectors are the vectors obtained by multiplying successive powers of  $\mathbf{R}$  by the cross correlation vector  $\tilde{\mathbf{c}}$ . The advantage of this choice and the performance of the corresponding receivers will be discussed throughout the thesis.

In this chapter, we present the Krylov subspace reduced-rank filtering techniques. We discuss both exact and approximate methods. These techniques can be applied to train the optimum Wiener receiver in the case of short code CDMA. The main part of this chapter is the extension of these techniques to the equalization in long-code CDMA (UMTS-FDD for example). Simulations results are presented and general conclusions are given.

## 2.2 Reduced-Rank Methods

Let us begin with the generic signal model

$$\mathbf{x}(m) = \tilde{\mathbf{c}} b(m) + \mathbf{I}(m), \quad (2.1)$$

where  $\mathbf{x}(m)$  is the  $N \times 1$  received signal,  $\tilde{\mathbf{c}}$  is a  $N \times 1$  vector,  $b(m)$  is a unit-variance scalar signal to be estimated and  $\mathbf{I}(m)$  is a signal decorrelated from  $b(m)$  modelling interferences and/or noise. The  $N \times N$  covariance matrix of  $\mathbf{I}(m)$  is denoted  $\mathbf{R}_I$  and will be assumed invertible.

We consider the problem of estimating the scalar  $b(m)$  from the received signal  $\mathbf{x}(m)$  using a  $N \times 1$  linear receiver  $\mathbf{w}$ . The soft estimate  $\tilde{b}(m)$  is given by:

$$\tilde{b}(m) = \mathbf{w}^H \mathbf{x}(m), \quad (2.2)$$

where  $\mathbf{w}$  is a  $N \times 1$  vector (filter). In particular, the filter corresponding to the MMSE detector (the Wiener filter) can be obtained as a solution of the following linear system

(normal equations):

$$\mathbf{R}\mathbf{w}_{opt}^N = \tilde{\mathbf{c}}, \quad (2.3)$$

where the covariance matrix of  $\mathbf{x}(m)$  is given by:

$$\mathbf{R} \stackrel{\text{def}}{=} \mathbb{E}[\mathbf{x}(m)\mathbf{x}^H(m)] = \tilde{\mathbf{c}}\tilde{\mathbf{c}}^H + \mathbf{R}_f,$$

and the observation-desired signal cross correlation signal

$$\tilde{\mathbf{c}} = \mathbb{E}[\mathbf{x}(m)b^*(m)].$$

The important property of the Wiener filter is that it is the only filter that minimizes the Mean-Squared estimation Error (MSE), or, in other words, average error energy. In our notations, the MSE can be written as:

$$J(\mathbf{w}) = \mathbb{E}[\|b(m) - \tilde{b}(m)\|^2] = 1 + \mathbf{w}^H \mathbf{R} \mathbf{w} - \mathbf{w}^H \tilde{\mathbf{c}} - \tilde{\mathbf{c}}^H \mathbf{w}. \quad (2.4)$$

The Wiener filter owes its popularity not only to this property but also to its relatively simple expression as a solution of a linear system (2.3). However, in most practical applications, including multiuser detection in CDMA systems, exact values of the covariance matrix and of the cross-covariance vector are not available. For example, in a synchronous CDMA system, such characteristics as number of CDMA users, user spreading codes, user fading and the signal-to-noise ratio are partially or completely unknown. Moreover, noise and signal powers, as well as the overall channel matrix may exhibit slow variations due to user's motion and, generally, changes in signal propagation conditions. Therefore, one has to deal with some estimates of  $\mathbf{R}$  and  $\tilde{\mathbf{c}}$ . By way of example, the estimate of  $\mathbf{R}$  can be obtained as:

$$\hat{\mathbf{R}}(m) = \gamma \hat{\mathbf{R}}(m-1) + (1-\gamma)\mathbf{x}(m)\mathbf{x}^H(m), \quad (2.5)$$

where  $0 < \gamma < 1$  is a forgetting factor. As soon as exact values of  $\mathbf{R}$  and  $\tilde{\mathbf{c}}$  are replaced by the time-varying estimates  $\hat{\mathbf{R}}(m)$  and  $\hat{\tilde{\mathbf{c}}}(m)$ , the system (2.3) has to be resolved each time these estimates are updated in order to take into account the most recent samples of  $\mathbf{x}(m)$ . The observation dimension  $N$  can be very high. In the case of CDMA  $N$  represents the processing gain (the spreading factor) which can be as high as 512. This can be further combined with multi antennas reception and/or oversampling. For these reasons, it may be quite a problem from the computational viewpoint to calculate the Wiener filter. For example, using Recursive Least-Squares (RLS) algorithm for adaptive inversion of  $\hat{\mathbf{R}}(m)$  leads to the computational cost of  $O(N^2)$  multiplications per symbol. Moreover, as the system to solve has the form

$$\hat{\mathbf{R}}(m)\mathbf{w}(m) = \hat{\tilde{\mathbf{c}}}(m), \quad (2.6)$$

natural questions arise such as the speed of the convergence of  $\mathbf{w}(m)$  to the Wiener filter  $\mathbf{w}_{opt}^N$  and the tracking ability of the solution  $\mathbf{w}(m)$  in a non-stationary environment. These questions can only be answered taking into account the particular method

of solving (2.6). Unfortunately, the answers provided by conventional adaptive filtering techniques (the Sample Matrix Inversion (SMI), Recursive Least Squares (RLS) and Least Mean Squares (LMS) algorithms [37]) are often unsatisfactory for applications when the amount of training data (that is, the number of observations) is limited: for example, multiuser detection in fast fading environment.

Reduced-rank methods, as an alternative to full-rank Wiener filter optimization, provide fast and efficient (approximate) solutions to (2.6). The idea behind reduced-rank filtering is to try to adapt only some of the coefficients of  $\mathbf{w}$  that are needed to keep reasonable performance.

### 2.2.1 Filter rank reduction

Let  $\mathbb{S}^D$  be a  $D$ -dimensional subspace of  $\mathbb{C}^N$ . The *reduced-rank Wiener filter in subspace*  $\mathbb{S}^D$  is defined as

$$\mathbf{w}_{opt}^D \stackrel{\text{def}}{=} \arg \min_{\mathbf{w} \in \mathbb{S}^D} J(\mathbf{w}). \quad (2.7)$$

The above definition includes the full-rank Wiener filter as a particular case when  $D = N$ . Let  $\{\mathbf{q}_j\}$ ,  $j = 1, \dots, D$ , be a basis (not necessarily orthogonal) of  $\mathbb{S}^D$ . Define *the projection matrix*  $\mathbf{Q} \stackrel{\text{def}}{=} [\mathbf{q}_1 \mathbf{q}_2 \dots \mathbf{q}_D]$ . As  $\mathbf{w}_{opt}^D = \mathbf{Q}\boldsymbol{\mu}$  for some  $\boldsymbol{\mu} \in \mathbb{C}^D$ , (2.7) can be rewritten as

$$\mathbf{w}_{opt}^D = \mathbf{Q} \left( \arg \min_{\boldsymbol{\mu} \in \mathbb{C}^D} J(\mathbf{Q}\boldsymbol{\mu}) \right) = \mathbf{Q}\boldsymbol{\mu}_{opt}^D. \quad (2.8)$$

Substituting  $\mathbf{w} = \mathbf{Q}\boldsymbol{\mu}$  into (2.4) yields

$$J(\mathbf{Q}\boldsymbol{\mu}) = 1 + \boldsymbol{\mu}^H \mathbf{R}_t \boldsymbol{\mu} - \boldsymbol{\mu}^H \tilde{\mathbf{c}}_t - \tilde{\mathbf{c}}_t^H \boldsymbol{\mu}, \quad (2.9)$$

where the *transformed covariance matrix*  $\mathbf{R}_t$  and the *transformed signal-data cross-correlation vector*  $\tilde{\mathbf{c}}_t$  are defined as

$$\mathbf{R}_t \stackrel{\text{def}}{=} \mathbf{Q}^H \mathbf{R} \mathbf{Q}, \quad (2.10)$$

$$\tilde{\mathbf{c}}_t \stackrel{\text{def}}{=} \mathbf{Q}^H \tilde{\mathbf{c}}. \quad (2.11)$$

It then follows that  $\boldsymbol{\mu}_{opt}^D$  in (2.8) is the solution of

$$\mathbf{R}_t \boldsymbol{\mu}_{opt}^D = \tilde{\mathbf{c}}_t. \quad (2.12)$$

Therefore, the reduced-rank Wiener filter is found by solving (2.12) and substituting  $\boldsymbol{\mu}_{opt}^D$  into (2.8). The rank- $D$  estimate of the  $b(m)$  is given by:

$$\tilde{b}^D(m) = \mathbf{w}_{opt}^D \mathbf{Q}^H \mathbf{x}(m) = \tilde{\mathbf{c}}_t^H \mathbf{Q} (\mathbf{Q}^H \mathbf{R} \mathbf{Q})^{-1} \mathbf{Q}^H \mathbf{x}(m). \quad (2.13)$$

Note that the reduced-rank filter  $\mathbf{w}_{opt}^D$  operates on the projection of  $\mathbf{x}(m)$  on  $\mathbf{Q}$  and not directly on  $\mathbf{x}(m)$ .

Contrary to (2.3), (2.12) is a system of  $D$  linear equations. Therefore, confining the filtering operation to a low-dimensional subspace  $\mathbb{S}^D$  leads to substantial gains in complexity when  $D \ll N$ . Better convergence and tracking properties can also be expected [60, 77]. On the other hand, confining the Wiener filter to a low-dimensional subspace implies a loss of degrees of freedom of the filter and, therefore, this operation should increase the minimum MSE achieved by a reduced-rank method:

$$J(\mathbf{w}_{opt}^D) \geq J(\mathbf{w}_{opt}^N). \quad (2.14)$$

As for the complexity, the computational overhead due to eventual estimation of  $\mathbf{Q}$  also has to be taken into account.

Different reduced-rank methods differ in the choice of the subspace  $\mathbb{S}^D$  or equivalently the projection matrix  $\mathbf{Q}$ . A ‘good’ choice of  $\mathbb{S}^D$  (and of the rank-reduction method) is always a compromise dictated by the requirements of a given application. In the next section, we briefly discuss the Krylov subspace that is common to many of the reduced-rank algorithms proposed recently. For more information, the reader is referred to [22] and to thesis [20].

### 2.2.2 The Krylov subspace $\mathcal{K}^D(\mathbf{R}, \tilde{\mathbf{c}})$ .

**Definition.** Given a square matrix  $\mathbf{A}$  and a nonzero vector  $\mathbf{v}$ , the subspace defined by

$$\mathcal{K}^D \equiv \text{span} \{ \mathbf{v}, \mathbf{A}\mathbf{v}, \mathbf{A}^2\mathbf{v}, \dots, \mathbf{A}^{D-1}\mathbf{v} \} \quad (2.15)$$

is referred to as a  $D$ th Krylov subspace associated with the pair  $(\mathbf{A}, \mathbf{v})$  and is denoted  $\mathcal{K}^D(\mathbf{A}, \mathbf{v})$  [64].

In this work, we deal with a family of reduced-rank methods for which  $\mathbb{S}^D = \mathcal{K}^D(\mathbf{R}, \tilde{\mathbf{c}})$ . The natural question is: what kind of reasoning leads to this particular choice for  $\mathbb{S}^D$ ? To answer this question, consider the gradient of the MSE (2.4):

$$\nabla J(\mathbf{w}) = 2(\mathbf{R}\mathbf{w} - \tilde{\mathbf{c}}). \quad (2.16)$$

Now let us take an arbitrary  $i$ -dimensional subspace  $\mathbb{S}^i$ . Let  $\mathbf{w}_{opt}^i$  be the reduced-rank Wiener filter in  $\mathbb{S}^i$ , i.e.,

$$\mathbf{w}_{opt}^i = \arg \min_{\mathbf{w} \in \mathbb{S}^i} J(\mathbf{w}). \quad (2.17)$$

Suppose that one seeks to extend the subspace  $\mathbb{S}^i$  to a  $(i+1)$ -dimensional subspace  $\mathbb{S}^{i+1}$ . Since  $J(\mathbf{w})$  decreases most rapidly in the direction of  $-\nabla J(\mathbf{w})$ , a reasonable strategy is

to require that

$$\nabla J(\mathbf{w}_{opt}^i) \in \mathbb{S}^{i+1}. \quad (2.18)$$

It follows from (2.16) that for the condition above to be satisfied it is sufficient for  $\mathbb{S}^{i+1}$  to contain the pair  $(\tilde{\mathbf{c}}, \mathbf{R}\mathbf{w}_{opt}^i)$ .

Now let  $\{\mathbb{S}^i, i = 1, 2, \dots, D\}$  be a chain of Krylov subspaces, i.e.,  $\mathbb{S}^i = \mathcal{K}^i(\mathbf{R}, \tilde{\mathbf{c}})$ ,  $i = 1, 2, \dots, D$ . It is then easy to prove by induction that in this case the condition (2.18) is satisfied for each  $i$  within the range  $1 \dots D$ . Therefore, the Krylov subspace  $\mathcal{K}^D(\mathbf{R}, \tilde{\mathbf{c}})$  results from  $D$  steps of a sequential procedure, which i) is initialized with the matched filter ( $\mathbb{S}^1 = \tilde{\mathbf{c}}$ ); ii) at step  $i$ , solves the reduced-rank minimization problem (2.17) and extends the minimization subspace  $\mathbb{S}^i$  with the gradient of the cost function (MSE) taken at the point  $\mathbf{w}_{opt}^i$ .

**Remark 2.1** *Other approaches leading to Krylov subspaces can be found in literature. For example, one can consider the polynomial decomposition of  $\mathbf{R}^{-1}$ :*

$$\mathbf{R}^{-1} = \alpha_0 \mathbf{I} + \alpha_1 \mathbf{R} + \dots + \alpha_{N-1} \mathbf{R}^{N-1}. \quad (2.19)$$

A reduced-rank filter is obtained by truncating the right-hand side of (2.19) to  $D$  terms and by multiplying the result by  $\tilde{\mathbf{c}}$ :

$$\mathbf{w}_{opt}^N = \mathbf{R}^{-1} \tilde{\mathbf{c}} \Rightarrow \mathbf{w}_{opt}^D = \alpha'_0 \tilde{\mathbf{c}} + \alpha'_1 \mathbf{R} \tilde{\mathbf{c}} + \dots + \alpha'_{D-1} \mathbf{R}^{D-1} \tilde{\mathbf{c}}. \quad (2.20)$$

The coefficients  $\{\alpha'_i\}$  are chosen in order to minimize the MSE (the Cayley-Hamilton Receiver of [58]) or to maximize the Signal-to-Interference ratio [59]. In [34], the MSWF is developed through the decomposition of the full-rank Wiener filter into a linear combination of the matched filter  $\tilde{\mathbf{c}}^N$  and of the reduced-rank Wiener filter  $\mathbf{v}_{opt}^{N-1}$  in the orthogonal to  $\tilde{\mathbf{c}}^N$  subspace:

$$\mathbf{w}_{opt}^N = \beta_1 \tilde{\mathbf{c}}^N + \beta_2 \mathbf{v}_{opt}^{N-1}. \quad (2.21)$$

The filter  $\mathbf{v}_{opt}^{N-1}$  can be further represented as a linear combination of the matched filter  $\tilde{\mathbf{c}}^{N-1}$  (in the subspace orthogonal to  $\tilde{\mathbf{c}}^N$ ) and of the Wiener filter  $\mathbf{v}_{opt}^{N-2}$  of rank  $N - 2$  (in the subspace orthogonal to  $\text{span}\{\tilde{\mathbf{c}}^N, \tilde{\mathbf{c}}^{N-1}\}$ ), and so on. The vectors  $\tilde{\mathbf{c}}^i$  so obtained again generate the Krylov subspace.

## 2.3 Reduced-rank techniques based on the Krylov subspace projection

In this section, we present three methods to calculate the reduced-rank Wiener filter. The subspace of the three methods is the Krylov subspace associated to the observation covariance matrix and the signal-observation cross-correlation vector.

### 2.3.1 The Powers of $\mathbf{R}$ (POR) receiver

The most direct way to implement a Krylov subspace reduced-rank receiver is to construct the Krylov matrix as the successive powers of the covariance matrix multiplied by the cross-correlation vector. The POR receiver [43] can be considered as the simplest reduced-rank filter because it directly uses this remark. Vectors  $\mathbf{t}_i, i = 1, 2 \dots D$ , which generate the Krylov subspace  $\mathcal{K}^D(\mathbf{R}, \tilde{\mathbf{c}})$  are computed as

$$\mathbf{t}_i = \mathbf{R}^{i-1} \tilde{\mathbf{c}}. \quad (2.22)$$

The algorithm is summarized in Table 2.1. It is noteworthy that for the POR receiver,  $[i, j]$ th element of  $\mathbf{R}_t$  can be written as

$$\mathbf{R}_t[i, j] = \tilde{\mathbf{c}}^H \mathbf{R}^{i+j-1} \tilde{\mathbf{c}}, \quad (2.23)$$

therefore,  $\mathbf{R}_t$  is a Hankel matrix. This fact can be used to simplify calculations.

$\mathbf{t}_1$	$= \tilde{\mathbf{c}}$
$\mathbf{t}_i$	$= \mathbf{R} \mathbf{t}_{i-1}, i = 2, \dots, D$
$\mathbf{T}$	$= [\mathbf{t}_1 \mathbf{t}_2 \dots \mathbf{t}_D]$
$\mathbf{R}_t$	$= \mathbf{T}^H \mathbf{R} \mathbf{T}$
$\tilde{\mathbf{c}}_t$	$= \mathbf{T}^H \tilde{\mathbf{c}}$
Solve $\mathbf{R}_t \boldsymbol{\mu} = \tilde{\mathbf{c}}_t$ for $\boldsymbol{\mu}$	
$\mathbf{w}_{opt}^D$	$= \mathbf{T} \boldsymbol{\mu}$

Table 2.1: Summary of the POR algorithm

### 2.3.2 The Multi-Stage Wiener Filter (MSWF)

The Multi-Stage Wiener Filter [34] consists of two distinct iterative procedures. The first one (*forward recursion*, Table 2.2) builds an orthonormal basis of the Krylov subspace  $\mathcal{K}^D(\mathbf{R}, \tilde{\mathbf{c}})$  giving the projection matrix  $\mathbf{Q} = [\mathbf{q}_1 \mathbf{q}_2 \dots \mathbf{q}_D]$ . The second procedure (*backward recursion*, Table 2.3) solves the system (2.12) giving the transformed Wiener filter  $\boldsymbol{\mu}_{opt}^D$ , or, equivalently, the weighting of basis vectors. The resulting structure of the MSWF is depicted in Fig. 2.1. At stage  $i$  of the MSWF, the received signal is projected onto the subspace orthogonal to the filters  $\mathbf{q}_j$  ( $j = 1, 2, \dots, i$ ) of the preceding stages giving the projected observation

$$\mathbf{x}_0(m) \stackrel{\text{def}}{=} \mathbf{x}(m), \quad \mathbf{x}_i(m) = \prod_{j=1}^i (\mathbf{I} - \mathbf{q}_j \mathbf{q}_j^H) \mathbf{x}(m) \quad (i > 0).$$

The projected observation  $\mathbf{x}_{i-1}(m)$  is subsequently filtered with the filter  $\mathbf{q}_i$  giving the output  $d_i(m)$  of the  $i$ th stage. The outputs of all  $D$  stages of the MSWF are then linearly combined. The derivation of the equations of Tables 2.2 and 2.3 can be found, for example, in [22]. The  $D$ -stage MSWF computes the rank  $D$  Wiener filter in Krylov subspace  $\mathcal{K}^D(\mathbf{R}, \tilde{\mathbf{c}})$ . Hence, the MSWF is mathematically equivalent to POR.

**Remark 2.2** *It can be verified that the basis vectors of the MSWF  $\mathbf{q}_j$  result from the Gram-Schmidt orthonormalization procedure applied to the POR basis vectors  $\mathbf{t}_i = \mathbf{R}^i \tilde{\mathbf{c}}$   $i = 1 \dots D$ .*

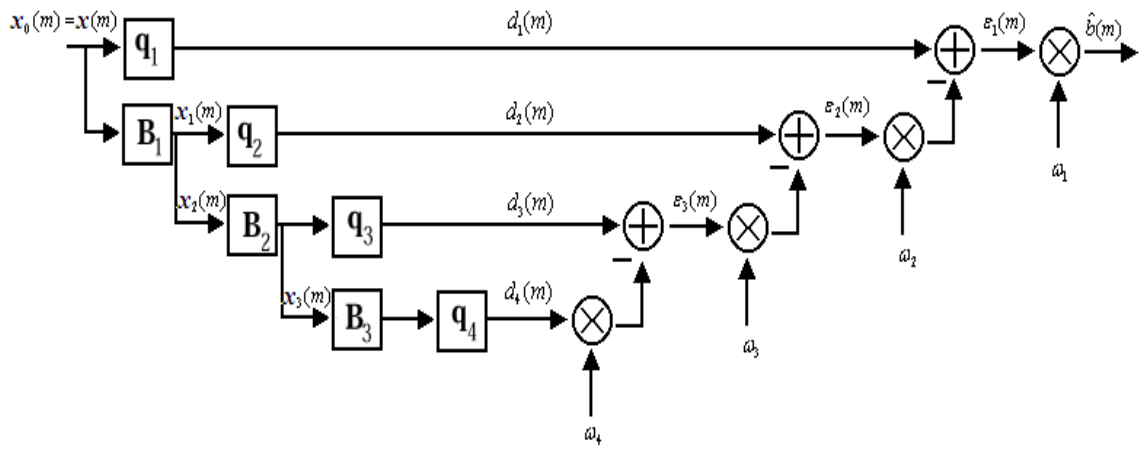


Figure 2.1: Multi-Stage Wiener Filter (rank  $D = 4$ ).

<i>Initialization:</i>	
$\mathbf{p}_1$	$= \tilde{\mathbf{c}}$
$\delta_1$	$= \ \tilde{\mathbf{c}}\ $
$\mathbf{x}_0(m)$	$= \mathbf{x}(m)$
$i$	$:= 1$
<i>Do While</i> ( $\delta_i \neq 0$ ) <i>and</i> ( $i \leq D$ )	
$\mathbf{q}_i$	$= \mathbf{p}_i / \delta_i$
$\mathbf{x}_i(m)$	$= (\mathbf{I} - \mathbf{q}_i \mathbf{q}_i^H) \mathbf{x}_{i-1}(m)$
$d_i(m)$	$= \mathbf{q}_i^H \mathbf{x}_{i-1}(m)$
$i$	$:= i + 1$
$\mathbf{p}_i$	$= \mathbb{E}[\mathbf{x}_{i-1}(k) d_{i-1}^*(m)]$
$\delta_i$	$= \ \mathbf{p}_i\ $

Table 2.2: Forward recursion of the rank  $D$  MSWF.

<p><i>Initialization:</i>  <math>\varepsilon_D(m) = d_D(m)</math>  <i>Decrement</i> <math>i = D, \dots, 1</math>  <math>\omega_i = \delta_i / \mathbb{E} [ \varepsilon_i(m) ^2]</math>  if <math>i = 1</math>  <math>\hat{b}(m) = \omega_1 \varepsilon_1(m)</math>  else  <math>\varepsilon_{i-1}(m) = d_{i-1}(m) - \omega_i \varepsilon_i(m)</math></p>
--------------------------------------------------------------------------------------------------------------------------------------------------------------------------------------------------------------------------------------------------------------------------------------------------------------------------------------------------------------------------------------

Table 2.3: Backward recursion of the rank  $D$  MSWF.

### 2.3.3 The Conjugate-Gradient Reduced-Rank Filter (CGRRF)

The Conjugate Gradient Reduced-Rank Filter [21] or Conjugate Gradient Implementation of the MSWF [31] are inspired directly from the Conjugate Gradient Algorithm (CGA) for systems of linear equations [35]. For that reason, we start by a brief introduction into conjugate gradient methods.

Consider the following general iterative procedure:

$$\mathbf{w}^0 = \mathbf{0} \quad (2.24)$$

$$\mathbf{w}^i = \mathbf{w}^{i-1} + c_i \mathbf{u}_i, \quad i = 1, 2, \dots, D \quad (2.25)$$

with the sequences of complex coefficients  $c_i$  and of vectors  $\mathbf{u}_i$  chosen according to some optimization criterion.

The criterion considered here is  $J(\mathbf{w}^i)$ , so it is natural to require that  $J(\mathbf{w}^i) \leq J(\mathbf{w}^{i-1})$ . Note also from (2.25) that  $\mathbf{w}^i$  is always in  $\mathcal{U}^i = \text{span}\{\mathbf{u}_1, \mathbf{u}_2, \dots, \mathbf{u}_i\}$ . The question is: whether it is possible to choose  $c_i$  and  $\mathbf{u}_i$  to give the reduced-rank Wiener filter in  $\mathcal{U}^i$ ? In other words, we require that

$$\mathbf{w}^i = \mathbf{w}_{opt}^i = \arg \min_{\mathbf{w} \in \mathcal{U}^i} J(\mathbf{w}). \quad (2.26)$$

The following lemma answers this question.

**Lemma 2.1** *For the requirement (2.26) to be satisfied, it is sufficient that*

1.  $\mathbf{u}_i$  be mutually  $\mathbf{R}$ -conjugate, that is,

$$\mathbf{u}_i^H \mathbf{R} \mathbf{u}_j = 0, \quad i \neq j \quad (2.27)$$

2.  $c_i$  be given by

$$c_i = \mathbf{u}_i^H \mathbf{e}_{i-1} / \mathbf{u}_i^H \mathbf{R} \mathbf{u}_i, \quad (2.28)$$

where

$$\mathbf{e}_i \stackrel{\text{def}}{=} \mathbf{c} - \mathbf{R} \mathbf{w}^i. \quad (2.29)$$

**Proof 2.1.** See [35].

It is easy to show that the value of the coefficient  $c_i$  as given by (2.28) minimizes the MSE in the direction of the line  $\mathcal{L} = \{\mathbf{w}^{i-1} + c\mathbf{u}_i\}$ . Therefore, the condition (2.27) guarantees that the reduced-rank Wiener filter  $\mathbf{w}_{opt}^i$  lies on  $\mathcal{L}$ .

Different versions of the conjugate-gradient algorithm result from different ways to compute the sequence of  $\mathbf{R}$ -conjugate vectors  $\mathbf{u}_i$  [35]. The version shown in Table 2.4 requires only one matrix-by-vector multiplication per iteration.  $D$  iterations of the algorithm result in a sequence  $\{\mathbf{w}_{opt}^i\}$  of  $D$  reduced-rank Wiener filters in  $\mathcal{U}^i$ . The following lemma establishes the equivalence between the CGA and other exact methods (MSWF, POR).

**Lemma 2.2** For all  $1 \leq i \leq D$ ,  $\mathcal{U}^i = \mathcal{K}^{i-1}(\mathbf{R}, \tilde{\mathbf{c}})$ .

**Proof 2.2.** See [35].

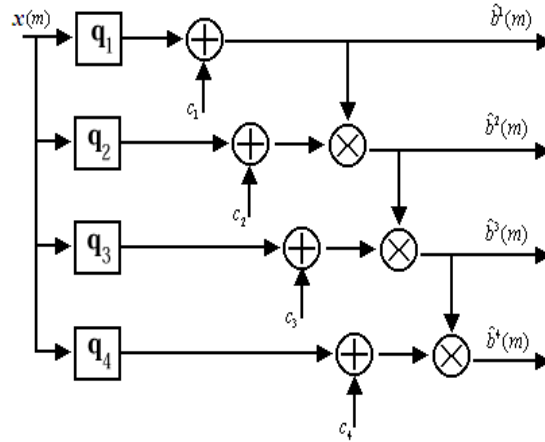
Therefore, the reduced-rank Wiener filter in  $\mathcal{U}^i$  generated at the  $i$ th CGA iteration is also the reduced-rank Wiener filter in the Krylov subspace  $\mathcal{K}^{i-1}(\mathbf{R}, \tilde{\mathbf{c}})$ .

Basically, the CGRRF of rank  $D$  performs  $D$  CGA iterations. The CGRRF has a multi-stage structure, as shown in Fig. 2.2, with the stage  $i$  computing the reduced-rank Wiener filter of the rank  $i$  and filtering the received signal to give the estimate  $\tilde{b}^i(m)$ .

<i>Initialization:</i>	
$\mathbf{w}_{opt}^0$	$= \mathbf{0}$
$\mathbf{u}_1$	$= \mathbf{e}_0 = \tilde{\mathbf{c}}$
For $i = 1, 2, \dots, D$	
if	$i > 1$
$\beta_i$	$= -\ \mathbf{e}_{i-1}\ ^2 / \ \mathbf{e}_{i-2}\ ^2$ (1)
$\mathbf{u}_i$	$= \mathbf{e}_{i-1} - \beta_i \mathbf{u}_{i-1}$ (2)
End	
$\mathbf{z}_i$	$= \mathbf{R}\mathbf{u}_i$ (3)
$c_i^{opt}$	$= \mathbf{u}_i^H \mathbf{e}_{i-1} / \mathbf{u}_i^H \mathbf{z}_i$ (4)
$\mathbf{e}_i$	$= \mathbf{e}_{i-1} - c_i^{opt} \mathbf{z}_i$ (5)
$\mathbf{w}_{opt}^i$	$= \mathbf{w}_{opt}^{i-1} + c_i \mathbf{u}_i$ (6)

Table 2.4: The Conjugate-Gradient Algorithm.

The complexity of block implementations of exact methods is given in Table 2.5. Here  $T$  is the block size. Note the complexity gain of reduced-rank methods (linear in  $N$ ) with respect to Sample Matrix Inversion (SMI) which varies as  $N^3$  and the RLS which varies as  $N^2$ .

Figure 2.2: The Conjugate-Gradient Reduced-Rank Filter (rank  $D = 4$ ).

Algorithm	Number of multiplications per block
SMI	$N^3/6 + TN^2$
RLS	$TN^2 + 3NT + 2T$
POR	$2TND + 3ND - N + 2D^2$
MSWF	$3TN(D - 1) + (N + T)(2D - 1) + D$
CGRRF	$2TND + 7ND - 3N + D$

Table 2.5: Complexity of block implementations [20].

### 2.3.4 Low-complexity approximate implementations

Low-complexity sample-by-sample adaptive implementations of exact methods can also be derived. By replacing some of the quantities that involve matrix-vector multiplications by some sample averages as a function of the previous samples. It should be noted, however, that these approximations incur a loss in performance especially for rapidly varying channels.

#### The Adaptive Conjugate Gradient Reduced Rank Filter

Let us take, as an example, the following equation of the CGRRF (equation (3) in Table 2.4):

$$\mathbf{z}_i = \mathbf{R}\mathbf{u}_i. \quad (2.30)$$

Implemented as it is, the matrix multiplication in (2.30) costs  $N^2$  flops. Instead, one may write:

$$\mathbf{z}_i(m) = \mathbf{R}(m)\mathbf{u}_i(m) = (\alpha_1(m)\mathbf{R}(m-1) + \alpha_2(m)\mathbf{r}(m)\mathbf{r}^H(m))\mathbf{u}_i(m),$$

where the coefficients  $\alpha_1$  and  $\alpha_2$  depend on the estimator of  $\mathbf{R}^1$ . Approximation

$$\mathbf{R}(m-1)\mathbf{u}_i(m) \approx \mathbf{R}(m-1)\mathbf{u}_i(m-1) \quad (2.31)$$

leads to

$$\mathbf{z}_i(m) = \alpha_1(m)\mathbf{z}_i(m-1) + \alpha_2(m)\mathbf{r}(m)\mathbf{r}^H(m)\mathbf{u}_i(m).$$

If  $\mathbf{z}_i(m)$  is computed as above, it costs only  $3N$  flops. The resulting low-complexity version of CGRRF proposed in [22] is given in Table 2.6.

#### The Stochastic Gradient Multi-Stage Wiener Filter

A similar adaptive implementation based on the MSWF: the Stochastic Gradient MSWF (SG-MSWF) was proposed in [40]. As for the CGRRF algorithm, the MSWF algorithm requires matrix-vector multiplications. In fact, when the statistics are not known, we concatenate the received signal vector  $\mathbf{x}(1), \dots, \mathbf{x}(T)$ , where  $T$  is the block size, in a single Matrix  $\mathbf{X}$ . The training symbols  $b(1), \dots, b(T)$  are also grouped in a single vector  $\mathbf{b}$ . The vector  $\mathbf{p}_1$  is then estimated by:  $\mathbf{p}_1 = \mathbf{X}\mathbf{b}$ . The vectors  $\mathbf{p}_i$   $i = 2 \dots D$  are estimated similarly after filtering  $\mathbf{X}$  by the blocking matrix (see [40] for a batch version of the MSWF based on training when the statistics are not known). In order to avoid the matrix-vector multiplication, it was proposed in [40] to approximate the MSWF parameters by sample averages. This means that the vectors  $\mathbf{p}_i$   $i = 1 \dots D$  are updated using the forgetting factor  $\gamma$  as:

$$\mathbf{p}_i(m) = \gamma\mathbf{p}_i(m-1) + (1-\gamma)d_{i-1}^*(m)\mathbf{x}_{i-1}(m). \quad (2.32)$$

---

<sup>1</sup>For example, if exponentially-forgetting window is used, then  $\alpha_1(m) = 1$  and  $\alpha_2(m) = \gamma$  (with  $0 \leq \gamma \leq 1$  being the forgetting factor).

The details of the SG-MSWF are given in Table 2.7.

Because of the approximations of the type (2.31), performance degradation (with the respect to exact versions of these algorithms) is generally observed. This point will be highlighted when discussing simulation results.

<i>Initialization:</i>	
$\mathbf{w}^0(m)$	$= \mathbf{0}$
$\beta_1(k)$	$= 0$
$\gamma$	$\in [0; 1]$ (forgetting factor)
$\mathbf{u}_1(m)$	$= \mathbf{e}_0(m) = \tilde{\mathbf{c}}$
<i>For <math>i = 1, 2, \dots, D</math></i>	
<i>if <math>i &gt; 1</math></i>	
$\beta_i(m) = \ \mathbf{e}_{i-1}(m)\ ^2 / \ \mathbf{e}_{i-2}(m)\ ^2$	
$\mathbf{u}_i(m) = \mathbf{e}_{i-1}(m) + \beta_i(n)\mathbf{u}_{i-1}(m)$	
<i>End</i>	
$\mathbf{z}_i(m)$	$= \gamma\mathbf{z}_i(m-1) + \mathbf{r}(m)\mathbf{r}^H(m)\mathbf{u}_i(m)$
$\alpha_i(m)$	$= \gamma\alpha_i(m-1) +  \mathbf{u}_i^H(m)\mathbf{r}(m) ^2$
$c_i(m)$	$= \mathbf{u}_i^H(m)\mathbf{e}_{i-1}(m) / \alpha_i(m)$
$\mathbf{e}_i(m)$	$= \mathbf{e}_{i-1}(m) - c_i(k)\mathbf{z}_i(m)$
$\mathbf{w}^i(m)$	$= \mathbf{w}^{i-1}(m-1) + c_i(m)\mathbf{u}_i(m)$

Table 2.6: Summary of the Adaptive Conjugate Gradient Reduced-Rank Filter.

The complexity of approximate sample-by-sample implementations is given in table 2.8.

## 2.4 Optimum Reduced-Rank CDMA Wiener Receivers

An optimum reduced-rank Wiener receiver stands for a reduced-rank version of the full-rank Wiener receiver. The full-rank receiver is the classical Wiener receiver. To explain how reduced-rank filtering can be applied to CDMA systems, we consider the faded CDMA model (1.14) that is repeated here for convenience:

$$\mathbf{x}(m) = \mathbf{H}_0\mathbf{W}(m)\mathbf{b}(m) + \mathbf{H}_1\mathbf{W}(m-1)\mathbf{b}(m-1) + \mathbf{v}(m), \quad (2.33)$$

where the quantities are defined in Chapter 1. We first precise that this model is a particular case of (2.1). We consider that user 1 is the user of interest and partition  $\mathbf{W}(m)$  and  $\mathbf{b}(m)$  as:

$$\mathbf{W}(m) = [\mathbf{w}_1(m) \ \mathbf{U}(m)],$$

<i>Forward recursion: Initialization:</i>	
$d_0(m)$	$= b(m)$
$\mathbf{x}_0(m)$	$= \mathbf{x}(m)$
$i$	$:= 1$
<i>At each <math>n</math>; Do While (<math>\delta_i \neq 0</math>) and (<math>i \leq D</math>)</i>	
$\mathbf{p}_i(m)$	$= \gamma \mathbf{p}_i(m-1) + (1-\gamma)d_{i-1}^*(m)\mathbf{x}_{i-1}(m)$
$\delta_i$	$=  \mathbf{p}_i(m) ^2$
$\mathbf{q}_i$	$= \mathbf{p}_i/\delta_i$
$d_i(m)$	$= \mathbf{q}_i^H(m)\mathbf{x}_{i-1}(m)$
$i$	$:= i+1$
$\mathbf{x}_i(m)$	$= (\mathbf{I} - \mathbf{q}_i\mathbf{q}_i^H)\mathbf{x}_{i-1}(m)$
<i>Backward Recursion: Initialization</i>	
$\varepsilon_D(m)$	$= d_D(m)$
<i>Decrement <math>i = D, \dots, 1</math></i>	
$\zeta_i(m)$	$= \gamma \zeta_i(m-1) + (1-\gamma)$
$\omega_i$	$= \delta_i/\zeta_i(m) \varepsilon_i(m) ^2$
<i>if <math>i = 1</math></i>	
	$\hat{b}(m) = \omega_1\varepsilon_1(m)$
<i>else</i>	
	$\varepsilon_{i-1}(m) = d_{i-1}(m) - \omega_i\varepsilon_i(m)$

Table 2.7: Summary of the Stochastic-Gradient MSWF.

Algorithm	Number of multiplications per sample
RLS	$N^2 + 3N + 2$
SG-MSWF	$7ND$
Adaptive CGRRF	$8ND - 2N$

Table 2.8: Complexity of some sample-by-sample algorithms

and

$$\mathbf{b}(m) = [b_1(m) \mathbf{b}_I(m)^T]^T,$$

where  $\mathbf{w}_1(m)$  and  $b_1(m)$  are the code and the transmitted symbol of the user of interest at time instant  $m$  whereas  $\mathbf{U}(m)$  and  $\mathbf{b}_I(m)$  are the interferers code matrix and transmitted symbol vector. If we let:

$$\mathbf{r}_{xb}(m) = \tilde{\mathbf{c}} \stackrel{\text{def}}{=} \mathbf{H}_0 \mathbf{w}_1(m) \quad (2.34)$$

$$\mathbf{I}_N \stackrel{\text{def}}{=} \mathbf{H}_0 \mathbf{U}(m) \mathbf{b}_I(m) + \mathbf{H}_1 \mathbf{U}(m-1) \mathbf{b}(m-1) + \mathbf{v}(m) \quad (2.35)$$

Then model (2.33) appears as a particular form of (2.1). The Wiener receiver is given by:

$$\mathbf{w} = \mathbf{R}_{xx}^{-1}(m) \mathbf{r}_{xb}(m) \quad (2.36)$$

where

$$\mathbf{R}_{xx}(m) = \mathbb{E}\{\mathbf{x}(m)\mathbf{x}(m)^H\} = \mathbf{H}_0 \mathbf{W}(m) \mathbf{W}(m)^H \mathbf{H}_0^H + \mathbf{H}_1 \mathbf{W}(m-1) \mathbf{W}(m-1)^H \mathbf{H}_1^H + \sigma^2 \mathbf{I}_N.$$

The reduced-rank receiver of rank  $D$  corresponding to this receiver is obtained by constructing the Krylov matrix:

$$\mathbf{K}^D(m) = [\mathbf{r}_{xb}(m) \quad \mathbf{R}_{xx}(m) \mathbf{r}_{xb}(m) \quad \dots \quad \mathbf{R}_{xx}^{D-1}(m) \mathbf{r}_{xb}(m)], \quad (2.37)$$

and calculating the reduced-rank filter:

$$\mathbf{w}^D = \left( \{\mathbf{K}^D(m)\}^H \mathbf{R}_{xx}(m) \mathbf{K}^D(m) \right)^{-1} \{\mathbf{K}^D(m)\}^H \mathbf{r}_{xb}(m). \quad (2.38)$$

The corresponding estimate of  $b_1^D(m)$  is given by:

$$\tilde{b}_1^D(m) = (\mathbf{w}^D)^H \{\mathbf{K}^D(m)\}^H \mathbf{x}(m). \quad (2.39)$$

This kind of receiver can be implemented if we know all the quantities. The scrambling code should be known at each time instant  $m$ . This is usually the case, but one has to reevaluate the covariance matrix each time. In the case of short-code CDMA, the interferers spreading codes are not known, but we know that  $\mathbf{W}(m) = \mathbf{W}(m-1)$ .  $\mathbf{R}_{xx}$  becomes independent of time and can be estimate by

$$\tilde{\mathbf{R}}_{xx} = \frac{1}{T} \sum_{m=1}^T \mathbf{x}(m) \mathbf{x}(m)^H,$$

and the methods discussed previously can be used to calculate the reduced-rank estimate of  $b_1(m)$ . The asymptotic performance of this kind of receivers will be discussed in chapter 4. For more information about the performance of different adaptive algorithms with this kind of receiver the reader is referred to thesis [20].

## 2.5 Suboptimum Reduced-Rank CDMA Wiener Receivers

The conventional detector for CDMA systems is the RAKE receiver. The RAKE receiver is known to suffer from Multiple Access Interference (MAI) that is created due to multipath channels. The use of multiuser detection gives a huge performance gain [74] but requires a substantial increase in the computational cost. Therefore, it cannot be used in the downlink where severe limitations are imposed on the mobile unit in terms of power consumption and computational complexity. Furthermore, most of the proposed multiuser detection algorithms, like the MMSE detector discussed previously, assume the knowledge of codes allocated to the active users present in the system. In the downlink, however, the mobile unit has very limited knowledge and cannot take advantage of multiuser detection.

Most of the methods for multiuser detection in CDMA rely on the cyclostationarity of the received signal [41] (no scrambling). Those methods cannot be used in W-CDMA systems where the short spreading codes are multiplied by a long cell specific pseudo-random scrambling code [15]. The received signal cyclostationarity is broken by the scrambling sequence. To overcome these difficulties, chip-level equalization was proposed to restore the orthogonality between spreading codes, thus reducing MAI [49, 48].

A Suboptimum Reduced-Rank receiver stands for a class of receivers that consist of a reduced-rank MMSE channel equalizer followed by descrambling and despreading. This receiver structure is shown in Figure 2.3. The main difference with optimum reduced rank Wiener receiver resides in the fact that interferers codes are not needed to implement this receiver. The channel effect is inverted by using an equalizer and any of the users can be detected without the need to know other codes.

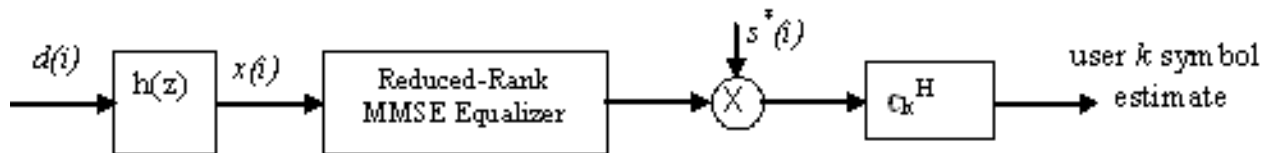


Figure 2.3: Suboptimum reduced-rank receiver structure.

To explain reduced-rank equalization, let the  $(N_g \times 1)$  discrete-time received signal be given by:

$$\mathbf{x}(i) = \mathbf{H}\mathbf{d}(i) + \mathbf{v}(i), \quad (2.40)$$

where  $N_g$  is the length of the equalizer to be introduced later, and

$$\begin{aligned} \mathbf{d}(i) &= [d(i-L+1), \dots, d(i), \dots, d(i+N_g-1)]^T, \\ \mathbf{x}(i) &= [x(i), x(i+1), \dots, x(i+N_g-1)]^T, \\ \mathbf{H} &= \begin{bmatrix} h_{L-1} & \cdots & h_0 & \cdots & 0 \\ 0 & h_{L-1} & \cdots & h_0 & \vdots \\ 0 & & \ddots & \ddots & \ddots & 0 \\ \vdots & 0 & h_{L-1} & \cdots & h_0 \end{bmatrix}, \end{aligned}$$

where  $h_k \triangleq h(t)|_{t=kT_c}$ ,  $\mathbf{v}(i)$  is defined as  $\mathbf{x}(i)$  with  $v(k) \triangleq v(t)|_{t=kT_c}$  and  $LT_c$  is the overall channel length.

### 2.5.1 Adaptive Chip Level MMSE Equalization

Chip level channel equalization is needed in order to restore the orthogonality between chip signals prior to despreading and descrambling. We will adopt the MMSE equalizer because it outperforms both Zero Forcing and RAKE [49].

Suppose that we want to design an MMSE equalizer of length  $N_g$  and delay  $D_g$  to restore  $d(i)$  from the observation  $\mathbf{x}(i)$ . Under the assumption that the chip sequence is an i.i.d sequence<sup>2</sup>, the MMSE equalizer is given by [49]:

$$\mathbf{g} = \{\sigma_d^2 \mathbf{H}\mathbf{H}^H + \sigma^2 \mathbf{I}_{N_g}\}^{-1} \mathbf{h} \quad (2.41)$$

where  $\sigma_d^2$  is the average chip sequence power,  $\mathbf{h}$  is the  $(D_g + 1)$ th column of  $\mathbf{H}$ . Let  $\mathbf{R}_{xx} = \sigma_d^2 \mathbf{H}\mathbf{H}^H + \sigma^2 \mathbf{I}_{N_g}$  and  $\mathbf{r}_{xd} = \mathbf{h}$ .  $\mathbf{R}_{xx}$  can be shown to coincide with:

$$\lim_{M \rightarrow \infty} \frac{1}{MN} \sum_{i=0}^{MN-1} \mathbb{E} \{\mathbf{x}(i)\mathbf{x}(i)^H\}, \quad (2.42)$$

where  $\mathbf{x}(m)$  is generated using the model (1.14).

$\mathbf{R}_{xx}$  can be estimated consistently by:

$$\tilde{\mathbf{R}}_{xx} = \frac{1}{MN} \sum_{i=0}^{MN-1} \mathbf{x}(i)\mathbf{x}(i)^H. \quad (2.43)$$

---

<sup>2</sup>The scrambling sequence is a realization of an i.i.d sequence that is known by the receiver. Note that the chip sequence can be considered i.i.d if the scrambling sequence is a realization of an i.i.d sequence unknown to the receiver.

Similarly,

$$\mathbf{r}_{xd} = \lim_{M \rightarrow \infty} \frac{1}{MN} \sum_{i=0}^{MN-1} \mathbb{E}\{\mathbf{x}(i + D_g)d^*(i)\} \quad (2.44)$$

$\mathbf{r}_{xd}$  can be estimated consistently by:

$$\tilde{\mathbf{r}}_{xd} = \frac{1}{MN} \sum_{i=0}^{MN-1} \mathbf{x}(i + D_g)d^*(i), \quad (2.45)$$

where the expectation is over all the symbols  $b_k(m)$  and noise.

The equalizer restores the orthogonality of the spreading codes. The reconstructed chip sequence ( $\hat{d}(i)$ ) is obtained by filtering the received signal  $x(i)$  by the equalizer filter  $g(z)$  corresponding to vector  $\mathbf{g}$ . An estimate of the symbol  $\hat{b}_k(m)$  is then obtained by descrambling and despreading the equalized chip sequence  $\hat{d}(i)$ :

$$\begin{aligned} \hat{b}_k(m) &= \sum_{i=0}^{N-1} \hat{d}(mN + i)s^*(mN + i)c_k^*(i) \\ &= \sum_{i=0}^{N-1} \sum_{l=0}^{N_g-1} g_l^* x(mN - l + i)s^*(mN + i)c_k^*(i) \\ &= \sum_{l=0}^{N_g-1} g_l^* y_{l,k}(m) = \mathbf{g}^H \mathbf{C}_k^H(m) \tilde{\mathbf{x}}(m) \\ &= \mathbf{g}^H \mathbf{y}_k(m) \end{aligned} \quad (2.46)$$

where

$$\begin{aligned} \mathbf{g} &= [g_0, \dots, g_{N_g-1}]^T \\ \mathbf{y}_k(m) &= [y_{0,k}(m), \dots, y_{N_g-1,k}(m)]^T \\ y_{l,k}(m) &= \sum_{i=0}^{N-1} x(mN - l + i)s^*(mN + i)c_k^*(i) \\ \tilde{\mathbf{x}}(m) &= [x(mN + N - 1), \dots, x(mN), \dots, x(mN - N_G + 1)]^T \\ \tilde{\mathbf{c}}_k(m) &= [s(mN + N - 1)c_k(N - 1), \dots, s(mN)c_k(0)]^T \end{aligned}$$

and  $\mathbf{C}_k(m) = \mathcal{T}(\tilde{\mathbf{c}}_k(m))$  is the  $(N + N_g - 1) \times N_g$  Toeplitz matrix associated with the vector  $\tilde{\mathbf{c}}_k(m)$  (padded with zeros) given by:

$$\mathbf{C}_k(m) = \begin{bmatrix} s(mN + N - 1)c_k(N - 1) & 0 & \dots & 0 \\ \vdots & \ddots & & \vdots \\ s(mN + 1)c_k(1) & & \ddots & s(mN + N - 1)c_k(N - 1) \\ s(mN)c_k(0) & & & s(mN + N - 2)c_k(N - 2) \\ & & \ddots & \vdots \\ 0 & \dots & \ddots & s(mN)c_k(0) \end{bmatrix}.$$

Equations 2.46 show that the order of the equalization step and the despreading (+ descrambling) step can be changed since they are two linear operations. This is a very important remark since it allows to train the equalizer using the known pilot symbols. Equation (2.41) is of the form of the well known Wiener-Hopf Equation. As for the symbol level receiver, the equalization step can be done in a reduced-rank fashion. The reduced-rank equalizer of rank  $D$  is given by:

$$\mathbf{g}^D = \mathbf{K}^D \left( \{\mathbf{K}^D\}^H \mathbf{R}_{xx} \mathbf{K}^D \right)^{-1} \{\mathbf{K}^D\}^H \mathbf{r}_{xd}, \quad (2.47)$$

where  $\mathbf{K}^D$  is now the Krylov matrix associated to the pair  $(\mathbf{R}_{xx}, \mathbf{r}_{xd})$  given by:

$$\mathbf{K}^D = [\mathbf{r}_{xd} \quad \mathbf{R}_{xx} \mathbf{r}_{xd} \quad \dots \quad \mathbf{R}_{xx}^{D-1} \mathbf{r}_{xd}]. \quad (2.48)$$

We cannot train the MMSE equalizer on the chip sequence (because the mobile is not supposed to know other users' codes and symbols). Future 3G CDMA systems (like the UMTS-FDD) consider the use of a permanent pilot channel which employs a code of all 1's, this sequence will be used to train the equalizer. The preceding set of equation show that the order of the equalization step and the despreading (+ descrambling) step can be interchanged. The error-driven adaptive algorithm is thus fed by the despread pilot signal and the desired signal is the pilot symbol. The resulting coefficients are the equalizer coefficients used for equalization. We need, however, to show that the resulting equalizer is the same. For this purpose we need to use the following proposition:

**Proposition 2.1** *under the assumption that the scrambling sequence is i.i.d (so that the chip sequence is i.i.d), the solution of:*

$$\mathbf{R}_{xx} \mathbf{g} = \mathbf{r}_{xd} \quad (2.49)$$

*is equal up to a constant multiplicative factor to the solution of:*

$$\mathbf{R}_{yy} \mathbf{g} = \mathbf{r}_{yb}, \quad (2.50)$$

where

$$\mathbf{R}_{yy} = \lim_{M \rightarrow \infty} \frac{1}{M} \sum_{m=0}^{M-1} \mathbb{E} \{ \mathbf{y}_k(m) \mathbf{y}_k(m)^H \} \quad (2.51)$$

and

$$\mathbf{r}_{yb} = \lim_{M \rightarrow \infty} \frac{1}{M} \sum_{n=0}^{M-1} \mathbb{E} \{ \mathbf{y}_k(m) b_k^*(m) \}. \quad (2.52)$$

**Proof.** See Appendix A.1.

Consistent estimate of  $\mathbf{R}_{yy}$  and  $\mathbf{r}_{yb}$  can be obtained by:

$$\tilde{\mathbf{R}}_{yy} = \frac{1}{M} \sum_{m=0}^{M-1} \mathbf{y}_k(m) \mathbf{y}_k(m)^H, \quad (2.53)$$

$$\tilde{\mathbf{r}}_{yb} = \frac{1}{M} \sum_{m=0}^{M-1} \mathbf{y}_k(m) b_k^*(m) \quad (2.54)$$

The reduced-rank algorithms discussed previously can be used by using implicitly the proposition 2.1. They provide a reduced rank MMSE equalizer using  $\mathbf{y}_1(m)$  as input and the known pilot sequence  $b_1(m)$  as desired output instead of using  $\mathbf{x}(m)$  and the unknown chip sequence  $d(i)$  and update the equalizer at each symbol.

Once the equalizer is updated, it is applied to  $\mathbf{y}_k(m)$  to estimate the symbol  $b_k(m)$  where  $k$  is the index of the user of interest. The corresponding performances are presented in the next section.

## 2.6 Simulation Results

In what follows, we present extensive simulation results to highlight the performance of reduced-rank equalization in the forward link of UMTS-FDD. Both exact and approximate methods are considered in static and time-varying channels environment.

### 2.6.1 Exact methods for available $\mathbf{R}_{xx}$ and $\mathbf{r}_{dx} = \mathbf{h}$

We begin by considering the case where we have exact estimates of the covariance matrix  $\mathbf{R}_{xx}$  and the cross-correlation vector  $\mathbf{r}_{xd}$ . We consider the physical channel of UMTS-FDD. All users are considered to have the same spreading factor  $N$ . We consider a system with  $N = 32$  and a number of users  $K = 16$ , all fixed to 10 dB. The propagation channel is the Vehicular A channel (The profile of the Vehicular A channel is shown in table 2.9). On each frame a different realization of channel following this profile is generated. The equalizer length  $N_g$  is taken to be 20. Figure 2.4 shows the BER of exact methods (either MSWF or CGRRF) as a function of the rank  $D$ . The BER of the MMSE equalizer solution and the RAKE receiver are given for comparison.

Path Delay in chips	0	1.19	2.73	4.19	6.65	9.65
Average Power (dB)	0	-1.0	-9.0	-10.0	-15.0	-20.0

Table 2.9: The Vehicular A channel power profile.

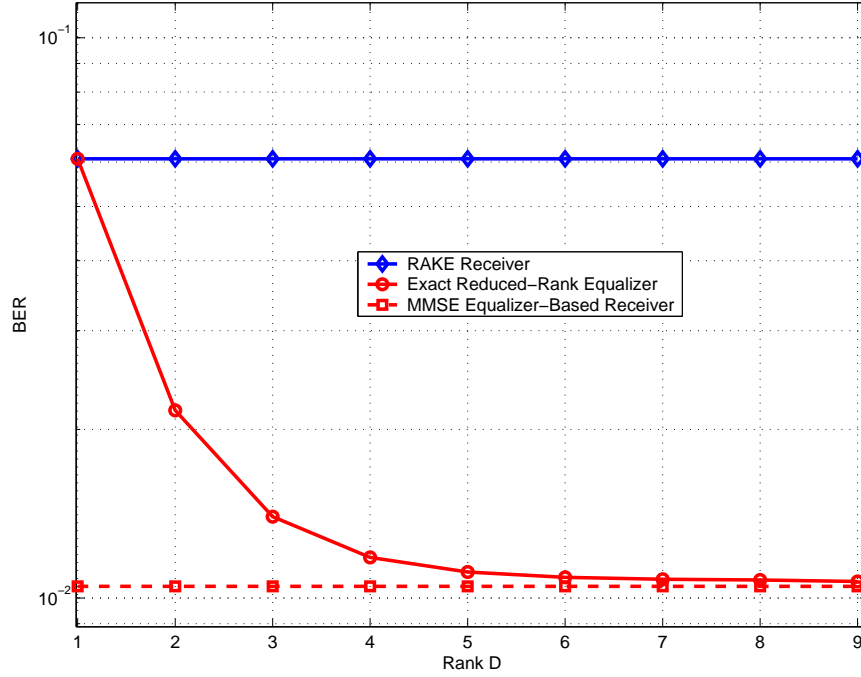


Figure 2.4: Performance of exact algorithms

We see that the reduced-rank BER converges rapidly to the full-rank (MMSE) BER. We see also that the rank  $D = 1$  corresponds to a RAKE receiver. The speed of convergence of the reduced-rank BER to the full-rank BER will be analyzed in Chapter 4 for optimum reduced-rank receivers. The speed of convergence of equalizer-based receivers considered in this chapter will be discussed in Chapter. 5.

### 2.6.2 Exact method with adaptive estimation of $\mathbf{R}_{yy}$ and $\mathbf{r}_{yb}$

We switch to the case where  $\mathbf{R}_{yy}$  and  $\mathbf{r}_{yb}$  are estimated using a forgetting factor. We start by evaluating the performance of exact methods (either MSWF or CGRRF). For this, we simulate a system with the following parameters: a Spreading Factor (SF)  $N = 32$ , a number of users  $K = 20$ . The user 1 is considered to be a pilot channel (CPICH) spread by a code of all ones and used to train the equalizer. The user of interest is taken to be one of the remaining users (we average the performance over the different spreading codes). The user of interest and the pilot are fixed to a power of 12 dB while all the remaining users are fixed to 10 dB. The propagation channel is taken to be the multipath "channel 1" with chip-spaced coefficients shown in Table. 2.10.

The equalizer length  $N_g$  is taken to be 20 and the forgetting factor  $\alpha = 0.99$ . The mobile is supposed to know neither interfering users codes nor the propagation channel, the only

Path Delay in chips	0	3	6	8
Channel Coefficient	0.45 - 0.45i	0.45 + 0.45i	-0.22 + 0.22i	0.22 - 0.22i

Table 2.10: The channels coefficients of “Channel 1” used in simulations.

knowledge required is the pilot sequence, the scrambling sequence and the spreading codes of the user of interest and the pilot.

We evaluate the convergence of exact methods versus time. The algorithm used to train the equalizer is the MSWF of rank  $D = 3^3$ . Figure 2.5 shows the BER convergence of MSWF and compare it to adaptive RAKE<sup>4</sup> and SMI. Exact RAKE and exact MMSE are given for comparison.

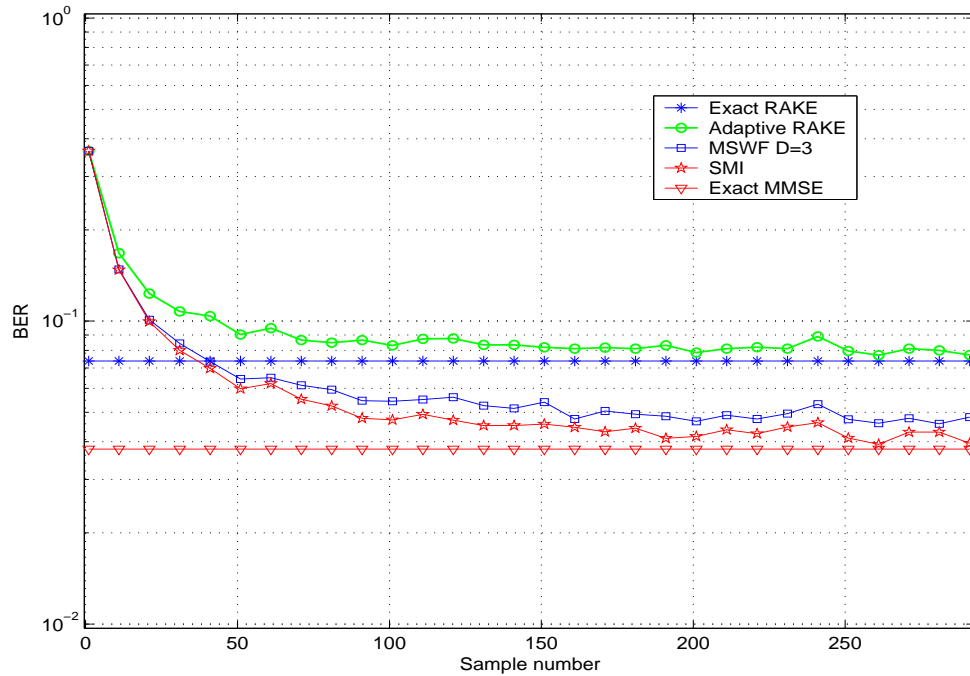


Figure 2.5: Performance of exact reduced rank equalization vs time (symbol period).

First, we note that adaptive RAKE and SMI tend to exact RAKE and exact MMSE respectively when the estimate  $\hat{\mathbf{R}}_{yy}$  and  $\hat{\mathbf{r}}_{yb}$  converge to  $\mathbf{R}_{yy}$  and  $\mathbf{r}_{yb}$  respectively. We remark also that the reduced-rank method give performance that is very close to the SMI.

<sup>3</sup>The same results are obtained for CGRRF and POR since exact algorithms are equivalent

<sup>4</sup>adaptive RAKE stands for a RAKE where the coefficients are estimated adaptively using a forgetting factor, where exact RAKE stands for a RAKE receiver which knows exactly the channel

Another important remark is that a reduced-rank equalizer *trained* only on the pilot gives a better performance than an *exact* RAKE.

In the next experiment, we keep the same setting as the previous experiment ( $N=32$ ,  $K=20$ ) and the same propagation channel. We evaluate the BER after convergence (after 300 samples) as a function of the SNR of each user. All users are considered to have the same SNR and are varied together. Figure 2.6 shows the results for different values of the Rank  $D$ .

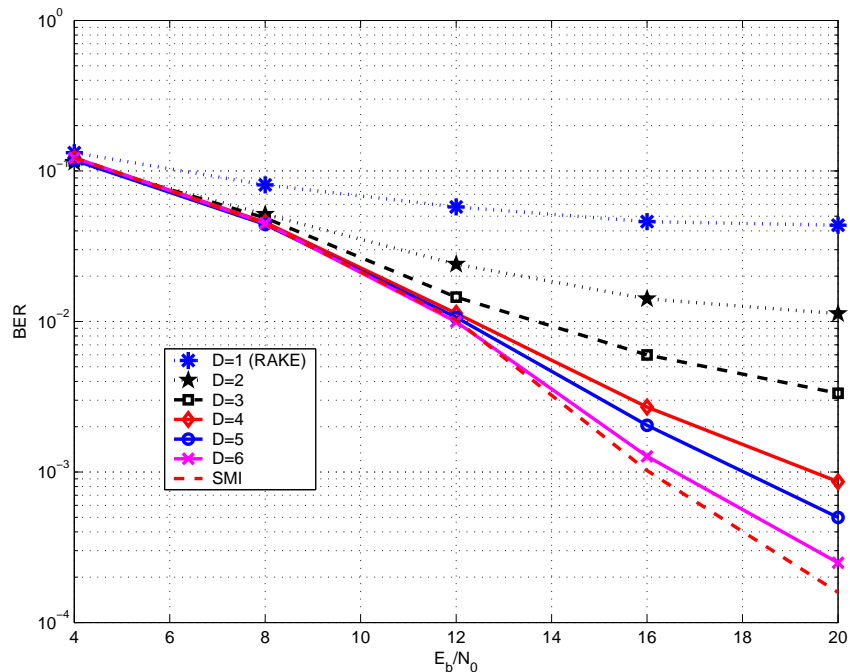


Figure 2.6: Performance of reduced rank exact algorithms.

We notice that the reduced-rank BER converges rapidly to the full-rank. This is more remarkable for low SNRs. We also remark that the RAKE receiver (which corresponds to  $D = 1$ ) flattens for high values of SNR because it is interference limited. This means that after a certain SNR, there is no interest in increasing the SNR because the limiting factor is no more noise, but interference. The MMSE equalizer (corresponding to SMI), on the other hand, as well as its reduced-rank versions suffer less from the interference and do not flatten for high values of the SNR.

### 2.6.3 Approximate sample by sample methods

In the next experiment, we test the performance of approximate methods (Adaptive CGRRF and Stochastic Gradient MSWF), we keep the same setting as the exact methods case: a Spreading Factor (SF)  $N = 32$ , a number of users  $K = 20$ . The user of interest and the pilot are fixed to a power of 12 dB while all the remaining users are fixed to 10 dB. We keep the same multipath channel "channel 1". The equalizer length  $N_g$  is taken to be 20 and the forgetting factor  $\alpha = 0.99$ . The results are shown in figure 2.7.

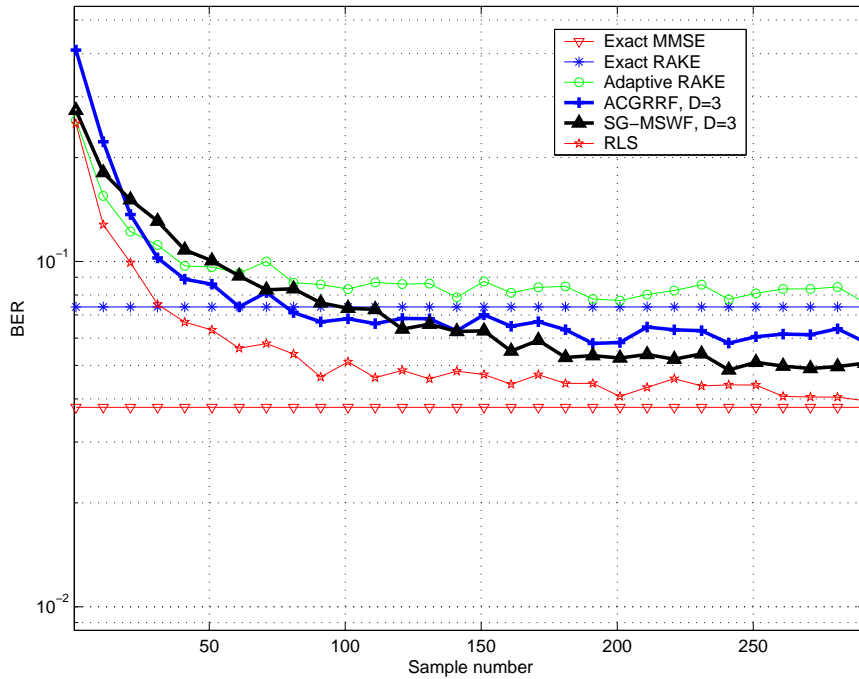


Figure 2.7: Performance of approximate reduced rank methods vs time.

We notice that the BER provided by approximate methods is slightly worse than exact methods due to the inherent approximations discussed previously. We also remark that the SG-MSWF converges slowly after some 50 samples but outperforms the ACGRFF after 150 samples. This means that the ACGRFF has better convergence properties when the training data are limited, whereas the SG-MSWF is better if the training data is sufficient to attain steady state performance.

### 2.6.4 Time-varying channels with exact methods

In the next experiments, we test the performance of the discussed algorithms under time-varying channels. Using Jakes model [46] we simulate a time-varying channel with Vehicular A profile and a mobile speed of 80 kmh. The forgetting factor  $\gamma = 0.98$ , the spreading

factor  $N=32$ ,  $K=15$  users all fixed to 11 dB. The results for CGRRF of  $D=3$  are shown in Figure 2.8. Note that the RLS gives no improvement over CGRRF. It is even worse

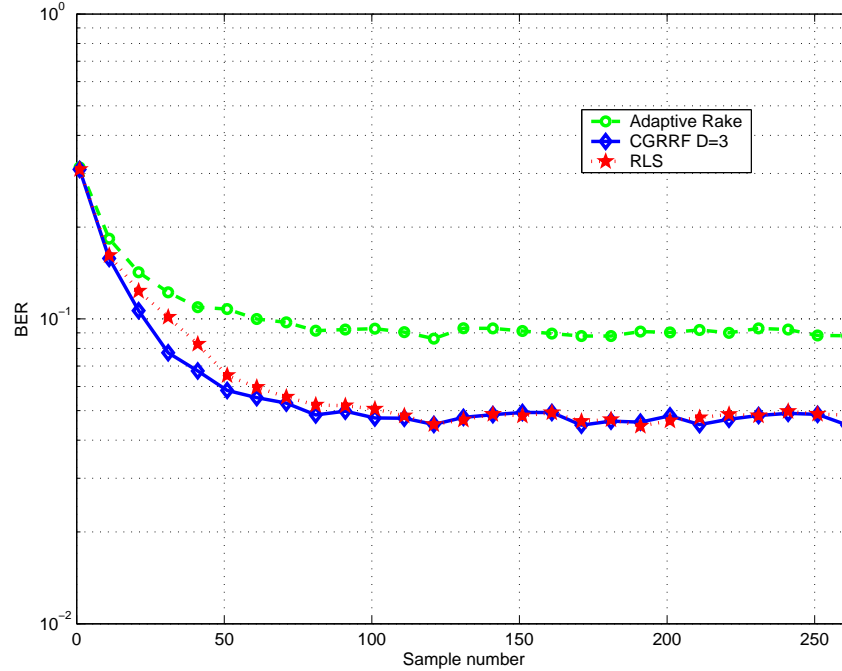


Figure 2.8: Performance of exact algorithms In time-varying channels environment.

at the beginning, this is a very important property of reduced-rank filtering. When the number of training data is not sufficient, the reduced-rank performance is better than the full-rank (Sample matrix inversion) performance.

In Figure 2.9, we plot the BER after convergence (i.e. after  $N_s=200$  samples) of the MSWF of rank  $D=3$  as a function of the mobile speed for a system with  $N = 16$ ,  $K = 10$  all fixed to 11 dB. Vehicular A channel profile and a forgetting factor  $\gamma = 0.98$ .

We remark that the performance gap between Sample Matrix Inversion (SMI) and MSWF decreases as the mobile speed increases. At 200 Km/h there is practically no difference between the two methods.

### 2.6.5 Time-Varying Channels with approximate methods

In the last experiment, We consider the performance of approximate methods in Time-Varying environment. We test the performance of both SG-MSWF and ACGRRF for the following setting: a vehicular A profile, a mobile speed of 80 km/h, a forgetting factor  $\gamma = 0.98$ , a spreading factor  $N=32$ ,  $K=15$  users all fixed to 11 dB. The results are shown

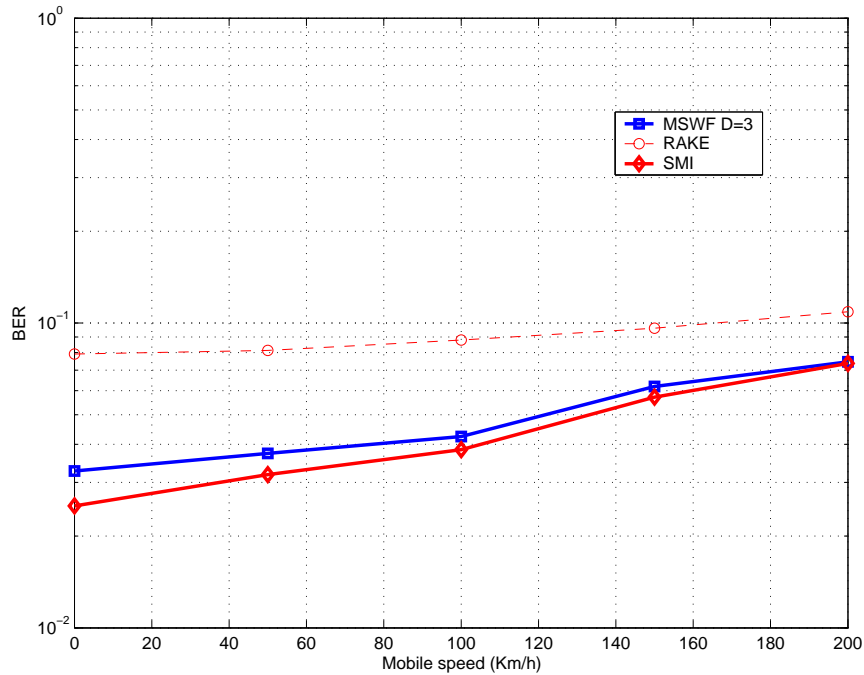


Figure 2.9: Performance of RAKE, MSWF and SMI as a function of the mobile speed.

in Figure 2.10.

The first remark is that the performance of approximate methods degrades completely for time varying environment. The improvement with respect to RAKE becomes almost negligible. We note also that the ACGRRF provides a better BER (recall that the SG-MSWF is better for static channels and sufficient training samples).

## 2.7 Conclusion

Reduced-rank filtering methods were discussed in this chapter. We started by a brief presentation of existing exact methods that are based on the Krylov subspace, namely: The MSWF the CGRRF and the POR algorithms. We then discussed approximate methods such as the Adaptive CGRRF and the Stochastic Gradient MSWF. The difference between optimum and suboptimum reduced-rank receivers was highlighted. Extensive simulation results were given to explain the performance of reduced-rank equalization in the CDMA downlink.

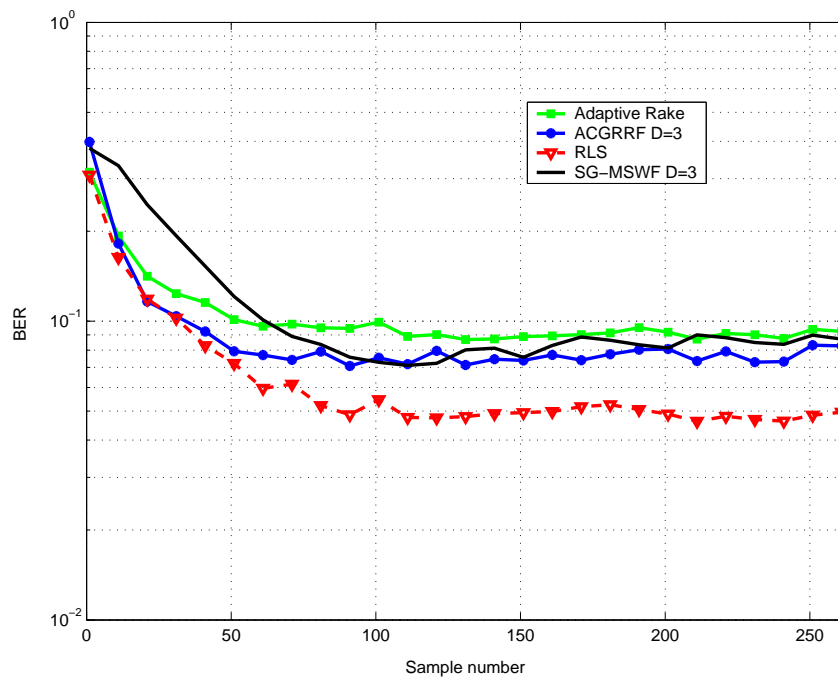


Figure 2.10: Performance of approximate algorithms In time-varying channels environment.



# Chapter 3

## Blind Interference Cancellation for Multi-rate Long-Code CDMA

---

### 3.1 Introduction

Third Generation (3G) mobile communication systems like UMTS are intended to provide a large variety of services like voice communication and internet browsing. This diversity of services implies the use of different data rates. 3G systems are termed as "*multi-rate*". In Code Division Multiple Access (CDMA) systems, data rates depend on the Spreading Factor (SF). Thus, different spreading factors are used depending on the rate intended for each physical channel.

As discussed in Chapter 2, because of the scrambling code, the cyclostationarity of the received signal is broken. Thus, the statistics of the channel and the received signal cannot be estimated. Wiener receivers and multiuser methods in general cannot be used. Equalization prior to descrambling and despreading allows to improve the performances of the RAKE receiver and overcome the MAI limitation.

Intercell Parallel Interference Cancellation (PIC) is another way of reducing MAI. If we know the codes that are active, we can make decision on some (or all) of the users interfering with the user of interest. Those decisions (either hard decisions, or soft estimations) are passed through a channel estimate thus producing a reliable version of MAI. This MAI can be removed either by subtraction or projection methods [55].

In this chapter, we propose a new blind interference cancellation scheme suitable for downlink multi-rate CDMA systems. The received signal is passed through a channel equalizer to restore orthogonality between spreading codes. Fast Walsh Transform (FWT) is used to produce estimates of the transmitted bits corresponding to all effective codes. Comparing with a threshold at the output of the FWT, the active codes are decided for. A Parallel Interference Cancellation stage follows the equalization and FWT. Simulations are carried for UMTS-FDD and show the gain in performance when using the proposed scheme with respect to Interference Cancellation with a RAKE receiver<sup>1</sup>.

## 3.2 Preliminaries

We consider a single base station transmitting the sum of  $K$  users chip signals given by:

$$d(i) = s(i) \sum_{k=1}^K \mu_k c_k(i \bmod N_k) b_k(\lfloor \frac{i}{N_k} \rfloor), \quad (3.1)$$

where  $s(i)$  is the base-station dependent QPSK (long) scrambling code,  $N_k$ ,  $b_k(\lfloor \frac{i}{N_k} \rfloor)$ ,  $\mu_k$  and  $c_k(i \bmod N_k)$  are the spreading factor, the BPSK symbol sequence, the gain and the ( $N_k$ -periodic) spreading code of user  $k$ , respectively. (*mod* stands for the modulo and  $\lfloor \cdot \rfloor$  for the integer part).

In this chapter, we deal with BPSK users symbols because the Effective Spreading Code concept to be presented in the sequel is valid for BPSK symbols only. The PIC algorithms is based on the Effective Spreading Code concept. In the case of QPSK symbols, the PIC should be carried out into two distinct branches: the I branch and the Q branch.

Let the index of the user of interest be 1. The sum chip signal (3.1) is transmitted through a multipath channel whose impulse response is given by:

$$h(t) = \sum_{q=0}^{P-1} \lambda(q) p(t - \tau_q), \quad (3.2)$$

where  $p(t)$  is the total shaping filter (including the transmitter and the receiver matched filters),  $\lambda(q)$  and  $\tau_q$  are the complex gain and the delay associated with path  $q$ , and  $P$  is the total number of resolvable paths.

The complex envelope of the received signal at the desired user terminal is then given by:

$$x(t) = \sum_i d(i) h(t - iT_c) + v(t), \quad (3.3)$$

---

<sup>1</sup>To concentrate on the PIC stage, we consider only ideal MMSE equalization. It is obvious, however, that reduced-rank adaptive equalization discussed in chapter 2 can be adapted to this situation.

where  $v(t)$  is a noise process (that we will assume to be white and gaussian) and  $T_c$  is the chip period.

Assume for a while that all spreading factors  $N_k$  are equal to  $N$ . The extension to the multi-rate case will be explained later.

It is more convenient to express the received vector  $\mathbf{x}(m)$  defined by:

$$\mathbf{x}(m) = [x(mN), x(mN + 1), \dots, x(mN + N - 1)]^T$$

as a function of the transmitted chip sequence  $\mathbf{d}(m)$  defined by:

$$\mathbf{d}(m) = [d(mN), d(mN + 1), \dots, d(mN + N - 1)]^T.$$

The transmitted chip sequence is given by:

$$\mathbf{d}(m) = \mathbf{S}(m)\mathbf{C}\sqrt{\mathbf{P}}\mathbf{b}(m), \quad (3.4)$$

where  $\mathbf{S}(m)$  and  $\mathbf{P}$  are  $N \times N$  and  $K \times K$  diagonal matrices whose diagonal elements are  $s(mN), s(mN + 1), \dots, s(mN + N - 1)$  and  $\mu_1^2, \mu_2^2, \dots, \mu_K^2$  respectively,  $\mathbf{C}$  is a  $N \times K$  matrix whose columns are the spreading codes assigned to different users and  $\mathbf{b}(m) = [b_1(m), \dots, b_K(m)]^T$ .

The received signal can be written as:

$$\mathbf{x}(m) = \mathbf{H}_0\mathbf{d}(m) + \mathbf{H}_1\mathbf{d}(m - 1) + \mathbf{v}(m), \quad (3.5)$$

where

$$\mathbf{H}_0 = \begin{bmatrix} h[0] & 0 & & 0 \\ \vdots & h[0] & & \\ h[L-1] & & \ddots & \\ & & \ddots & \ddots \\ 0 & & & h[L-1] & h[0] \end{bmatrix}, \quad (3.6)$$

and

$$\mathbf{H}_1 = \begin{bmatrix} & h[L-1] & \dots & h[1] \\ & & \ddots & \vdots \\ 0 & & & h[L-1] \end{bmatrix}, \quad (3.7)$$

$h(q) \triangleq h(t)|_{t=qT_c}$ ,  $LT_c$  is the overall channel length, and  $\mathbf{v}(m) = [v(mN), v(mN+1), \dots, v(mN+N-1)]^T$ .

### 3.3 Parallel Interference Cancellation

The conventional detector of CDMA systems is the RAKE receiver. The RAKE receiver estimates the transmitted symbol of the user of interest by:

$$\hat{b}_1(m) = Dec\{\mathbf{c}_1^T \mathbf{S}^H(m) \mathbf{H}_0^H \mathbf{x}(m)\}, \quad (3.8)$$

where  $Dec$  is a decision operator that transforms the soft estimate into a hard decision. For BPSK signals we use the signum function as decision operator.

Now, suppose that we know the active users in the system (i.e. their spreading codes) along with their powers. we denote by  $\mathbf{U}$  the  $N \times (K - 1)$  matrix obtained by deleting the first column of  $\mathbf{C}$ , or equivalently:

$$\mathbf{C} = [\mathbf{c}_1 \ \mathbf{U}]. \quad (3.9)$$

Similarly, let  $\mathbf{Q}$  be the  $K - 1 \times K - 1$  matrix obtained from  $\mathbf{P}$  by deleting its first row and column.

We can obtain estimates of all the interferers by:

$$\hat{\mathbf{b}}_{2:K}(m) \triangleq \begin{bmatrix} \hat{b}_2(m) \\ \vdots \\ \hat{b}_K(m) \end{bmatrix} = Dec\{\mathbf{U}^T \mathbf{S}^H(m) \mathbf{H}_0^H \mathbf{x}(m)\}. \quad (3.10)$$

Then regenerate the Multi Access Interference (MAI)<sup>2</sup>:

$$\bar{\mathbf{x}}(m) = \mathbf{H}_0 \mathbf{S}(m) \mathbf{U} \mathbf{Q} \hat{\mathbf{b}}_{2:K}(m). \quad (3.11)$$

Then use Parallel Interference Cancellation (PIC) to cancel the effects of the interferers on the received signal, thus obtaining an *Interference Free* signal (provided that the decisions are correct)

$$\mathbf{z}(m) = \mathbf{x}(m) - \bar{\mathbf{x}}(m). \quad (3.12)$$

Finally a better estimate of the symbol of interest can be obtained by applying RAKE detection on the interference free observation  $\mathbf{z}$  by:

$$\hat{b}_1(m) = Dec\{\mathbf{c}_1^T \mathbf{S}^H(m) \mathbf{H}_0^H \mathbf{z}(m)\}. \quad (3.13)$$

Now, to apply PIC in W-CDMA we have to consider different spreading factors. We will show that the model (3.4) remains valid to some extent by using the concept of Effective Spreading Code (ESC) and virtual symbols introduced in [55].

---

<sup>2</sup>In this chapter, we neglect the InterSymbol Interference (ISI), i.e. we assume that  $\|\mathbf{H}_1 \mathbf{d}(m-1)\| \ll \|\mathbf{H}_0 \mathbf{d}(m)\|$ . This is a valid assumption especially for large spreading factors

### 3.3.1 Effective Spreading Codes and Virtual data symbols

Different spreading factors are used in W-CDMA. The orthogonal variable spreading factors (OVSF) used in W-CDMA [15] have a very important property: they are of different lengths (which may be any power of two between 4 and 256), but still, they remain orthogonal. As a consequence of this property, each user sees a set of orthogonal codes regardless of his spreading factor. This can be represented mathematically by the following condition:

$$\forall l, k \text{ such that } N_l \geq N_k,$$

$$\sum_{i=0}^{N_k-1} c_k(i)c_l(i + mN_k) = \delta(l - k),$$

for  $m = 0, 1, \dots, \frac{N_l}{N_k} - 1$ .

If we know all the spreading codes and, thus, their spreading factors (which is the case in the uplink), we can estimate all the transmitted symbols and use standard PIC to suppress interference. In the downlink however, only limited knowledge is available at the mobile unit, and standard PIC cannot be used.

It was shown in [55, 23] that the knowledge of all the active codes is not mandatory to remove interference. The lack of knowledge can be circumvented by using the concept of Effective Spreading Code (ESC) introduced in [55]. This concept can be explained as follows: any active user can be seen as a virtual user with the same spreading factor as the user of interest and with virtual symbols and effective spreading codes that depend on the actual spreading factor, the actual spreading code, and actual symbols.

To explain the ESC concept suppose that we have a user of interest (user 1) with Spreading Factor  $N$ , and three interfering users (users 2,3 and 4) with Spreading Factors  $N/2$ ,  $N/4$  and  $2N$  respectively. In one symbol period (of user 1), the spread signal corresponding to user 1 can be written in vector form as  $[b_1(1)\mathbf{c}_1^T]$  while users 2, 3 and 4 transmit  $[b_2(1)\mathbf{c}_2^T \quad b_2(2)\mathbf{c}_2^T]$ ,  $[b_3(1)\mathbf{c}_3^T \quad b_3(2)\mathbf{c}_3^T \quad b_3(3)\mathbf{c}_3^T \quad b_3(4)\mathbf{c}_3^T]$   $[b_4(1)\mathbf{c}_1^T(0 : \frac{2N}{2} - 1)]$  respectively. User 2 can be seen as a  $N$ -Spreading Factor user with virtual symbol  $b_2(1)$  and code  $\tilde{\mathbf{c}}_2^T = [\mathbf{c}_2^T \quad b_2(1)b_2(2)\mathbf{c}_2^T]$ ; user 3 can be seen as a  $N$ -Spreading Factor user with virtual symbol  $b_3(1)$  and code  $\tilde{\mathbf{c}}_3^T = [\mathbf{c}_3^T \quad b_3(1)b_3(2)\mathbf{c}_3^T \quad b_3(1)b_3(3)\mathbf{c}_3^T \quad b_3(1)b_3(4)\mathbf{c}_3^T]$  while user 4 can be seen as a  $N$ -Spreading Factor user with virtual symbol  $b_4(1)$  and code  $\tilde{\mathbf{c}}_4^T = \mathbf{c}_1^T(0 : \frac{2N}{2} - 1)$ .

In the sequel we will refer to users 2, 3 and 4 as “actual” users, and refer to users of the same spreading factor as the user of interest, i.e. users with *Effective Spreading Codes*  $\tilde{\mathbf{c}}_2$ ,  $\tilde{\mathbf{c}}_3$  and  $\tilde{\mathbf{c}}_4$  as “virtual” users. Note that the symbols are required to be BPSK for the analysis to hold.

Like the case of single spreading factor (3.4), the transmitted chip sequence can be given by:

$$\mathbf{d}(m) = \mathbf{S}(m)\tilde{\mathbf{C}}(m)\sqrt{\mathbf{P}}\mathbf{b}(m), \quad (3.14)$$

where  $\tilde{\mathbf{C}}(m)$  is the effective code matrix at time  $m$ . Note that the effective spreading codes belong to the set of Walsh Hadamard codes of the same length as the user of interest.

Madkour *et. al* [55] proposed to use this interference cancellation scheme for downlink W-CDMA. Interference Cancellation is carried out using the combining correlation values after the Maximal Ratio Combining (MRC) that combines the contribution from all the fingers. On each finger of the RAKE we estimate the received symbols of all users and decide on the active users. After MRC, interference is removed and better estimates of the user of interest transmitted symbols are obtained. We propose to combine this technique with equalization in order to obtain better estimates of virtual interferers.

### 3.4 Equalization

The RAKE receiver could be applied to (3.5) to give an estimate of the transmitted bit of the user of interest. However, Due to the multipath channel, Multiple Access Interference (MAI) is created. The RAKE receiver is no more optimal in the presence of MAI. Chip-level equalization was proposed to restore the orthogonality between the spreading codes and hence MAI is reduced [49, 48].

The most popular equalizers are the Zero Forcing (ZF) and the Minimum Mean Squared Error (MMSE) equalizers. the ZF completely eliminates MAI at the expense of enhanced noise. The MMSE, on the other hand, strives to keep a balance between MAI elimination and noise enhancement. Chip-level MMSE equalization was compared to Zero Forcing (ZF) and RAKE [49], where it was shown that the MMSE equalizer outperforms both ZF and RAKE.

In Chapter 2, we discussed chip-rate equalization. For the sake of simplicity, we work on symbol level, i.e. we try to design a MMSE equalizer matrix  $\mathbf{G}$  that acts on a single symbol interval and minimizes

$$\mathbb{E}\|\mathbf{d}(m) - \mathbf{G}^H \mathbf{x}(m)\|^2. \quad (3.15)$$

Using (3.5), the MMSE Equalizer  $\mathbf{G}$  is given by (we neglect the ISI term):

$$\mathbf{G} = (\mathbf{H}_0 \mathbf{P} \mathbf{H}_0^H + \sigma^2 \mathbf{I})^{-1} \mathbf{H}_0 \sqrt{\mathbf{P}}, \quad (3.16)$$

where  $\sigma^2$  is the noise variance. After equalization, a "better" version of the chip sequence is obtained by:

$$\hat{\mathbf{d}}(m) = \mathbf{G}^H \mathbf{x}(m). \quad (3.17)$$

Now, we can descramble and despread with the code of the user of interest to obtain an estimate of the transmitted symbol:

$$\tilde{b}_1(m) = Dec\{\mathbf{c}_1^T \mathbf{S}^H(m) \hat{\mathbf{d}}(m)\}. \quad (3.18)$$

MMSE equalization was shown to improve the performance of a plain RAKE receiver. In what follows, we propose a new blind PIC scheme for multi-rate systems. The PIC stage is preceded by a MMSE equalizer that restores code orthogonality, and thus leads to better estimates of interferers symbols than those of section 3.3.

**Remark 3.1** *The assumption  $L \ll N$  and the related expressions of the MMSE equalizer in (3.16) are made here for simplicity. The equalization being done at chip level, this assumption is clearly not necessary and the chip level equalizer implementation can be performed without such an assumption such as in Chapter 2.*

## 3.5 Improvement Through BPIC

Equalization allows to have better estimates of the user of interest symbols, and even of interferers. We propose to combine both PIC and equalization for multi-rate systems as explained below.

Let us assume first that we know the virtual codes of active users along with their powers (i.e.  $\mathbf{K}$  and  $\mathbf{U}$  are known to the receiver). We can obtain estimates of the active (virtual) users by:

$$\hat{\mathbf{b}}_{2:K}(m) \triangleq \begin{bmatrix} \hat{b}_2(m) \\ \vdots \\ \hat{b}_K(m) \end{bmatrix} = Dec\{\mathbf{U}^T \mathbf{S}^H(m) \hat{\mathbf{d}}(m)\}. \quad (3.19)$$

The interference is recalculated:

$$\bar{\mathbf{x}}(m) = \mathbf{H}_0 \mathbf{S}(m) \mathbf{U} \mathbf{Q} \hat{\mathbf{b}}_{2:K}(m). \quad (3.20)$$

Then, it is subtracted from the received signal:

$$\mathbf{z}(m) = \mathbf{x}(m) - \bar{\mathbf{x}}(m). \quad (3.21)$$

Thanks to the Interference Cancellation stage, the estimate of the user of interest can be calculated according to:

$$\hat{b}_1(m) = Dec\{\mathbf{c}_1^T \mathbf{S}^H(m) \mathbf{G}^H \mathbf{z}(m)\}. \quad (3.22)$$

Now, we discuss how to obtain the effective codes. To estimate  $\mathbf{U}$  we proceed as follows: we descramble and despread with respect to every possible (virtual) spreading code, thus obtaining soft estimates:

$$\begin{bmatrix} \tilde{b}_1 \\ \vdots \\ \tilde{b}_N \end{bmatrix} = \mathbf{C}_N^T \mathbf{S}^H(m) \hat{\mathbf{d}}(m) \quad (3.23)$$

where  $\mathbf{C}_N$  is the  $N \times N$  Hadamard matrix.

Equation (3.23) seems to be demanding in terms of calculation. However, the Fast Walsh Transform (FWT) [55, 18] can be used to calculate the output of the despreader in  $O(N \log N)$  flops per symbol duration. Furthermore, the scrambling matrix  $\mathbf{S}$  is a diagonal matrix, its multiplication with the output of the despreader is of the order of a scalar by matrix multiplication.

Depending on the estimates in (3.23), we decide on the active codes by comparing the outputs with a carefully chosen threshold (or if we know the number of users, we can take the  $K - 1$  codes that give the strongest outputs).

Concerning the power matrix  $\mathbf{Q}$ , we can estimate it by averaging the received powers over a many symbols, typically a frame duration by taking into account the structure of the OVFSF codes. In our simulations we suppose that the power matrix  $\mathbf{Q}$  is known.

Once estimates of  $\mathbf{U}$  and  $\mathbf{Q}$  are available, we carry out interference cancellation similar to equations. (3.12) and (3.13). The proposed receiver structure is shown in Fig 3.1.

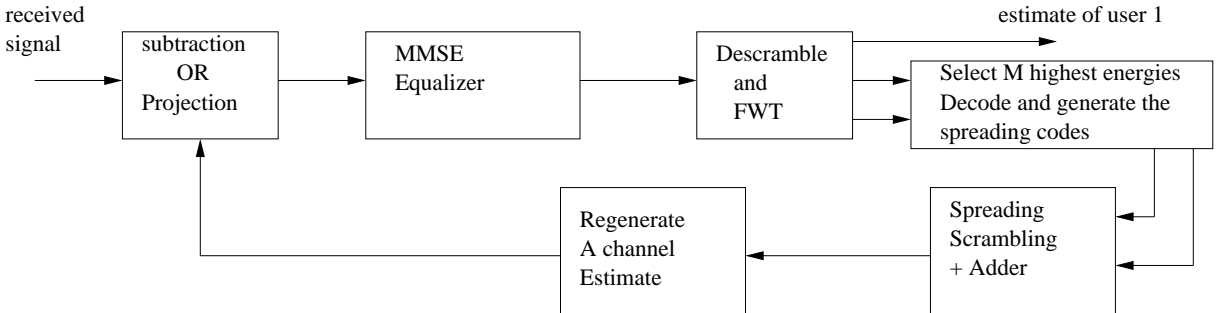


Figure 3.1: The proposed receiver structure.

**Remark 3.2** *Efficient implementations of an approximate MMSE equalizer using reduced rank filtering theory discussed in Chapter 2 can be used. For example, using a  $D$ -rank MMSE equalizer together with FWT in an adaptive scheme leads to a reasonable computational complexity of order  $O(DN + N \log(N) + LN)$  flops per symbol duration.*

**Remark 3.3** *In order to further reduce the computational complexity, it is possible to skip the second stage of PIC if not necessary. This may be the case for example in a weakly-loaded system context. To chose whether to perform the PIC or not, we can use a measure of the SINR at the output of the MMSE equalizer and activate the PIC stage only if smaller than a properly chosen threshold (target SINR).*

## 3.6 Simulation Results

### 3.6.1 Comparison of Rake and Equalized PIC for Single Rate CDMA

To evaluate the performances of the proposed algorithm, we start by considering a down-link synchronous CDMA system in which each user transmits BPSK information symbols. Those symbols are spread with a spreading code of length 32. After spreading, the resulting sum signal is scrambled using an i.i.d QPSK scrambling sequence. The chip sequence is then transmitted through a 10 path channel with a delay spread of 10 chips. The chips spaced coefficients of the propagation channel, that will be referred as channel 2 are given in table 3.1. We assume that the receivers have a priori obtained exact estimates of the powers and the spreading codes of interfering users.

Figures 3.2 and 3.3 show the performance of 4 reception schemes as a function of the SNR of each user for 31 and 15 users respectively (all users are considered with the same SNR). The considered receivers are the following: the RAKE receiver, PIC with decisions obtained using a RAKE receiver [55], MMSE equalizer followed by despreading and descrambling and finally the proposed "PIC + equalization" scheme. Note the huge gain in performance between PIC + RAKE and PIC + MMSE equalization.

We see that, for the first configuration (a fully loaded system), the MMSE equalization is better than the PIC scheme with decisions obtained by RAKE reception, while for the second configuration (a half loaded system) the PIC is better. This can be explained by the fact that for the first configuration, the RAKE receiver sees too much interference, which makes its decisions about interfering users not very reliable. In the second configuration, the system is only half loaded, and the RAKE decisions are more reliable. Consequently, IC provides better results. The equalization, on the other hand, consists of inverting the channel, and is unaffected (to some extent) by the number of users.

Delay in chips	Complex coefficient
0	-0.2607 + 0.2718i
1	0.0965 - 0.1268i
2	0.2255 + 0.1755i
3	-0.4047 + 0.2077i
4	0.3612 + 0.1438i
5	-0.2885 - 0.1588i
6	-0.2123 + 0.1985i
8	0.3661 - 0.2572i

Table 3.1: Channel 2 coefficients

### 3.6.2 Comparison of Rake and Equalized PIC for Multi-Rate CDMA

Next, We consider the case of different spreading factors. We simulate the physical channel of the downlink of UMTS-FDD with the following configuration: 4 users with a spreading factor of 16, 8 users with a spreading factor of 32, and 16 users (including the user of interest) with a spreading factor 64. We evaluate the performances of the four reception schemes in two cases: hard decisions and soft estimates. In the case of hard decisions, we assume that we know the number of active users and the powers allocated to them. If a users is detected at the output of FWT, we remove its hard decision weighted by its exact power. In the soft estimation case, we assume no knowledge about the powers, only the number of users is known. We decide for the active virtual users by taking those with the highest energies at the output of the FWT, and we subtract their soft estimates. No (hard) decision is taken since we assume no knowledge of the users powers.

The simulations results for hard decisions are shown in Fig. 3.4. We compare the BER versus the SNR per virtual user (i.e. we consider that all the users have the same chip energy which makes the energy of higher rate "actual" users greater. The virtual user

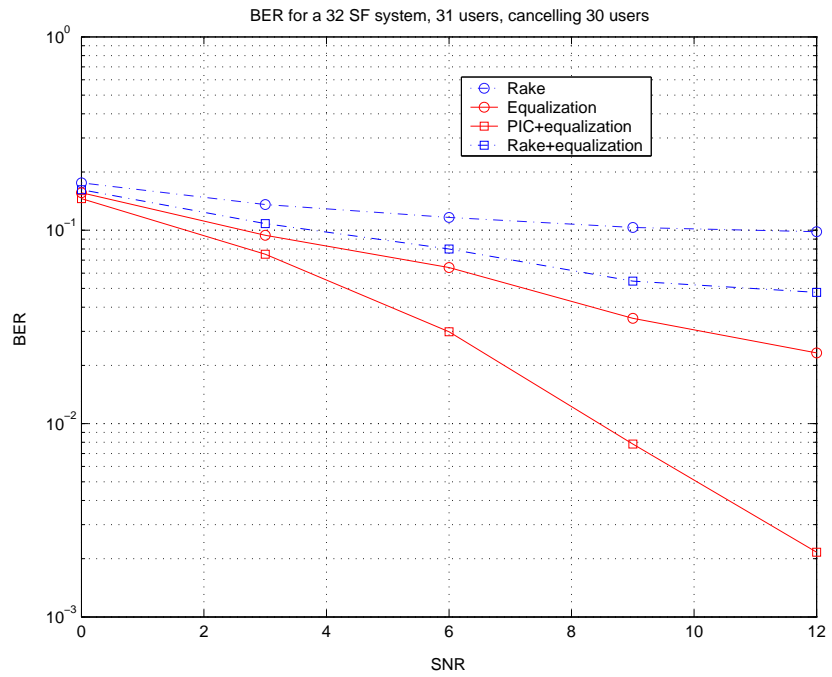


Figure 3.2: Performance of different reception schemes Vs the SNR for a loaded system.

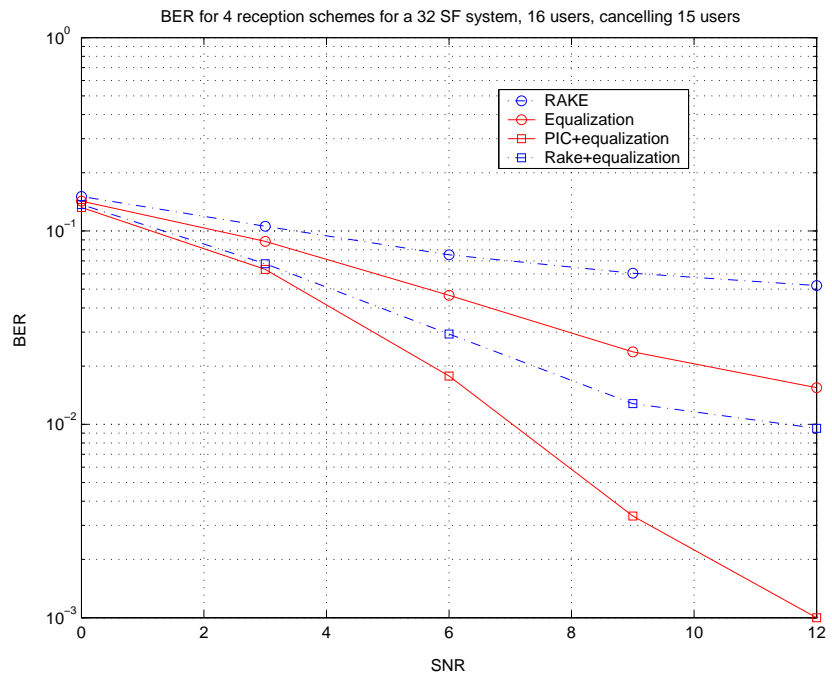


Figure 3.3: Performance of different reception schemes Vs the SNR for a half loaded system.

power, corresponding to a spreading factor of 64 is, on the other hand, considered the same). We see that the PIC schemes improve the BER in both cases (with RAKE and with equalization). The improvement after equalization, however, is much larger than that obtained after RAKE reception.

Fig. 3.5 shows the results for soft decisions versus the SNR per virtual user. In this case, RAKE reception followed by PIC deteriorates the BER performance of a plain RAKE receiver. While PIC after equalization still gives some improvement, albeit with a limited degree. This is a very important result, because this reception scheme does not require any power or active users prior knowledge.

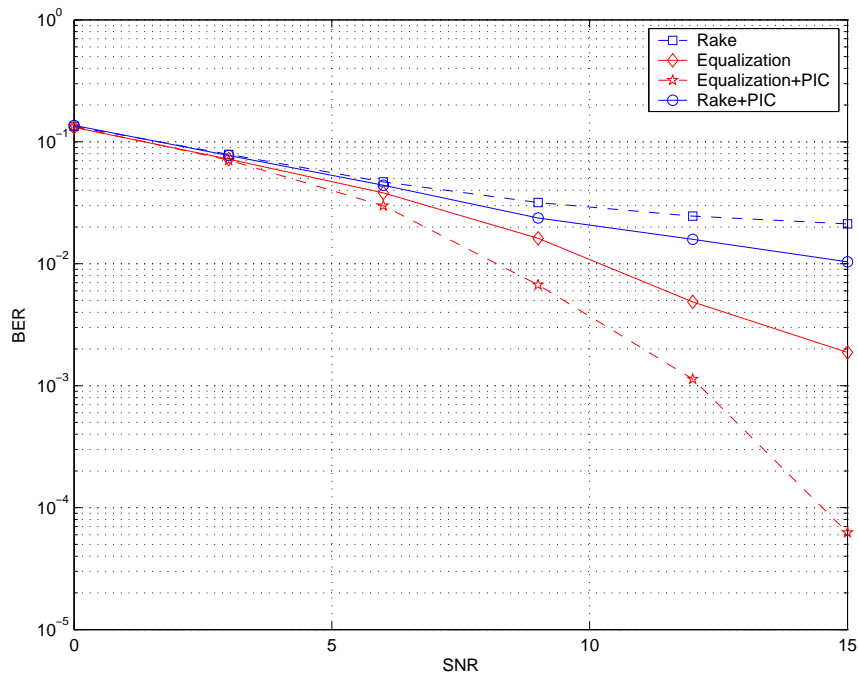


Figure 3.4: Performance of reception schemes for different SF and hard decisions.

### 3.6.3 Comparison of Blind PIC with Known Codes PIC

Finally, to assess the utility of virtual spreading codes we compare the performance of our Blind PIC method with the case where we perform classical PIC with known multi-rate codes. For this, we keep the same setting as the previous experiment and add two curves that assume perfect knowledge of multi-rate interfering codes. The first curve is for the RAKE-based PIC receiver and the second is for equalizer-based PIC receiver. The results are shown in Figure 3.6. We see that the gap between Blind PIC and known codes PIC is not negligible. But the RAKE-based PIC performs only as good as an equalizer based receiver for SNR=15dB. We remark also that the equalizer-based PIC with estimated

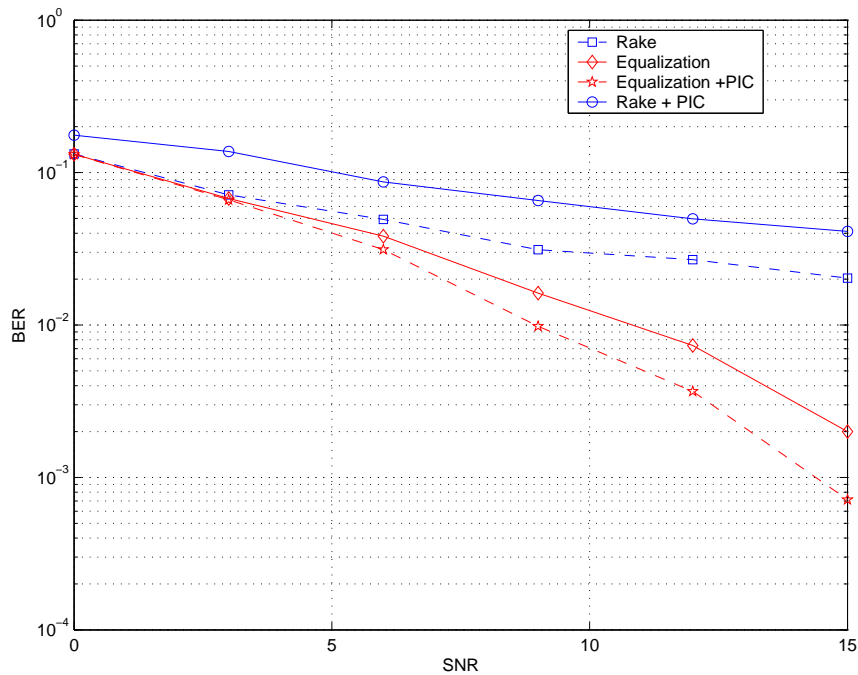


Figure 3.5: Performance of reception schemes for different SF and soft estimates.

codes performs much better than RAKE-based PIC even with exact codes knowledge. This means that the codes ignorance can be compensated by using equalization. Another very important remark is the additional diversity provided by equalization. We note that the slope of the three equalizer curves (blue dashed curves) is better than the three RAKE curves (black solid curves). This means that the RAKE curves flatten after a certain SNR and equalizer curves perform better with less knowledge. This is due to the MAI limitation of the RAKE.

### 3.7 Conclusion

In this chapter, we have proposed a new reception scheme consisting of MMSE equalization and blind Parallel Interference Cancellation (PIC). Our scheme is suitable for multi-rate CDMA systems like the 3G W-CDMA. The proposed methods takes advantage of the virtual users and Effective Spreading Codes (ESC) concepts. Simulation results show that the proposed scheme allows a significant gain with respect to RAKE-based PIC.

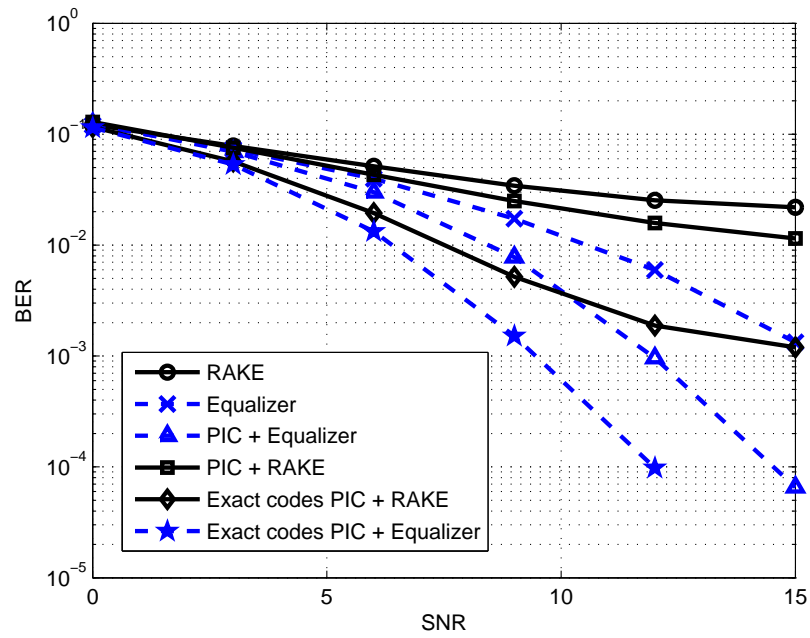


Figure 3.6: Comparison of reception schemes with and without code knowledge.

Part Two:

---

Asymptotic Performance of Downlink CDMA  
Receivers



# Chapter 4

## Asymptotic Performance of Reduced-Rank Wiener Receivers

---

### 4.1 Introduction

The performance evaluation of existing CDMA receivers has received considerable attention recently. In this course, several works were devoted to the performance study of linear detectors such as the conventional matched filter, the decorrelator, the Minimum Mean-Squared Error (MMSE) receiver, and various kinds of linear interference cancellers. The main measure of performance used in evaluating the performance is the output Signal to Interference plus Noise Ratios (SINR). The reason why the study of the whole system can be replaced by the study of the SINR is that the Multi Access Interference (MAI) at the output of these receivers can be approximated by a Gaussian distribution. This was thoroughly justified in [63] and quite recently in [78]. It was pointed out in [71] that the SINR analytical expressions depend on several parameters such as the received powers and the code sequences allocated to the users. In particular, no clear insight on the compared performance of the detectors can be obtained directly from the SINR formulas. To overcome this conceptual difficulty, it has become now classical to model the code sequences as random sequences following a certain distribution. The various SINRs can in this situation be interpreted as random variables, and it has been shown that, under certain conditions, they converge almost surely toward deterministic quantities when the spreading factor and the number of users tend to infinity with fixed ratio. The forms of these limit SINRs become more explicit, and allow to obtain more insight on the parameters that influence the performance of the detectors.

Recently, the asymptotic (large-system) performance analysis under random spreading was applied to reduced-rank receivers. The same problem arises when trying to extract useful information about the SINR  $\beta^{(N)}$  provided by a reduced-rank receiver for a given spreading factor  $N$ . More precisely, studying the convergence rate of the the rank  $n$  SINR  $\beta_n^{(N)}$  toward the full-rank SINR  $\beta^{(N)}$  is impossible<sup>1</sup>. Honig and Xiao proposed to follow the same philosophy as in [71] and showed that SINRs  $\beta_n^{(N)}$  and  $\beta^{(N)}$  tend toward deterministic limits  $\beta_n$  and  $\beta$  respectively when  $N$  and  $K$  tend to infinity with fixed ratio. They replaced the study of the rate of convergence of  $\beta_n^{(N)}$  toward  $\beta^{(N)}$  by that of  $\beta_n$  toward  $\beta$ . The study proved to be very useful in the case where all the users are allocated the same power. In this case, a recursive relation between  $\beta_{n+1}$  and  $\beta_n$  was derived. Computer simulations were carried out and it was concluded that full-rank performance was attained for moderate values of  $n$ .

In this chapter, we revisit previous work concerning the large-system performance. We start by the pioneering work of Tse and Hanly [71] on full-rank MMSE receiver performance. We then review the work of Honig and Xiao [44] on reduced-rank receivers performance under equal-powers. New results of Loubaton and Hachem [53], (see also [3]), will be discussed. These results can be used to study the asymptotic performance of reduced rank receivers corrupted by frequency selective fading channels. A paper that discusses this issue is given in the appendix E. In the next chapter we use these results to study the large-system performance of reduced-rank suboptimum receivers.

## 4.2 Asymptotic Analysis of Wiener receivers for i.i.d spread CDMA (Tse-Hanly)

We consider a CDMA system with  $K$  users and spreading factor  $N$ . The received signal  $\mathbf{y}_N$  obtained by concatenating  $N$  received chips is given by:

$$\mathbf{y}_N = \mathbf{W}_{N,K} \sqrt{\mathbf{P}_K} \mathbf{b}_K + \mathbf{v}_N \quad (4.1)$$

where  $\mathbf{b}_K$  is the  $K$  dimensional vector of transmitted symbols, the  $N \times K$  matrix  $\mathbf{W}_{N,K}$  contains in its columns the codes allocated to different users,  $\mathbf{P}_K$  is the  $K \times K$  diagonal matrix containing users powers. Finally,  $\mathbf{v}_N$  represents the AWGN matrix of variance  $\sigma^2 \mathbf{I}_N$ .

We want to retrieve the symbol transmitted by user 1. i.e.  $b_1$  the first entry of vector  $\mathbf{b}_K$ .

---

<sup>1</sup>From here on, we denote by  $n$  the rank of equalizer in the asymptotic study. The full-rank is the spreading factor  $N$ .

We let

$$\mathbf{W}_{N,K} = (\mathbf{w}_1, \mathbf{U}_{N,K}),$$

where  $\mathbf{w}_1$  is the code of user 1 and  $\mathbf{U}_{N,K}$  is the interferers code matrix. We also call  $\mathbf{Q}_K$  the interferers power matrix obtained from  $\mathbf{P}_K$  by suppressing its first row and column. i.e.

$$\mathbf{P}_K = \begin{bmatrix} p_1 & \\ & \mathbf{Q}_K \end{bmatrix}$$

In order to simplify the notations, we suppose that the power of the first user  $p_1$  is equal to 1. If we can estimate matrices  $\mathbf{W}_{N,K}$ ,  $\mathbf{P}_K$  and the noise variance  $\sigma^2$ , then the classical Wiener receiver can be used. The symbol  $b_1$  is estimated by

$$\hat{b}_1 = \mathbf{w}_1^H \mathbf{R}_N^{-1} \mathbf{y}_N \quad (4.2)$$

where

$$\mathbf{R}_N = \mathbb{E}(\mathbf{y}_N \mathbf{y}_N^H) = \mathbf{W}_{N,K} \mathbf{P}_K \mathbf{W}_{N,K}^H + \sigma^2 \mathbf{I}_N \quad (4.3)$$

is the  $N \times N$  covariance matrix of  $\mathbf{y}_N$ . In the sequel, we call  $\mathbf{R}_{I,N}$  the "Interference+Noise" matrix given by

$$\mathbf{R}_{I,N} = \mathbf{U}_{N,K} \mathbf{Q}_K \mathbf{U}_{N,K}^H + \sigma^2 \mathbf{I}_N. \quad (4.4)$$

It is classical to use the SINR as a measure of performance. The SINR of the Wiener receiver,  $\beta^{(N)}$ , is given by

$$\beta^{(N)} = \mathbf{w}_1^H \mathbf{R}_{I,N}^{-1} \mathbf{w}_1 \quad (4.5)$$

It is sometimes more convenient to use the equivalent form:

$$\beta^{(N)} = \frac{\eta^{(N)}}{1 - \eta^{(N)}} \quad (4.6)$$

where  $\eta^{(N)}$  is defined by

$$\eta^{(N)} = \mathbf{w}_1^H \mathbf{R}_N^{-1} \mathbf{w}_1. \quad (4.7)$$

The MMSE SINR (4.5) can be rewritten as:

$$\beta^{(N)} = \mathbf{w}_1^H (\mathbf{U}_{N,K} \mathbf{Q}_K \mathbf{U}_{N,K}^H + \sigma^2 \mathbf{I}_N)^{-1} \mathbf{w}_1 \quad (4.8)$$

In order to obtain a more informative expression, Tse and Hanly [71] proposed to study the behavior of  $\beta^{(N)}$  when  $N$  and  $K$  tend to infinity with fixed ratio. The code matrix  $\mathbf{W}_{N,K}$  was modelled as a random matrix with *i.i.d* entries of variance  $\frac{1}{N}$ . The hope is that due to a certain averaging effect,  $\beta$  would converge toward a simpler-to-interpret deterministic expression independent of the code matrix  $\mathbf{W}_{N,K}$ . This turns out to be the case. The following lemmas are needed in order to present the results:

**Lemma 4.1** *Let  $\mathbf{z}_N$  be a  $N \times 1$  random vector and  $\mathbf{B}_N$  a  $N \times N$  random matrix independent of  $\mathbf{z}_N$ . Assume that the elements of  $\mathbf{z}_N$  are centered i.i.d with variance  $\frac{1}{N}$ , and that  $\sup_{N \in \mathbb{N}} \|\mathbf{B}_N\| < +\infty$  where ( $\|\cdot\|$  denotes the spectral norm). Then,*

$$\mathbf{z}_N^H \mathbf{B}_N \mathbf{z}_N - \frac{\text{Trace}(\mathbf{B}_N)}{N} \rightarrow 0$$

when  $N \rightarrow \infty$  and the convergence stands for the convergence in probability.

**Lemma 4.2** *Suppose that the powers allocated to different users converge to a limit distribution with compact support  $[p_{\min}, p_{\max}]$ . Then, the empirical distribution of the eigenvalues of the interference+noise covariance matrix  $\mathbf{R}_{I,N}$ , namely the distribution with CDF  $F_N$  given by :*

$$F_N(\lambda) = \frac{\text{number of eigenvalues of } \mathbf{R}_{I,N} \text{ smaller than } \lambda}{N},$$

converges almost surely when  $N$  and  $K$  tend to  $\infty$  and  $K/N \rightarrow \alpha$  to a **deterministic** probability measure  $\omega$  with compact support  $[\delta_1, \delta_2]$ , where  $\delta_1 \geq \sigma^2$ . In other words, if we note  $(\lambda_{N,k})_{k=1, \dots, N}$  the eigenvalues of  $\mathbf{R}_{I,N}$ , then

$$\lim_{N \rightarrow \infty} \frac{1}{N} \sum_{k=1}^N \phi(\lambda_{N,k}) = \int \phi(\lambda) d\omega(\lambda) \quad (4.9)$$

for every continuous function  $\phi$  bounded on  $[\delta_1, \delta_2]$ .

Lemma 4.1 show that  $\beta^{(N)}$  and  $\frac{1}{N} \text{Trace}(\mathbf{R}_{I,N}^{-1})$  have the same asymptotic behavior. Moreover, it is clear that

$$\frac{1}{N} \text{Trace}(\mathbf{R}_{I,N}^{-1}) = \frac{1}{N} \sum_{k=1}^N (\lambda_{N,k})^{-1}$$

Now using lemma 4.2, we have:

$$\lim_{N \rightarrow \infty} \frac{1}{N} \sum_{k=1}^N (\lambda_{N,k})^{-1} = \int_{\delta_1}^{\delta_2} \frac{1}{\lambda} d\omega(\lambda) \quad (4.10)$$

the preceding equality means that  $\beta^{(N)}$  converges almost surely towards a deterministic constant

$$\beta = \int \frac{1}{\lambda} d\omega(\lambda)$$

We now introduce the Stieltjes transform  $G_\omega(z)$  of the measure  $\omega$  defined by<sup>2</sup>:

$$G_\omega(z) = \int \frac{1}{\lambda - z} d\omega(\lambda) \quad (4.11)$$

we note that  $\beta$  coincides with  $G_\omega(0)$ . In order to compute  $\beta$ , we need the following theorem proved in [65]:

**Theorem 4.1** *Let  $\mathbf{W}_{N,K}$  be a random  $N \times K$  matrix with zero mean and variance  $\frac{1}{N}$  i.i.d. entries, and let  $\mathbf{T}_N$  be a random  $N \times N$  hermitian matrix independent of  $\mathbf{W}_{N,K}$  admitting a limiting eigenvalue distribution  $\mu_T$ . Consider a deterministic diagonal  $K \times K$  matrix  $\mathbf{P}_K$  admitting a limit eigenvalue distribution  $\mu_P$  and let  $\mathbf{R}$  be the matrix defined by:*

$$\mathbf{R}_N = \mathbf{W}_{N,K} \mathbf{P}_K \mathbf{W}_{N,K}^H + \mathbf{T}_N$$

*When  $N$  and  $K$  tend toward  $+\infty$  in such a way that  $\frac{K}{N} \rightarrow \alpha$  ( $0 < \alpha < \infty$ ), then the empirical eigenvalue distribution  $\omega_N$  of  $\mathbf{R}_N$  converges weakly almost everywhere to a deterministic probability distribution  $\omega$ .  $\omega$  is characterized by its Stieltjes transform  $G_\omega(z)$  defined as the unique solution of the functional equation:*

$$G_\omega(z) = G_{\mu_T} \left( -z + \alpha \int \frac{\lambda}{1 - \lambda G_\omega(z)} d\mu_P(\lambda) \right). \quad (4.12)$$

Comparing with matrix  $\mathbf{R}_{I,N}$ , we see that matrix  $\mathbf{T}_N$  coincides with  $\sigma^2 \mathbf{I}$ . The distribution  $\mu_T$  is reduced to  $\delta(\lambda - \sigma^2)$  and the corresponding Stieltjes transform is equal to

$$G_{\mu_T}(z) = \frac{1}{\sigma^2 - z}.$$

By substituting its value in (4.12), we get that the Stieltjes transform  $G_\omega(z)$  of measure  $\omega$  is given by:

$$G_\omega(z) = \left( -z + \sigma^2 + \alpha \int \frac{\lambda}{1 - \lambda G_\omega(z)} d\mu_P(\lambda) \right)^{-1} \quad (4.13)$$

Where are now in a position to present the main result of [71]. Using (4.13) for  $z = 0$  we get the following theorem:

**Theorem 4.2** *Let  $N, K \rightarrow \infty$  such that  $\frac{K}{N} \rightarrow \alpha$ . The SINR  $\beta^{(N)}$  converges in probability to  $\beta$  the unique solution of the fixed point equation:*

---

<sup>2</sup>The Stieltjes Transform is also known as the Cauchy transform and it is equal to  $-\pi$  times the Hilbert transform when defined on the real axis. As with the Fourier transform, there is no universal agreement on its definition, as sometimes the Stieltjes transform is defined as  $G_\omega(-z)$  or  $-G_\omega(z)$ [72].

$$\beta = \frac{1}{\sigma^2 + \alpha \int_0^\infty I(\lambda, \beta) d\mu_P(\lambda)} \quad (4.14)$$

where

$$I(p, x) = \frac{p}{1 + px}$$

It is interesting to recall how this result was interpreted in [71]. Heuristically, the result says that in a large system,

$$\beta^{(N)} \approx \frac{1}{\sigma^2 + \frac{1}{N} \sum_{k=2}^K I(p_k, \beta^{(N)})} \quad (4.15)$$

For a target SINR  $\beta$ , the term  $I(p_k, \beta) = \frac{p_k}{1+p_k\beta}$  can be interpreted as the variance of the interference produced by user  $k$  on the output of the MMSE receiver. This term is called in [71] the *Effective Interference* of user  $k$  at target SINR  $\beta$ . The factor  $\frac{1}{N}$  can be interpreted as the spreading gain on the interference produced by user  $k$ . Moreover, the total multiuser interference can be decoupled into a sum of interference terms from each of the interfering users

### 4.3 Asymptotic Analysis of Reduced Rank Receivers for i.i.d spread CDMA (Honig-Xiao)

As discussed in chapter 2, the covariance matrix  $\mathbf{R}_N$  has to be inverted in order to implement the Wiener receiver. When the spreading factor is high, this may be very costly. Reduced-rank filtering solves this problem. We estimate  $b_1$  by its projection on the  $n$ -dimensional space  $n < N$  produced by the components of  $\mathbf{y}_{n,N} = \mathbf{K}_n^H \mathbf{y}_N$  where  $\mathbf{K}_n$  is the Krylov-subspace matrix defined by:

$$\mathbf{K}_n = [\mathbf{w}_1, \mathbf{R}_{I,N} \mathbf{w}_1, \dots, \mathbf{R}_{I,N}^{n-1} \mathbf{w}_1] \quad (4.16)$$

As pointed out in [44], the matrix  $\mathbf{R}_{I,N}$  can be replaced by  $\mathbf{R}_N$  in expression (4.16) since the subspace generated by  $\mathbf{K}_n(\mathbf{R}_{I,N}, \mathbf{w}_1)$  is identical to that generated by  $\mathbf{K}_n(\mathbf{R}_N, \mathbf{w}_1)$ . However, the form (4.16) is more convenient for the analysis to be presented.

The symbol of interest is estimated by a reduced-rank filter of rank  $n$  as:

$$\hat{b}_{1,n} = \mathbf{w}_1^H \mathbf{K}_n (\mathbf{K}_n^H \mathbf{R}_N \mathbf{K}_n)^{-1} \mathbf{K}_n^H \mathbf{y}_N. \quad (4.17)$$

The SINR  $\beta_n^{(N)}$  associated to the rank- $n$  reduced-rank filter is given by:

$$\beta_n^{(N)} = \mathbf{w}_1^H \mathbf{K}_n (\mathbf{K}_n^H \mathbf{R}_{I,N} \mathbf{K}_n)^{-1} \mathbf{K}_n^H \mathbf{w}_1 \quad (4.18)$$

As for,  $\beta^{(N)}$ , the reduced-rank SINR  $\beta_n^{(N)}$  can be written as

$$\beta_n^{(N)} = \frac{\eta_n^{(N)}}{1 - \eta_n^{(N)}} \quad (4.19)$$

where  $\eta_n^{(N)}$  is now defined by

$$\eta_n^{(N)} = \mathbf{w}_1^H \mathbf{K}_n (\mathbf{K}_n^H \mathbf{R}_N \mathbf{K}_n)^{-1} \mathbf{K}_n^H \mathbf{w}_1 \quad (4.20)$$

Reduced-rank receivers are useful if close to optimal performance is obtained for moderate values of the rank  $n$ . In terms of the SINR, this would mean that  $\beta_n^{(N)} \approx \beta^{(N)}$  for  $n \ll N$ . It is very difficult to extract any conclusion about the convergence rate by looking at the expressions of  $\beta^{(N)}$  and  $\beta_n^{(N)}$ .

Honig and Xiao proposed to replace the study of the convergence of  $\beta_n^{(N)}$  toward  $\beta^{(N)}$  by that of the limiting values  $\beta_n$  toward  $\beta = \int_{\delta_1}^{\delta_2} \frac{1}{\lambda} d\sigma(\lambda)$ . (see [70] for a simpler proof). They have established that if  $\mathbf{P}_K = \mathbf{I}_K$  ( the same power is allocated to all users), then  $\beta_{n+1}$  can be written as a function of  $\beta_n$ . The main result of [44] is the following theorem:

**Theorem 4.3** *As  $K = \alpha N \rightarrow \infty$ , the output SINR of the rank- $n$  reduced-rank MMSE receiver converges in probability to the limit  $\beta_n$  which satisfies:*

$$\beta_{n+1} = \frac{1}{\sigma^2 + \alpha \frac{1}{1+\beta_n}} \quad (4.21)$$

where  $\beta_0 = 0$  and  $\beta_1 = \frac{1}{\sigma^2 + \alpha}$  is the large-system limit of the matched filter.

The importance of equation (4.21) resides in the fact that it is independent of  $n$ . Thus, the speed of convergence of  $\beta_n$  towards  $\beta$  can be very fast and can be evaluated easily by simulations. Honig and Xiao noticed that  $\beta_n$  is very close to  $\beta$  as far as  $n \geq 8$ . This means that one can obtain performances very close to the optimal Wiener filter without the need to invert the covariance matrix.

The Honig-Xiao recurrence relation (4.21) is closely related to the Tse-Hanly fixed-point equation (4.14). In fact, for a uniform power distribution ( $\mathbf{P} = \mathbf{I}_K$ ), formula (4.14) boils down to:

$$\beta = \frac{1}{\sigma^2 + \alpha \frac{1}{1+\beta}} \quad (4.22)$$

Now, looking at the Honig-Xiao formula (4.21), we note that  $\beta_{n+1} = \beta_n$  when  $n \rightarrow \infty$ . Furthermore, the reduced rank SINR  $\beta_n$  converges to the full-rank SINR  $\beta$  when  $n \rightarrow \infty$ .

replacing  $\beta_{n+1}$  and  $\beta_n$  by  $\beta$  in (4.21) we obtain (4.22)<sup>3</sup>.

In the case of non-equal powers, Honig and Xiao claimed that it was not possible to obtain a recurrence relation like (4.21). They provided an *approximate* relation very similar to (4.14):

$$\beta_{n+1} \approx \frac{1}{\sigma^2 + \alpha \int_0^\infty \frac{\lambda}{1+\lambda\beta_n} d\mu_P(\lambda)} \quad (4.23)$$

Honig and Xiao claimed that this relation works quiet well for most of the cases but remains an approximation. they did not specify, however, the cases for which it works.

### Illustration of Tse-Hanly and Honig-Xiao formulas

In what follows, we check whether the asymptotic analysis discussed allows to understand real-life systems (with finite spreading factors and number of users). For this, we simulate a CDMA system with a spreading factor  $N = 64$  and  $K = 32$  users (which corresponds to  $\alpha = 0.5$ ). All users are received with power=1, and  $\sigma^2$  is fixed such that the SNR ( $E_b/N_0$ ) per user is equal to 10dB. We plot the (empirical) SINR provided by a reduced-rank Wiener receiver under random spreading. We also plot the (asymptotic) theoretical SINR given by the Honig-Xiao Formula (4.21). In the same figure we plot the SINR provided by a (full-rank) Wiener receiver and the corresponding (asymptotic) theoretical SINR given by the Tse-Hanly Formula (4.14). the results are shown in figure 4.3.

We remark that even for moderate values of the spreading factor  $N$ , the asymptotic evaluation allows to approximate very well the empirical results (the fit is quasi-total for  $N = 256$ ). We also remark that the reduced-rank SINR converges very rapidly to the full-rank SINR. This confirms the utility of reduced-rank filtering based on the Krylov subspace. The convergence rate is the same for finite-values and asymptotic-values of  $N$  and  $K$ , this means that the rank  $n$  required for a given performance does not scale with  $N$  and  $K$ . This is a very important result since this claim is not true for reduced-rank techniques based on other methods (other subspaces) like Principal Component (PC) [44].

## 4.4 New results of Loubaton-Hachem

Using a more general model than Honig and Xiao, Loubaton and Hachem [53] proposed to study "analytically" the convergence of  $\beta_n$  towards  $\beta$  even when the powers allocated to the different users are not equal. Consider the following model:

$$\mathbf{y}_N = \mathbf{h}_N b_1 + \mathbf{x}_N, \quad (4.24)$$

---

<sup>3</sup>Amazingly enough, if we want to find the SINR  $\beta$  of the Tse-Hanly formula (4.22) we will use the recurrence relation of (4.21) and take  $\beta_{n+1}$  after a sufficient number of iteration as a solution (i.e. when we notice that  $\beta_{n+1} \approx \beta_n$ )

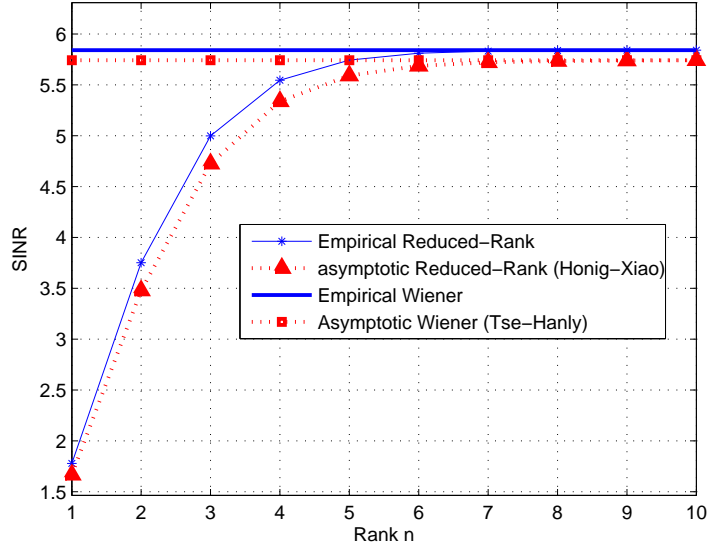


Figure 4.1: Simulated and Asymptotic SINR for reduced-rank and full-rank receivers.

where  $\mathbf{y}_N$  is the received  $N \times 1$  signal,  $b_1$  is the unit-variance scalar signal to be estimated,  $\mathbf{h}_N$  is the signature of the desired symbol and  $\mathbf{x}_N$  is a signal decorrelated from  $b_1$  representing interference and/or background noise but not necessarily resulting from i.i.d spreading of interfering users. The  $N \times N$  covariance matrix of  $\mathbf{x}_N$  is denoted  $\mathbf{R}_{I,N}$  and will be assumed invertible.  $\mathbf{R}_N = \mathbf{h}_N \mathbf{h}_N^H + \mathbf{R}_{I,N}$  is the received signal  $\mathbf{y}_N$  covariance matrix.

It is clear that model (4.24) is a more general case of model (4.1). In fact, if we let  $\mathbf{h}_N = \mathbf{w}_1$  and

$$\mathbf{x}_N = \mathbf{U}_{N,K} \sqrt{\mathbf{Q}_K} \mathbf{b}_I + \mathbf{v}_N$$

where  $\mathbf{b}_K = [b_1 \ \mathbf{b}_I^T]^T$ , then model (4.1) appears as a particular case of (4.24). The Wiener receiver estimates the symbol  $b_1$  by:

$$\tilde{b}_1 = \mathbf{h}_N^H \mathbf{R}_N^{-1} \mathbf{y}_N. \quad (4.25)$$

The output SINR provided corresponding to the Wiener receiver is given by the standard expression

$$\beta^{(N)} = \mathbf{h}_N^H \mathbf{R}_N^{-1} \mathbf{h}_N. \quad (4.26)$$

The  $n^{\text{th}}$  Krylov matrix associated to the pair  $(\mathbf{R}_{I,N}, \mathbf{h}_N)$  is given by:

$$\mathbf{K}_n = [\mathbf{h}_N, \mathbf{R}_{I,N} \mathbf{h}_N, \dots, \mathbf{R}_{I,N}^{n-1} \mathbf{h}_N].$$

The rank- $n$  reduced-rank receiver estimates  $b_1$  by:

$$\tilde{b}_{1,n} = \mathbf{h}_N^H \mathbf{K}_n (\mathbf{K}_n^H \mathbf{R}_N \mathbf{K}_n)^{-1} \mathbf{K}_n^H \mathbf{y}_N. \quad (4.27)$$

As for,  $\beta^{(N)}$ , the reduced-rank SINR  $\beta_n^{(N)}$  provided by this receiver is given by:

$$\beta_n^{(N)} = \mathbf{h}_N^H \mathbf{K}_n (\mathbf{K}_n^H \mathbf{R}_{I,N} \mathbf{K}_n)^{-1} \mathbf{K}_n^H \mathbf{h}_N. \quad (4.28)$$

In order to present the results, we need to formulate the following assumptions:

**Assumption 4.1** *We assume that for each  $k$ ,  $s_k^{(N)} = \mathbf{h}_N^H \mathbf{R}_{I,N}^k \mathbf{h}_N$  converges when  $N \rightarrow +\infty$  to a finite limit  $s_k$ , and that  $s_0 = 1$ .*

It is easily seen that  $\beta_n^{(N)}$  is equal to

$$(s_0^{(N)}, \dots, s_{n-1}^{(N)}) \begin{pmatrix} s_1^{(N)} & s_2^{(N)} & \dots & s_n^{(N)} \\ s_2^{(N)} & s_3^{(N)} & \dots & s_{n+1}^{(N)} \\ \vdots & \vdots & \vdots & \vdots \\ s_n^{(N)} & s_{n+1}^{(N)} & \dots & s_{2n-1}^{(N)} \end{pmatrix}^{-1} \begin{pmatrix} s_0^{(N)} \\ \vdots \\ s_{n-1}^{(N)} \end{pmatrix} \quad (4.29)$$

Assumption 4.1 thus implies that for each  $n$ ,  $\beta_n^{(N)}$  converges to the quantity  $\beta_n$  obtained by replacing  $(s_k^{(N)})_{k=1,2n-1}$  in (4.29) by sequence  $(s_k)_{k=1,2n-1}$ . Moreover,  $\mathbf{K}_n^H \mathbf{K}_n$  and  $\mathbf{K}_n^H \mathbf{R}_{I,N} \mathbf{K}_n$  are positive Hankel matrices converging to the Hankel matrices  $(s_{k+l})_{(k,l)=0,\dots,n-1}$  and  $(s_{k+l+1})_{(k,l)=0,\dots,n-1}$ . Therefore, matrices  $(s_{k+l})_{(k,l)=0,\dots,n-1}$  and  $(s_{k+l+1})_{(k,l)=0,\dots,n-1}$  are also positive. Using well known results (see e.g. [16]), there exists a probability measure  $\omega$  such that

$$s_k = \int_0^\infty \lambda^k d\omega(\lambda). \quad (4.30)$$

**Assumption 4.2** *Measure  $\omega$  is carried by an the interval  $[\delta_1, \delta_2]$ , and is thus uniquely defined by (4.30) (see [16]). Moreover,  $\omega$  is absolutely continuous, and its density is almost surely strictly positive on  $[\delta_1, \delta_2]$ .*

**Assumption 4.3** *There exist  $D_1 > 0$  and  $D_2 > 0$  such that  $\|\mathbf{R}_{I,N}^{-1}\| \leq D_1$  and  $\|\mathbf{R}_{I,N}\| \leq D_2$  for each  $N$ .*

The assumption that measure  $\omega$  is absolutely continuous (Assumption 4.2) implies in particular that  $\alpha$  defined as the limit of  $\frac{K}{N}$  is greater than 1. otherwise, the limit distribution  $\omega$  has clearly a mass at point  $\sigma^2$ . The case  $\frac{K}{N} < 1$  can be treated using a slightly different approach explained in Remark 4.2.

Under the above assumptions,  $\beta^{(N)} = \mathbf{h}_N \mathbf{R}_{I,N}^{-1} \mathbf{h}_N$  can be shown to converge to  $\beta = \int_{\delta_1}^{\delta_2} \frac{1}{\lambda} d\omega(\lambda)$ . Therefore, we have to evaluate the convergence rate of:

$$\beta_n = (s_0, \dots, s_{n-1}) \begin{pmatrix} s_1 & s_2 & \dots & s_n \\ s_2 & s_3 & \dots & s_{n+1} \\ \vdots & \vdots & \vdots & \vdots \\ s_n & s_{n+1} & \dots & s_{2n-1} \end{pmatrix}^{-1} \begin{pmatrix} s_0 \\ \vdots \\ s_{n-1} \end{pmatrix}$$

towards  $\beta = \int_{\delta_1}^{\delta_2} \frac{1}{\lambda} d\omega(\lambda)$ .

The analysis of this kind of convergence is a classical mathematical problem. Let us suppose that the measure  $\omega$  is absolutely continuous and that its density is almost surely positive in  $[\delta_1, \delta_2]$ . We mention that the Stieltjes transform is analytic in  $\mathbb{C} - [\delta_1, \delta_2]$ , and can be developed in the neighborhood of the infinity as

$$G_\sigma(z) = - \sum_{k=0}^{\infty} \frac{s_k}{z^{k+1}}$$

As mentioned previously, it is important to recall that the SINR  $\beta$  of the Wiener filter coincides with  $G_\omega(0)$ . We define in the space of square-integrable function with respect to  $\omega$  the scalar product

$$\langle f(\lambda), g(\lambda) \rangle = \int_{\delta_1}^{\delta_2} f(\lambda)g(\lambda)d\omega(\lambda) .$$

We also define the family  $(p_k(\lambda))_{k \geq 0}$  of orthonormal polynomials obtained by using the Gram-Schmidt orthogonalization procedure of the functions  $1, \lambda, \lambda^2, \dots, \lambda^k, \dots$ . Polynomials  $(p_k)_{k \geq 0}$  are called orthogonal polynomials of the first kind. The polynomials of the second kind  $(q_k)_{k \geq 0}$  are defined from the polynomials of the first kind  $(p_k)_{k \geq 0}$  by the following recurrence equation

$$q_k(\lambda) = \int_{\delta_1}^{\delta_2} \frac{p_k(\lambda) - p_k(u)}{\lambda - u} d\omega(u) \quad (4.31)$$

It is known that the sequence of functions  $(-\frac{q_n(z)}{p_n(z)})_{n \geq 0}$  converges uniformly in every compact support of  $\mathbb{C} - [\delta_1, \delta_2]$  toward  $G_\omega(z)$  (see for example [16]). The link with the analysis of the rate of convergence of  $\beta_n$  towards  $\beta$  resides in the following proposition:

**Proposition 4.1** *The SINR  $\beta_n$  of a reduced-rank filter of rank  $n$  coincides with  $-\frac{q_n(0)}{p_n(0)}$ .*

By using useful results of [68], [19] et [67], we can prove the following result:

**Theorem 4.4** *Let  $\mu > 1$  and  $\phi < 1$  be defined by  $\mu = \frac{1+\frac{\delta_1}{\delta_2}}{1-\frac{\delta_1}{\delta_2}}$  and  $\phi = \frac{1}{\mu+\sqrt{\mu^2-1}}$ . Then, there exist 2 strictly positive constants  $A$  and  $B$  such that*

$$A\phi^{2n} \leq |\beta - \beta_n| \leq B\phi^{2n} \quad (4.32)$$

for  $n$  large enough.

This result is derived from the fact that:

$$|p_n(0)| \sim C\phi^{-n} \text{ if } n \rightarrow \infty \quad (4.33)$$

where  $C$  is a constant (see for example [68]), and from the inequality:

$$\frac{1}{\delta_2}|p_n(0)|^{-2} \leq |\beta - \beta_n| \leq \frac{1}{\delta_1}|p_n(0)|^{-2} \text{ for every } n \quad (4.34)$$

(see for example [67] and [19]). Under these conditions, the constants  $A$  and  $B$  are of the order of  $\frac{1}{C^2\delta_2}$  et  $\frac{1}{C^2\delta_1}$  respectively, if  $n$  is chosen so that  $p_n(0)$  is sufficiently close to  $C\phi^{-n}$ .

**Remark 4.1** *As  $\delta_1 \geq \omega^2 > 0$ ,  $\mu$  is strictly greater than 1, and the factor  $\phi$  is strictly smaller than 1. Thus,  $\beta_n$  converges locally exponentially towards  $\beta$  at a speed that depends on the support  $[\delta_1, \delta_2]$  of measure  $\omega$ . It is interesting to remark that the factor that can slow down the convergence rate is the proximity from zero of the ratio  $\frac{\delta_1}{\delta_2}$ . In order to express this in terms more significant parameters, we note that the condition  $\alpha \geq 1$  implies that  $\delta_1 \geq p_{min}(\sqrt{\alpha} - 1)^2 + \sigma^2$  and that  $\delta_2 \leq p_{max}(\sqrt{\alpha} + 1)^2 + \sigma^2$ . Furthermore, if all the users have the same power (i.e.  $p_{min} = p_{max} = 1$ ), then  $\delta_1$  is equal to  $(\sqrt{\alpha} - 1)^2 + \sigma^2$  and  $\delta_2 = (\sqrt{\alpha} + 1)^2 + \sigma^2$ . consequently, the factors that can slow down the speed of convergence of  $\beta_n$  towards  $\beta$  are i) a weak noise, ii) a dispersed distribution of powers and iii) a factor  $\alpha$  close to 1.*

The theorem 4.4 is a local convergence result. This means that inequality (4.34) holds for values of  $n$  for which  $p_n(0)$  is close to  $C\phi^{-n}$ . In the case of Honig-Xiao (equal powers case), we have  $p_{min} = p_{max} = 1$ . It is possible in this case to calculate explicitly the limit distribution  $\omega$  (which coincides with the Marchenko-Pastur distribution), and the corresponding orthogonal polynomials. We can thus deduce that (see [53])

$$p_n(0) = r_n(0) + \frac{1}{\sqrt{\alpha}}r_{n-1}(0) \quad (4.35)$$

where  $r_n(0)$  is given by

$$r_n(0) = (-1)^n \frac{(\phi^{-(n+1)} - \phi^{(n+1)})}{(\phi^{-1} - \phi)} \quad (4.36)$$

Consequently,  $|p_n(0)| \simeq C\phi^{-n}$  if  $n \rightarrow \infty$  with  $C = (1 - \frac{\phi}{\alpha})$ . Furthermore, It is easy to see that  $|p_n(0)|$  is close from  $C\phi^{-n}$  as far as  $\phi^{2n}$  is negligible with respect to 0. We can thus perfectly predict the values of  $n$  for which the behavior of  $|\beta - \beta_n|$  is controlled by inequality (4.34).

**Remark 4.2** *The full-rank SINR  $\beta^{(N)}$  can be written as:*

$$\beta^{(N)} = \frac{\eta^{(N)}}{1 - \eta^{(N)}} \quad (4.37)$$

where  $\eta^{(N)}$  is defined by

$$\eta^{(N)} = \mathbf{h}_N^H \mathbf{R}_N^{-1} \mathbf{h}_N \quad (4.38)$$

while the SINR  $\beta_n^{(N)}$  provided by a reduced-rank receiver of rank  $n$  can be written as:

$$\beta_n^{(N)} = \frac{\eta_n^{(N)}}{1 - \eta_n^{(N)}} \quad (4.39)$$

where  $\eta_n^{(N)}$  is now defined by

$$\eta_n^{(N)} = \mathbf{h}_N^H \mathbf{K}_n (\mathbf{K}_n^H \mathbf{R}_N \mathbf{K}_n)^{-1} \mathbf{K}_n^H \mathbf{h}_N. \quad (4.40)$$

Since  $\beta_n^{(N)}$  and  $\beta^{(N)}$  are functions of  $\eta_n^{(N)}$  and  $\eta^{(N)}$  respectively, we can study the convergence of  $\eta_n^{(N)}$  toward  $\eta^{(N)}$ . In fact, if we define:  $s_k^{(N)} = \mathbf{h}_N^H \mathbf{R}_N^k \mathbf{h}_N$  and assume that, for each  $k$ ,  $s_k^{(N)}$  converges when  $N \rightarrow +\infty$  to a finite limit  $s_k$  (like Assumption 4.1), then there exists a probability measure  $\omega$  such that

$$s_k = \int_0^\infty \lambda^k d\omega(\lambda). \quad (4.41)$$

$\eta_n^{(N)}$  converges when  $N, K \rightarrow +\infty$  with  $\frac{K}{N} \rightarrow \alpha$  to a deterministic limit  $\eta_n$  given by:

$$\eta_n = (s_0, \dots, s_{n-1}) \begin{pmatrix} s_1 & s_2 & \dots & s_n \\ s_2 & s_3 & \dots & s_{n+1} \\ \vdots & \vdots & \vdots & \vdots \\ s_n & s_{n+1} & \dots & s_{2n-1} \end{pmatrix}^{-1} \begin{pmatrix} s_0 \\ \vdots \\ s_{n-1} \end{pmatrix}$$

while  $\eta^{(N)}$  converges to  $\eta$  given by:

$$\int_{\delta_1}^{\delta_2} \frac{1}{\lambda} d\omega(\lambda).$$

By using similar arguments, we can find a relation similar to (4.32) that controls the behavior of  $|\eta - \eta_n|$ . We conclude then that the convergence of  $\eta_n$  towards  $\eta$  is locally exponential. It is noteworthy that, in this case, the restriction  $\frac{K}{N} > 1$  is no more required. The study of  $\eta_n$  is more convenient for the analysis to be presented in Chapter 5.

## 4.5 Conclusion

In this chapter, previous work on the asymptotic performance of Wiener receivers [71] and reduced-rank Wiener receivers [44] under random spreading was discussed. New results [53, 3] that are more general were also presented. The results of [53] will be used in the next chapter to discuss the asymptotic performance of suboptimum reduced-rank CDMA Wiener receivers. The study of optimum-reduced rank receivers corrupted by frequency selective fading channels can be carried out using the same results. In appendix E, a paper that was published in Eusipco 2004 and discusses this issue is presented.

## Chapter 5

# Asymptotic Performance of Reduced-Rank Equalization in CDMA Downlink

---

In long-code downlink CDMA systems, the receiver is aware of the code allocated to the user of interest, but not of the codes allocated to the other users. The covariance matrix of the observation is therefore unknown nor it can be estimated at the receiver side. Therefore, conventional MMSE receivers cannot be used in this context. Chip rate MMSE equalization followed by despreading was proposed as an alternative ([32], [49], [51], [45]). The corresponding receiver is usually called the suboptimum Wiener receiver because, unlike the optimum Wiener receiver, it has no knowledge about the interfering users codes. For the same reasons as in the short-code case, the chip rate MMSE equalization step can be done in a reduced-rank fashion.

Since the suboptimum Wiener receiver (both full-rank and reduced-rank) are more recent than their optimum counterparts, their large system asymptotic performance analysis has received much less attention. The suboptimum MMSE receiver was analyzed in [25] in the context of certain random orthogonal code matrices. However, to our knowledge, the asymptotic performance of reduced-rank suboptimum receivers was not performed yet.

In this chapter, we study the performance of reduced-rank suboptimum CDMA downlink Wiener receivers consisting of a reduced-rank equalizer MMSE equalizer followed by despreading. We use the results of Loubaton-Hachem [53] to show that the convergence of the reduced-rank SINR toward the full-rank SINR is locally exponential. We provide simulation results where we highlight the fact that for very moderate values of the rank

$n$  the output reduced-rank SINR can be very close to the full-rank SINR.

## 5.1 Reduced-Rank Equalization for CDMA Downlink

We consider a downlink CDMA system. A base station transmits  $K$  symbol sequences  $(b_k)_{k=1,\dots,K}$  to  $K$  mobile units of the corresponding cell. It is assumed that the number of users  $K$  is smaller than the spreading factor  $N$ . Motivated by the specifications of the downlink of the Third Generation (3G) mobile communication systems (UMTS) [14], we assume that the spreading codes change from one symbol to another, and that at time  $m$ , code matrix  $\mathbf{W}_{N,K}(m)$  is obtained as follows

$$\mathbf{W}_{N,K}(m) = \mathbf{S}(m)\mathbf{C}_{N,K} \quad (5.1)$$

where:

- $\mathbf{C}_{N,K}$  is a time-invariant orthogonal  $N \times K$  matrix obtained by extracting  $K$  columns from a  $N \times N$  Walsh-Hadamard matrix (this implies that each entry of  $\mathbf{C}_{N,K}$  is equal to  $\pm \frac{1}{\sqrt{N}}$ ),
- $\mathbf{S}(m) = \text{diag}(s_1(m), \dots, s_N(m))$  is a time-varying diagonal matrix whose entries  $(s_l(m))_{l=1,\dots,N}$  are QPSK distributed ( $s_l(m) \in \{\pm \frac{1}{\sqrt{2}} + \pm i \frac{1}{\sqrt{2}}\}$ ) and represent the long scrambling code of the cell under consideration.

We remark that  $\mathbf{W}_{N,K}(m)^H \mathbf{W}_{N,K}(m) = \mathbf{I}_K$  for each  $m$ . We take into account the effect of the propagation channel between the base station and the mobile of interest (say mobile 1), and we denote by

$$h(z) = \sum_{l=0}^L h_l z^{-l}$$

its chip rate discrete-time equivalent transfer function.  $h(z)$  is assumed to be known at the receiver side, and is normalized in such a way that  $\sum_{l=0}^L |h_l|^2 = 1$ .  $(d(i))_{i \in \mathbb{Z}}$  represents the chip sequence transmitted by the base station. Therefore, the received signal  $(y(i))_{i \in \mathbb{Z}}$  sampled at the chip rate can be written as

$$y(i) = \sum_{l=0}^L h_l d(i-l) + v(i) \quad (5.2)$$

where  $v$  is an additive white Gaussian noise of variance  $\sigma^2$ . It is more convenient to express this in matrix form. Let

$$\mathbf{d}_N(m) = (d(mN), d(mN+1), \dots, d(mN+N-1))^T$$

be the transmitted chip-vector sequence at symbol instant  $m$ .  $\mathbf{d}_N(m)$  is of course given by

$$\mathbf{d}_N(m) = \mathbf{W}_{N,K}(m)\mathbf{b}_K(m) \quad (5.3)$$

where  $\mathbf{b}_K(m) = (b_1(m), \dots, b_K(m))^T$  represents the  $K$  symbols transmitted at time  $m$  by the base station. We put  $\mathbf{y}_N(m) = (y(mN), y(mN + 1), \dots, y(mN + N - 1))^T$ . Then, (5.2) is equivalent to

$$\mathbf{y}_N(m) = \mathbf{H}_{0,N}\mathbf{d}_N(m) + \mathbf{H}_{1,N}\mathbf{d}_N(m - 1) + \mathbf{v}_N(m) \quad (5.4)$$

where

$$\mathbf{H}_{0,N} = \begin{bmatrix} h[0] & 0 & & 0 \\ \vdots & h[0] & & \\ h[L-1] & & \ddots & \\ & & & \ddots \\ 0 & & & h[L-1] & h[0] \end{bmatrix}$$

and

$$\mathbf{H}_{1,N} = \begin{bmatrix} & h[L-1] & \dots & h[1] \\ & & \ddots & \vdots \\ & & & h[L-1] \\ 0 & & & \end{bmatrix}$$

In contrast with the uplink context, the mobile of interest is not supposed to be aware of the codes allocated to the other users of the cell. Moreover, the covariance matrix cannot be estimated consistently using the cyclostationarity of the received signal like the short-code CDMA case. It is therefore impossible to implement neither the optimum Wiener filter nor reduced-rank Wiener filters since they are based on the complete knowledge of the code matrix or the covariance matrix. To overcome this difficulty, chip-rate equalization prior to despreading was proposed. Chip-rate equalization allows to partially restore the orthogonality between the spreading codes, thus reducing Multiple Access Interference (MAI) (see e.g. [32], [45], [48], [49], [51]). More precisely, chip sequence  $(d(i))_{i \in \mathbb{Z}}$  is estimated by a filtered version  $\hat{d}(i) = [g(z)]y(i)$  of the received signal. If the action of filter  $g(z)$  compensates the effect of channel  $h(z)$ , vector  $\hat{\mathbf{d}}_N(m) = (\hat{d}(mN), \dots, \hat{d}(mN + N - 1))^T$  can nearly be written as

$$\hat{\mathbf{d}}_N(m) \simeq \mathbf{W}_{N,K}(m)\mathbf{b}_K(m) + \mathbf{u}_N(m),$$

where  $\mathbf{u}_N(m)$  is the contribution of the background noise to the chip rate equalized output. In this case, the orthogonality between the spreading codes is restored, and  $\mathbf{w}_{N,1}^H(m)\hat{\mathbf{d}}_N(m)$  is a quite relevant estimate of symbol  $b_1(m)$ . Here,  $\mathbf{w}_{N,1}(m)$  represents the code allocated

to user 1 at time  $m$ , i.e. the first column of matrix  $\mathbf{W}_{N,K}(m)$ .

In this chapter, we consider non causal FIR chip rate (reduced-rank) MMSE equalizers with transfer functions  $g(z) = \sum_{k=-(N-1)}^N g_k z^{-k}$ , the coefficients of which are designed as if the chip sequence  $(d(i))_{i \in \mathbb{Z}}$  were a decorrelated sequence with variance  $\frac{K}{N}$ . This property is of course not verified because (5.3) implies that the covariance matrix of  $\mathbf{d}_N(m)$  is rank deficient. The variance  $\frac{K}{N}$  is justified by the fact that as  $\mathbf{W}_{N,K}(m)^H \mathbf{W}_{N,K}(m) = \mathbf{I}_K$ , then  $\mathbb{E}\|\mathbf{d}_N(m)\|^2 = \mathbb{E}\|\mathbf{b}_K(m)\|^2 = K$ . If  $(d(i))_{i \in \mathbb{Z}}$  were an i.i.d. sequence, its variance would therefore be equal to  $\frac{K}{N}$ . In the following, we collect the coefficients of any of the above equalizers  $g(z)$  into the  $2N$ -dimensional vector  $\mathbf{g} = (g_N, \dots, g_0, g_{-1}, \dots, g_{-(N-1)})^T$ . The plain MMSE chip-rate equalizer thus corresponds to vector  $\mathbf{g}_{2N}$  given by

$$\mathbf{g}_{2N} = \mathbf{h}_{2N}^H \left( \mathcal{H}_{2N} \mathcal{H}_{2N}^H + \frac{\sigma^2}{K/N} \mathbf{I} \right)^{-1} \quad (5.5)$$

where  $\mathbf{h}_{2N}$  is defined by  $\mathbf{h} = (0, \dots, 0, h_0, \dots, h_L, 0, \dots, 0)^T$  and where  $\mathcal{H}_{2N}$  is the  $2N \times 3N$  Sylvester matrix given by

$$\mathcal{H}_{2N} = \begin{bmatrix} \mathbf{H}_{1,N} & \mathbf{H}_{0,N} & \mathbf{0} \\ \mathbf{0} & \mathbf{H}_{1,N} & \mathbf{H}_{0,N} \end{bmatrix} \quad (5.6)$$

In the following, we denote by  $\mathbf{R}_{2N}$  the  $2N \times 2N$  matrix

$$\mathbf{R}_{2N} = \mathcal{H}_{2N} \mathcal{H}_{2N}^H + \frac{\sigma^2}{K/N} \mathbf{I} \quad (5.7)$$

and by  $\mathbf{K}_{n,2N}$  the  $n \times 2N$  Krylov matrix associated to the pair  $(\mathbf{R}_{2N}, \mathbf{h}_{2N})$ , i.e.

$$\mathbf{K}_{n,2N} = [\mathbf{h}_{2N}, \mathbf{R}_{2N} \mathbf{h}_{2N}, \dots, \mathbf{R}_{2N}^{n-1} \mathbf{h}_{2N}]$$

The  $n$ -th stage reduced-rank Wiener equalizer corresponds to vector  $\mathbf{g}_n$  given by

$$\mathbf{g}_n = \mathbf{h}_{2N}^H \mathbf{K}_{n,2N}^H (\mathbf{K}_{n,2N}^H \mathbf{R}_{2N} \mathbf{K}_{n,2N})^{-1} \mathbf{K}_{n,2N}^H \quad (5.8)$$

We denote by  $g_n(z)$  the transfer function associated to vector  $\mathbf{g}_n$  and define  $\hat{d}_n(i)$  as the corresponding estimated chip sequence  $\hat{d}_n(i) = [g_n(z)]y(i)$ . We propose to study the effect of  $n$  on the performance of the estimator of symbol  $b_1(m)$  defined by

$$\hat{b}_{1,n}(m) = \mathbf{w}_{N,1}^H(m) \hat{\mathbf{d}}_{n,N}(m) \quad (5.9)$$

where  $\hat{\mathbf{d}}_{n,N}(m) = (\hat{d}_n(mN), \dots, \hat{d}_n(mN + N - 1))^T$ .

## 5.2 Asymptotic analysis of reduced-rank equalizers.

From now on, we formulate the following realistic assumption:

**Assumption 5.1** *The long code sequence is a realization of a QPSK i.i.d. sequence.*

Therefore, due to the presence of the matrix  $\mathbf{S}(m)$ , matrix  $\mathbf{W}_{N,K}(m)$  can be seen as the realization of a quite particular random matrix. In the following, we study the performance of the above reduced-rank receivers in the asymptotic regime  $N$  and  $K$  tend to  $+\infty$  in such a way that  $\frac{K}{N} \rightarrow \alpha$  where  $0 < \alpha < 1$ . For the sake of simplicity, we also assume that the length  $L$  of the impulse response of the channel is assumed to be kept constant. However, we conjecture that our results can be extended if  $L$  also converges to  $\infty$  in such a way that  $L < N$  provided that  $\sup_N \sum_{l=0}^L |h_l| < +\infty$ . As the proofs of the main results are more technical in this context, we do not address this case. However, some simulations are given to support this claim.

As  $\frac{K}{N} \rightarrow \alpha$ , we replace factor  $\frac{K}{N}$  by  $\alpha$  in definition (5.7) of matrix  $\mathbf{R}_{2N}$  in order to simplify the exposition. This, of course, modifies the expressions of matrices  $\mathbf{K}_{n,2N}$  and of vectors  $\mathbf{g}_n$ .

In order to characterize the performance of receiver (5.9), we first evaluate its output SINR. For this, we consider the filter  $f_n(z) = \sum_{l=-(N-1)}^{N+L} f_{n,l} z^{-l} = g_n(z)h(z)$ , and remark that the estimated chip sequence  $\hat{d}_n(i)$  is given by

$$\hat{d}_n(i) = [f_n(z)]d(i) + [g_n(z)]v(i) \quad (5.10)$$

Vector  $\hat{\mathbf{d}}_{n,N}(m)$  can thus be written as

$$\hat{\mathbf{d}}_{n,N}(m) = \mathcal{F}_{n,N} \begin{bmatrix} \mathbf{d}_N(m-2) \\ \mathbf{d}_N(m-1) \\ \mathbf{d}_N(m) \\ \mathbf{d}_N(m+1) \end{bmatrix} + \mathcal{G}_{n,N} \begin{bmatrix} \mathbf{v}_N(m-1) \\ \mathbf{v}_N(m) \\ \mathbf{v}_N(m+1) \end{bmatrix} \quad (5.11)$$

Here, matrix  $\mathcal{G}_{n,N}$  is the  $N \times 3N$  Sylvester matrix associated to filter  $g_n(z)$ , i.e.

$$\mathcal{G}_{n,N} = \begin{pmatrix} g_{n,N} & \cdots & g_{n,0} & \cdots & g_{n,-(N-1)} & 0 & \cdots & \cdots & 0 \\ 0 & g_{n,N} & \cdots & g_{n,0} & \cdots & g_{n,-(N-1)} & 0 & \ddots & 0 \\ \vdots & \ddots & \ddots & \ddots & \ddots & \ddots & \ddots & \ddots & \vdots \\ 0 & \cdots & 0 & g_{n,N} & \cdots & g_{n,0} & \cdots & g_{n,-(N-1)} & 0 \end{pmatrix}$$

and  $\mathcal{F}_{n,N}$  is the  $N \times 4N$  Sylvester matrix associated to  $f_n(z)$  defined as  $\mathcal{G}_{n,N}$  from  $3N$ -dimensional vector  $\mathbf{f}_n = (0, \dots, 0, f_{N+L}, \dots, f_0, f_{-1}, \dots, f_{-(N-1)})^T$ . As  $f_n(z) = g_n(z)h(z)$ , vector  $\mathbf{f}_n$  is equal to  $\mathbf{g}_n \mathcal{H}_{2N}$  and matrix  $\mathcal{F}_{n,N}$  can be written as

$$\mathcal{F}_{n,N} = \mathcal{G}_{n,N} \mathcal{H}_{3N}$$

where  $\mathcal{H}_{3N}$  is the  $3N \times 4N$  Sylvester matrix defined in the same way that matrix  $\mathcal{H}_{2N}$  (see eq. (5.6)). For convenience, we partition  $\mathcal{F}_{n,N}$  as  $\mathcal{F}_{n,N} = (\mathbf{F}_{n,2,N}, \mathbf{F}_{n,1,N}, \mathbf{F}_{n,0,N}, \mathbf{F}_{n,-1,N})$  where the 4 blocks are  $N \times N$ .

For the sake of simplicity and readability, we simplify from now on the previous notations as follows:

- Matrix  $\mathbf{C}_{N,K}$  is denoted  $\mathbf{C}$ .  $\mathbf{c}_1$  represents its first column, and  $\mathbf{C}$  is partitioned as  $\mathbf{C} = (\mathbf{c}_1, \mathbf{C}_2)$ .

In order to express the output SINR provided by receiver (5.9), it is necessary to identify in (5.9) the contribution of symbol  $b_1(m)$ , of symbols  $(b_j(m))_{j=2,\dots,K}$  and symbols  $(b_j(m-k))_{j=1,\dots,K,k=-1,1,2}$ , and of the noise. After straightforward calculations, we get that the output SINR at time  $m$ , denoted  $\tilde{\beta}_n^{(N)}(m)$ , is given by

$$\tilde{\beta}_n^{(N)}(m) = \frac{|\mathbf{c}_1^H \mathbf{S}(m)^H \mathbf{F}_{n,0,N} \mathbf{S}(m) \mathbf{c}_1|^2}{\sum_{k=-1}^2 T_{n,k,N} + \sigma^2 \mathbf{c}_1^H \mathbf{S}(m)^H \mathcal{G}_{n,N} \mathcal{G}_{n,N}^H \mathbf{S}(m) \mathbf{c}_1} \quad (5.12)$$

where the terms  $(T_{n,k})_{k=-1,\dots,2}$  are defined by

$$T_{n,0,N} = \mathbf{c}_1^H \mathbf{S}(m)^H \mathbf{F}_{n,0,N} \mathbf{S}(m) \mathbf{C}_2 \mathbf{C}_2^H \mathbf{S}(m)^H \mathbf{F}_{n,0,N}^H \mathbf{S}(m) \mathbf{c}_1 \quad (5.13)$$

$$T_{n,k,N} = \mathbf{c}_1^H \mathbf{S}(m)^H \mathbf{F}_{n,k,N} \mathbf{S}(m-k) \mathbf{C} \mathbf{C}^H \mathbf{S}(m-k)^H \mathbf{F}_{n,k,N}^H \mathbf{S}(m) \mathbf{c}_1 \text{ for } k \neq 0 \quad (5.14)$$

In order to simplify the notations, the SINR  $\tilde{\beta}_N^{(N)}(m)$  of the plain MMSE receiver (i.e.  $n = N$ ) is denoted  $\tilde{\beta}^{(N)}(m)$ .

The expression (5.12) is quite complicated, and does not allow to obtain any insight on the performance of the reduced-rank receivers, in particular on the influence of  $n$  on the SINR. We also note that, considered as symbol rate receivers, the chip rate (reduced-rank) Wiener equalizers followed by a despreading **are not Wiener filters** in the classical sense. This explains why  $\tilde{\beta}^{(N)}(m)$  and  $\tilde{\beta}_n^{(N)}(m)$  are not given by expressions similar to (4.37) and (4.39). Therefore, some work is needed in order to be able to use the results of Loubaton-Hachem [53].

$\tilde{\beta}_n^{(N)}(m)$  depends on the values of the scrambling code. It can thus be interpreted as a random variable. The key point of this chapter is the following result, which states that

as  $N$  and  $K$  converge to  $+\infty$  in such a way that  $\frac{K}{N} \rightarrow \alpha$ , then  $\tilde{\beta}_n^{(N)}(m)$  has the same behavior as a certain deterministic quantity which does not depend on the entries of the code matrix  $\mathbf{W}_{N,K}(m)$  (not only of the values of the scrambling code, but also of the entries of the Walsh-Hadamard part  $\mathbf{C}$  of  $\mathbf{W}_{N,K}(m)$ ).

**Theorem 5.1** *For each  $n \leq N$ , we define  $\eta_n^{(N)}$  by*

$$\eta_n^{(N)} = \mathbf{h}_{2N}^H \mathbf{K}_{n,2N} (\mathbf{K}_{n,2N}^H \mathbf{R}_{2N} \mathbf{K}_{n,2N})^{-1} \mathbf{K}_{n,2N}^H \mathbf{h}_{2N} \quad (5.15)$$

*Then, for any fixed  $n$ ,*

$$\lim_{N \rightarrow +\infty, K/N \rightarrow \alpha} \tilde{\beta}_n^{(N)}(m) - \frac{1}{\alpha} \frac{\eta_n^{(N)}}{(1 - \eta_n^{(N)})} = 0 \quad (5.16)$$

*where the convergence stands for the convergence in probability.*

*We also define  $\eta^{(N)}$  by  $\eta^{(N)} = \mathbf{h}_{2N}^H \mathbf{R}_{2N}^{-1} \mathbf{h}_{2N}$ . Then,*

$$\lim_{N \rightarrow +\infty, K/N \rightarrow \alpha} \left( \tilde{\beta}^{(N)}(m) - \frac{1}{\alpha} \frac{\eta^{(N)}}{(1 - \eta^{(N)})} \right) = 0 \quad (5.17)$$

This result is quite useful because, up to the term  $\frac{1}{\alpha}$ , eq. (5.16) shows that asymptotically, the SINR has an expression similar to (4.39). The results of [53] can therefore be used in order to study the influence of  $n$  on the performance of the receiver (see below). Moreover, expressions at the righthand side of (5.17) and (5.16) have a simple interpretation. In fact, it is easy to check that  $\frac{\eta_n^{(N)}}{(1 - \eta_n^{(N)})}$  coincides with the SINR provided by the plain Wiener filter  $g_N(z)$  ((5.10) for  $n = N$ ) **if the chip sequence  $(d(i))_{i \in \mathbb{Z}}$  in (5.10) were an i.i.d. sequence of variance  $\alpha$** . The term  $\frac{1}{\alpha}$  at the righthand side of (5.17) can thus be interpreted as the gain produced in (5.9) by the despreading. (5.16) can be interpreted similarly. It is also interesting to notice that (5.17) coincides with the asymptotic SINR found in [25] in the case where the code matrix  $\mathbf{W}_{N,K}$  is obtained by extracting  $K$  columns from a Haar distributed random unitary matrix<sup>1</sup>. This is a surprising result because our actual code matrix model (equation (5.1) and assumption 5.1) looks very different from a Haar distributed matrix.

The proof of Theorem 5.1 needs some work. We just outline the main steps of (5.16) and provide more details in the Appendix B. We finally briefly justify (5.17).

---

<sup>1</sup>A random unitary matrix  $\mathbf{U}$  is said to be Haar distributed if for each deterministic unitary matrix  $\mathbf{Q}$ , the distribution of  $\mathbf{U}$  coincides with the distribution of  $\mathbf{U}\mathbf{Q}$

In order to study the asymptotic behavior of  $\tilde{\beta}_n^{(N)}(m)$ , it is necessary to study separately the various terms of the righthand side of (5.12).

**First step: study of  $|\mathbf{c}_1^H \mathbf{S}(m)^H \mathbf{F}_{n,0,N} \mathbf{S}(m) \mathbf{c}_1|^2$  and  $\mathbf{c}_1^H \mathbf{S}(m)^H \mathcal{G}_{n,N} \mathcal{G}_{n,N}^H \mathbf{S}(m) \mathbf{c}_1$ .**

The above terms can be studied by using the following useful lemma.

**Lemma 5.1** *Let  $\mathbf{B}_N$  be a deterministic  $N \times N$  uniformly bounded matrix, that is  $\sup_N \|\mathbf{B}_N\| < +\infty$ . Then,*

$$\lim_{N \rightarrow +\infty} \mathbb{E} \left| \mathbf{c}_1^H \mathbf{S}(m)^H \mathbf{B}_N \mathbf{S}(m) \mathbf{c}_1 - \frac{1}{N} \text{Trace}(\mathbf{B}_N) \right|^2 = 0 \quad (5.18)$$

This result is an immediate consequence of a classical result used extensively in previous work like [71] (See section 4.2, Lemma 4.1).

In order to be able to use Lemma 5.1, we need to verify that matrices  $\mathbf{F}_{n,0,N}$  and  $\mathcal{G}_{n,N} \mathcal{G}_{n,N}^H$ , or equivalently  $\mathcal{G}_{n,N}$ , are uniformly bounded.

**Lemma 5.2** *For each  $n$  fixed, matrix  $\mathcal{G}_{n,N}$  is uniformly bounded, i.e.  $\sup_N \|\mathcal{G}_{n,N}\| < +\infty$ .*

The proof is given in Appendix B.1. Matrix  $\mathcal{F}_{n,N}$  is given by  $\mathcal{F}_{n,N} = \mathcal{G}_{n,N} \mathcal{H}_{3N}$ . Matrix  $\mathcal{H}_{3N}$  is a Toeplitz matrix associated to the filter  $h(z) = \sum_{l=0}^L h_l z^{-L}$ . Therefore, for each  $N$ ,  $\|\mathcal{H}_{3N}\| \leq \|h\|_\infty = \sup_f |h(e^{2i\pi f})|$ . This shows that  $\mathcal{H}_{3N}$  is uniformly bounded. As  $\|\mathcal{F}_{n,N}\| \leq \|\mathcal{G}_{n,N}\| \|\mathcal{H}_{3N}\|$ , Lemma 5.2 implies that  $\mathcal{F}_{n,N}$ , and thus matrices  $(\mathbf{F}_{n,k,N})_{k=-1,\dots,2}$  are uniformly bounded.

Lemma 5.1 and the above discussion imply the following corollary:

**Corollary 5.1**

$$\mathbf{c}_1^H \mathbf{S}(m)^H \mathbf{F}_{n,0,N} \mathbf{S}(m) \mathbf{c}_1 - \eta_n^{(N)} \rightarrow 0 \quad (5.19)$$

$$\mathbf{c}_1^H \mathbf{S}(m)^H \mathcal{G}_n \mathcal{G}_n^H \mathbf{S}(m) \mathbf{c}_1 - \|\mathbf{g}_n\|^2 \rightarrow 0 \quad (5.20)$$

where the convergence stands for the convergence in probability.

**Proof.** In order to prove the first statement of Corollary 5.1, we remark that Lemma 5.1 and the fact that  $\mathbf{F}_{n,0,N}$  is uniformly bounded imply that

$$\mathbf{c}_1^H \mathbf{S}(m)^H \mathbf{F}_{n,0,N} \mathbf{S}(m) \mathbf{c}_1 - \frac{1}{N} \text{Trace}(\mathbf{F}_{n,0,N})$$

converges in the mean-square sense, and thus in probability, to 0. As  $\mathbf{F}_{n,0}$  is a Toeplitz matrix, its normalized trace coincides with the constant term  $f_{n,0}$  of transfer function  $f_n(z) = g_n(z)h(z)$ , which is equal to  $f_{n,0} = \mathbf{g}_n \mathbf{h} = \eta_n^{(N)}$ . The second statement of Corollary 5.1 follows directly from Lemmas 5.1 and 5.2 and from the observation that

$$\frac{1}{N} \text{Trace}(\mathcal{G}_n \mathcal{G}_n^H) = \|\mathbf{g}_n\|^2.$$

**Second step: study of  $T_{n,0,N}$ .**

The asymptotic behaviour of  $T_{n,0,N} = \mathbf{c}_1^H \mathbf{S}(m)^H \mathbf{F}_{n,0,N} \mathbf{S}(m) \mathbf{C}_2 \mathbf{C}_2^H \mathbf{S}(m)^H \mathbf{F}_{n,0,N}^H \mathbf{S}(m) \mathbf{c}_1$  is a straightforward consequence of the following Lemma.

**Lemma 5.3** *Let  $\mathbf{B}_N$  be a  $N \times N$  uniformly bounded Toeplitz matrix, i.e.  $\sup_N \|\mathbf{B}_N\| < +\infty$ . Then, the limit when  $N \rightarrow +\infty$  and  $\frac{K}{N} \rightarrow \alpha$  of*

$$\mathbb{E} \left| \mathbf{c}_1^H \mathbf{S}(m)^H \mathbf{B}_N \mathbf{S}(m) \mathbf{C}_2 \mathbf{C}_2^H \mathbf{S}(m)^H \mathbf{B}_N^H \mathbf{S}(m) \mathbf{c}_1 - \alpha \left( \frac{1}{N} \text{Trace}(\mathbf{B}_N \mathbf{B}_N^H) - \left| \frac{1}{N} \text{Trace}(\mathbf{B}_N) \right|^2 \right) \right|^2 \quad (5.21)$$

is equal to 0.

**Proof.** See Appendix B.2.

Lemma 5.2 implies that matrix  $\mathbf{F}_{n,0,N}$  is uniformly bounded. As the mean-square convergence implies the convergence in probability, Lemma 5.3 shows that  $T_{n,0,N}$  converges in probability to  $\alpha \left( \frac{1}{N} \text{Trace}(\mathbf{F}_{n,0,N} \mathbf{F}_{n,0,N}^H) - \left| \frac{1}{N} \text{Trace}(\mathbf{F}_{n,0,N}) \right|^2 \right)$ . As  $\frac{1}{N} \text{Trace}(\mathbf{F}_{n,0,N}) = \eta_m^{(N)}$ , we get immediately the following Corollary.

**Corollary 5.2**

$$T_{n,0,N} \rightarrow \alpha \left( \frac{1}{N} (\text{Trace}(\mathbf{F}_{n,0,N} \mathbf{F}_{n,0,N}^H) - (\eta_m^{(N)})^2) \right) \quad (5.22)$$

where the convergence stands for the convergence in probability.

**Third step: study of  $T_{n,k,N}$  for  $k = -1, 1, 2$ .**

The following lemma allows to precise the behaviour of  $T_{n,k,N}$  for  $k = -1, 1, 2$ .

**Lemma 5.4** *Let  $\mathbf{B}_N$  be a uniformly bounded  $N \times N$  matrix. Then, for  $k = -1, 1, 2$ ,*

$$\lim_{N \rightarrow +\infty, \frac{K}{N} \rightarrow \alpha} \mathbb{E} \left| \mathbf{c}_1^H \mathbf{S}(m)^H \mathbf{B}_N \mathbf{S}(m-k) \mathbf{C} \mathbf{C}^H \mathbf{S}(m-k)^H \mathbf{B}_N^H \mathbf{S}(m) \mathbf{c}_1 - \alpha \frac{1}{N} \text{Trace}(\mathbf{B}_N \mathbf{B}_N^H) \right|^2 = 0 \quad (5.23)$$

**Proof.** See Appendix B.3 for a sketch of the proof.

Lemma 5.2 implies that matrices  $\mathbf{F}_{n,k,N}$  are bounded. As the mean-square convergence implies the convergence in probability, Lemma 5.4 shows that

$$T_{n,k,N} \rightarrow \alpha \frac{1}{N} \text{Trace}(\mathbf{F}_{n,k,N} \mathbf{F}_{n,k,N}^H) \quad (5.24)$$

where the convergence stands for the convergence in probability.

#### Fourth step: proof of (5.16)

We are now in position to complete the proof of (5.16). From the above discussions, we get that

$$\tilde{\beta}_n^{(N)} - \frac{(\eta_n^{(N)})^2}{\alpha \left( \sum_{k=-1}^2 \frac{1}{N} \text{Trace}(\mathbf{F}_{n,k,N} \mathbf{F}_{n,k,N}^H) - (\eta_n^{(N)})^2 \right) + \sigma^2 \|\mathbf{g}_n\|^2}$$

converges to 0 in probability. We remark that

$$\sum_{k=-1}^2 \frac{1}{N} \text{Trace}(\mathbf{F}_{n,k,N} \mathbf{F}_{n,k,N}^H) = \frac{1}{N} \text{Trace}(\mathcal{F}_{n,N} \mathcal{F}_{n,N}^H)$$

As  $\mathcal{F}_{n,N} \mathcal{F}_{n,N}^H$  is a  $N \times N$  Toeplitz matrix, its normalized trace coincides with its diagonal term which is equal to  $\|\mathbf{f}_n\|^2$ . As  $\mathbf{f}_n = \mathbf{g}_n \mathcal{H}_{2N}$ , we get that

$$\frac{1}{N} \text{Trace}(\mathcal{F}_{n,N} \mathcal{F}_{n,N}^H) = \mathbf{g}_n \mathcal{H}_{2N} \mathcal{H}_{2N}^H \mathbf{g}_n^H$$

and that

$$\alpha \sum_{k=-1}^2 \frac{1}{N} \text{Trace}(\mathbf{F}_{n,k,N} \mathbf{F}_{n,k,N}^H) + \sigma^2 \|\mathbf{g}_n\|^2 = \alpha \mathbf{g}_n \left( \mathcal{H}_{2N} \mathcal{H}_{2N}^H + \frac{\sigma^2}{\alpha} \mathbf{I}_{2N} \right) \mathbf{g}_n^H = \alpha \mathbf{g}_n \mathbf{R}_{2N} \mathbf{g}_n^H$$

But, as  $\mathbf{g}_n$  is given by (5.8),  $\mathbf{g}_n \mathbf{R}_{2N} \mathbf{g}_n^H$  coincides with  $\mathbf{h}_{2N}^H \mathbf{K}_{n,2N}^H (\mathbf{K}_{n,2N} \mathbf{R}_{2N} \mathbf{K}_{n,2N}^H)^{-1} \mathbf{K}_{n,2N} \mathbf{h}_{2N}$ , i.e. with  $\eta_n^{(N)}$ . Putting all pieces together, we get that

$$\frac{(\eta_n^{(N)})^2}{\alpha \left( \sum_{k=-1}^2 \frac{1}{N} \text{Trace}(\mathbf{F}_{n,k,N} \mathbf{F}_{n,k,N}^H) - (\eta_n^{(N)})^2 \right) + \sigma^2 \|\mathbf{g}_n\|^2} = \frac{1}{\alpha} \frac{\eta_n^{(N)}}{1 - \eta_n^{(N)}}$$

which, eventually, proves (5.16).

We finally justify (5.17). For this, we just mention that, as the full rank Wiener filter  $g_N(z)$  converges when  $N \rightarrow +\infty$  to the usual non causal filter  $g_\infty(z) = \frac{h^*(z^{-1})}{h(z)h^*(z^{-1}) + \sigma^2}$ , which verifies  $\|g_\infty\|_\infty < +\infty$ , then  $\sup_N \|g_N\|_\infty < +\infty$ . Therefore, matrices  $\mathcal{G}_{N,N}$  and  $\mathcal{F}_{N,N}$  are uniformly bounded. One may check that this allows to generalize the above arguments to the case where  $n = N$ .

Theorem 5.1 is important in that it allows to use the material of section 4.4 in order to obtain insights on the convergence speed of  $\tilde{\beta}_n^{(N)}$  toward  $\tilde{\beta}^{(N)}$  when  $N$  and  $K$  are large

enough. In fact, relation (5.16) implies that it is sufficient to evaluate the convergence speed of  $\eta_n^{(N)}$  toward  $\eta^{(N)}$  when  $N \rightarrow +\infty, K/N \rightarrow \alpha$ , a simpler problem. For this, it is possible to use the results of section 4.4. Formula (5.15) coincides with (4.38) when  $N$  is exchanged with  $2N$ . In our context, matrix  $\mathbf{R}_{2N}$  is  $\mathbf{R}_{2N} = \mathcal{H}_{2N} \mathcal{H}_{2N}^H + \frac{\sigma^2}{\alpha} \mathbf{I}$  while vector  $\mathbf{h}_{2N}$  is  $\mathbf{h}_{2N} = (0, \dots, 0, h_0, \dots, h_L, 0, \dots, 0)^T$ . We have thus only to check that Assumptions 4.1, 4.2, 4.3 hold.

As  $\mathbf{R}_{2N}$  is a Toeplitz matrix associated to the spectral density  $|h(e^{2i\pi f})|^2 + \frac{\sigma^2}{\alpha}$ , the term  $s_k^{(2N)} = \mathbf{h}_{2N}^H \mathbf{R}_{2N}^k \mathbf{h}_{2N}$  defined in Assumption 4.1 is easily seen to converge towards  $s_k$  defined by

$$s_k = \int_0^1 |h(e^{2i\pi f})|^2 \left( |h(e^{2i\pi f})|^2 + \frac{\sigma^2}{\alpha} \right)^k df$$

when  $N \rightarrow +\infty$ . We put  $\delta_1 = |h_{min}|^2 + \frac{\sigma^2}{\alpha}$  and  $\delta_2 = |h_{max}|^2 + \frac{\sigma^2}{\alpha}$  where  $|h_{min}| = \min_f |h(e^{2i\pi f})|$  and  $|h_{max}| = \max_f |h(e^{2i\pi f})|$ . Then, it is easy to check that  $s_k$  can be written as

$$s_k = \int_{\delta_1}^{\delta_2} \lambda^k d\nu(\lambda)$$

where  $\nu$  is the probability measure supported by  $[\delta_1, \delta_2]$  defined by

$$\int_{\delta_1}^{\delta_2} \phi(\lambda) d\nu(\lambda) = \int_0^1 |h(e^{2i\pi f})|^2 \phi \left( |h(e^{2i\pi f})|^2 + \frac{\sigma^2}{\alpha} \right) df$$

for each continuous function  $\phi$ . Measure  $\nu$  is easily seen to be absolutely continuous and to have a strictly positive density on  $[\delta_1, \delta_2]$ . Thus Assumptions 4.1 and 4.2 hold. As for Assumption 4.3, we remark that as  $\mathbf{R}_{2N}$  is a Toeplitz matrix associated to the spectral density  $|h(e^{2i\pi f})|^2 + \frac{\sigma^2}{\alpha}$ , then,

$$\begin{aligned} \|\mathbf{R}_{2N}\| &\leq \max_f \left( |h(e^{2i\pi f})|^2 + \frac{\sigma^2}{\alpha} \right) = \delta_2 \\ \|\mathbf{R}_{2N}^{-1}\| &\leq \left( \min_f \left( |h(e^{2i\pi f})|^2 + \frac{\sigma^2}{\alpha} \right) \right)^{-1} = \frac{1}{\delta_1} \end{aligned} \quad (5.25)$$

Theorem 4.4 thus shows that  $\eta_n^{(N)}$  and  $\eta^{(N)}$  converge toward  $\eta_n$  and  $\eta$  defined in section 4.4. Hence,  $\beta_n^{(N)}$  and  $\beta^{(N)}$  converge toward  $\beta_n$  and  $\beta$  defined by

$$\begin{aligned} \beta_n &= \frac{1}{\alpha} \frac{\eta_n}{1 - \eta_n} \\ \beta &= \frac{1}{\alpha} \frac{\eta}{1 - \eta} \end{aligned} \quad (5.26)$$

Moreover, the convergence speed of  $\eta_n$  and  $\beta_n$  toward  $\eta$  and  $\beta$  is locally exponential, and the rate of convergence essentially depends on the ratio  $\mu = \frac{1 + \frac{\delta_1}{\delta_2}}{1 - \frac{\delta_1}{\delta_2}}$ . If  $\mu$  is close to 1, or

equivalently if  $\frac{\delta_1}{\delta_2} \ll 1$ , the convergence speed is low. Using standard results on Toeplitz matrices, the smallest and the largest eigenvalue of  $\mathbf{R}_{2N}$  converge to  $\delta_1$  and  $\delta_2$  respectively when  $N \rightarrow \infty$ . Therefore, the ratio  $\frac{\delta_1}{\delta_2}$  is for  $N$  large enough nearly equal to the condition number of matrix  $\mathbf{R}_{2N}$ . It thus appears that, for  $N$  large enough, the convergence rate is poor if  $\mathbf{R}_{2N}$  is ill conditioned and vice and versa. Our result also allows to evaluate the influence of the load of the cell, i.e. parameter  $\alpha$ . In effect,  $\frac{\delta_1}{\delta_2}$  can be written as

$$\frac{\delta_1}{\delta_2} = \frac{\sigma^2 + \alpha|h_{min}|^2}{\sigma^2 + \alpha|h_{max}|^2}$$

Therefore, the smaller  $\alpha$  is, the better the convergence rate is.

**Remark 5.1** *It can be shown that the same results are obtained if, instead of working with a matrix  $\mathbf{R}_{2N}$  of size  $2N$ , we work with a matrix  $\mathbf{R}_N$  of size  $N$  and neglect the Inter Symbol Interference (ISI). This is equivalent to replacing model (5.4) by:*

$$\mathbf{y}_N(m) = \mathbf{H}_N \mathbf{d}_N(m) + \mathbf{v}_N(m), \quad (5.27)$$

where  $\mathbf{H}_N$  is the circulant matrix defined by

$$\mathbf{H}_N = \mathbf{H}_{0,N} + \mathbf{H}_{1,N}.$$

However, this approach is not convenient in our case because the proofs are tedious. For more details see [4, 25]. This idea is also used in Chapter 6.

## 5.3 Simulation results

### 5.3.1 Comparison of empirical and theoretical (asymptotic) BER

In this section, we first verify that our asymptotic SINR evaluations allow to predict the empirical performance of the studied receivers. For this, we have implemented the physical layer of the downlink of the UMTS-FDD, and have compared the measured bit error rate with its asymptotic evaluation given by  $Q(\sqrt{\beta_n})$ . The results are presented in Figure 5.3.1. Here, the propagation channel is the so-called Vehicular A the profile of which is given in Table. 5.1. (on each frame, a different realization of the channel is generated). Note that the chip period  $T_c$  is equal to  $T_c = 260nsec$ . The signal to noise ratio (for each user)  $\frac{E_b}{N_0}$  is equal to 10 dB and the load factor  $\alpha$  is equal to  $\frac{1}{2}$ . Figure 5.3.1 shows that our asymptotic evaluations allow to predict rather accurately the performance of the true system even for spreading factors as low as  $N = 16$ <sup>2</sup>.

<sup>2</sup>This means that this asymptotic analysis can be used to study the reduced-rank equalizer raw BER performance in the context of the very recent High-Speed Downlink Packet Access (HSDPA) mode of the UMTS in which many spreading codes of length 16 are allocated to the same user with 16QAM constellation symbols.

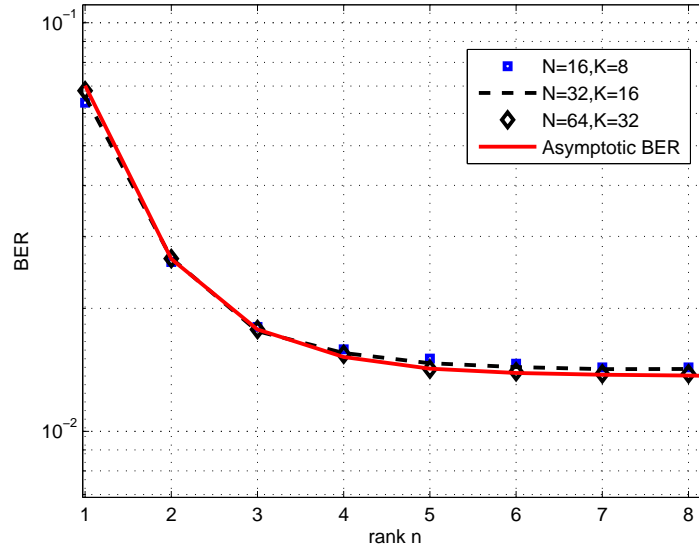


Figure 5.1: Comparison of empirical and theoretical BER for the Vehicular A channel.

Vehicular A Path Delay in nsec	0	310	710	1090	1730	2510
Vehicular A Average Power (dB)	0	-1.0	-9.0	-10.0	-15.0	-20.0
Vehicular B Path Delay in nsec	0	300	8900	12900	17100	20000
Vehicular B Average Power (dB)	-2.5	0	-12.8	-10.0	-25.2	-16.0

Table 5.1: The Vehicular A and Vehicular B channel profiles.

### 5.3.2 Comparison of empirical and theoretical BER for very long delay spread channels

In section 5.2, we claimed that the results remain valid even for channels with very long delay spread (comparable to  $N$ ). To verify this, we consider the Vehicular B channel (see Table. 5.1). The delay spread in this case is roughly equal to  $80T_c$ . We consider the case  $N = 128$  and  $\alpha = \frac{1}{2}$ . The SNR  $\frac{E_b}{N_0}$  is equal to 10 dB. The results are given in Figure 5.4. We see that the fit is as good as the Vehicular A case. Thus, the results remain valid for channels with delay spreads growing with the spreading factor (provided that  $L < N$ ).

### 5.3.3 Effect of the load factor $\alpha$ on the convergence rate

As we have verified that  $\beta_n$  and  $\beta$  allow to predict accurately the performance of the above real life system, we next study the influence of the different parameters on the convergence speed of  $\beta_n$  toward  $\beta$ . For this, we represent in the following figures the relative SINR defined as the ratio  $\frac{\beta_n}{\beta}$  as a function of the rank  $n$ . In Figure 5.4, , we first study the influence of  $\alpha$  on the convergence speed of the relative SINR toward 1. Here, the propagation channel is the Vehicular A channel, and the ratio  $\frac{E_b}{N_0}$  is equal to 7 dB. This figure confirms that the convergence speed of the reduced rank receivers depends crucially on the load factor.

### 5.3.4 Effect of the channel on the convergence rate

In Figure 5.4, we study the effect of the channel on the convergence speed of  $\beta_n$  toward  $\beta$ . For this, we consider a 2 taps channel with transfer function  $h(z) = h_0 + h_1 z^{-1}$  and change the relative power of the two taps. In this case, the ratio  $\frac{\delta_1}{\delta_2}$  is minimum if  $|h_0| = |h_1|$  and is equal to  $\frac{\sigma^2/\alpha}{2+\sigma^2/\alpha}$  :  $h(z)$  has a zero on the unit circle, so that  $|h_{min}| = 0$ , while  $|h_{max}| = 2|h_0| = \sqrt{2}$  (because  $|h_0|^2 + |h_1|^2 = 1$ ). Therefore, If  $|h_0| = |h_1|$ , the convergence speed of  $\beta_n$  toward  $\beta$  is expected to be minimum. This is confirmed by Figure 5.4 obtained for  $\alpha = \frac{1}{2}$  and  $\frac{E_b}{N_0} = 7dB$ .

## 5.4 Conclusion

In this chapter, we have addressed the performance of downlink CDMA receivers consisting of reduced rank Wiener equalizers followed by despreading. We have studied the convergence speed of their SINR versus their order in the asymptotic regime  $N \rightarrow +\infty, K/N \rightarrow \alpha$ . In this context, we have shown that for each  $n$ , the SINR provided by the rank  $n$  receiver converges to a deterministic term  $\beta_n$ , and that the convergence of  $\beta_n$  when  $n$  increases is locally exponential. We have evaluated the corresponding rate which only depends on the condition number of the covariance matrix to be inverted in order to calculate the full rank receiver. Simulation results have shown that our asymptotic results allow to predict the performance of finite dimension CDMA system even for very short spreading factors.

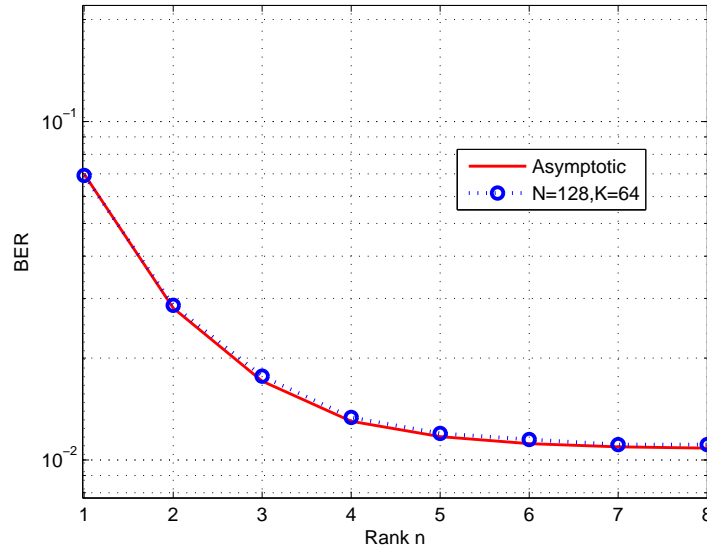


Figure 5.2: Comparison of empirical and theoretical BER for the Vehicular B channel

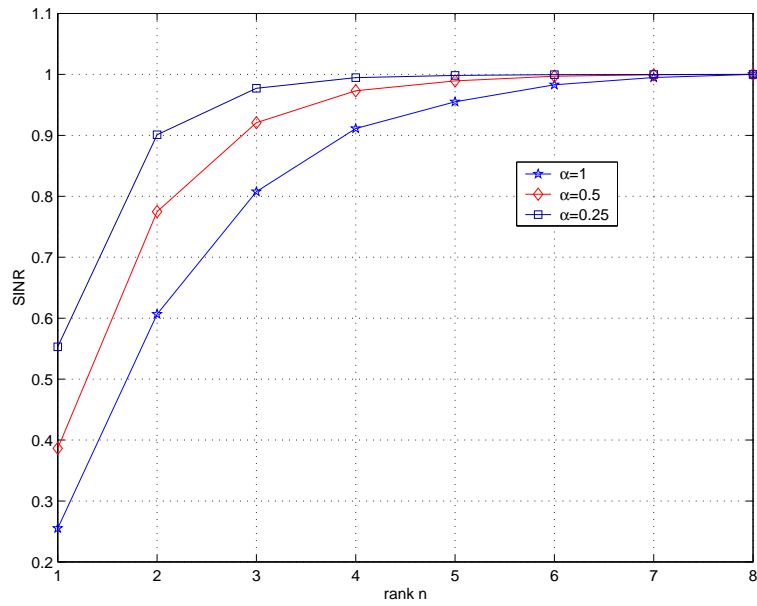


Figure 5.3: Influence of  $\alpha$  on the convergence of the relative SINR

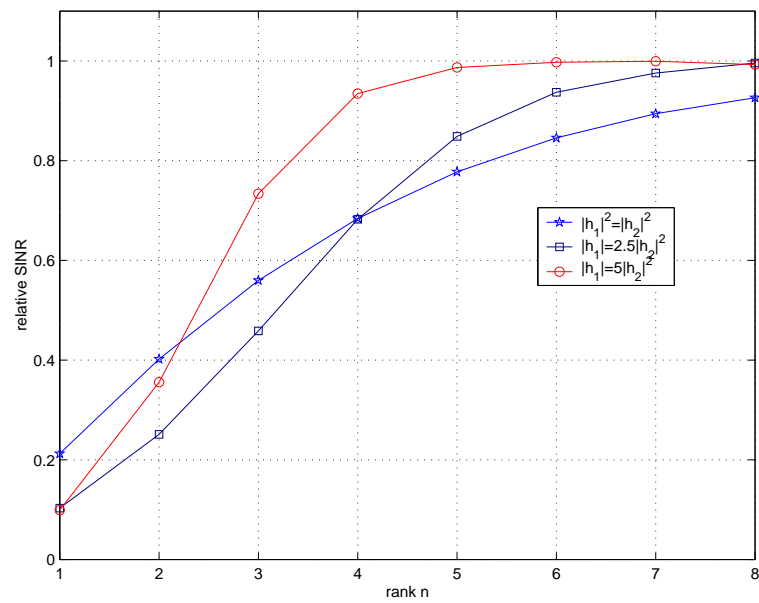


Figure 5.4: Influence of the propagation channel on the convergence of the relative SINR

# Chapter 6

## Asymptotic Analysis of Space-Time Transmit Diversity with and without Equalization

---

### 6.1 Introduction

Third generation (3G) mobile communications systems such cdma2000 and W-CDMA are intended to provide higher data rates than current second generation systems. High data rates can be achieved by combatting channel fading between the transmitter and the receiver. Diversity is one way to combat channel fading. Multiple antennas at the receiver can be used to provide diversity. The dilemma is that, in the downlink, multiple antennas at the receiver induces an increase in the size of the mobile unit, while significant effort is being done to make wireless mobile devices smaller and cheaper. By using a very simple Space-Time Block Code (STBC), Alamouti [17] has shown that the diversity provided by using two transmit antennas and one receive antenna is the same as that provided by one transmit antenna and two receive antennas. The Alamouti scheme allows to double the diversity without the need to include multiple antennas at the receiver side. However, this result is valid for flat fading channels only.

Space Time Transmit Diversity (STTD) based on the Alamouti STBC has been adopted in the W-CDMA norm [14]. In W-CDMA, the propagation channels are known to be frequency selective. It is then of great importance to study the performance of STTD in frequency selective fading channels when associated with the conventional receiver of

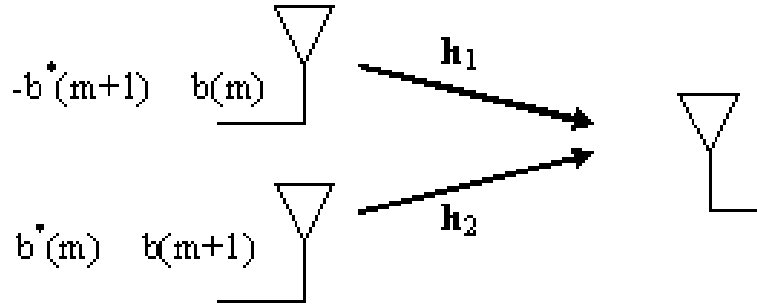


Figure 6.1: A Communication system with 2 transmit antennas and one receive antenna.

CDMA systems (the RAKE receiver).

A promising alternative to the RAKE reception is chip-rate Minimum Mean Squared Error (MMSE) equalization prior to descrambling and despreading (see Chapter 2). The orthogonality between the spreading codes is destroyed due to the multipath propagation channel. MMSE equalization allows to partially restore the orthogonality. Thus, after descrambling and despreading the symbol estimate is better than that obtained by the RAKE receiver. It is thus very useful to study the performance of STTD in frequency selective fading channels when associated with a MMSE equalizer-based receiver.

In this chapter, we consider the use of STTD in the downlink of W-CDMA. We discuss the applicability of the Alamouti scheme in the case of multipath (frequency-selective) fading channels when using a RAKE receiver or a MMSE equalizer-based receiver. We follow the classical approach used for the first time in [71], and assume that the spreading factor  $N$  and the number of users  $K$  tend to  $+\infty$  at the same rate. The spreading codes are supposed to coincide with Walsh Hadamard codes scrambled by an Independent Identically Distributed (i.i.d) sequence. In this context, the SINRs of the two receiver tend to deterministic limits independent of the scrambling and the spreading codes. We derive the asymptotic SINRs, compare the two receivers and discuss the gain that we obtain by using STTD for both of them.

## 6.2 The Alamouti Space Time Block Code (STBC)

In this section, we discuss the originally proposed Alamouti scheme proposed in [17]. Consider the scenario shown in figure 6.1. We have two Transmit antennas and one receive antenna. The transmission setting is shown in Table 1. At time instant  $m$  we transmit the symbol  $b(m)$  from antenna 1 and symbol  $b(m+1)$  from antenna 2. At time

instant  $m + 1$ ,  $-b^*(m + 1)$  is transmitted from antenna 1, while  $b^*(m)$  is transmitted from antenna 2.

	time m	time m+1
Antenna 1	$b(m)$	$-b^*(m + 1)$
Antenna 2	$b(m + 1)$	$b^*(m)$

**Table 1.** The Original Alamouti STBC

Now, the received signals at time instants  $m$  and  $m + 1$  are given by:

$$x(m) = h_1 b(m) + h_2 b(m + 1) + v(m) \quad (6.1)$$

$$x(m + 1) = -h_1 b^*(m + 1) + h_2 b^*(m) + v(m + 1) \quad (6.2)$$

The receiver calculates the following estimates:

$$\tilde{b}(m) = h_1^* x(m) + h_2 x^*(m + 1) \quad (6.3)$$

$$\tilde{b}(m + 1) = h_2^* x(m) - h_1 x^*(m + 1) \quad (6.4)$$

This is the decoding scheme. The trick behind the Alamouti scheme is to separate the two symbols by getting rid of the cross-channel interference i.e. terms that depends on both channels. In fact,

$$\begin{aligned} \tilde{b}(m) &= h_1^* (h_1 b(m) + h_2 b(m + 1) + v(m)) + h_2 (-h_1^* b(m + 1) + h_2^* b(m) + v^*(m + 1)) \\ &= (|h_1|^2 + |h_2|^2) b(m) + (h_1^* v(m) + h_2 v^*(m + 1)) \end{aligned} \quad (6.5)$$

similarly,

$$\tilde{b}(m + 1) = (|h_1|^2 + |h_2|^2) b(m + 1) + (h_2^* v(m) - h_1 v^*(m + 1)) \quad (6.6)$$

Note that, unlike the single antenna case, the estimate of each symbol depends on both channels. This provides extra diversity because the two channels are supposed independent and the probability of deep fades in both is smaller than a deep fade in each one separately. The Alamouti scheme provides the same diversity as the one with one transmit antennas and two receive antennas (if the same power is transmitted from each transmit antenna). Figure 6.2 show the BER performance as a function of the total transmitted power for three transmission schemes: one transmit antenna and one receive antenna, one transmit antenna and two receive antennas and finally two transmit antenna and one receive antenna employing the Alamouti Space Time Block Code. We note that the diversity provided by the Alamouti scheme is the same as that provided by the two receive antennas. The 3dB difference is due to the transmission of half the power from each

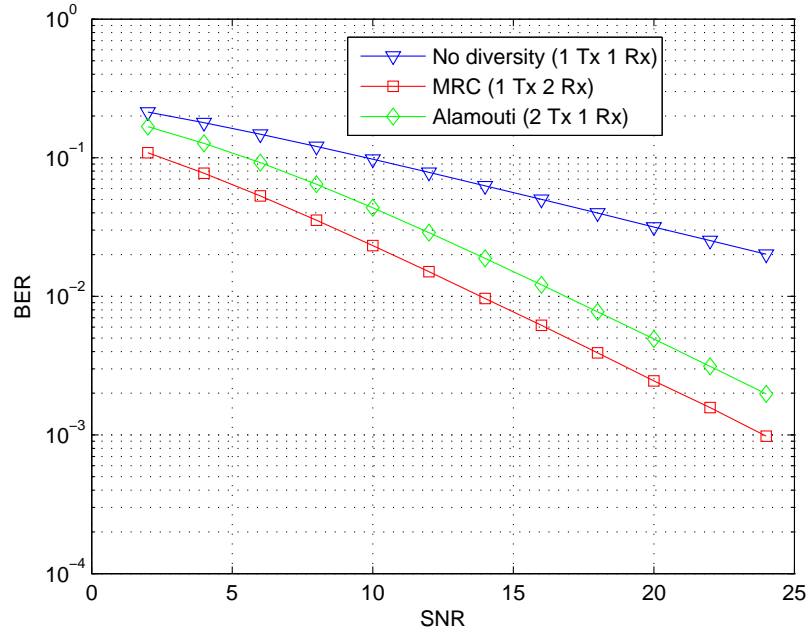


Figure 6.2: BER performance comparison for coherent QPSK of Alamouti scheme with other schemes.

transmit antenna for the comparison to be fair. The diversity, though, is the same <sup>1</sup>. If we double the power, the two curves will be identical.

In order to simplify the asymptotic analysis to be presented in the sequel, it is more convenient to write the previous equations in matrix form. The received samples in two consecutive time instants are given by:

$$\begin{bmatrix} x(m) \\ x^*(m+1) \end{bmatrix} = \begin{bmatrix} h_1 & h_2 \\ h_2^* & -h_1^* \end{bmatrix} \begin{bmatrix} b(m) \\ b(m+1) \end{bmatrix} + \begin{bmatrix} v(m) \\ v^*(m+1) \end{bmatrix}$$

Then the decoding scheme is to pre-multiply the received vector by the conjugate of the channel matrix, i.e.

$$\begin{bmatrix} \tilde{b}(m) \\ \tilde{b}(m+1) \end{bmatrix} = \begin{bmatrix} h_1^* & +h_2 \\ h_2^* & -h_1 \end{bmatrix} \begin{bmatrix} x(m) \\ x(m+1) \end{bmatrix}$$

<sup>1</sup>The diversity is sometimes defined as the slope of the BER curve as a function of the SNR

finally, we get:

$$\begin{bmatrix} \tilde{b}(m) \\ \tilde{b}(m+1) \end{bmatrix} = \begin{bmatrix} |h_1|^2 + |h_2|^2 & 0 \\ 0 & |h_1|^2 + |h_2|^2 \end{bmatrix} \begin{bmatrix} b(m) \\ b(m+1) \end{bmatrix} + \begin{bmatrix} h_1^*v(m) + h_2v^*(m+1) \\ h_2^*v(m) - h_1v^*(m+1) \end{bmatrix}$$

Note that the anti-diagonal entries of the matrix resulting for the product of channel matrix with its conjugate are equal to zero.

The Alamouti scheme is valid for frequency-flat fading channels. Its elegance and simplicity has helped in its standardization in the UMTS norm even though the radio communication channels are highly frequency selective. In the sequel, we study the effect of the presence of multipath (frequency selective) fading channels when using the Alamouti scheme.

### 6.3 CMDA System Model under STTD

We consider a single base station transmitting the sum of  $K$  users chip signals given by:

$$d(i) = s(i) \sum_{k=1}^K c_k(i \bmod N) b_k(\lfloor \frac{i}{N} \rfloor) \quad (6.7)$$

where  $s(i)$  is the base-station dependent QPSK (long) scrambling code,  $N$  is the spreading factor,  $K$  is the number of users,  $b_k(\lfloor \frac{i}{N} \rfloor)$  and  $c_k(i \bmod N)$  are the QPSK symbol sequence and the ( $N$ -periodic) normalized spreading code of user  $k$ , respectively. ( $\bmod$  stands for the modulo and  $\lfloor \cdot \rfloor$  for the integer part).

Throughout the chapter, we will assume that the scrambling sequence is i.i.d, and that the user's bits are independent zero mean QPSK signals. The index of the user of interest is 1. The transmitted chip vector in one symbol period  $\mathbf{d}(m) = [d(mN), d(mN+1), \dots, d(mN+N-1)]^T$  is given by:

$$\mathbf{d}(m) = \mathbf{S}(m)\mathbf{C}\mathbf{b}(m) \quad (6.8)$$

where  $\mathbf{S}(m)$  is the  $N \times N$  diagonal matrix whose diagonal elements are  $s(mN), s(mN+1), \dots, s(mN+N-1)$  and  $\mathbf{C}$  is a  $N \times K$  matrix whose columns are the spreading codes assigned to different users and  $\mathbf{b}(m) = [b_1(m), \dots, b_K(m)]^T$ .

The sum chip signal (6.7) is transmitted through two multipath frequency-selective fading channels whose impulse responses are given by

$$h_j(t) = \sum_{q=0}^{P-1} \lambda^j(q) p(t - \tau_q^i) \quad j = (1, 2) \quad (6.9)$$

where  $p(t)$  is the total shaping filter (including the transmitter and the receiver matched filters),  $\lambda^j(q)$  and  $\tau_q^j$  are the complex gain and the delay associated with path  $q$  of the channel between transmit antenna  $j = (1, 2)$  and the receiver, and  $P$  is the total number of resolvable paths. For the sake of simplicity we suppose that the number of resolvable paths is the same for both channels.

A symbol-level Alamouti STBC is applied at the base station. This is equivalent to transmitting the chip vectors defined by equation 6.8 according to Table. 2<sup>2</sup>.

time Antenna	$m - 2$	$m - 1$	$m$	$m + 1$
1	$\mathbf{d}(m - 2)$	$\mathbf{d}(m - 1)$	$\mathbf{d}(m)$	$\mathbf{d}(m + 1)$
2	$\bar{\mathbf{d}}(m - 1)$	$-\bar{\mathbf{d}}(m - 2)$	$\bar{\mathbf{d}}(m + 1)$	$-\bar{\mathbf{d}}(m)$

**Table 1.** The Alamouti STBC for W-CDMA

If we call the chips transmitted from antenna 1  $d_1(i)$  and the chips transmitted from antenna 2  $d_2(i)$  then the chip-rate sampled received signal is given by:

$$x(i) = \sum_{l=0}^{L-1} h_{1,l} d_1(i-l) + \sum_{l=0}^{L-1} h_{2,l} d_2(i-l) + v(i) \quad (6.10)$$

where  $h_{j,l} \triangleq h_j(t)|_{t=lT_c}$ ,  $L$  is the overall channel length (in chip periods) and  $v(i)$  is a centered white Gaussian noise process with variance  $\sigma^2$ .

It is more convenient to express the model (6.10) in matrix form. By concatenating the received signal in  $2N$  chips we get:

$$\begin{bmatrix} \mathbf{x}(m) \\ \bar{\mathbf{x}}(m+1) \end{bmatrix} = \begin{bmatrix} \mathbf{H}_{1,0} & \mathbf{H}_{2,0} \\ -\bar{\mathbf{H}}_{2,0} & \bar{\mathbf{H}}_{1,0} \end{bmatrix} \begin{bmatrix} \mathbf{d}(m) \\ \bar{\mathbf{d}}(m+1) \end{bmatrix} + \begin{bmatrix} \mathbf{H}_{1,1} & 0 \\ 0 & -\mathbf{H}_{1,2} \end{bmatrix} \begin{bmatrix} \mathbf{d}(m-1) \\ \bar{\mathbf{d}}(m-2) \end{bmatrix} \\ + \begin{bmatrix} \bar{\mathbf{H}}_{1,1} & 0 \\ 0 & \bar{\mathbf{H}}_{1,2} \end{bmatrix} \begin{bmatrix} \bar{\mathbf{d}}(m) \\ \mathbf{d}(m+1) \end{bmatrix} + \begin{bmatrix} \mathbf{v}(m) \\ \bar{\mathbf{v}}(m+1) \end{bmatrix} \quad (6.11)$$

where  $\mathbf{x}(m)$  and  $\mathbf{v}(m)$  are defined as  $\mathbf{d}(m)$ ,

$$\mathbf{H}_{j,0} = \begin{bmatrix} h_{j,0} & 0 & & 0 \\ \vdots & h_{j,0} & & \\ h_{j,L-1} & & \ddots & \\ 0 & & h_{j,L-1} & h_{j,0} \end{bmatrix}$$

<sup>2</sup>Note that the WCDMA STBC differs slightly from the original Alamouti STBC. This is done to ensure that one antenna operates under normal mode. i.e. by switching off the second antenna, we have the normal transmission of sequence  $\mathbf{d}(m)$

and

$$\mathbf{H}_{j,1} = \begin{bmatrix} & h_{j,L-1} & \cdots & h_{j,1} \\ & & \ddots & \vdots \\ & & & h_{j,L-1} \\ 0 & & & \end{bmatrix}$$

## 6.4 Asymptotic Performance of STTD

To study the asymptotic performance of the two considered receivers, we suppose that the spreading factor and the number of users tend to infinity while their ratio remains constant (see for example [71, 25]). In this scenario, it can be shown that the Inter Symbol Interference (ISI) term has no effect on the asymptotic SINR (see Chapter 5 and [25] for example). Model (6.11) can be replaced by the following model:

$$\begin{bmatrix} \mathbf{x}(m) \\ \bar{\mathbf{x}}(m+1) \end{bmatrix} = \begin{bmatrix} \mathbf{H}_1 & \mathbf{H}_2 \\ -\bar{\mathbf{H}}_2 & \bar{\mathbf{H}}_1 \end{bmatrix} \begin{bmatrix} \mathbf{d}(m) \\ \bar{\mathbf{d}}(m+1) \end{bmatrix} + \begin{bmatrix} \mathbf{v}(m) \\ \bar{\mathbf{v}}(m+1) \end{bmatrix} \quad (6.12)$$

where  $\mathbf{H}_j$  is the circulant Toeplitz matrix defined by:

$$\mathbf{H}_j = \begin{bmatrix} h_{j,0} & 0 & h_{j,L-1} & \cdots & h_{j,1} \\ \vdots & h_{j,0} & & \ddots & \vdots \\ h_{j,L-1} & & & & h_{j,L-1} \\ & \ddots & \ddots & & \\ 0 & & h_{j,L-1} & & h_{j,0} \end{bmatrix}$$

To simplify the analysis, we can replace (6.12) by the following equivalent model:

$$\mathbf{y} = \mathcal{H}\mathcal{C}\mathcal{B} + \mathcal{V} \quad (6.13)$$

where

$$\mathbf{y} = [x(mN+1) \ x^*((m+1)N+1) \dots x(mN+N) \ x^*((m+1)N+N)]^T$$

$\mathcal{H}$  is a block Toeplitz matrix of the same structure as  $\mathbf{H}_j$  whose  $2 \times 2$  blocks are equal to

$$\begin{bmatrix} h_{1,l} & h_{2,l} \\ -(h_{2,l})^* & (h_{1,l})^* \end{bmatrix}$$

$$\mathcal{C} = (\mathbf{S}(m)\mathbf{C}) \otimes \mathbf{A}_{1,1} + (\bar{\mathbf{S}}(m+1)\mathbf{C}) \otimes \mathbf{A}_{2,2}$$

$\mathbf{A}_{i,j}$  stands for a 2 by 2 matrix whose entry  $(i,j)$  is equal to 1 and all other entries are equal to zero,

$$\mathcal{B} = [b_1(m) \ b_1^*(m+1) \ b_2(m) \ b_2^*(m+1) \dots b_K(m) \ b_K^*(m+1)]^T$$

and  $\mathcal{V}$  has the same structure as  $\mathbf{y}$ .  $\mathcal{C}$  can be interpreted as the overall code matrix. Note we have omitted the time index as it is irrelevant.

### 6.4.1 The receivers

The RAKE receiver is a matched filter matched to the signature of the user of interest. Suppose that we want to retrieve  $b_1(m)$ , that is the symbol transmitted by user 1 at time instant  $m$  from antenna 1. Let  $\mathcal{C} = [\mathbf{w}_1 \ \mathbf{U}]$ , where  $\mathbf{w}_1$  is the overall code of the user of interest and  $\mathbf{U}$  represents the matrix of interferers codes.

The soft estimate of  $b_1(m)$  is given by:

$$\tilde{b}_1(m) = \mathbf{w}_1^H \mathcal{H}^H \mathbf{y} \quad (6.14)$$

The SINR, that we index by the spreading factor, corresponding to this receiver is given by :

$$\beta_{RAKE}^{(N)} = \frac{|\mathbf{w}_1^H \mathcal{H}^H \mathcal{H} \mathbf{w}_1|^2}{\mathbf{w}_1^H \mathcal{H}^H (\mathcal{H} \mathbf{U}_1 \mathbf{U}_1^H \mathcal{H}^H + \sigma^2 \mathbf{I}) \mathcal{H} \mathbf{w}_1} \quad (6.15)$$

The MMSE equalizer-based receiver consists of a MMSE channel-equalizer followed by a despreader. The MMSE equalizer is given by:

$$\mathbf{G} = \mathcal{H}^H (\mathcal{H} \mathcal{H}^H + \frac{N\sigma^2}{K} \mathbf{I})^{-1} \quad (6.16)$$

The soft estimate of  $b_1(m)$  is given by:

$$\tilde{b}_1(m) = \mathbf{w}_1^H \mathbf{G} \mathbf{y} \quad (6.17)$$

Note that this is exactly the Wiener receiver that would be implemented if the chip sequence were considered i.i.d with variance  $\frac{K}{N}$ . The corresponding SINR is:

$$\beta_{MMSE}^{(N)} = \frac{|\mathbf{w}_1^H \mathbf{G} \mathcal{H} \mathbf{w}_1|^2}{\mathbf{w}_1^H \mathbf{G} (\mathcal{H} \mathbf{U}_1 \mathbf{U}_1^H \mathcal{H}^H + \sigma^2 \mathbf{I}) \mathbf{G}^H \mathbf{w}_1} \quad (6.18)$$

### 6.4.2 Asymptotic analysis

The expressions of the MMSE and the RAKE SINRs depend in a complex way on the spreading codes. To overcome the difficulty of interpreting them, we study their limit in the asymptotic regime, i.e. we suppose that  $N \rightarrow \infty$ ,  $K \rightarrow \infty$  while  $\frac{K}{N} \rightarrow \alpha$  where  $1 > \alpha > 0$ . Under these conditions  $\beta_{MMSE}^{(N)}$  and  $\beta_{RAKE}^{(N)}$  can be shown to converge to deterministic limits  $\beta_{MMSE}$  and  $\beta_{RAKE}$  respectively. These limits depend only on the channel, the noise variance and the load factor (and not on the spreading codes or the specific realization of the scrambling code anymore). Note that, asymptotically, model (6.13) is equivalent to the following chip-rate  $2 \times 2$  MIMO system:

$$\begin{bmatrix} x(n) \\ \bar{x}(n+N) \end{bmatrix} = H(z) \begin{bmatrix} d(n) \\ \bar{d}(n+N) \end{bmatrix} + \begin{bmatrix} v(n) \\ \bar{v}(n+N) \end{bmatrix} \quad (6.19)$$

for  $2kN < n \leq (2k+1)N$ ,

where  $H(z) = \begin{bmatrix} h_1(z) & h_2(z) \\ -\bar{h}_2(z) & \bar{h}_1(z) \end{bmatrix}$

The MMSE equalizer designed to recover  $d(n)$  from  $x(n)$  is thus given by:

$$\begin{bmatrix} g_1(z) & g_2(z) \end{bmatrix} = [\bar{h}_1(z^{-1}) - h_2(z^{-1})](H(z)H^H(z^{-1}) + \frac{\sigma^2}{\alpha})^{-1} \quad (6.20)$$

where we have replaced  $\frac{K}{N}$  by  $\alpha$ .

We are now in a position to give the two main results of this chapter. The limit SINR of the RAKE and MMSE-equalizer are given in theorems 6.1 and 6.2. A sketch of the proof are given in appendix C.1.

**Theorem 6.1** *Under the assumption that the scrambling sequence is i.i.d with variance 1,*

$$\lim_{N \rightarrow \infty, \frac{K}{N} \rightarrow \alpha} \beta_{RAKE}^{(N)} \rightarrow \beta_{RAKE}$$

given by:

$$\beta_{RAKE} = \frac{|R_{h_1}(0)|^2}{\alpha(\sum_{k \neq 0} |R_{h_1}(k)|^2 + \sum_k |R_{h_2}(k)|^2) + \sigma^2 R_{h_1}(0)} \quad (6.21)$$

where:

$$|h_1(e^{2i\pi kf})|^2 + |h_2(e^{2i\pi kf})|^2 = \sum_k R_{h_1}(k) e^{-2i\pi kf} \quad (6.22)$$

$$\bar{h}_1(e^{-2i\pi f}) h_2(e^{2i\pi f}) - h_2(e^{-2i\pi f}) \bar{h}_1(e^{2i\pi f}) = \sum_k R_{h_2}(k) e^{-2i\pi kf} \quad (6.23)$$

and the convergence stands for the convergence in probability.

**Theorem 6.2** *Under the assumption that the scrambling sequence is i.i.d with variance 1,*

$$\lim_{N \rightarrow \infty, \frac{K}{N} \rightarrow \alpha} \beta_{MMSE}^{(N)} \rightarrow \beta_{MMSE}$$

given by:

$$\beta_{MMSE} = \frac{|R_{g_1}(0)|^2}{\alpha(\sum_{k \neq 0} |R_{g_1}(k)|^2 + \sum_k |R_{g_2}(k)|^2) + \sigma^2(\sum_k |g_1(k)|^2 + |g_2(k)|^2)} \quad (6.24)$$

where:

$$g_1(e^{2i\pi f})h_1(e^{2i\pi f}) - g_2(e^{2i\pi f})\overline{h_2}(e^{2i\pi f}) = \sum_k R_{g_1}(k)e^{-2i\pi kf} \quad (6.25)$$

$$g_1(e^{2i\pi f})h_2(e^{2i\pi f}) + g_2(e^{2i\pi f})\overline{h_1}(e^{2i\pi f}) = \sum_k R_{g_2}(k)e^{-2i\pi kf} \quad (6.26)$$

and the convergence stands for the convergence in probability.

### 6.4.3 Discussion of the two theorems

The expression of the RAKE receiver SINR contains the desired signal term in the numerator and three undesired terms in the denominator. The third term stems from the effect of noise and will not be discussed. The first undesired term

$$\alpha \left( \sum_{k \neq 0} |R_{h_1}(k)|^2 \right)$$

is the classical Multi Access Interference (MAI) which is due to the non-perfect nature of each channel separately. The second undesired term  $\alpha \left( \sum_k |R_{h_2}(k)|^2 \right)$  is more interesting and can be interpreted as the Cross-Channel Interference (CCI) due to the simultaneous use of two multipath channels (see equation 6.22). Note that if the channels were single path (flat-fading), then we would have (by virtue of equation 6.22)  $R_{h_1}(k) = 0$  and  $R_{h_2}(k) = 0$  for  $k \neq 0$ . This means that the first term in the denominator would vanish. The second term would also vanish because:

$$\sum_k R_{h_2}(k)e^{-2i\pi kf} = (h_{1,0})^* h_{2,0} - h_{2,0}(h_{1,0})^* = 0$$

and only the noise term would remain in the denominator. On the other hand, when there is no transmit diversity (i.e.  $h_2(z) = 0$ ), part of the first term ( $\alpha \sum_{k \neq 0} |R_{h_1}(k)|^2$ ) would still be present (see equation (6.22)), while the second term would vanish.

The remark that the CCI vanishes for single path channels was behind the original Alamouti STBC proposed for single-user flat-fading channels. For multipath channels, however, the CCI can be very high, and the STBC may deteriorate the performances when used with a RAKE receiver. The MAI and CCI terms are both weighted by the load factor  $\alpha$ . This explains the fact that the SINR is higher for lightly loaded systems and vice versa.

Concerning  $\beta_{MMSE}$ , we first mention how  $R_{g_1}(k)$  and  $R_{g_2}(k)$  behave. The MMSE-equalizer tries to recover  $\mathbf{d}(m)$  from  $\mathbf{x}(m)$  and  $\mathbf{x}(m+1)$  (see equation 6.19). It strives to make  $R_{g_1}(e^{2i\pi f})$  close to a single path channel (which is the case in the absence of noise). This is done by concentrating the energy of in the central term  $R_{g_1}(0)$ . On the other hand, the coefficients  $R_{g_2}(k)$  are made as close to zero as possible. Now, looking at

the expression of  $\beta_{MMSE}$ , we see that the first term in the denominator decreases with respect to the first term in the denominator of  $\beta_{RAKE}$ . The second term, the CCI, also decreases and the noise is this time filtered by the two equalizers. The numerator, on the other hand, remains comparable to the RAKE case. By decreasing the first and second terms in the denominator while keeping the third term and the numerator comparable, the SINR is increased.

## 6.5 Simulation Results

### 6.5.1 Comparison of empirical BER and asymptotic BER

We begin by verifying that our asymptotic analysis allows to predict the performance of W-CDMA. We have implemented the physical layer of the downlink of the UMTS-FDD, and we have compared the measured Bit Error Rate (BER) obtained for  $N = 256$  and  $K = 128$  with its asymptotic evaluation given by  $Q(\sqrt{\beta_{MMSE}})$  and  $Q(\sqrt{\beta_{RAKE}})$ . The results are presented in Figure 6.3. The propagation channel is the Vehicular A channel. The profile of the vehicular A channels is shown in Table 6.1. Recall that the chip period  $T_c$  is equal to  $T_c = 260nsec$ .

Vehicular A Path Delay in nsec	0	310	710	1090	1730	2510
Vehicular A Average Power (dB)	0	-1.0	-9.0	-10.0	-15.0	-20.0
Pedestrian A Path Delay in nsec	0	110	190	410		
Pedestrian A Average Power (dB)	0	-9.7	-19.2	-22.8		

Table 6.1: The Vehicular A and Pedestrian A channel profiles.

It is noteworthy that the receiver we implemented is based on the correct model (6.10), thus showing that the approximation (6.12) is justified in this context. Figure 6.3. shows that our asymptotic evaluations allow to predict rather accurately the BER performance for  $N = 256$ .

### 6.5.2 Gain of STTD for non-severe channels

We next study the gain obtained by using the Alamouti scheme in CDMA with multipath channels. For this, we represent in the following the asymptotic BER for a half-loaded CDMA system obtained by using a RAKE receiver and a MMSE equalizer-based receiver. We compare the performances in the case where we use transmit diversity with the case

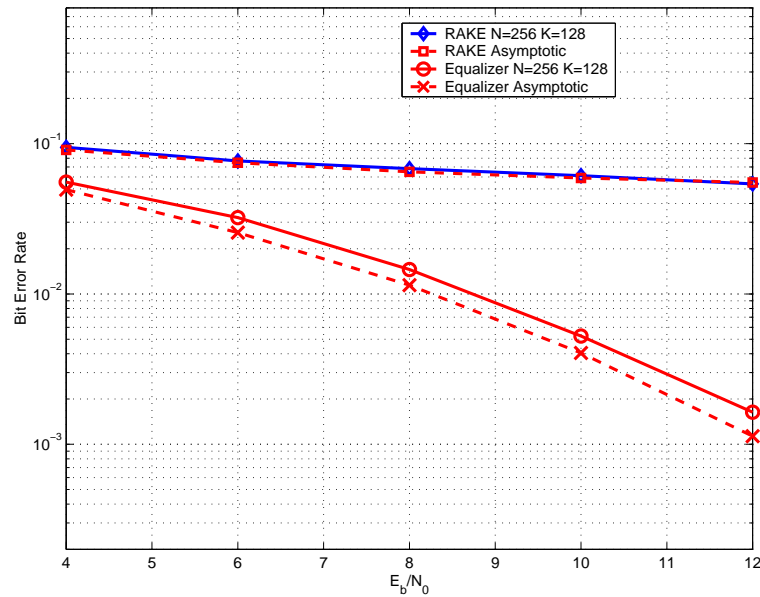


Figure 6.3: Comparison of empirical and theoretical BER.

where there is no transmit diversity<sup>3</sup>. We start first by considering a case where STTD gives some improvement. For this we consider the propagation channel to be the Pedestrian A channel. The power profile of the Pedestrian A channel is given in Table 6.1. The load factor is equal to 1/2. The results are shown in Figure 6.4.

We remark that the use of STTD allows a very important gain for both receivers: The RAKE and the Equalizer-based one. Note, however, that the Pedestrian A channel is not a severe channel because the power profile decreases very rapidly as a function of the channel path. The gain provided in severe channels will be investigated in the following figures.

### 6.5.3 Gain of STTD for severe channels

We keep the same setting as the previous experiment and consider the propagation channel to have three equal power paths spaced by twice the chip period. The results are shown in Figure 6.5. We note that in this setting, the transmit diversity deteriorates the performances of the RAKE receiver because the CCI is greater than the diversity provided. In the case of the equalizer-based receiver, not only does it outperform the RAKE receiver in both cases, but it gives a better performance in the case of STTD because the

<sup>3</sup>For the comparison to be fair, the total transmitted power should be the same in both cases.

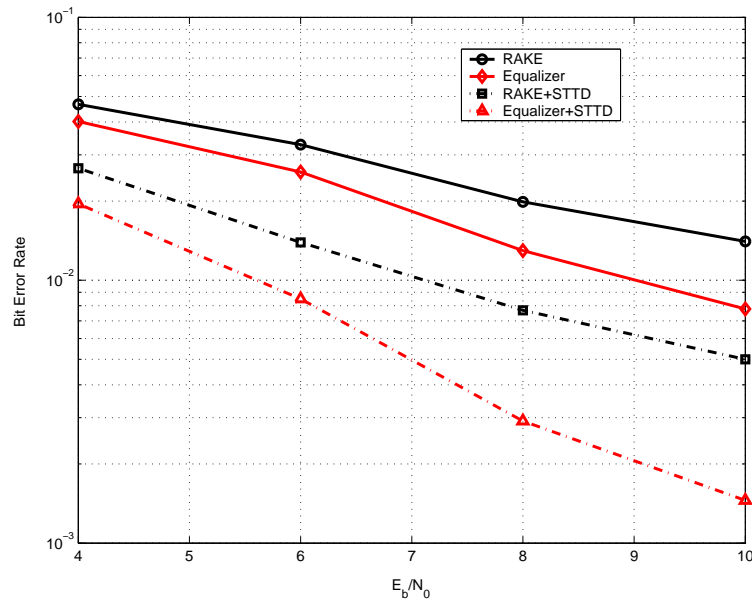


Figure 6.4: The BER of the two receivers with and without transmit diversity for the Pedestrian A channel,  $\alpha = 0.5$

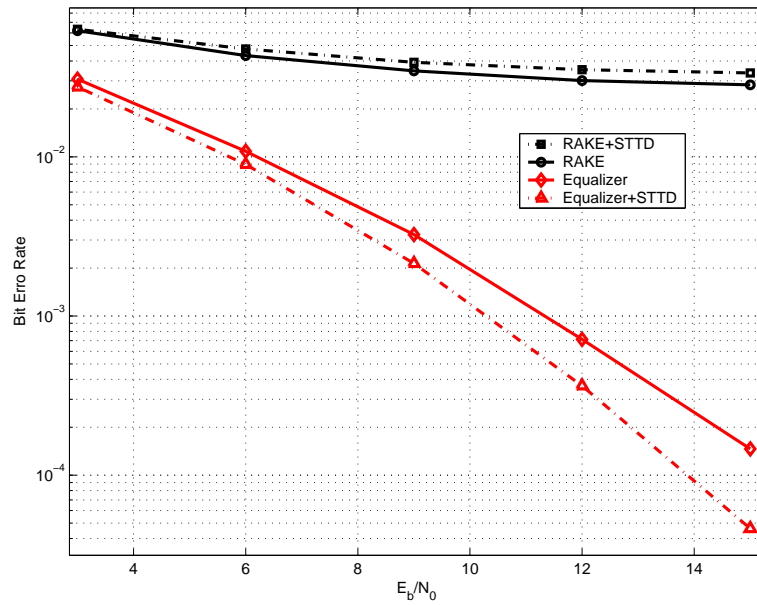


Figure 6.5: The BER of the two receivers with and without transmit diversity for a three equal path channel,  $\alpha = 0.5$ .

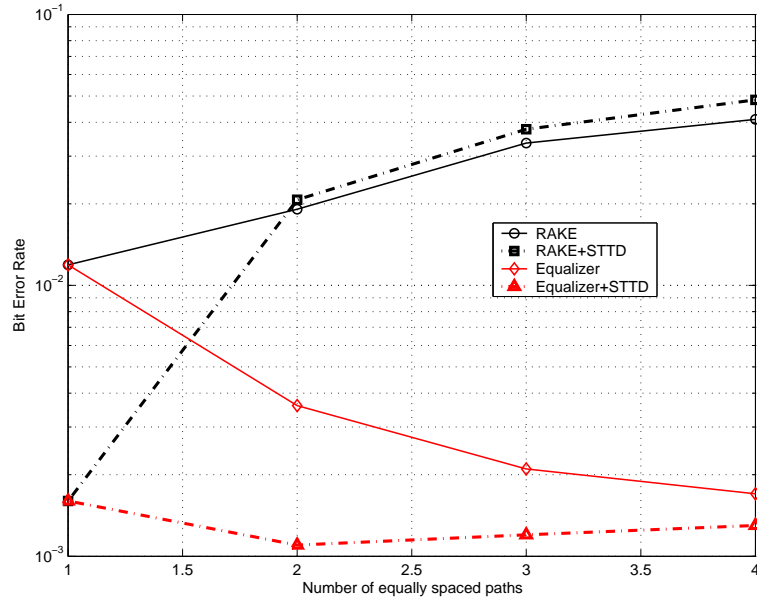


Figure 6.6: BER with and without transmit diversity Vs the number of channel paths

CCI is partially cancelled out.

#### 6.5.4 Effect of multipath channels on the performance of STTD

To have a clearer idea about the effect of multipath channels on the performance of STTD, we plot the BER obtained by using the two receivers (with and without diversity) as a function of the number of the channel paths. All the paths are assumed to have the same power and to be spaced by a chip period,  $E_b/N_0 = 10dB$ . The results are shown in Figure 6.6. The MMSE equalizer is known to outperform the RAKE receiver (without diversity). We note that the use of STTD deteriorates the BER performance when using a RAKE receiver, while it improves the BER performance when using a MMSE equalizer. This is a very important remark since it is another argument toward the use of equalizer-based receivers for third generation systems.

## 6.6 Conclusion

In this chapter, we have addressed the performance of Space Time Transmit Diversity in the downlink of W-CDMA over frequency-selective fading channels. We have derived asymptotic expressions of SINR provided by two kinds of receiver: the RAKE receiver and the chip-level MMSE equalizer-based receiver. Simulation results show that our

asymptotic expressions allow to predict the performance of UMTS-FDD for  $N = 256$ . We have noticed that for some channels, the RAKE receiver deteriorates the BER performance when using STTD, while the equalizer based receiver still gives some improvement. This is another reason to use equalizer based receiver for 3G systems other than the fact that the MMSE equalizer outperforms the RAKE receiver when used without diversity.



# Chapter 7

## Concluding remarks

---

In this thesis, we study the performance of reduced-rank receivers for Downlink Code Division Multiple Access (CDMA) systems. A reduced-rank receiver stands for a receiver that differs from the full-rank one in that only some of the filter coefficients are optimized. This represents an important gain in the computational complexity and can speed up the convergence in the case of rapidly varying channels. Two kinds of receivers are considered: the optimum reduced-rank receiver and the suboptimum reduced-rank receivers. The optimum reduced-rank receiver, sometimes called symbol-level receiver, stands for the classical Wiener receiver whose output is the estimated user symbols. The suboptimum reduced-rank receiver, on the other hand, stands for a class of receivers which consist of a reduced-rank chip-level equalizer followed by despreading. These receivers are strong candidates to replace the conventional receiver for CDMA: the RAKE receiver. Two other techniques that allow to improve the RAKE performance are discussed: the Parallel Interference Cancellation (PIC) and Space Time Transmit Diversity (STTD). In what follows, we present a summary of the contributions with possible improvement and future work.

### **7.1 Equalizer and Blind Interference Cancellation based receivers**

#### **7.1.1 Reduced-rank equalization algorithms**

In the first part, we consider the reduced-rank filtering algorithms and their application to the equalization in the forward link of W-CDMA. The problem that arises in W-CDMA

is the presence of a long scrambling code that breaks the received signal cyclostationarity. For this reason, symbol level receivers cannot be used. The solution is to use equalization prior to despreading (and descrambling). The equalization can be used in a reduced-rank fashion, thus reducing the overall complexity. In chapter 2, we adapt two algorithms originally proposed for periodic CDMA to long-code CDMA with a permanent code-multiplexed pilot. The error driven filter can be trained using the received signal as an input and the pilot chips as a desired output. The problem with this method of adaptation is that it suffers from Multi Access Interference (MAI) because we only know part of the desired output (the pilot chips). An alternative approach would be to perform despreading (and descrambling) of shifted versions of the received signal. The resulting modified received signal is then used as an input to the error-driven filter. The corresponding desired output is the pilot symbols. We show that the Wiener equalizer obtained in the two cases is equal up to a constant multiplicative factor. Extensive simulation results are presented where we remark that the BER performance is very close to the optimal (MMSE) equalizer even for moderate values of the rank. This phenomenon can be understood better by using the asymptotic performance discussed in the second part of the thesis.

### 7.1.2 Blind Interference Cancellation

#### Blind PIC for multi-rate CDMA

Another way to improve the BER performance is to use Parallel Interference Cancellation (PIC) in which interferers symbols are estimated and their effect is subtracted from the received signal. This allows a better detection of the desired user symbols. The problem that arises in WCDMA is that the users codes are not known and cannot be estimated by averaging because they are of different lengths (multi-rate). In chapter 3, we propose to combine equalization with a partial PIC technique that assumes the presence of (virtual) codes of the same length as the user of interest. By doing this, we remove a very important part of the interference while keeping reasonable complexity.

#### Noise-subspace based PIC for periodic CDMA

In the case of short code CDMA, the cyclostationarity of the received signal can be exploited to estimate the signal and noise subspaces. Following a previously proposed method based on signal subspace, we propose a new method: the Code Detection Blind Interfering Cancellation (CD-BIC) algorithm, based on the noise subspace that performs very well for a weak number of users using Walsh-Hadamard codes. The corresponding

article is given in appendix D.

It is possible to further reduce the computational cost of the CD-BIC by considering only few noise vectors instead of the whole noise subspace. Indeed, it can be shown that both the subspace-based channel estimation and the code-detection can be achieved consistently using one or few noise vectors only. This would lead to a considerable reduction of the computational cost. A further improvement would be to design an adaptive algorithm of the CD-BIC algorithm by tracking the noise-subspace using existing work on this subject.

## 7.2 Asymptotic performance of CDMA receivers

The second part of the thesis concerns the analysis of the performance of reduced-rank Wiener receivers, reduced-rank MMSE equalizers and Space Time Transmit Diversity (STTD). The study of these receivers for finite size of the spreading factor  $N$  is very difficult. In fact, the Signal to Interference Noise Ratios (SINRs) of these receivers, usually considered as a performance measure, depends in a complicated way on the spreading codes, the powers, the system load and the channel. It has become classical now to model the code matrix as a random matrix following a certain distribution. The SINR can be interpreted in this case as a random variable. Due to some averaging phenomena, the SINR converges in probability to a *deterministic* limit when the number of users  $K$  and the spreading factor  $N$  tend to infinity at the same rate. We apply the same technique to study the performance of the reduced-rank receivers. Both optimal and suboptimal receivers are considered. The Space-Time Transmit diversity is also studied when combined with the RAKE receiver and the MMSE equalizer based receiver.

### 7.2.1 Asymptotic performance of reduced-rank Wiener receivers

In the context of randomly spread CDMA, Tse and Hanly have obtained a fixed point equation for the asymptotic SINR of the Wiener receiver. This equation allows a better understanding of the parameters influencing the performance of the Wiener receiver. In the same context, Honig and Xiao obtained a recurrence relation between the asymptotic SINRs of reduced-rank receivers of successive ranks. The Honig-Xiao formula is valid for equal power case but allows nevertheless to show by simulations that the convergence of the reduced-rank SINR to the full-rank SINR is very rapid. In chapter 4, we review the main results of Tse-Hanly and Honig-Xiao. We then present new results that were developed during this thesis with the work of Loubaton and Hachem. We show that the

convergence of the reduced-rank SINR to the full-rank SINR is locally exponential (thus very rapid) and exhibit the different parameters that can speed up or slow down the convergence.

The results of chapter 4 concern mainly the randomly spread CDMA with i.i.d spreading and no fading. In appendix E, we use the results of Loubaton-Hachem to study the performance of reduced-rank Wiener receivers for CDMA systems corrupted by frequency selective fading channels. The spreading matrix is considered to be extracted from a Haar matrix. Thus, although this matrix is random, it remains orthogonal. This allows a better approximation of real life systems in which orthogonal Walsh-Hadamard codes are used.

### 7.2.2 Asymptotic performance of reduced-rank equalization

The performance of suboptimum Wiener receivers (both full-rank and reduced-rank) has received much less attention than their optimum counterparts. Apart from some work on the asymptotic performance of full-rank suboptimum Wiener receivers, we could not find any previous work that treats this aspect. In chapter 5, we consider the performance of reduced-rank suboptimum Wiener receivers in the context of downlink W-CDMA in frequency-selective fading channels. Motivated by the specifications of the UMTS-FDD, we consider a random scrambling code and orthogonal Walsh-Hadamard codes. In this context, we show that, like the optimum case, the convergence of the reduced-rank SINR to the full-rank SINR is locally exponential. We exhibit the different parameters that influence the convergence.

### 7.2.3 Asymptotic performance of Space Time Transmit Diversity

Besides equalization and Parallel Interference Cancellation, Space-Time Transmit Diversity represents a simple, yet powerful, technique to improve the system performance. By using two transmit antennas and one receive antenna, we can take advantage of increased diversity without the need to include additional antennas at the receiver side. In the current specifications, the STTD is intended to work with the RAKE receiver. However, the MMSE equalizer can be used with STTD and gives a better performance. Following similar arguments as in chapters 4 and 5, we study in chapter 6 the asymptotic performance of Space Time Transmit Diversity when used with a RAKE receiver and an equalizer-based receiver. We notice that the performance of the RAKE receiver can be worse when used with STTD for some very selective channels. The equalizer based STTD, however, does

not suffer from this problem. Thanks to channel "inversion", the diversity provided is made higher than the cross-channel interference created due to the simultaneous use of two multipath channels.

Chapter 6 considers the performance of the RAKE (rank 1) and the MMSE equalizer (full-rank) when coupled with Space Time Transmit Diversity. In the same context, it would be interesting to consider the performance of reduced-rank equalization (of different ranks ranging from 1 to full rank) when used with STTD. Other forms of Transmit Diversity have been proposed and standardized in the UMTS-FDD. The other main open loop transmit diversity scheme is the Orthogonal Transmit Diversity (OTD). In OTD, two transmit antennas and one receive antenna are used. The symbols are transmitted through different antennas using spreading codes that are twice longer than the spreading factor (to keep the same rate). The Asymptotic analysis can be extended Orthogonal Transmit Diversity (OTD) since the principle is very close to STTD.



# Appendix A

## Appendix to chapter 2

### A.1 Proof of proposition 2.1

In this appendix, we will show that  $\mathbf{R}_{yy}^{-1}\mathbf{r}_{yb}$  is equal up to a constant multiplicative factor to  $\mathbf{R}_{xx}^{-1}\mathbf{r}_{xd}$ .

i) **The first step:** It can be shown that:

$$\mathbf{R}_{yy} = \mathbf{R}_{xx} + \gamma_1 \mathbf{h}\mathbf{h}^H, \quad (\text{A.1})$$

where  $\gamma_1$  is a scalar, See [32, 24]. Then, matrix  $\mathbf{R}_{yy}$  differs from  $\mathbf{R}_{xx}$  by a rank 1 matrix.

ii) **The second step:** is to show that:

$$\mathbf{r}_{yb} = a\mathbf{r}_{xd} \quad (\text{A.2})$$

That is  $\mathbf{r}_{yb}$  and  $\mathbf{r}_{xd}$  are equal up to a constant multiplicative factor. In fact,

$$\begin{aligned} & \mathbb{E}\{y_{l,1}(m)b_1^*(m)\} \\ &= \mathbb{E}\left\{\sum_i x(nN - l + i)]s^*(mN + i)c_1^*(i)b_1^*(m)\right\} \\ &= \mathbb{E}\left\{\sum_i x(mN - l + i)d_1^*(mN + i)\right\} \end{aligned}$$

recall that for each  $m$ , the sequence  $d_1(mN + i)$  is a known deterministic sequence (it represents the  $N$  pilot chips at the  $m^{\text{th}}$  symbol), thus we can write:

$$\mathbb{E}\{y_{l,1}(m)b_1^*(m)\} = \sum_i \left\{ \mathbb{E}\left\{x(mN - l + i)\right\} d_1^*(mN + i) \right\}$$

Now,  $x(mN - l + i)$  is the sum of the received signal due to the pilot chips and all the remaining users. because of the assumption that users symbols are independent, the

received signal of all the remaining users is a zero-mean one. Then we can write:

$$\mathbb{E}\{y_{l,1}(m)b_1^*(m)\} = \sum_i x_1(mN - l + i) d_1^*(mN + i)$$

Now, the  $l^{\text{th}}$  coefficient of vector  $\mathbf{r}_{yb}$  is given by:

$$\begin{aligned} & \lim_{M \rightarrow \infty} \frac{1}{M} \sum_{m=0}^{M-1} \left\{ \mathbb{E}\{y_{l,1}(m)b_1^*(m)\} \right\} \\ &= \sum_i \lim_{M \rightarrow \infty} \frac{1}{M} \sum_{m=0}^{M-1} x_1(mN - k + i) d_1^*(mN + i) \\ &= \sum_i \lim_{M \rightarrow \infty} \frac{1}{M} \sum_{m=0}^{M-1} \mathbb{E}\{x(mN - l + i) d^*(mN + i)\} \\ &= \sum_i \lim_{M \rightarrow \infty} \frac{1}{M} \sum_{m=0}^{M-1} \mathbb{E}\{x(mN - l + i) d^*(mN)\} \end{aligned}$$

the last expression is equal up to a constant multiplicative factor to

$$\lim_{M \rightarrow \infty} \frac{1}{M} \sum_{m=0}^{M-1} \mathbb{E}\{x(m - l) d^*(mN)\}$$

which is the  $(l)^{\text{th}}$  channel coefficient.

then  $\mathbf{r}_{yb} = a\mathbf{h} = a\mathbf{r}_{xd}$ . This completes the second step

iii) **The third step:** Let us compute  $\mathbf{R}_{yy}^{-1}\mathbf{r}_{yb}$

$$\mathbf{R}_{yy}^{-1} = (\mathbf{R}_{xx} + \gamma_1 \mathbf{h}\mathbf{h}^H)^{-1} \quad (\text{A.3})$$

using the matrix inversion lemma

$$\mathbf{R}_{yy}^{-1} = \mathbf{R}_{xx}^{-1} + \mathbf{R}_{xx}^{-1} \mathbf{h} \left( \frac{1}{\gamma_1} + \mathbf{h}^H \mathbf{R}_{xx}^{-1} \mathbf{h} \right)^{-1} \mathbf{h}^H \mathbf{R}_{xx}^{-1} \quad (\text{A.4})$$

now

$$\mathbf{R}_{yy}^{-1} \mathbf{r}_{yb} = a \mathbf{R}_{xx}^{-1} \mathbf{h} + \beta \mathbf{R}_{xx}^{-1} \mathbf{h} \mathbf{h}^H \mathbf{R}_{xx}^{-1} \mathbf{h} \quad (\text{A.5})$$

$$= \mathbf{R}_{xx}^{-1} \mathbf{h} a (1 + \beta \zeta) \quad (\text{A.6})$$

where  $\zeta = \mathbf{h}^H \mathbf{R}_{xx}^{-1} \mathbf{h}$ .

It is clear from A.6 that  $\mathbf{R}_{yy}^{-1} \mathbf{r}_{yb} = \kappa \mathbf{R}_{xx}^{-1} \mathbf{r}_{xd}$ .

This completes the proof.

# Appendix B

## Appendix to chapter 5

### B.1 Proof of Lemma 5.2

We show that  $\sup_N \|\mathcal{G}_{n,N}\| < +\infty$ . For this, we note that matrix  $\mathcal{G}_{n,N}$  is a Toeplitz matrix associated to the transfer function  $g_n(z)$ . Therefore, for each  $N$ ,  $\|\mathcal{G}_{n,N}\| < \|g_n\|_\infty = \sup_f |g_n(e^{2i\pi f})|$ . Hence,

$$\sup_N \|\mathcal{G}_{n,N}\| < \sup_N \|g_n\|_\infty$$

We now prove that  $\sup_N \|g_n\|_\infty < +\infty$ . As  $h(z)$  is a degree  $L$  FIR filter, we claim that if  $N$  is large enough, then the number of non zero coefficients of  $g_n(z)$  is less than  $(2n-1)L$ , and thus remains finite when  $N \rightarrow +\infty$ . In effect, row vector  $\mathbf{g}_n$  is a linear combination of the rows  $(\mathbf{h}_{2N}^H, \mathbf{h}_{2N}^H \mathbf{R}_{2N}, \dots, \mathbf{h}_{2N}^H \mathbf{R}_{2N}^{n-1})$  of matrix  $\mathbf{K}_{n,2N}^H$ . If  $N$  is large enough, for each  $1 \leq k \leq (n-1)$ ,  $\mathbf{R}_{2N}^k$  is a band matrix whose entries  $(\mathbf{R}_{2N}^k)_{i,j}$  are zero if  $|i-j| > kL$ . It is therefore easy to check that components 1 to  $N - kL - 1$  and  $N + (k+1)L + 1$  to  $2N$  of vector  $\mathbf{h}_{2N}^H \mathbf{R}_{2N}^k$  are zero. This implies that components 1 to  $N - (n-1)L - 1$  and  $N + nL + 1$  to  $2N$  of any linear combination of the rows of  $\mathbf{K}_{n,2N}^H$  are zero if  $N$  is large enough. In order to establish that  $\sup_N \|g_n\|_\infty < +\infty$ , it is therefore sufficient to show that the (euclidian) norm  $\|\mathbf{g}_n\|$  of vector  $\mathbf{g}_n$  remains bounded when  $N$  increases. For this, we remark that

$$\|\mathbf{g}_n\|^2 = \mathbf{h}_{2N}^H \mathbf{K}_{n,2N} (\mathbf{K}_{n,2N}^H \mathbf{R}_{2N} \mathbf{K}_{n,2N})^{-1} \mathbf{K}_{n,2N}^H \mathbf{K}_{n,2N} (\mathbf{K}_{n,2N}^H \mathbf{R}_{2N} \mathbf{K}_{n,2N})^{-1} \mathbf{K}_{n,2N}^H \mathbf{h}_{2N}.$$

As  $\mathbf{R}_{2N} \geq \frac{\sigma^2}{\alpha} \mathbf{I}_{2N}$ , it is clear that  $(\mathbf{K}_{n,2N}^H \mathbf{R}_{2N} \mathbf{K}_{n,2N})^{-1} \leq \alpha \sigma^{-2} (\mathbf{K}_{n,2N}^H \mathbf{K}_{n,2N})^{-1}$ , and that  $\mathbf{K}_{n,2N} (\mathbf{K}_{n,2N}^H \mathbf{R}_{2N} \mathbf{K}_{n,2N})^{-1} \mathbf{K}_{n,2N}^H \leq \alpha \sigma^{-2} \mathbf{K}_{n,2N} (\mathbf{K}_{n,2N}^H \mathbf{K}_{n,2N})^{-1} \mathbf{K}_{n,2N}^H$ , which is itself less than  $\alpha \sigma^{-2} \mathbf{I}_{2N}$ . This, in turn, shows that  $\|\mathbf{g}_n\|^2 \leq \frac{\alpha \|\mathbf{h}_{2N}\|^2}{\sigma^2}$ , and that the norm  $\|\mathbf{g}_n\|$  remains bounded when  $N$  increases.

## B.2 Proof of Lemma 5.3.

The proof of Lemma 5.3 needs some work. In order to make the proof easier to follow, we simplify the notations: As the parameter  $m$  is irrelevant here,  $\mathbf{S}(m)$  is denoted  $\mathbf{S}$ . Finally, matrix  $\mathbf{B}_N$  is denoted  $\mathbf{B}$ . We denote by  $b_0$  the diagonal term of  $\mathbf{B}$ , and put  $\mathbf{A} = \mathbf{B} - b_0\mathbf{I}$  and

$$T_N = \mathbf{c}_1^H \mathbf{S}^H \mathbf{B} \mathbf{S} \mathbf{C}_2 \mathbf{C}_2^H \mathbf{S}^H \mathbf{B}^H \mathbf{S} \mathbf{c}_1$$

We remark that, as the entries of matrix  $\mathbf{C}$  are equal to  $\pm \frac{1}{\sqrt{N}}$ , then, the diagonal entries of  $\mathbf{C}_2 \mathbf{C}_2^H$  are equal to  $\frac{K-1}{N}$ . We denote by  $\mathbf{D}$  the matrix  $\mathbf{D} = \mathbf{C}_2 \mathbf{C}_2^H - \frac{K-1}{N} \mathbf{I}$ . The diagonal entries of  $\mathbf{A}$  and  $\mathbf{D}$  are of course zero.  $T_N$  can be written as

$$T_N = \mathbf{c}_1^H \mathbf{S}^H (\mathbf{A} + b_0 \mathbf{I}) \mathbf{S} \mathbf{C}_2 \mathbf{C}_2^H \mathbf{S}^H (\mathbf{A} + b_0 \mathbf{I})^H \mathbf{S} \mathbf{c}_1$$

As  $\mathbf{c}_1^H \mathbf{C}_2 = 0$  and  $\mathbf{S}$  is unitary, this reduces to

$$T_N = \mathbf{c}_1^H \mathbf{S}^H \mathbf{A} \mathbf{S} \mathbf{C}_2 \mathbf{C}_2^H \mathbf{S}^H \mathbf{A}^H \mathbf{S} \mathbf{c}_1$$

Writing  $\mathbf{C}_2 \mathbf{C}_2^H$  as  $\mathbf{D} + \frac{K-1}{N} \mathbf{I}$ , we get that  $T_N$  is given by

$$T_N = \frac{K-1}{N} \mathbf{c}_1^H \mathbf{S}^H \mathbf{A} \mathbf{A}^H \mathbf{S} \mathbf{c}_1 + \mathbf{c}_1^H \mathbf{S}^H \mathbf{A} \mathbf{S} \mathbf{D} \mathbf{S}^H \mathbf{A}^H \mathbf{S} \mathbf{c}_1$$

$\mathbf{B}$  uniformly bounded implies that  $\mathbf{A} \mathbf{A}^H$  is uniformly bounded. Therefore, Lemma 5.1 implies that  $\frac{K-1}{N} \mathbf{c}_1^H \mathbf{S}^H \mathbf{A} \mathbf{A}^H \mathbf{S} \mathbf{c}_1$  converges in quadratic mean to  $\alpha \frac{1}{N} \text{Trace}(\mathbf{A} \mathbf{A}^H)$ . But, it is easy to check that

$$\frac{1}{N} \text{Trace}(\mathbf{A} \mathbf{A}^H) = \frac{1}{N} \text{Trace}(\mathbf{B} \mathbf{B}^H) - \left| \frac{1}{N} \text{Trace}(\mathbf{B}) \right|^2$$

Therefore, in order to establish that  $T_N$  converges in the least-squares sense toward

$$\alpha \left( \frac{1}{N} \text{Trace}(\mathbf{B} \mathbf{B}^H) - \left| \frac{1}{N} \text{Trace}(\mathbf{B}) \right|^2 \right)$$

it is sufficient to show that  $\epsilon_N = \mathbf{c}_1^H \mathbf{S}^H \mathbf{A} \mathbf{S} \mathbf{D} \mathbf{S}^H \mathbf{A}^H \mathbf{S} \mathbf{c}_1$  converges in the least-squares sense to 0, i.e. that  $\lim_{N \rightarrow +\infty, \frac{K}{N} \rightarrow \alpha} \mathbb{E}(\epsilon_N^2) = 0$  (note that  $\epsilon_N$  is real). For this, we have to express  $\mathbb{E}(\epsilon_N^2)$  by taking benefit that the entries  $(s_i)_{i=1, \dots, N}$  of  $\mathbf{S}$  are independent QPSK sequences and that the diagonal entries of  $\mathbf{D}$  and  $\mathbf{A}$  are zero.  $\epsilon_N$  can be written as

$$\epsilon_N = \sum_{i_1, j_1, i_2, j_2} \mathbf{c}_{i_1, 1} s_{i_1}^* \mathbf{A}_{i_1, j_1} s_{j_1} \mathbf{D}_{j_1, i_2} s_{i_2}^* (\mathbf{A}^H)_{i_2, j_2} s_{j_2} \mathbf{c}_{j_2, 1}$$

Hence,  $\mathbb{E}(\epsilon_N^2)$  is equal to

$$\sum_{(i_1, i_2, i_3, i_4), (j_1, j_2, j_3, j_4)} \mathbf{c}_{i_1, 1} \mathbf{A}_{i_1, j_1} \mathbf{D}_{j_1, i_2} (\mathbf{A}^H)_{i_2, j_2} \mathbf{c}_{j_2, 1} \mathbf{c}_{i_3, 1} \mathbf{A}_{i_3, j_3} \mathbf{D}_{j_3, i_4} (\mathbf{A}^H)_{i_4, j_4} \mathbf{c}_{j_4, 1} \mathbb{E}(s_{i_1}^* s_{j_1} s_{i_2}^* s_{j_2} s_{i_3}^* s_{j_3} s_{i_4}^* s_{j_4})$$

As  $(s_i)_{i=1,\dots,N}$  is an independent QPSK sequence, the term  $\mathbb{E}(s_{i_1}^* s_{j_1} s_{i_2}^* s_{j_2} s_{i_3}^* s_{j_3} s_{i_4}^* s_{j_4})$  is non zero if and only if it exists a permutation  $\pi$  (depending on the multi-index  $(i_1, i_2, i_3, i_4)$ ) from the set  $\{1, 2, 3, 4\}$  for which  $j_k = i_{\pi(k)}$  for each  $k \in \{1, 2, 3, 4\}$ . In this case,  $\mathbb{E}(s_{i_1}^* s_{j_1} s_{i_2}^* s_{j_2} s_{i_3}^* s_{j_3} s_{i_4}^* s_{j_4})$  is equal to 1. As the diagonal entries of  $\mathbf{A}$  and  $\mathbf{D}$  are zero, coefficient

$$\mathbf{c}_{i_1,1} \mathbf{A}_{i_1,j_1} \mathbf{D}_{j_1,i_2} (\mathbf{A}^H)_{i_2,j_2} \mathbf{c}_{j_2,1} \mathbf{c}_{i_3,1} \mathbf{A}_{i_3,j_3} \mathbf{D}_{j_3,i_4} (\mathbf{A}^H)_{i_4,j_4} \mathbf{c}_{j_4,1}$$

is possibly non zero only if  $j_k \neq i_k$  for  $k \in \{1, 2, 3, 4\}$  and  $j_{k-1} \neq i_k$  for  $k \in \{2, 3, 4\}$ , that is if

$$\pi(1) \neq 1, \pi(1) \neq 2, \pi(2) \neq 2, \pi(3) \neq 3, \pi(3) \neq 4, \pi(4) \neq 4$$

Therefore, a permutation  $\pi$  corresponds to a possibly non zero term if

$$\pi(1) \in \{3, 4\}, \pi(2) \in \{1, 3, 4\}, \pi(3) \in \{1, 2\}, \pi(4) \in \{1, 2, 3\}$$

This corresponds to the following 5 possible permutations:

- $\pi(1) = 3, \pi(3) = 1, \pi(2) = 4, \pi(4) = 2$ , permutation  $\pi_1$ ,
- $\pi(1) = 3, \pi(3) = 2, \pi(2) = 4, \pi(4) = 1$ , permutation  $\pi_2$ ,
- $\pi(1) = 4, \pi(3) = 1, \pi(2) = 3, \pi(4) = 2$ , permutation  $\pi_3$ ,
- $\pi(1) = 4, \pi(3) = 2, \pi(2) = 1, \pi(4) = 3$ , permutation  $\pi_4$ ,
- $\pi(1) = 4, \pi(3) = 2, \pi(2) = 3, \pi(4) = 1$ , permutation  $\pi_5$ .

In the following, we denote by  $\mathbf{i} = (i_1, i_2, i_3, i_4)$  a four-dimensional multi-index, and for each  $k = 1, \dots, 5$ , by  $\pi_k(\mathbf{i})$  the multi-index  $(i_{\pi_k(1)}, i_{\pi_k(2)}, i_{\pi_k(3)}, i_{\pi_k(4)})$ . We will show below that for each  $k = 1, 2, \dots, 5$ , then,

$$\sum_{\mathbf{i}} \sum_{\mathbf{j}=\pi_k(\mathbf{i})} \mathbf{c}_{i_1,1} \mathbf{A}_{i_1,j_1} \mathbf{D}_{j_1,i_2} (\mathbf{A}^H)_{i_2,j_2} \mathbf{c}_{j_2,1} \mathbf{c}_{i_3,1} \mathbf{A}_{i_3,j_3} \mathbf{D}_{j_3,i_4} (\mathbf{A}^H)_{i_4,j_4} \mathbf{c}_{j_4,1} \rightarrow 0 \quad (\text{B.1})$$

Unfortunately, this does not show that  $\mathbb{E}(\epsilon_N^2)$  converges to 0 because

$$\mathbb{E}(\epsilon_N^2) \neq \sum_{k=1}^5 \sum_{\mathbf{i}} \sum_{\mathbf{j}=\pi_k(\mathbf{i})} \mathbf{c}_{i_1,1} \mathbf{A}_{i_1,j_1} \mathbf{D}_{j_1,i_2} (\mathbf{A}^H)_{i_2,j_2} \mathbf{c}_{j_2,1} \mathbf{c}_{i_3,1} \mathbf{A}_{i_3,j_3} \mathbf{D}_{j_3,i_4} (\mathbf{A}^H)_{i_4,j_4} \mathbf{c}_{j_4,1} \quad (\text{B.2})$$

This is because, for certain multi-indices  $\mathbf{i}$  having identical components, it may exist  $k \neq l$  for which  $\pi_k(\mathbf{i}) = \pi_l(\mathbf{i})$ . For example, if  $i_1 = i_2$ , then  $\pi_1(\mathbf{i}) = \pi_2(\mathbf{i})$ . These multi-indices are thus taken into account at least 2 times in the righthandside of equation (B.2). In order to show that  $\mathbb{E}(\epsilon_N^2)$  converges toward 0, the reader may check that it is sufficient to prove (B.1) for  $k = 1, \dots, 5$ , as well as (B.1) but in which the summation over  $\mathbf{i}$  is

restricted to indices for which  $(i_1 = i_2)$ ,  $(i_1 = i_3)$ ,  $(i_3 = i_4)$ ,  $(i_1 = i_2)$  and  $(i_3 = i_4)$ .

We now prove (B.1) for  $k = 1$ , i.e. that

$$\sum_{\mathbf{i}} \mathbf{c}_{i_1,1} \mathbf{A}_{i_1,i_3} \mathbf{D}_{i_3,i_2} (\mathbf{A}^H)_{i_2,i_4} \mathbf{c}_{i_4,1} \mathbf{c}_{i_3,1} \mathbf{A}_{i_3,i_1} \mathbf{D}_{i_1,i_4} (\mathbf{A}^H)_{i_4,i_2} \mathbf{c}_{i_2,1} \rightarrow 0 \quad (\text{B.3})$$

For this, we replace  $\mathbf{D}$  by  $\mathbf{C}_2 \mathbf{C}_2^H - \frac{K-1}{N} \mathbf{I}$ , and verify that

$$\sum_{\mathbf{i}} \mathbf{c}_{i_1,1} \mathbf{A}_{i_1,i_3} (\mathbf{C}_2 \mathbf{C}_2^H)_{i_3,i_2} (\mathbf{A}^H)_{i_2,i_4} \mathbf{c}_{i_4,1} \mathbf{c}_{i_3,1} \mathbf{A}_{i_3,i_1} (\mathbf{C}_2 \mathbf{C}_2^H)_{i_1,i_4} (\mathbf{A}^H)_{i_4,i_2} \mathbf{c}_{i_2,1} \rightarrow 0, \quad (\text{B.4})$$

and

$$\begin{aligned} \sum_{\mathbf{i}} \mathbf{c}_{i_1,1} \mathbf{A}_{i_1,i_3} \delta_{i_3-i_2} (\mathbf{A}^H)_{i_2,i_4} \mathbf{c}_{i_4,1} \mathbf{c}_{i_3,1} \mathbf{A}_{i_3,i_1} (\mathbf{C}_2 \mathbf{C}_2^H)_{i_1,i_4} (\mathbf{A}^H)_{i_4,i_2} \mathbf{c}_{i_2,1} &\rightarrow 0 \\ \sum_{\mathbf{i}} \mathbf{c}_{i_1,1} \mathbf{A}_{i_1,i_3} (\mathbf{C}_2 \mathbf{C}_2^H)_{i_3,i_2} (\mathbf{A}^H)_{i_2,i_4} \mathbf{c}_{i_4,1} \mathbf{c}_{i_3,1} \mathbf{A}_{i_3,i_1} \delta_{i_1-i_4} (\mathbf{A}^H)_{i_4,i_2} \mathbf{c}_{i_2,1} &\rightarrow 0 \end{aligned} \quad (\text{B.5})$$

as well as

$$\sum_{\mathbf{i}} \mathbf{c}_{i_1,1} \mathbf{A}_{i_1,i_3} \delta_{i_3-i_2} (\mathbf{A}^H)_{i_2,i_4} \mathbf{c}_{i_4,1} \mathbf{c}_{i_3,1} \mathbf{A}_{i_3,i_1} \delta_{i_1-i_4} (\mathbf{A}^H)_{i_4,i_2} \mathbf{c}_{i_2,1} \rightarrow 0 \quad (\text{B.6})$$

We first check (B.4). We recall that matrix  $(\mathbf{C}_{i,k})_{i=1,\dots,N,k=1,\dots,K}$  is obtained by extracting  $K$  columns from a  $N \times N$  (unitary) Walsh-Hadamard matrix. In order to simplify the notations, we denote by  $(\mathbf{c}_k)_{k=1,\dots,N}$  the columns of this unitary matrix, and by  $(\mathbf{c}_{i,k})_{i=1,\dots,N}$  the components of vector  $\mathbf{c}_k$ . In particular, matrix  $\mathbf{C}_2$  is equal to  $\mathbf{C}_2 = (\mathbf{c}_2, \dots, \mathbf{c}_K)$ . The term to be studied, denoted  $u_{1,N}$ , is equal to

$$u_{1,N} = \sum_{k=2}^K \sum_{l=2}^K \sum_{(i_1,i_2,i_3,i_4)} \mathbf{c}_{i_1,1} \mathbf{A}_{i_1,i_3} \mathbf{c}_{i_3,k} \mathbf{c}_{i_2,k} (\mathbf{A}^H)_{i_2,i_4} \mathbf{c}_{i_4,1} \mathbf{c}_{i_3,1} \mathbf{A}_{i_3,i_1} \mathbf{c}_{i_1,l} \mathbf{c}_{i_4,l} (\mathbf{A}^H)_{i_4,i_2} \mathbf{c}_{i_2,1}$$

It can also be written as

$$u_{1,N} = \sum_{k=2}^K \sum_{l=2}^K \left| \sum_{i_1,i_3} \mathbf{c}_{i_1,1} \mathbf{c}_{i_3,1} \mathbf{c}_{i_1,l} \mathbf{c}_{i_3,k} \mathbf{A}_{i_1,i_3} \mathbf{A}_{i_3,i_1} \right|^2$$

It is clear that  $u_{1,N}$  is smaller than the term  $v_{1,N}$  defined by

$$v_{1,N} = \sum_{k=1}^N \sum_{l=1}^N \left| \sum_{i_1,i_3} \mathbf{c}_{i_1,1} \mathbf{c}_{i_3,1} \mathbf{c}_{i_1,l} \mathbf{c}_{i_3,k} \mathbf{A}_{i_1,i_3} \mathbf{A}_{i_3,i_1} \right|^2$$

$v_{1,N}$  is equal to

$$v_{1,N} = \sum_{\mathbf{i}} \sum_{k=1}^N \sum_{l=1}^N \mathbf{c}_{i_1,1} \mathbf{c}_{i_3,1} \mathbf{c}_{i_2,1} \mathbf{c}_{i_4,1} \mathbf{c}_{i_1,l} \mathbf{c}_{i_2,l} \mathbf{c}_{i_3,k} \mathbf{c}_{i_4,k} \mathbf{A}_{i_1,i_3} \mathbf{A}_{i_3,i_1} \mathbf{A}_{i_2,i_4}^* \mathbf{A}_{i_4,i_2}^*$$

As  $\sum_{l=1}^N \mathbf{c}_{i_1,l} \mathbf{c}_{i_2,l} = \delta_{i_1-i_2}$  and  $\sum_{k=1}^N \mathbf{c}_{i_3,k} \mathbf{c}_{i_4,k} = \delta_{i_3-i_4}$ , we get that

$$v_{1,N} = \sum_{i_1, i_3} (\mathbf{c}_{i_1,1})^2 (\mathbf{c}_{i_3,1})^2 |\mathbf{A}_{i_1, i_3}|^2 |\mathbf{A}_{i_3, i_1}|^2 = \frac{1}{N^2} \sum_{i_1, i_3} |\mathbf{A}_{i_1, i_3}|^2 |\mathbf{A}_{i_3, i_1}|^2$$

because the entries of  $\mathbf{C}$  are equal to  $\pm \frac{1}{\sqrt{N}}$ . We finally show that  $v_{1,N} \rightarrow 0$ , which in turn, implies that  $u_{1,N} \rightarrow 0$ . For this, we have to check that  $\frac{1}{N} \sum_{i_1, i_3} |\mathbf{A}_{i_1, i_3}|^2 |\mathbf{A}_{i_3, i_1}|^2$  is bounded. If  $\mathbf{E}$  and  $\mathbf{F}$  are  $N \times N$  matrices, we denote by  $\mathbf{E} \bullet \mathbf{F}$  the Schur-Hadamard product of  $\mathbf{E}$  and  $\mathbf{F}$  defined by  $(\mathbf{E} \bullet \mathbf{F})_{k,l} = \mathbf{E}_{k,l} \mathbf{F}_{k,l}$ . It is easily seen that  $\|\mathbf{E} \bullet \mathbf{F}\| \leq \|\mathbf{E}\| \|\mathbf{F}\|$ . We remark that

$$\frac{1}{N} \sum_{i_1, i_3} |\mathbf{A}_{i_1, i_3}|^2 |\mathbf{A}_{i_3, i_1}|^2 = \frac{1}{N} \text{Trace}(\mathbf{A} \bullet \mathbf{A}^T) (\mathbf{A} \bullet \mathbf{A}^T)^H$$

and is thus upper bounded by  $\|\mathbf{A} \bullet \mathbf{A}^T\|^2 \leq \|\mathbf{A}\|^4$ . As  $\mathbf{A}$  is uniformly bounded,

$$\sup_N \frac{1}{N} \text{Trace}(\mathbf{A} \bullet \mathbf{A}^T) (\mathbf{A} \bullet \mathbf{A}^T)^H < +\infty$$

This shows that  $v_{1,N}$ , and thus  $u_{1,N}$  converges to 0.

We now prove the first part of (B.5). We put

$$u_{2,N} = \sum_{\mathbf{i}} \mathbf{c}_{i_1,1} \mathbf{A}_{i_1, i_3} \delta_{i_3-i_2} (\mathbf{A}^H)_{i_2, i_4} \mathbf{c}_{i_4,1} \mathbf{c}_{i_3,1} \mathbf{A}_{i_3, i_1} (\mathbf{C}_2 \mathbf{C}_2^H)_{i_1, i_4} (\mathbf{A}^H)_{i_4, i_2} \mathbf{c}_{i_2,1}$$

Using that  $(\mathbf{c}_{i_3,1})^2 = \frac{1}{N}$ , we get immediately that

$$u_{2,N} = \frac{1}{N} \sum_{i_1, i_4} \mathbf{c}_{i_1,1} \mathbf{c}_{i_4,1} (\mathbf{C}_2 \mathbf{C}_2^H)_{i_1, i_4} \mathbf{E}_{i_1, i_4}$$

where  $\mathbf{E}$  is the  $N \times N$  matrix defined by

$$\mathbf{E}_{i_1, i_4} = \sum_{i_3} \mathbf{A}_{i_1, i_3} \mathbf{A}_{i_3, i_1} (\mathbf{A}^H)_{i_3, i_4} (\mathbf{A}^H)_{i_4, i_3}$$

It is easy to check that  $\mathbf{E} = (\mathbf{A} \bullet \mathbf{A}^T) (\mathbf{A} \bullet \mathbf{A}^T)^H$ . Therefore,  $u_{2,N}$  can be rewritten as

$$u_{2,N} = \frac{1}{N} \mathbf{c}_1^H ((\mathbf{C}_2 \mathbf{C}_2^H) \bullet \mathbf{E}) \mathbf{c}_1$$

As  $\mathbf{A}$  and  $\mathbf{C}_2 \mathbf{C}_2^H$  are uniformly bounded, matrix  $(\mathbf{C}_2 \mathbf{C}_2^H) \bullet \mathbf{E}$  is uniformly bounded. As  $\|\mathbf{c}_1\| = 1$ , this implies that

$$\sup_N \mathbf{c}_1^H ((\mathbf{C}_2 \mathbf{C}_2^H) \bullet \mathbf{E}) \mathbf{c}_1 < +\infty$$

thus showing that  $u_{2,N} \rightarrow 0$ .

The second part of (B.5) and (B.6) are obtained similarly. This establishes (B.1) for  $k = 1$ . The proof of (B.1) for  $k \in \{2, 3, 4, 5\}$ , and of (B.1),  $k \in \{1, 2, 3, 4, 5\}$  restricted to multi-indices satisfying  $i_1 = i_2$ ,  $i_1 = i_3$ ,  $i_3 = i_4$ ,  $i_1 = i_2$  and  $i_3 = i_4$  are similar, and thus omitted.

### B.3 Proof of Lemma 5.4.

As in the proof of Lemma 5.3, we simplify the notations. We put  $\mathbf{B}_N = \mathbf{B}$ ,  $\mathbf{S}(m) = \mathbf{S}$ ,  $\mathbf{S}(m-k) = \mathbf{S}'$ , and denote  $(s_i)_{i=1,\dots,N}$  and  $(s'_i)_{i=1,\dots,N}$  their diagonal entries. The diagonal terms of matrix  $\mathbf{C}\mathbf{C}^H$  all coincide with  $\frac{K}{N}$ , and we denote by  $\mathbf{D}$  the matrix  $\mathbf{D} = \mathbf{C}\mathbf{C}^H - \frac{K}{N}\mathbf{I}$ . Finally, we denote by  $T_N$  the term to be studied, i.e.

$$T_N = \mathbf{c}_1^H \mathbf{S}^H \mathbf{B} \mathbf{S}' \mathbf{C} \mathbf{C}^H \mathbf{S}'^H \mathbf{B}^H \mathbf{S} \mathbf{c}_1 - \alpha \frac{1}{N} \text{Trace}(\mathbf{B}\mathbf{B}^H)$$

Writing  $\mathbf{C}\mathbf{C}^H$  as  $\mathbf{D} + \frac{K}{N}\mathbf{I}$  and using that  $\mathbf{S}'$  is unitary, we get that

$$T_N = \epsilon_N + \frac{K}{N} \mathbf{c}_1^H \mathbf{S}^H \mathbf{B} \mathbf{B}^H \mathbf{S} \mathbf{c}_1 - \alpha \frac{1}{N} \text{Trace}(\mathbf{B}\mathbf{B}^H)$$

where

$$\epsilon_N = \mathbf{c}_1^H \mathbf{S}^H \mathbf{B} \mathbf{S}' \mathbf{D} \mathbf{S}'^H \mathbf{B}^H \mathbf{S} \mathbf{c}_1$$

As  $\mathbf{B}\mathbf{B}^H$  is uniformly bounded, Lemma 5.1 implies that

$$\mathbf{c}_1^H \mathbf{S}^H \mathbf{B} \mathbf{B}^H \mathbf{S} \mathbf{c}_1 - \frac{1}{N} \text{Trace}(\mathbf{B}\mathbf{B}^H)$$

converges to 0 in the mean square sense. As  $\frac{K}{N} \rightarrow \alpha$ ,  $\mathbb{E}(\epsilon_N^2) \rightarrow 0$  implies that  $\mathbb{E}(T_N^2) \rightarrow 0$ . In the following, we therefore prove that  $\mathbb{E}(\epsilon_N^2) \rightarrow 0$ . For this, we expand  $\mathbb{E}(\epsilon_N^2)$  as

$$\sum_{(i_1, i_2, i_3, i_4), (j_1, j_2, j_3, j_4)} \mathbf{c}_{i_1,1}^H \mathbf{B}_{i_1, j_1} \mathbf{D}_{j_1, i_2}(\mathbf{B}^H)_{i_2, j_2} \mathbf{c}_{j_2, 1} \mathbf{c}_{i_3, 1}^H \mathbf{B}_{i_3, j_3} \mathbf{D}_{j_3, i_4}(\mathbf{B}^H)_{i_4, j_4} \mathbf{c}_{j_4, 1} \mathbb{E}(s_{i_1}^* s'_{j_1} s_{i_2}^* s'_{j_2} s_{i_3}^* s'_{j_3} s_{i_4}^* s'_{j_4})$$

As sequences  $(s_i)_{i=1,\dots,N}$  and  $(s'_i)_{i=1,\dots,N}$  are independent, it is clear that

$$\mathbb{E}(s_{i_1}^* s'_{j_1} s_{i_2}^* s'_{j_2} s_{i_3}^* s'_{j_3} s_{i_4}^* s'_{j_4}) = \mathbb{E}(s_{i_1}^* s_{j_2} s_{i_3}^* s_{j_4}) \mathbb{E}(s'_{j_1} s_{i_2}^* s'_{j_3} s_{i_4}^*)$$

But,

$$\begin{aligned} \mathbb{E}(s_{i_1}^* s_{j_2} s_{i_3}^* s_{j_4}) &= \delta_{i_1-j_2} \delta_{i_3-j_4} + \delta_{i_1-j_4} \delta_{j_2-i_3} - \delta_{i_1-j_2} \delta_{i_3-j_4} \delta_{i_1-j_4} \delta_{j_2-i_3} \\ \mathbb{E}(s'_{j_1} s_{i_2}^* s'_{j_3} s_{i_4}^*) &= \delta_{j_1-i_2} \delta_{j_3-i_4} + \delta_{j_1-i_4} \delta_{i_2-j_3} - \delta_{j_1-i_2} \delta_{j_3-i_4} \delta_{j_1-i_4} \delta_{i_2-j_3} \end{aligned}$$

As the diagonal terms of  $\mathbf{D}$  are 0, the terms for which  $j_1 = i_2$  or  $j_3 = i_4$  do not contribute to  $\mathbb{E}(\epsilon_N^2)$ . Therefore,  $\mathbb{E}(\epsilon_N^2)$  reduces to

$$\sum_{(i_1, i_2, i_3, i_4), (j_1, j_2, j_3, j_4)} \mathbf{c}_{i_1,1}^H \mathbf{B}_{i_1, j_1} \mathbf{D}_{j_1, i_2}(\mathbf{B}^H)_{i_2, j_2} \mathbf{c}_{j_2, 1} \mathbf{c}_{i_3, 1}^H \mathbf{B}_{i_3, j_3} \mathbf{D}_{j_3, i_4}(\mathbf{B}^H)_{i_4, j_4} \mathbf{c}_{j_4, 1} \mathbb{E}(s_{i_1}^* s_{j_2} s_{i_3}^* s_{j_4}) \delta_{j_1-i_4} \delta_{i_2-j_3}$$

Starting from this expression, it is easy to check that  $\mathbb{E}(\epsilon_N^2) \rightarrow 0$ .

# Appendix C

## Appendix to chapter 6

### C.1 Proof of Theorems 6.1 and 6.2

Suppose that we want to use a receiver  $\mathbf{G}(z)$  to recover  $\begin{bmatrix} \tilde{d}(n) \\ \tilde{d}(n+N) \end{bmatrix}$  from  $\begin{bmatrix} x(n) \\ \bar{x}(n+N) \end{bmatrix}$  (see equation(6.19)). The overall transfer function between  $\begin{bmatrix} d(n) \\ \bar{d}(n+N) \end{bmatrix}$  and  $\begin{bmatrix} \tilde{d}(n) \\ \tilde{d}(n+N) \end{bmatrix}$  is given by the multiplication of the two transfer functions  $\mathbf{G}(z)$  and  $\mathbf{H}(z)$

$$\mathbf{F}(z) = \mathbf{G}(z)\mathbf{H}(z) = \begin{bmatrix} g_{11}(z) & g_{12}(z) \\ g_{21}(z) & g_{22}(z) \end{bmatrix} \begin{bmatrix} h_1(z) & h_2(z) \\ -\bar{h}_2(z) & \bar{h}_1(z) \end{bmatrix} \quad (\text{C.1})$$

$$\mathbf{F}(z) = \mathbf{G}(z)\mathbf{H}(z) = \begin{bmatrix} g_{11}(z)h_1(z) - g_{12}(z)\bar{h}_2(z) & g_{11}(z)h_2(z) + g_{12}(z)\bar{h}_1(z) \\ g_{21}(z)h_1(z) - g_{22}(z)\bar{h}_2(z) & g_{21}(z)h_2(z) - g_{22}(z)\bar{h}_1(z) \end{bmatrix} \quad (\text{C.2})$$

evaluating this expression on the unit circle  $z = e^{2i\pi f}$ , we get:

$$\begin{bmatrix} g_{11}(e^{2i\pi f})h_1(e^{2i\pi f}) - g_{12}(e^{2i\pi f})\bar{h}_2(e^{2i\pi f}) & g_{11}(e^{2i\pi f})h_2(e^{2i\pi f}) + g_{12}(e^{2i\pi f})\bar{h}_1(e^{2i\pi f}) \\ g_{21}(e^{2i\pi f})h_1(e^{2i\pi f}) - g_{22}(e^{2i\pi f})\bar{h}_2(e^{2i\pi f}) & g_{21}(e^{2i\pi f})h_2(e^{2i\pi f}) - g_{22}(e^{2i\pi f})\bar{h}_1(e^{2i\pi f}) \end{bmatrix} \quad (\text{C.3})$$

Now, recall that the SINR associated to this receiver is given by

$$\beta^{(N)} = \frac{|\mathbf{w}_1^H \mathbf{G} \mathcal{H} \mathbf{w}_1|^2}{\mathbf{w}_1^H \mathbf{G} (\mathcal{H} \mathbf{U}_1 \mathbf{U}_1^H \mathcal{H}^H + \sigma^2 \mathbf{I}) \mathbf{G}^H \mathbf{w}_1} \quad (\text{C.4})$$

and that

$$\mathcal{C} = \begin{bmatrix} s(mN)c_1(1) & 0 & s(mN)c_2(1) & 0 & \dots \\ 0 & s^*(mN+N)c_1(1) & 0 & s^*(mN+N)c_2(1) & \dots \\ s(mN+1)c_1(2) & 0 & s(mN+1)c_2(1) & 0 & \dots \\ 0 & s^*(mN+N+1)c_1(2) & 0 & s^*(mN+N+1)c_2(1) & \dots \\ \vdots & \vdots & \vdots & \vdots & \vdots \end{bmatrix} \quad (\text{C.5})$$

or

$$\mathcal{C} = [ \mathbf{w}_{1,1} \ \mathbf{w}_{2,1} \ \mathbf{w}_{1,2} \ \mathbf{w}_{2,2} \ \dots \ \mathbf{w}_{1,K} \ \mathbf{w}_{2,K} ] \quad (\text{C.6})$$

so that the first column  $\mathbf{w}_1 = \mathbf{w}_{1,1}$  is given by:

$$\mathbf{w}_1 = [s(mN)c_1(1) \ 0 \ s(mN+1)c_1(2) \ 0 \ \dots \ s(mN+N-1)c_1(N)]^T \quad (\text{C.7})$$

We Now consider the asymptotic behavior of the numerator:

$$(\mathbf{w}_1^H \mathbf{G} \mathbf{H} \mathbf{w}_1) = [X \ 0 \ X \ 0 \ \dots] \mathbf{F} \begin{bmatrix} X \\ 0 \\ X \\ 0 \\ \vdots \end{bmatrix}, \quad (\text{C.8})$$

where we denote by  $X$  the non-zero entries of  $\mathbf{w}_1$  and replace  $\mathbf{G} \mathbf{H}$  by  $\mathbf{F}$ .  $\mathbf{F}$  is the block circulant matrix with  $(2 \times 2)$  blocks having the same structure as the matrix in C.2. This means that the non-zero entries of  $(\mathbf{w}_1$  act on the matrix  $\mathbf{F}_{1,1}$  resulting from  $\mathbf{F} = \mathbf{G} \mathbf{H}$  by taking entries  $(1, 1)$  from each  $(2 \times 2)$  block. Using lemma 4.1,  $(\mathbf{w}_1^H \mathbf{G} \mathbf{H} \mathbf{w}_1)$  coincides with  $\frac{1}{N} \text{Trace}(\mathbf{F}_{1,1})$ . But  $\mathbf{F}_{1,1}$  is the filtering Toeplitz matrix associated to the transfer function

$$g_{11}(e^{2i\pi f})h_1(e^{2i\pi f}) - g_{12}(e^{2i\pi f})\overline{h_2}(e^{2i\pi f})$$

(see equation C.2) and  $\text{Trace}(\mathbf{F}_{1,1})$  coincides with  $\frac{1}{N} \sum_i \lambda_{i, \mathbf{F}_{1,1}}$ , where  $\lambda_{i, \mathbf{F}_{1,1}}$  stands for the  $i$ -th eigenvalue of  $\mathbf{F}_{1,1}$ . By using Lemma 4.2, this is seen to coincide with

$$g_{11}(e^{2i\pi f})h_1(e^{2i\pi f}) - g_{12}(e^{2i\pi f})\overline{h_2}(e^{2i\pi f}).$$

Then, asymptotically, we have:

$$(\mathbf{w}_1^H \mathbf{G} \mathbf{H} \mathbf{w}_1)^2 \longleftrightarrow \left[ \int_0^1 g_{11}(e^{2i\pi f})h_1(e^{2i\pi f}) - g_{12}(e^{2i\pi f})\overline{h_2}(e^{2i\pi f}) df \right]^2 \quad (\text{C.9})$$

Now, we consider the denominator:

$$\mathbf{w}_1^H \mathbf{G}(\mathbf{H}\mathbf{U}\mathbf{U}^H \mathbf{H}^H) \mathbf{G}^H \mathbf{w}_1 + \sigma^2 \mathbf{w}_1 \mathbf{G} \mathbf{G}^H \mathbf{w}_1 \quad (\text{C.10})$$

$\mathbf{U}$  can be divided into  $\mathbf{W}_2 \mathbf{U}_1$  so that

$$\mathbf{U}\mathbf{U}^H = \mathbf{W}_2 \mathbf{W}_2^H + \mathbf{U}_1 \mathbf{U}_1^H$$

where

$$\mathbf{W}_2 = [\mathbf{w}_{2,1} \ \mathbf{w}_{2,2} \ \mathbf{w}_{2,3} \ \dots \ \mathbf{w}_{2,K}]$$

and

$$\mathbf{U}_1 = [\mathbf{w}_{1,2} \ \mathbf{w}_{1,3} \ \mathbf{w}_{1,4} \ \dots \ \mathbf{w}_{1,K}]$$

Now, the denominator C.10 can be rewritten as:

$$\mathbf{w}_1^H \mathbf{G}(\mathbf{H}\mathbf{U}_1 \mathbf{U}_1^H \mathbf{H}^H) \mathbf{G}^H \mathbf{w}_1 + \mathbf{w}_1^H \mathbf{G}(\mathbf{H}\mathbf{W}_2 \mathbf{W}_2^H \mathbf{H}^H) \mathbf{G}^H \mathbf{w}_1 + \sigma^2 \mathbf{w}_1 \mathbf{G} \mathbf{G}^H \mathbf{w}_1 \quad (\text{C.11})$$

Taking (C.11) term by term. The first term can be written as:

$$\mathbf{w}_1^H \mathbf{F} \mathbf{U}_1 \mathbf{U}_1^H \mathbf{F}^H \mathbf{w}_1 = \tilde{\mathbf{w}}_1^H \mathbf{F}_{1,1} \tilde{\mathbf{U}}_1 \tilde{\mathbf{U}}_1^H \mathbf{F}_{1,1}^H \tilde{\mathbf{w}}_1 \quad (\text{C.12})$$

where  $\tilde{\mathbf{w}}_1$  (resp.  $\tilde{\mathbf{U}}_1$ ) is obtained from  $\mathbf{w}_1$  (resp.  $\mathbf{U}_1$ ) by removing even all-zeros elements (resp. rows). and  $\mathbf{F}_{1,1}$  is obtained by taking entries 1,1 of the  $(2 \times 2)$  blocks of  $\mathbf{F}$ . equation (C.12) has the same asymptotic behavior as:

$$\alpha \tilde{\mathbf{w}}_1^H \mathbf{F}_{1,1} (\mathbf{I} - \tilde{\mathbf{w}}_1 \tilde{\mathbf{w}}_1^H) \mathbf{F}_{1,1}^H \tilde{\mathbf{w}}_1 \quad (\text{C.13})$$

or equivalently,

$$\alpha [\tilde{\mathbf{w}}_1^H (\mathbf{F}_{1,1})^2 \tilde{\mathbf{w}}_1 - (\tilde{\mathbf{w}}_1^H \mathbf{F}_{1,1} \tilde{\mathbf{w}}_1)^2]. \quad (\text{C.14})$$

Following the same arguments as the numerator, equation C.14 has the same asymptotic behavior as:

$$\alpha \left\{ \frac{1}{N} \text{Trace}(\mathbf{F}_{1,1})^2 - \left( \frac{1}{N} \text{Trace} \mathbf{F}_{1,1} \right)^2 \right\}, \quad (\text{C.15})$$

which coincides with

$$\alpha \left\{ \frac{1}{N} \sum_i \lambda_{i, \mathbf{F}_{1,1}}^2 - \left( \frac{1}{N} \sum_i \lambda_{i, \mathbf{F}_{1,1}} \right)^2 \right\} \quad (\text{C.16})$$

Finally the asymptotic behavior of the first term boils down to the product of  $\alpha$  with:

$$\int_0^1 \left\{ g_{11}(e^{2i\pi f}) h_1(e^{2i\pi f}) - g_{12}(e^{2i\pi f}) \overline{h_2(e^{2i\pi f})} \right\}^2 df - \left[ \int_0^1 g_{11}(e^{2i\pi f}) h_1(e^{2i\pi f}) - g_{12}(e^{2i\pi f}) \overline{h_2(e^{2i\pi f})} df \right]^2 \quad (\text{C.17})$$

The second term is given by:

$$\mathbf{w}_1^H \mathbf{F} \mathbf{W}_2 \mathbf{W}_2^H \mathbf{F}^H \mathbf{w}_1 \quad (\text{C.18})$$

note that  $\mathbf{W}_2$  has all-zeros in the odd rows. Thus,  $\mathbf{w}_1^H \mathbf{F} \mathbf{W}_2$  takes into account the entry (1,2) of the blocks of the matrix  $\mathbf{F}$ . Therefore, (C.18) has the same behavior as:

$$\frac{\alpha}{N} \text{trace}(\mathbf{F}_{1,2} \mathbf{F}_{1,2}^H)$$

which has the same asymptotic behavior as:

$$\alpha \left[ \int_0^1 \left\{ g_{11}(e^{2i\pi f}) h_2(e^{2i\pi f}) + g_{12}(e^{2i\pi f}) \overline{h_1}(e^{2i\pi f}) \right\}^2 df \right] \quad (\text{C.19})$$

The third terms stems from the noise effect, it is given by:

$$\sigma^2 \mathbf{w}_1^H \mathbf{G} \mathbf{G}^H \mathbf{w}_1 \quad (\text{C.20})$$

for the same reason as (C.8), the result includes only entries (1,1) of the  $(2 \times 2)$  blocks of the matrix  $\mathbf{G} \mathbf{G}^H$  and asymptotically the third term of the denominator is given by:

$$\sigma^2 \int_0^1 (|g_{11}(e^{2i\pi f})|^2 + |g_{12}(e^{2i\pi f})|^2) df = \sigma^2 \left( \sum_q |g_{11,q}|^2 + |g_{12,q}|^2 \right) \quad (\text{C.21})$$

Now, putting all pieces together, we get the asymptotic SINR of a receiver  $\mathbf{G}$  is given by:

$$\beta_G = \frac{[\int_0^1 \{R_{g1}(e^{2i\pi f})\} df]^2}{\alpha \{ \int_0^1 \{R_{g1}(e^{2i\pi f})\}^2 df - [\int_0^1 \{R_{g1}(e^{2i\pi f})\} df]^2 \} + \alpha [\int_0^1 \{R_{g2}(e^{2i\pi f})\} df]^2 + \sigma^2 (\sum_q |g_{11,q}|^2 + |g_{12,q}|^2)} \quad (\text{C.22})$$

where

$$R_{g1}(e^{2i\pi f}) = g_{11}(e^{2i\pi f}) h_1(e^{2i\pi f}) - g_{12}(e^{2i\pi f}) \overline{h_2}(e^{2i\pi f}) \quad (\text{C.23})$$

$$R_{g2}(e^{2i\pi f}) = g_{11}(e^{2i\pi f}) h_2(e^{2i\pi f}) + g_{12}(e^{2i\pi f}) \overline{h_1}(e^{2i\pi f}) \quad (\text{C.24})$$

Expression (C.22) gives the SINR of a general receiver

$$\mathbf{G}(z) = \begin{bmatrix} g_{11}(z) & g_{12}(z) \\ g_{21}(z) & g_{22}(z) \end{bmatrix}$$

Expressing  $\beta_G$  as a function of the coefficients  $R_{g1}(k)$  and  $R_{g2}(k)$  we get for the MMSE equalizer SINR (it is understood that we replace  $g_{11}(z)$  and  $g_{12}(z)$  by  $g_1(z)$  and  $g_2(z)$  the MMSE equalizers):

$$\beta_{MMSE} = \frac{|R_{g1}(0)|^2}{\alpha (\sum_{k \neq 0} |R_{g1}(k)|^2 + \sum_k |R_{g2}(k)|^2) + \sigma^2 (\sum_k |g_1(k)|^2 + |g_2(k)|^2)} \quad (\text{C.25})$$

The RAKE receiver corresponds to:

$$g_{11}(z) = \overline{h_1}(z^{-1}) \quad \text{and} \quad g_{12}(z) = -h_2(z^{-1}).$$

Substituting these expressions in (C.22) we get the SINR of the RAKE receiver with:

$$\beta_{RAKE} = \frac{[\int_0^1 \{R_{h1}(e^{2i\pi f})\} df]^2}{\alpha \{ \int_0^1 \{R_{h1}(e^{2i\pi f})\}^2 df - [\int_0^1 R_{h1}(e^{2i\pi f}) df]^2 \} + \alpha [\int_0^1 \{R_{h2}(e^{2i\pi f})\} df]^2 + \sigma^2 \sum_q |h_{1,q}|^2 + |h_{2,q}|^2} \quad (C.26)$$

where

$$R_{h1}(e^{2i\pi f}) = |h_1(e^{2i\pi f})|^2 + |h_2(e^{2i\pi f})|^2 \quad (C.27)$$

$$R_{h2}(e^{2i\pi f}) = \overline{h_1}(e^{-2i\pi f})h_2(e^{2i\pi f}) + h_2(e^{-2i\pi f})\overline{h_1}(e^{2i\pi f}) \quad (C.28)$$

Expressing  $\beta_{RAKE}$  as a function of the coefficients  $R_{h1}(k)$  and  $R_{h2}(k)$  we get:

$$\beta_{RAKE} = \frac{|R_{h1}(0)|^2}{\alpha (\sum_{k \neq 0} |R_{h1}(k)|^2 + \sum_k |R_{h2}(k)|^2) + \sigma^2 R_{h1}(0)} \quad (C.29)$$



# Appendix D

## Appendix to Chapter 3, Article Published in ISSSTA 2004 Proceedings

---

### Spreading Code Detection and Blind Interference Cancellation for DS/CDMA Downlink.

Belkacem Mouhouche, Karim Abed-Meraim, Serguei Burykh

---

- Abstract
- Introduction
- Data Model
- Review of the BIC algorithm [23]
- BIC based on subspace decomposition and FWT projection
- Discussion
- Computer Simulations
- Conclusion

## D.1 Abstract

In this paper, We propose a new blind interference cancellation algorithm suitable for the Direct-Sequence Code-Division Multiple Access (DS/CDMA) downlink. Interferers codes are unknown but the family to which they belong is supposed to be known. The proposed technique is blind in the sense that only the desired user's spreading code is assumed to be known *a priori*. The remaining parameters required for the interference cancellation such as spreading codes and energies of interfering users are estimated using subspace decomposition and projection on the family of codes. Fast and efficient implementations are discussed. Therefore, unlike standard interference cancellers which can be used only in the uplink, the proposed method can be implemented at the mobile terminal.

## D.2 Introduction

In DS/CDMA communications, it is well known that channel orthogonality at the receiver is impossible to ensure in practice, whether on the forward or reverse link. This leads to a loss in capacity compared to the orthogonal case, regardless of the type of receiver used. The capacity loss is however greatest for RAKE (or conventional) receiver, and smallest for the optimal detector which performs joint maximum likelihood decoding of all users. In between these two extremes, there are the linear mean squared error (MMSE) and decorrelating detectors [74]. Still, the performance gap between the linear and optimal multiuser detectors becomes considerable when the number of users increase, which acts as a strong inducement to find non-linear, computationally tractable detectors.

An important class of non-linear sub-optimal receivers is the interference cancellers (IC) [39, 73], where an estimate of the Multiple-Access Interference (MAI) is subtracted from the received signal before making the decision on the desired user. Unlike linear multiuser detectors, IC has the potential to approach the single-user performance bound when the MAI estimate is reliable. Because of the need to re-generate the interfering signal at the receiver, all existing IC schemes have been proposed for the uplink as they require the knowledge of all users' codes and energies. As a result, ICs have thus far been assumed to be applicable at a base station, and not at the mobile terminal where only one information stream is to be decoded and the spreading codes of interfering users are unknown.

In [23], a blind interference cancellation (BIC) scheme that estimates the energies and codes of interfering users using subspace decomposition and the constant modulus (CM) property of the transmitted symbols has been proposed. the BIC algorithm is suitable when the number of users is small, because its complexity is of the order of  $O((N+T)K^2)$ , where  $N$  is the spreading factor,  $T$  is the sample size and  $K$  is the number of users.

In this paper, a new interference cancellation scheme is proposed for DS/CDMA downlink which estimates blindly<sup>1</sup> the spreading codes and energies of interfering users. As a consequence, this cancellation scheme can be implemented at the mobile terminal. The estimation procedures

---

<sup>1</sup>Meaning that no pilot nor training symbols are required, but the desired user's signature is known.

are based on subspace decomposition and Fast Walsh Transform (FWT) projection. Unlike the algorithm proposed in [23], this algorithm is more convenient when the number of users is high because its complexity is proportional to the number of excess codes, i.e. the number of codes that are not being used by the system.

Notations: Throughout the paper,  $T$ ,  $*$ ,  $H$  and  $\dagger$  are used to denote transpose, conjugate, conjugate transpose and Moore-Penrose pseudoinverse operations, respectively.  $\Re\{x\}$  and  $\Im\{x\}$  denote real and imaginary parts of  $x$ , respectively.  $\mathbf{M}_{i,j}$  denotes the  $\{i,j\}$ th element of matrix  $\mathbf{M}$ .

## D.3 Data model

In CDMA downlink, the received baseband continuous-time signal is given by

$$r(t) = \sum_{k=1}^K \sqrt{\epsilon_k} \sum_n b_k(n) a_k(t - nT_b) + v(t), \quad (\text{D.1})$$

where  $K$ ,  $\epsilon_k$ ,  $b_k(n)$  and  $a_k(t)$  denote the number of active system users, the received energy, the unit-power transmitted symbols and the channel signature of the  $k^{\text{th}}$  user, respectively;  $T_b$  is the symbol period and  $v(t)$  stands for the additive channel noise.

The channel signature  $a_k(t)$  can be written as

$$a_k(t) = \sum_{m=0}^{N-1} c_k(m) h(t - mT_c),$$

where  $T_c \stackrel{\text{def}}{=} T_b/N$ ,  $\{c_k(m)\}$  is the normalized spreading sequence of user  $k$  ( $N$ -periodic spreading codes are assumed in this work) and  $h(t)$  is the composite channel impulse response having finite support  $[0; (L-1)T_c]$ .

Chip-rate sampling of  $r(t)$  with subsequent stacking of  $N$  samples so obtained gives the following model<sup>2</sup>:

$$\mathbf{r}(n) \stackrel{\text{def}}{=} [r(0) \dots r(N-1)]^T = \mathbf{HCEb}(n) + \mathbf{v}(n), \quad (\text{D.2})$$

where

$$\mathbf{H} \stackrel{\text{def}}{=} \begin{pmatrix} h_0 & 0 & \dots & \dots & 0 \\ h_1 & h_0 & & & \vdots \\ \vdots & & \ddots & & \\ h_{L-1} & h_{L-2} & \dots & h_0 & \\ \vdots & \ddots & & & \ddots \\ 0 & \dots & h_{L-1} & h_{L-2} & \dots & h_0 \end{pmatrix},$$

---

<sup>2</sup>Here we assume that  $L \ll N$  so that the intersymbol interference can be ignored. The generalization of the presented technique to the case of non-negligible ISI is straightforward, but cumbersome.

$\mathbf{C} \stackrel{\text{def}}{=} [\mathbf{c}_1, \mathbf{c}_2, \dots, \mathbf{c}_K]$ ,  $\mathbf{c}_k \stackrel{\text{def}}{=} [c_k(0) c_k(1) \dots c_k(N-1)]^T$ ,  $\mathbf{E} \stackrel{\text{def}}{=} \text{diag}(\sqrt{\epsilon_1}, \dots, \sqrt{\epsilon_K})$ ,  $\mathbf{b}(n) \stackrel{\text{def}}{=} [b_1(n), \dots, b_K(n)]^T$  and  $\mathbf{v}(n) \stackrel{\text{def}}{=} [v(0) v(1) \dots v(N-1)]^T$ .

In the sequel, the matrix  $\mathbf{A} \stackrel{\text{def}}{=} \mathbf{CE}$  will be called ‘signature matrix’ and the matrix  $\mathbf{A}_{cs} \stackrel{\text{def}}{=} \mathbf{HCE} = \mathbf{HA}$  will be called ‘channel signature matrix’. Finally,  $T$  vectors  $\mathbf{r}(n)$ ,  $n = 0, 1, \dots, T-1$  can be stacked into one  $N \times T$  observation matrix  $\mathbf{X}$ :

$$\mathbf{X} \stackrel{\text{def}}{=} [\mathbf{r}(0), \mathbf{r}(1), \dots, \mathbf{r}(T-1)] = \mathbf{A}_{cs}\mathbf{B} + \mathbf{V}, \quad (\text{D.3})$$

where  $\mathbf{B} \stackrel{\text{def}}{=} [\mathbf{b}(0), \dots, \mathbf{b}(T-1)]$  and  $\mathbf{V} \stackrel{\text{def}}{=} [\mathbf{v}(0), \dots, \mathbf{v}(T-1)]$ .

Our further assumptions<sup>3</sup> will be: 1) information symbols  $b_k(n)$  belong to a CM constellation, for example, QAM-4 or M-PSK; 2) the number of users  $K < N$  and their corresponding spreading codes are extracted from a Walsh-Hadamard matrix; 3) additive noise  $v(t)$  is white so that  $\mathbb{E}[\mathbf{v}(n)\mathbf{v}^H(n)] = \sigma^2\mathbf{I}$ ; 4) information symbols are mutually decorrelated so that  $\mathbb{E}[\mathbf{b}(n)\mathbf{b}^H(n)] = \mathbf{I}$ .

In further developments, we will need the concepts of signal and noise subspaces. Consider the covariance matrix of the observation vector  $\mathbf{r}(n)$ :

$$\mathbf{R} \stackrel{\text{def}}{=} \mathbb{E}[\mathbf{r}(n)\mathbf{r}^H(n)] = \mathbf{A}_{cs}\mathbf{A}_{cs}^H + \sigma^2\mathbf{I}. \quad (\text{D.4})$$

As  $\mathbf{A}_{cs}$  is of column rank  $K$ , it follows that  $K$  principal eigenvectors of  $\mathbf{R}$  correspond to eigenvalues  $\lambda_i > \sigma^2$ ,  $i = 1, 2, \dots, K$ . These eigenvectors span the *signal subspace*. The remaining  $N - K$  eigenvectors constitute a basis of the *noise subspace* and correspond to eigenvalues  $\lambda_i = \sigma^2$ ,  $i = K + 1, \dots, N$ . Therefore, the eigendecomposition of  $\mathbf{R}$  can be written as

$$\mathbf{R} = \mathbf{U}_s\mathbf{\Lambda}_s\mathbf{U}_s^H + \sigma^2\mathbf{U}_n\mathbf{U}_n^H, \quad (\text{D.5})$$

where  $\mathbf{\Lambda}_s$  is the diagonal matrix of signal subspace eigenvalues and  $\mathbf{U}_s$  ( $\mathbf{U}_n$ ) are the matrices of signal (repectively, noise) subspace eigenvectors.

## D.4 Review of the BIC algorithm [23]

In this section we review the main aspects of the BIC algorithm proposed in [23]. To discuss the BIC algorithm, we need to introduce the following proposition:

**Proposition D.1** *There exists a certain  $K \times K$  unitary matrix  $\mathbf{Q}$  such that*

$$\mathbf{A}_{cs} = \mathbf{HCE} = \mathbf{U}_s(\mathbf{\Lambda}_s - \sigma^2\mathbf{I})^{1/2}\mathbf{Q}.$$

Therefore, the channel signature matrix (which contains the information about the spreading codes of all system users and their corresponding energies) can be obtained from the following parameters: the matrix of signal subspace eigenvectors  $\mathbf{U}_s$ , the matrix of signal subspace eigenvalues  $\mathbf{\Lambda}_s$ , noise variance  $\sigma^2$  and a certain unitary factor  $\mathbf{Q}$ . The former three can be extracted

---

<sup>3</sup>Assumption 1 is needed only for the BIC algorithm while assumption 2 is needed for the new proposed algorithm.

directly from the SVD of the covariance matrix (or its sample estimate)<sup>4</sup>. Hence, it remains to find a way to estimate the unitary matrix  $\mathbf{Q}$ .

For the notational convenience, define  $\mathbf{M}_0 \stackrel{\text{def}}{=} \mathbf{U}_s(\mathbf{\Lambda}_s - \sigma^2 \mathbf{I})^{1/2}$  so that  $\mathbf{A}_{cs} = \mathbf{M}_0 \mathbf{Q}$ . Consider the following set of linear detectors parametrized by a certain  $K \times K$  unitary matrix  $\mathbf{V}$ :

$$\mathbf{W}_{\mathbf{V}} = \mathbf{V}^H \mathbf{M}_0^\dagger. \quad (\text{D.6})$$

It follows easily from Proposition D.1 that  $\mathbf{V} = \mathbf{Q}$  results in the decorrelating detector [74]. Hence, in the absence of noise, one would have

$$\mathbf{W}_{\mathbf{Q}} \mathbf{X} = \mathbf{B}. \quad (\text{D.7})$$

Next, recall that the transmitted symbols belong to a CM constellation<sup>5</sup>. Using (D.7), this can be expressed as

$$C(\mathbf{Q}) \stackrel{\text{def}}{=} \sum_{k=1}^K \sum_{n=0}^{T-1} (|(\mathbf{W}_{\mathbf{Q}} \mathbf{X})_{k,n}|^2 - 1)^2 = 0.$$

Generally, consider the following criterion:

$$C(\mathbf{V}) \stackrel{\text{def}}{=} \sum_{k=1}^K \sum_{n=0}^{T-1} (|(\mathbf{W}_{\mathbf{V}} \mathbf{X})_{k,n}|^2 - 1)^2. \quad (\text{D.8})$$

Clearly,  $C(\mathbf{V}) \geq 0$  and  $C(\mathbf{V})$  reaches its global minimum (zero) for  $\mathbf{V} = \mathbf{Q}$ . Therefore, the following estimate of  $\mathbf{Q}$  can be proposed:

$$\hat{\mathbf{Q}} = \arg \min_{\mathbf{V}} C(\mathbf{V}), \quad (\text{D.9})$$

where the minimization is carried over all unitary  $K \times K$  matrices  $\mathbf{V}$ . A practical method for the minimization of (D.9) relying on the Givens rotations is proposed in [23].

Having obtained an estimate of  $\mathbf{Q}$ , one may compute the channel signature matrix  $\mathbf{A}_{cs}$  as

$$\hat{\mathbf{A}}_{cs} = \mathbf{M}_0 \hat{\mathbf{Q}} = \mathbf{A}_{cs} + \mathbf{N}_e = \mathbf{H} \mathbf{A} + \mathbf{N}_e, \quad (\text{D.10})$$

where  $\mathbf{N}_e$  represents the estimation noise. In order to get the unknown spreading codes and energies, we would like to have an estimate of the signature matrix  $\mathbf{A} = \mathbf{C} \mathbf{E}$ . Let us assume that the channel  $\mathbf{H}$  (or its estimate, e.g., [75]) is available at the receiver. Then, the zero-forcing estimate of  $\mathbf{A}$  has the form

$$\hat{\mathbf{A}} = \mathbf{H}^\dagger \hat{\mathbf{A}}_{cs}. \quad (\text{D.11})$$

However, similarly to the zero-forcing equalizer or decorrelating detector [74], this estimate will suffer from noise enhancement. To counter this problem, we propose the ‘regularized’ zero-forcing estimate:

$$\hat{\mathbf{A}} = \mathbf{H}^H (\mathbf{H} \mathbf{H}^H + \delta \mathbf{I})^{-1} \hat{\mathbf{A}}_{cs}.$$

<sup>4</sup>The noise variance  $\sigma^2$  can be estimated as the mean value of  $N - K$  smallest singular values of  $\mathbf{R}$ .

<sup>5</sup>As for the standard CDMA algorithm, the BIC algorithm proposed in [23] can be generalized and applied to sub-gaussian non-CM signals.

The regularized ZF estimate differs from (D.11) in that it introduces into the pseudo-inverse the term  $\delta \mathbf{I}$ , where  $\delta$  is a small constant (regularization parameter). The regularization can also be seen as modelling the estimation noise as white noise process with the variance  $\delta$ .

The users' powers matrix  $\mathbf{E}$  can be estimated from the norm values of the column vectors of  $\hat{\mathbf{A}}$  (the spreading sequences are assumed to be of unit norm) and hard decisions on the entries of  $\mathbf{A}$  can be used as well:  $\tilde{\mathbf{A}} = \text{Dec}(\hat{\mathbf{A}}\mathbf{E}^{-1})$ , where  $\text{Dec}$  represents the hard symbol decision operator.

## D.5 BIC based on subspace decomposition and FWT projection

In this section, we propose a new blind interference cancellation algorithm that we will call Code-Detection Blind Interference Cancellation (CD-BIC).

To explain the code-detection scheme, assume that we have correctly estimated the channel matrix  $\mathbf{H}$  and the noise subspace  $\mathbf{U}_n$ . let  $\mathbf{C}_N = [\mathbf{C} \ \tilde{\mathbf{C}}]$  where  $\mathbf{C}_N$  is the complete family of Walsh Hadamard codes, and  $\tilde{\mathbf{C}}$  is the matrix of unused codes. The noise subspace is orthogonal to the signature matrix  $\mathbf{HC}$  which spans the signal subspace. this means that:

$$(\mathbf{HC})^H \mathbf{U}_n = \mathbf{0}$$

or equivalently:

$$\mathbf{C}^H \mathbf{H}^H \mathbf{U}_n = 0$$

In other words, the projection of  $\mathbf{H}^H \mathbf{U}_n$  on the active spreading codes is null. This can be used as a criterion to distinguish the active from excess (unused) codes by projecting on the complete code set and comparing the outputs. This is done by calculating:

$$\mathbf{F} = \mathbf{C}_N^H \mathbf{H}^H \mathbf{U}_n = \begin{bmatrix} \mathbf{C}^H \mathbf{H}^H \mathbf{U}_n \\ \tilde{\mathbf{C}}^H \mathbf{H}^H \mathbf{U}_n \end{bmatrix} = \begin{bmatrix} \mathbf{0} \\ \tilde{\mathbf{C}}^H \mathbf{H}^H \mathbf{U}_n \end{bmatrix},$$

This suggests to detect the active codes as those corresponding to the  $K$  rows of  $\mathbf{F}$  with smallest norm values.

The projection of any vector on a Walsh-Hadamard matrix can be performed efficiently by using the Fast Walsh Transform (FWT) which costs  $N \log(N)$  instead of  $N^2$ . This means that the above operation can be carried using FWT and the total number of operations is  $(N - K)N \log(N)$ .

The proposed (CD-BIC) algorithm can be summarized as follows:

1. Accumulate  $T$  observations of the received signal:  $\mathbf{X} = [\mathbf{r}(0), \mathbf{r}(1), \dots, \mathbf{r}(T - 1)]$  and estimate the received covariance matrix  $\hat{\mathbf{R}} = \mathbf{X}\mathbf{X}^H/T$ .
2. Estimate the signal subspace eigenvalues and eigenvectors ( $\mathbf{U}_s$  and  $\mathbf{\Lambda}_s$ ) as well as the noise subspace eigenvalues  $\mathbf{U}_n$  from the SVD of  $\hat{\mathbf{R}}$ .

3. Estimate the channel coefficients vector  $\hat{\mathbf{h}}$  using subspace method [75] (see Remark D.1) or the pilot sequence if available.
4. Let  $\mathbf{M}_1 = \hat{H}^H \mathbf{U}_n$ , calculate  $\mathbf{F} = FWT(\mathbf{M}_1)$ .
5. For  $i=1$  to  $N$ , calculate the norm of the  $i^{th}$  row of  $\mathbf{F}$ . Decide for interfering users codes  $\hat{\mathbf{c}}_2 \dots \hat{\mathbf{c}}_K$  as the codes corresponding to the  $(K-1)$  smallest row norm values. the complete Code matrix  $\hat{\mathbf{C}} = [\mathbf{c}_1 \hat{\mathbf{c}}_2 \dots \hat{\mathbf{c}}_K]$
6. Compute  $K - 1$  MMSE detectors for the interferers  $\mathbf{w}_k = \mathbf{U}_s \mathbf{\Lambda}_s^{-1} \mathbf{U}_s^H \hat{\mathbf{H}} \hat{\mathbf{c}}_k$ ,  $k = 2, 3, \dots, K$ .
7. Interference cancellation: for  $n = 0, 1, \dots, T - 1$  do
  - (a) Detect the interfering bits:  $\tilde{b}_k(n) = \text{Dec}(\hat{b}_k(n))$  where  $\hat{b}_k(n) = (\mathbf{w}_k^H \mathbf{r}(n))$ .
  - (b) Estimate the interferers powers as:  
 $\sqrt{\hat{\epsilon}_k} = (\sum_{n=0}^{T-1} \hat{b}_k(n) \tilde{b}_k^*(n))^{-1}$  (see remark D.2)
  - (c) Subtract the estimated interference:  $\mathbf{r}_s(n) = \mathbf{r}(n) - \sum_{k=2}^K \sqrt{\hat{\epsilon}_k} \hat{\mathbf{H}} \hat{\mathbf{c}}_k \hat{b}_k(n)$ ;
  - (d) Perform the desired user's detection:  
 $\hat{b}_1(n) = \text{Dec}((\hat{\mathbf{H}} \mathbf{c}_1)^H \mathbf{r}_s(n))$ .

**Remark D.1** *The channel coefficients can be estimated as*

$$\hat{\mathbf{h}} = \arg \min_{\|\mathbf{h}\|=1} (\|\mathbf{U}_n^H \tilde{\mathbf{C}}_1 \mathbf{h}\|^2)$$

where  $\tilde{\mathbf{C}}_1 \mathbf{h} = \mathbf{H} \mathbf{c}_1$  with

$$\tilde{\mathbf{C}}_1 \stackrel{\text{def}}{=} \begin{pmatrix} c_1(0) & & \mathbf{0} \\ \vdots & \ddots & c_1(0) \\ \vdots & & \vdots \\ c_1(N-1) & \dots & c_1(N-L) \end{pmatrix},$$

**Remark D.2** *Indeed, the output of the MMSE detector  $\mathbf{w}_k$  is equal to  $\hat{b}_k(n) = \frac{1}{\sqrt{\hat{\epsilon}_k}} b_k(n) +$  noise. Consequently, under the assumption of correct decision ( $\tilde{b}_k(n) = b_k(n)$ ), we have:  $\mathbb{E}(\hat{b}_k(n) \tilde{b}_k^*(n)) = \frac{1}{\sqrt{\hat{\epsilon}_k}}$*

**Remark D.3** *It is noteworthy that the two algorithms (BIC and CD-BIC) differ in estimating the spreading codes only, this means that for sufficiently high SNRs, the interfering codes are detected correctly, and the two algorithms give the same performance.*

## D.6 Discussion

We provide here some coments to highlight certain points related to the proposed algorithm.

### D.6.1 Computational complexity

The overall computational cost of the proposed algorithm corresponds to  $O(NK^2)$  for the eigen-decomposition of  $\mathbf{R}$  [?] plus  $O((N-K)N\log_2(N))$  for the code detection using subspace orthogonality and FWT plus  $O((L+K)KN)$  for the interference cancellation. We can notice that the cost due to the code detection step is not the dominant one and, in general, the CD-BIC has an overall computational cost comparable to that of the blind MMSE detector in [75]. Moreover, comparatively to the BIC algorithm in [23], the CD-BIC is in most cases less expensive, especially for large number of users  $K$ .

### D.6.2 Blind channel estimation indeterminacy

In the blind context, the channel parameter vector  $\mathbf{h}$  can be estimated only up to a constant scalar, which corresponds to the phase and amplitude ambiguities inherent to the problem. Consequently the BIC scheme cannot be applied, in this case, unless a differential modulation is used for the transmitted symbols to get rid of the phase ambiguity.

### D.6.3 Channel estimation

At low SNRs, the subspace-based channel estimate may be too noisy and inadequate for the interference cancellation. In that case, we propose to use a two-step procedure to refine the channel estimation using an input output least squares fitting criterion. The inputs are decided for in the first step using a MMSE detector computed from the first channel estimate.

### D.6.4 Further improvements

It is possible to further reduce the computational cost of the CD-BIC by considering only few noise vectors instead of the whole noise subspace. Indeed, it can be shown that both the subspace-based channel estimation and the code-detection can be achieved consistently using one or few noise vectors only. This would lead to a considerable reduction of the computational cost. This point will be developed and presented in future works.

## D.7 Computer simulations

In this section, we provide computer simulations to validate both the code-detection scheme, and the interference cancellation algorithm based on it.

We start by evaluating the code detection scheme. We simulate a DS/CDMA system with a spreading factor  $N = 64$ , QPSK information symbols, Walsh-Hadamard Codes are used for spreading, the propagation channel is a 10 path channel generated randomly with a delay spread of 10 chips. All the users are assigned the same power.

We consider two configurations corresponding to a number of users  $K = 10$  (weakly loaded system) and  $K = 32$  (half loaded system), respectively. Figure D.1 shows the probability of

false detection (i.e. that a Walsh Hadamard Code would be detected given that it is not present in the system) under both configurations for two values of the block size  $T = 128$  and  $256$ . We see that the probability of false detection is higher for a weakly loaded system, this makes our algorithm suitable for moderately loaded systems (note that we have already mentioned that the complexity of the code-detection scheme is smaller when the number of users is high). We see also that the larger the sample size, the better the noise subspace estimation, and the lower the probability of false detection

Next, We evaluate the performance of the CD-BIC algorithm as compared to a MMSE detector (without interference cancellation) and a single user system. We simulate a DS/CDMA systems with a spreading factor  $N = 32$ ,  $K = 10$  users transmitting QPSK information symbols. The chip sequence is transmitted through a 5 path channel generated randomly, users powers (including the user of interest) are considered equal. Figure D.2 shows the BER performance of the three detection methods versus the symbol SNR per user. We see that the MMSE detector provides no improvement due to the residual interference, while the CD-BIC approaches the single user performance.

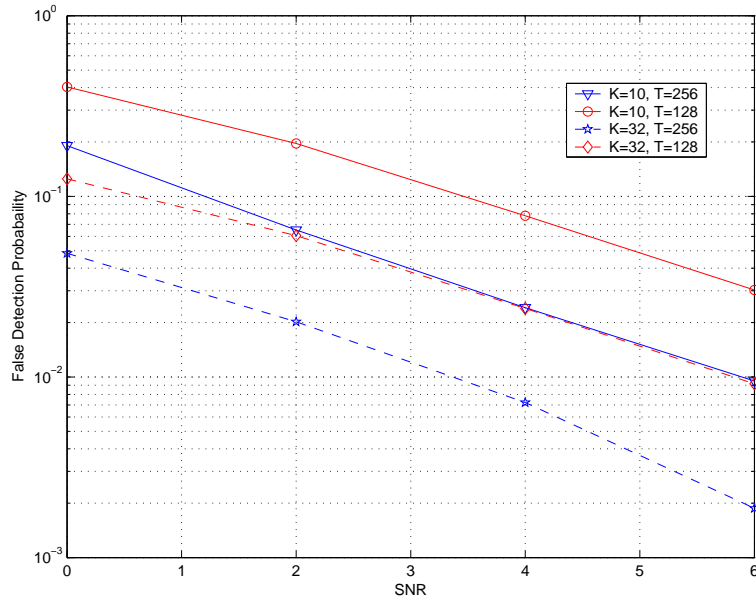


Figure D.1: Code Detection Probability of Error vs. SNR for a 64 SF system.

## D.8 Conclusions

In this paper we have proposed a new blind interference cancellation algorithms based on subspace decomposition and Fast Walsh Transform projection. The code detection method was shown to perform quite well especially for moderately or highly loaded systems. The proposed algorithm was shown to outperform the MMSE receiver and give performances that are close to single user detection.

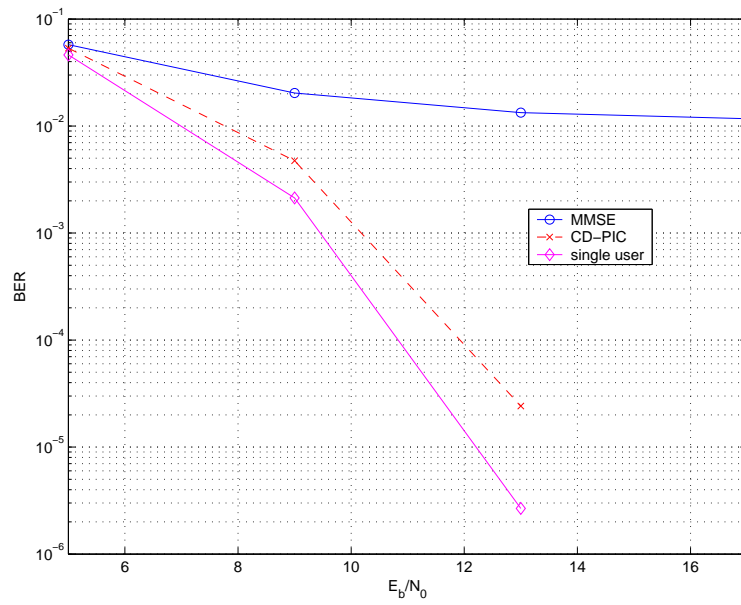


Figure D.2: BER vs.  $E_b/N_0$  for MMSE, single user and CD-PIC algorithm for  $N = 32$ ,  $K = 10$  system.

# Appendix E

## Appendix to Chapter 4, Article Published in Eusipco 2004 Proceedings

---

### Asymptotic Analysis of reduced rank downlink CDMA Wiener receivers.

Belkacem Mouhouche, Philippe Loubaton, Walid Hachem, Nicolas Ibrahim

---

- Abstract
- Introduction
- A review of the main results of Loubaton-Hachem
- The downlink CDMA model
- The reduced-rank Wiener receivers
- Simulation results
- Conclusion

## E.1 Abstract

In this paper, we study the performance of reduced rank Wiener filters in the context of downlink CDMA systems corrupted by a frequency selective channel. For this, we consider the output signal to interference plus noise ratio (SINR), and study its convergence speed versus the order of the receiver. Unfortunately, this is a difficult task because the SINR expressions depend on the spreading codes allocated to the various users in a rather complicated way. In order to be able to obtain positive results, we follow the classical approach used for the first time in [71]: the code matrix is modelled as the realization of a certain random matrix, and the behavior of the SINRs is studied when the spreading factor  $N$  and the number of users  $K$  converges to  $+\infty$  in such a way that  $\frac{K}{N} \rightarrow +\alpha$ . As the code matrices used in the downlink of CDMA systems are very often orthogonal, we model the code matrix allocated to the various users as a realization of a Haar distributed random unitary matrix. In this context, we show that the SINR of each order  $n$  reduced rank receiver converge toward a deterministic limit  $\beta_n$  independent of the spreading codes. In order to study the performance of the receiver versus  $n$ , we therefore study the convergence speed of  $\beta_n$  when  $n \rightarrow +\infty$ , a simpler problem. For this, we use the results of [53] based on the theory of orthogonal polynomials for the power moment problem. We obtain the convergence rate of  $\beta_n$ , and exhibit the parameters influencing the convergence speed.

## E.2 Introduction

In multidimensional signal processing, it is often useful to approximate the Wiener filter by a reduced rank version of this filter. The latter acts on a projection of the received signal on a judiciously chosen small dimensional subspace. The use of a reduced rank filter can be motivated by complexity constraints or, in an adaptive setting, by fast convergence requirements. It is then of major interest to quantify the SNR loss at the output of this filter due to its non optimum character.

The *Krylov subspaces*, widely used as projection subspaces, will be considered in this paper. To fix our ideas, let us begin with the generic signal model

$$\mathbf{y}_N = \mathbf{h}_N b + \mathbf{x}_N \quad (\text{E.1})$$

where  $\mathbf{y}_N$  is the received  $N \times 1$  signal,  $b$  is the unit-variance scalar signal to be estimated and  $\mathbf{x}_N$  is a signal decorrelated with  $b$  representing interference and/or background noise. The  $N \times N$  covariance matrix of  $\mathbf{x}_N$  is denoted  $\mathbf{R}_{N,I}$  and will be assumed invertible. Recall that the MMSE receiver is described by the equation  $s_{\text{MMSE}} = \mathbf{h}_N^H \mathbf{R}_N^{-1} \mathbf{y}$  where  $\mathbf{R}_N = \mathbf{h}_N \mathbf{h}_N^H + \mathbf{R}_{N,I}$  is the received signal  $\mathbf{y}_N$  covariance matrix. This receiver will be called in the sequel the full rank MMSE receiver. Its output SNR that we index by the number of dimensions of the received signal is given by the standard expression

$$\beta^{(N)} = \frac{\eta^{(N)}}{1 - \eta^{(N)}} \quad (\text{E.2})$$

where  $\eta^{(N)}$  is defined by

$$\eta^{(N)} = \mathbf{h}_N^H \mathbf{R}_N^{-1} \mathbf{h}_N . \quad (\text{E.3})$$

The  $n^{\text{th}}$  Krylov subspace associated to the pair  $(\mathbf{R}_N, \mathbf{h}_N)$  is the subspace of  $\mathbb{C}^N$  spanned by the columns of  $\mathbf{K}_{n,N} = [\mathbf{h}_N, \mathbf{R}_N \mathbf{h}_N, \dots, \mathbf{R}_N^{n-1} \mathbf{h}_N]$ . The  $n$ -th stage reduced rank Wiener filter considered in this paper is the MMSE estimator of  $b$  operating on the transformed signal  $\tilde{\mathbf{y}}_{n,N} = \mathbf{K}_{n,N}^H \mathbf{y}_N$ .

The motivation behind choosing the Krylov subspaces and the implementation of the subsequent filters are discussed in a number of works (see e.g. [44] and [34]).

The output SINR  $\beta_n^{(N)}$  of the  $n$ -th stage reduced rank Wiener filter is given by

$$\beta_n^{(N)} = \frac{\eta_n^{(N)}}{1 - \eta_n^{(N)}} \quad (\text{E.4})$$

where  $\eta_n^{(N)}$  is now defined by

$$\eta_n^{(N)} = \mathbf{h}_N^H \mathbf{K}_{n,N} (\mathbf{K}_{n,N}^H \mathbf{R}_N \mathbf{K}_{n,N})^{-1} \mathbf{K}_{n,N}^H \mathbf{h}_N . \quad (\text{E.5})$$

The use of reduced rank Wiener filters is of course attractive if close to optimum performance can be achieved for small values  $n$ . In order to precise in which contexts this nice condition holds, the convergence speed of  $\beta_n^{(N)}$  to  $\beta^{(N)}$ , or equivalently of  $\eta_n^{(N)}$  to  $\eta^{(N)}$  when  $n$  increases has to be studied. This problem has been successfully addressed in the recent work [44] (see also ([70], [69]) in the context of the following simple CDMA transmission model

$$\mathbf{y}_N = \mathbf{W}_{N,K} \mathbf{b}_K + \mathbf{v}_N . \quad (\text{E.6})$$

$\mathbf{b}_K = [b_1, \dots, b_K]^T$  is the  $K$ 1 symbol vector where  $K$  is the number of users,  $\mathbf{W}_{N,K}$  is the  $NK$  code matrix, and  $\mathbf{v}_N$  is the classical noise with covariance matrix  $\omega^2 \mathbf{I}_N$ . The purpose is to estimate the symbol  $b_1$ , so this equation appears as a particular case of (E.1) : if we partition  $\mathbf{W}_{N,K}$  and  $\mathbf{b}_K$  as  $\mathbf{W}_{N,K} = [\mathbf{w}_N \ \mathbf{U}_{N,K-1}]$  and  $\mathbf{b}_K = [b_1 \ \mathbf{b}_I^T]^T$ , then we replace  $\mathbf{h}_N$  by  $\mathbf{w}_N$  and  $\mathbf{x}_N$  by  $\mathbf{U}_{N,K-1} \mathbf{b}_I + \mathbf{v}_N$ . Honig and Xiao ([44]) assumed that the code matrix  $\mathbf{W}_{N,K}$  is a random matrix with centered i.i.d. elements having a variance of  $1/N$ , and studied the performance of the reduced rank filter in the "large system" regime where  $N$  tends to infinity in such a way that  $K/N$  converges toward a constant  $\alpha$ . They established that  $\eta_n^{(N)}$  and  $\eta^{(N)}$  converge to finite limits  $\eta_n$  and  $\eta$ , and were able to show that  $\eta$  is a continued fraction expansion whose order  $n$  truncation coincides with  $\eta_n$ . From this, they concluded for the rapid convergence of this SNR toward the full rank SNR.

Note that partial results have been obtained in more general models than (E.6) (see [29] and [52]). In these works, the convergence of  $\eta_n^{(N)}$  toward  $\eta_n$  is established. However, the convergence speed of  $\eta_n$  toward  $\eta$  is not addressed.

In [53], we also addressed the influence of  $n$  on the performance of the receiver in the asymptotic regime when  $N \rightarrow +\infty$ , but in the much more general context defined by model (E.1).

Under the hypothesis that for each integer  $k$ ,  $s_k^{(N)} = \mathbf{h}_N^H \mathbf{R}_N^k \mathbf{h}_N$  converges when  $N \rightarrow +\infty$  to a finite limit  $s_k$ , we showed that  $\eta^{(N)}$  and  $\eta_n^{(N)}$  also converge to certain finite limits  $\eta$  and  $\eta_n$  respectively. More importantly, the convergence speed of  $\eta_n$  toward  $\eta$  can be evaluated using properties of certain orthogonal polynomials.

The purpose of this paper is to show that the results of [53] can be used in order to study the convergence speed of reduced rank Wiener filters in the context of downlink CDMA systems corrupted by frequency selective channels. This paper is organized as follows. We first recall in section II the main results of [53]. In section III, we present the downlink CDMA system model as well as the reduced rank Wiener filters under consideration. The received data is corrupted by a frequency selective channel, and the code matrix is modelled as the realization of a orthogonal random Haar distributed matrix. In section IV, we study the performance of the above receivers in the asymptotic regime  $N$  and  $K$  converge to  $\infty$  in such a way that  $\frac{K}{N} \rightarrow \alpha$ . We show that the hypotheses formulated in section II are valid, and deduce the convergence speed of the reduced rank receivers.

### E.3 A review of the main results of Loubaton-Hachem

We still consider model E.1 and formulate the following assumption.

**Assumption E.1** *We assume that for each  $k$ ,  $s_k^{(N)} = \mathbf{h}_N^H \mathbf{R}_N^k \mathbf{h}_N$  converges when  $N \rightarrow +\infty$  to a finite limit  $s_k$ , and that  $s_0 = 1$ .*

It is easily seen that  $\eta_n^{(N)}$  is equal to

$$(s_0^{(N)}, \dots, s_{n-1}^{(N)}) \begin{pmatrix} s_1^{(N)} & s_2^{(N)} & \dots & s_n^{(N)} \\ s_2^{(N)} & s_3^{(N)} & \dots & s_{n+1}^{(N)} \\ \vdots & \vdots & \vdots & \vdots \\ s_n^{(N)} & s_{n+1}^{(N)} & \dots & s_{2n-1}^{(N)} \end{pmatrix}^{-1} \begin{pmatrix} s_0^{(N)} \\ \vdots \\ s_{n-1}^{(N)} \end{pmatrix} \quad (\text{E.7})$$

Assumption E.1 thus implies that for each  $n$ ,  $\eta_n^{(N)}$  converges to the quantity  $\eta_n$  obtained by replacing  $(s_k^{(N)})_{k=1,2n-1}$  in (E.7) by sequence  $(s_k)_{k=1,2n-1}$ . Moreover,  $\mathbf{K}_{n,N}^H \mathbf{K}_{n,N}$  and  $\mathbf{K}_{n,N}^H \mathbf{R}_N \mathbf{K}_{n,N}$  are positive Hankel matrices converging to the Hankel matrices  $(s_{k+l})_{(k,l)=0,\dots,n-1}$  and  $(s_{k+l+1})_{(k,l)=0,\dots,n-1}$ . Therefore, matrices  $(s_{k+l})_{(k,l)=0,\dots,n-1}$  and  $(s_{k+l+1})_{(k,l)=0,\dots,n-1}$  are also positive. Using well known results (see e.g. [16]), it exists a probability measure  $\sigma$  such that

$$s_k = \int_0^\infty \lambda^k d\sigma(\lambda). \quad (\text{E.8})$$

**Assumption E.2** *Measure  $\sigma$  is carried by an interval  $[\delta_1, \delta_2]$ , and is thus uniquely defined by (E.8) (see [16]). Moreover,  $\sigma$  is absolutely continuous, and its density is almost surely strictly positive on  $[\delta_1, \delta_2]$ .*

**Assumption E.3** *There exists  $A > 0$  and  $B > 0$  such that  $\|\mathbf{R}_N^{-1}\| \leq A$  and  $\|\mathbf{R}_N\| \leq B$  for each  $N$ .*

Under the above assumptions,  $\eta^{(N)} = \mathbf{h}_N \mathbf{R}_N^{-1} \mathbf{h}_N$  can be shown to converge to  $\eta = \int_{\delta_1}^{\delta_2} \frac{1}{\lambda} d\sigma(\lambda)$ . Therefore, we have to evaluate the convergence speed of

$$\eta_n = (s_0, \dots, s_{n-1}) \begin{pmatrix} s_1 & s_2 & \dots & s_n \\ s_2 & s_3 & \dots & s_{n+1} \\ \vdots & \vdots & \ddots & \vdots \\ s_n & s_{n+1} & \dots & s_{2n-1} \end{pmatrix}^{-1} \begin{pmatrix} s_0 \\ \vdots \\ s_{n-1} \end{pmatrix}$$

toward  $\eta = \int_{\delta_1}^{\delta_2} \frac{1}{\lambda} d\sigma(\lambda)$ . The main result of [53] is the following theorem.

**Theorem E.1** *Let  $\mu > 1$  and  $\phi < 1$  be defined by  $\mu = \frac{1 + \frac{\delta_1}{\delta_2}}{1 - \frac{\delta_1}{\delta_2}}$  and  $\phi = \frac{1}{\mu + \sqrt{\mu^2 - 1}}$ . Then, there exist 2 strictly positive constants  $C$  and  $D$  such that*

$$C\phi^{2n} \leq (\eta - \eta_n) \leq D\phi^{2n} \quad (\text{E.9})$$

for  $n$  large enough.

This results implies that the convergence is locally exponential, and that its rate only depends on the ratio  $\frac{\delta_1}{\delta_2}$ , and not on the particular form of measure  $\sigma$ . In particular, if  $\frac{\delta_1}{\delta_2}$  is close to 0, then  $\mu$  is close to 1, and the convergence is slow. If however  $\frac{\delta_1}{\delta_2}$  is close to 1, then  $\mu$  is large, and the convergence is fast.

## E.4 The downlink CDMA model.

We now show how to apply these results in order to evaluate the convergence speed of reduced rank suboptimum Wiener filters in the context of downlink CDMA systems. In this section, we first present the downlink CDMA model. We denote by  $N$  and  $K$  the spreading factor and the number of users of the cell respectively, and by  $h(z) = \sum_{l=0}^L h_l z^{-l}$  the transfer function of the chip rate discrete-time equivalent channel between the base station and the mobile station of interest.  $h(z)$  is assumed to be known at the receiver side, and is normalized in such a way that  $\sum_{l=0}^L |h_l|^2 = 1$ .  $(d(m))_{m \in \mathbb{Z}}$  represents the chip sequence transmitted by the base station. Therefore, the received signal  $(y(m))_{m \in \mathbb{Z}}$  sampled at the chip rate can be written as

$$y(m) = \sum_{l=0}^L h_l d(m-l) + v(m)$$

where  $v$  is an additive white noise of variance  $\omega^2$ . We denote by  $\mathbf{y}_N(n)$  the  $N$ -dimensional vector defined by  $\mathbf{y}_N(n) = (y(nN), \dots, y(nN + N - 1))^T$ .  $\mathbf{y}_N(n)$  can be written as

$$\mathbf{y}_N(n) = \mathbf{H}_{0,N} \mathbf{W}_{N,K}(n) \mathbf{b}_K(n) + \mathbf{H}_{1,N} \mathbf{W}_{N,K}(n-1) \mathbf{b}_K(n-1) + \mathbf{v}_N(n) \quad (\text{E.10})$$

$\mathbf{b}_K(n)$  represents the vector of transmitted symbols at time  $n$ , and we assume that the user of interest is user 1.  $\mathbf{H}_{0,N}$  and  $\mathbf{H}_{1,N}$  are 2 Toeplitz band matrices depending on sequence  $(h_l)_{l=0,\dots,L}$ . Matrix  $\mathbf{W}_{N,K}(n)$  represents the code matrix at time  $n$ . We denote  $\mathbf{w}_N(n)$  the first column of  $\mathbf{W}_{N,K}(n)$  (i.e. the code vector of the user of interest), and by  $\mathbf{U}_{N,K-1}(n)$  the orthogonal  $N \times (K-1)$  matrix such that  $\mathbf{W}_{N,K}(n) = (\mathbf{w}_N(n), \mathbf{U}_{N,K-1}(n))$ . In the following, we study the performance of reduced rank Wiener filters in the asymptotic regime  $N$  and  $K$  converge to  $+\infty$  in such a way that  $\frac{K}{N} \rightarrow \alpha$  where  $0 < \alpha < 1$ . It is important to notice that the length  $L$  of the impulse response of the channel is assumed to be kept constant. Therefore, the intersymbol interference term  $\mathbf{H}_{1,N}\mathbf{W}_{N,K}(n-1)$  can be shown to have no effect on the performance of our receivers. In particular, the term  $\mathbf{H}_{1,N}\mathbf{W}_{N,K}(n-1)$  can be replaced by  $\mathbf{H}_{1,N}\mathbf{W}_{N,K}(n)$  without changing the asymptotic behavior of the output SNRs of the receivers. We can therefore exchange (E.10) with

$$\mathbf{y} = \mathbf{H}_N \mathbf{W}_{N,K} \mathbf{b}_K + \mathbf{v} \quad (\text{E.11})$$

Here,  $\mathbf{H}_N$  is the circulant matrix  $\mathbf{H}_N = \mathbf{H}_{0,N} + \mathbf{H}_{1,N}$ , the first column of which is vector  $\mathbf{h}_N$  defined by

$$\mathbf{h}_N = (h_0, \dots, h_L, 0, \dots, 0)^T.$$

This observation allows to simplify many further calculations. Note that we omit from now on the time index  $n$  which is irrelevant.

We now explain how the random matrix  $\mathbf{W}_{N,K}$  is generated. For this purpose, some notations and definitions need to be introduced. Denote by  $\mathcal{U}$  the multiplicative group of  $N \times N$  unitary matrices, and by  $\mathbf{Q}$  a random  $N \times N$  unitary matrix.  $\mathbf{Q}$  is said to be Haar distributed if the probability distribution of  $\mathbf{Q}$  is invariant by left multiplication by constant unitary matrices. Since the group  $\mathcal{U}$  is compact, this condition is known to be equivalent to the invariance of the probability distribution of  $\mathbf{Q}$  by right multiplication by constant unitary matrices. In order to generate Haar distributed unitary random matrices, let  $\mathbf{X} = [x_{i,j}]_{1 \leq i,j \leq N}$  be a  $N \times N$  random matrix with independent complex Gaussian centered unit variance entries. The unitary matrix  $\mathbf{X}(\mathbf{X}^H \mathbf{X})^{-1/2}$  is Haar distributed. Unless otherwise stated, it will be assumed in the following that matrix  $\mathbf{W}_{N,K}$  is generated by extracting  $K$  columns from a  $N \times N$  Haar unitary random matrix  $\mathbf{Q}$ .

## E.5 The reduced rank Wiener receivers.

Model (E.11) coincides with model (E.1) for  $\mathbf{h}_N = \mathbf{H}_N \mathbf{w}_N$  and  $\mathbf{R}_N = \mathbf{H}_N \mathbf{W}_{N,K} \mathbf{W}_{N,K}^H \mathbf{H}_N^H + \omega^2 I$ . The SINRs of the plain Wiener filter and of the reduced rank Wiener filters are thus given by formulas (E.2) to (??). Moreover, in order to study the convergence speed of  $\eta_n^{(N)}$  to  $\eta^{(N)}$  in our asymptotic regime, the results of section (E.3) can be used provided assumptions E.1 to E.3 hold.

In order to check assumption E.1, we observe that  $s_k^{(N)}$  is given by  $s_k^{(N)} = \mathbf{w}_N^H \mathbf{H}_N^H (\mathbf{H}_N \mathbf{W}_{N,K} \mathbf{W}_{N,K}^H \mathbf{H}_N^H + \omega^2 I)^k \mathbf{H}_N \mathbf{w}_N$ . Using the properties of the Haar dis-

tribution, it can be shown as in [30] that  $s_k^{(N)}$  has the same asymptotic behavior that the term

$$\frac{1}{K} \text{Trace}(\mathbf{W}_{N,K}^H \mathbf{H}_N^H (\mathbf{H}_N \mathbf{W}_{N,K} \mathbf{W}_{N,K}^H \mathbf{H}_N^H + \omega^2 I)^k \mathbf{H}_N \mathbf{W}_{N,K}) \quad (\text{E.12})$$

Denote by  $(\lambda_l^{(N)})_{l=1,\dots,N}$  the eigenvalues of  $\mathbf{H}_N \mathbf{W}_{N,K} \mathbf{W}_{N,K}^H \mathbf{H}_N^H$ . Then, (E.12) is equal to  $\frac{1}{K} \sum_{l=1}^N \lambda_l^{(N)} (\lambda_l^{(N)} + \omega^2)^k$ .

In order to precise the asymptotic behavior of this term when  $N \rightarrow +\infty$  and  $K/N \rightarrow \alpha$ , we first note that the eigenvalue distributions of matrices  $\mathbf{W}_{N,K} \mathbf{W}_{N,K}^H$  and  $\mathbf{H}_N^H \mathbf{H}_N$  converge toward two probability distributions denoted  $\nu$  and  $\mu$  respectively. It is clear that  $d\nu(t) = \alpha\delta(t-1) + (1-\alpha)\delta(t)$ . In order to precise the behavior of  $\mu$ , we remark that the eigenvalues of  $\mathbf{H}_N^H \mathbf{H}_N$  coincide with  $(|h(e^{2i\pi l/N})|^2)_{l=0,\dots,N-1}$ . Therefore,  $\mu$  is carried by the interval  $[|h_{\min}|^2, |h_{\max}|^2]$  where  $|h_{\min}| = \min_f |h(e^{2i\pi f})|$  and  $|h_{\max}| = \max_f |h(e^{2i\pi f})|$ , and is defined by  $\int_0^1 \phi(|h(e^{2i\pi f})|^2) df$ .

As matrices  $\mathbf{W}_{N,K} \mathbf{W}_{N,K}^H$  and  $\mathbf{H}_N^H \mathbf{H}_N$  are almost surely asymptotically free (see [30], [38]), the eigenvalue distribution of matrix  $\mathbf{H}_N \mathbf{W}_{N,K} \mathbf{W}_{N,K}^H \mathbf{H}_N^H$  converges toward a probability measure, denoted  $\mu \otimes \nu$ , called the free multiplicative convolution product of  $\mu$  and  $\nu$ . This implies that

$$\lim_{N \rightarrow +\infty, K/N \rightarrow \alpha} s_k^{(N)} = \frac{1}{\alpha} \int t(t + \omega^2)^k d\mu \otimes \nu(t) \quad (\text{E.13})$$

We note  $s_k$  the above limit. This shows that assumption E.1 holds.

Assumption E.3 is obviously satisfied. We now verify assumption E.2. We first note that 0 is eigenvalue of matrix  $\mathbf{H}_N \mathbf{W}_{N,K} \mathbf{W}_{N,K}^H \mathbf{H}_N^H$  with multiplicity  $N-K$ . The remaining eigenvalues are strictly positive, and coincide with the eigenvalues of matrix  $\mathbf{W}_{N,K}^H \mathbf{H}_N^H \mathbf{H}_N \mathbf{W}_{N,K}$ . Therefore, measure  $d\mu \otimes \nu(t)$  can be written as  $d\mu \otimes \nu(t) = (1-\alpha)\delta(t) + \alpha d\gamma(t)$  where  $d\gamma(t)$  represents the limit eigenvalue distribution of  $\mathbf{W}_{N,K}^H \mathbf{H}_N^H \mathbf{H}_N \mathbf{W}_{N,K}$ . It can be checked that  $d\gamma(t)$  is absolutely continuous, and that its density is almost surely strictly positive on a certain interval  $[x_1, x_2]$ . It is clear that the eigenvalues of  $\mathbf{W}_{N,K}^H \mathbf{H}_N^H \mathbf{H}_N \mathbf{W}_{N,K}$  are contained in the interval  $[|h_{\min}|^2, |h_{\max}|^2]$  for each  $N$  and  $K$ . Therefore, the interval  $[x_1, x_2]$  is itself contained in  $[|h_{\min}|^2, |h_{\max}|^2]$ .

In order to complete the verification of assumption E.2, we remark that  $s_k$  can be written as  $s_k = \int_{x_1}^{x_2} t(t + \omega^2)^k d\gamma(t)$ , or equivalently

$$s_k = \int_{x_1 + \omega^2}^{x_2 + \omega^2} (\lambda - \omega^2) \lambda^k d\gamma(\lambda - \omega^2)$$

This shows that measure  $\sigma$  defined by  $s_k = \int \lambda^k d\sigma(\lambda)$  is given by

$$d\sigma(\lambda) = (\lambda - \omega^2) d\gamma(\lambda - \omega^2) \quad (\text{E.14})$$

As  $d\gamma(t)$  is compactly supported and absolutely continuous, so is  $\sigma$ . Moreover, the support of  $\sigma$  is the interval  $[\delta_1, \delta_2]$  where  $\delta_1 = x_1 + \omega^2$  and  $\delta_2 = x_2 + \omega^2$ , and its density is almost surely strictly positive on  $[\delta_1, \delta_2]$ .

As assumptions E.1 to E.3 hold, the results of [53] can be applied. It turns out that the convergence speed of  $\eta_n$  toward  $\eta$  is exponential, and depends on factor  $\frac{(x_1 + \omega^2)}{(x_2 + \omega^2)}$ : if this ratio

is close to 1, the convergence is fast, while if it is close to 0, the convergence is slow. In order to discuss this point, we assume that the effect of  $\omega^2$  on the ratio is negligible. The important term is thus  $\frac{x_1}{x_2}$ , which depends both on  $\alpha$  and  $|h_{min}|^2$  and  $|h_{max}|^2$ . It is clear that the ratio  $\frac{x_2 - x_1}{|h_{max}|^2 - |h_{min}|^2}$  increases from 0 to 1 when  $\alpha$  increases from 0 to 1. Moreover, one can expect that the condition number  $\frac{|h_{min}|^2}{|h_{max}|^2}$  also affects  $\frac{x_1}{x_2}$ . In order to be able to understand the influence of  $\alpha$  and  $(|h_{min}|^2, |h_{max}|^2)$  on  $(x_1, x_2)$ , we mention that  $x_1$  and  $x_2$  can be evaluated numerically rather easily. For this, we denote by  $G_\gamma(z)$  the Stieljs transform of  $d\gamma(t)$  defined by  $G_\gamma(z) = \int_{x_1}^{x_2} \frac{d\gamma(t)}{t-z}$ . For each  $z \in \mathbb{C} - [\sphericalcap, \sphericalcap]$ ,  $G_\gamma(z)$  can be shown to satisfy the equation  $\alpha(1 + zG_\gamma(z)) = T(z, G_\gamma(z))$  where  $T(z, g)$  is defined by

$$T(z, g) = \int_0^1 \frac{|h(e^{2i\pi f})|^2}{|h(e^{2i\pi f})|^2 - z + \frac{1-\alpha}{\alpha g}} \quad (\text{E.15})$$

Moreover,  $x_1$  is the unique positive real number for which there exists  $g_1 > 0$  satisfying

$$\begin{aligned} \alpha(1 + x_1 g_1) &= T(x_1, g_1) \\ \alpha x_1 &= \frac{\partial T}{\partial g}(x_1, g_1) \end{aligned} \quad (\text{E.16})$$

$x_2$  is characterized similarly, but the corresponding value  $g_2$  is strictly negative. This result will be used more extensively in a forthcoming paper.

## E.6 Simulation results

We now illustrate the influence of  $\alpha$  and  $(|h_{min}|^2, |h_{max}|^2)$  on the convergence speed of  $\beta_n = \frac{\eta_n}{1-\eta_n}$  toward  $\beta = \frac{\eta}{1-\eta}$ . For this, we represent in the following figures the relative SINR defined as the ratio  $\frac{\beta_n}{\beta}$ . In Figure E.6, we first study the influence of  $\alpha$  on the convergence speed of the relative SINR toward 1. Here, the ratio  $\frac{E_b}{N_0}$  is equal to 10 dB. This figure confirms that the convergence speed of the reduced rank receivers depends crucially on the load factor.

In figure E.6, we study the effect of the channel on the convergence speed of  $\beta_n$  toward  $\beta$ . For this, we consider a 2 taps channel with transfer function  $h(z) = h_1 + h_2 z^{-1}$ . In this case, if  $|h_1| = |h_2|$ ,  $h(z)$  has a zero on the unit circle, so that  $|h_{min}| = 0$ . If  $|h_1| = |h_2|$ , the convergence speed of  $\beta_n$  toward  $\beta$  is thus expected to be minimum. This is confirmed by ?? obtained for  $\alpha = \frac{1}{2}$  and  $\frac{E_b}{N_0} = 17dB$ .

We finally verify that our asymptotic SINR evaluations allow to predict the empirical performance of the studied receivers. For this, we have compared the measured bit error rate with its asymptotic evaluation given by  $Q(\sqrt{\beta_n})$  (we have used a QPSK constellation). The results are presented in figure E.6. Here, the propagation channel is the so-called Vehicular A (on each frame, a different realization of the channel is generated). The signal to noise ratio  $\frac{E_b}{N_0}$  is equal to 7dB and the load factor  $\alpha$  is equal to  $\frac{1}{2}$ . Figure 3 shows that our asymptotic evaluations allow to predict rather accurately the performance of the true system if  $N \geq 128$ . However, for smaller values of  $N$ , the asymptotic performance is too optimistic. We finally note that the receiver we implemented is based on the correct model (E.10), thus showing that the approximation (E.11)

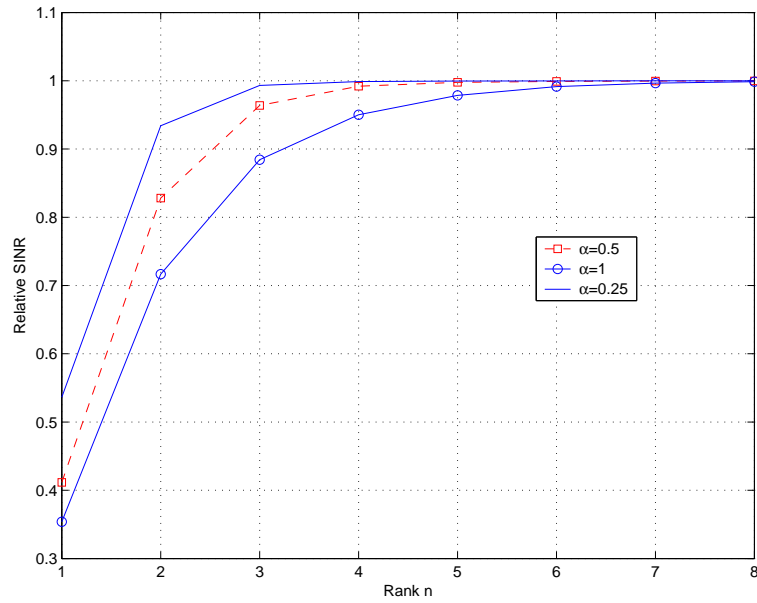
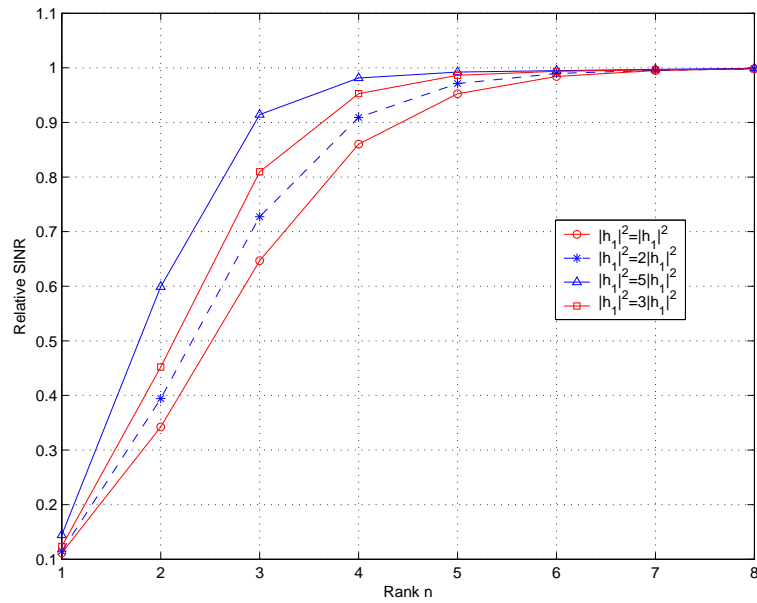
Figure E.1: Influence of  $\alpha$  on the convergence of the reduced-rank SINR.

Figure E.2: Influence of the propagation channel on the convergence of the reduced-rank SINR.

used in order to derive the asymptotic performance is justified in the context of the vehicular A channel

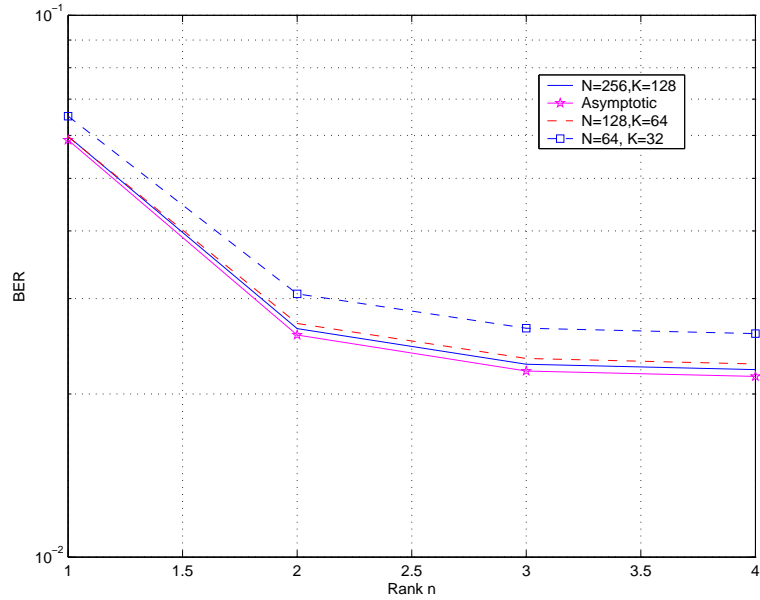


Figure E.3: Comparison of empirical and theoretical BER

## E.7 Conclusion

In this paper, we have shown that the results of [53] can be used in order to study the convergence speed of reduced rank Wiener filters in the context of downlink CDMA systems corrupted by frequency selective channels. we exhibited the different parameters affecting the convergence of a reduced-rank Wiener receiver to the full-rank Wiener receiver SINR. Simulation results show that the asymptotic SINRs can be used in order to predict real-life receivers performances.

# Bibliography

- [1] B. Mouhouche, K. Abed-Meraim, N. Ibrahim and Ph. Loubaton, “Reduced-Rank Adaptive Chip level MMSE Equalization for the forward link of long-code DS-CDMA Systems,” *In Proc. International Symposium on Signal Processing Applications (ISSPA)*., Paris, France. October 2001.
- [2] B. Mouhouche, K. Abed-Meraim, N. Ibrahim and Ph. Loubaton, “Chip-Level MMSE Equalization in the Forward Link of UMTS-FDD: A Low Complexity Approach,” *In Proc. Vehicular Technology Conference (VTC-fall)*., Orlando, Fl. USA. October 2003.
- [3] B. Mouhouche, Ph. Loubaton, W. Hachem, K. Abed-Meraim and N. Ibrahim, “Analyse Asymptotique de certains filtres de Wiener à rang réduit,” *in Proc. GretsI 2003*, Paris, France. September 2003.
- [4] B. Mouhouche, Ph. Loubaton and W. Hachem, “Asymptotic Analysis of Chip Level MMSE Equalizers in the Downlink of CDMA Systems,” *In Proc. IEEE. Workshop on Signal Processing Advances for Wireless Communications (SPAWC)*. Lisboa, Portugal. July 2004.
- [5] B. Mouhouche, K. Abed-Meraim, N. Ibrahim and Ph. Loubaton, “Combined MMSE Equalization and Blind Parallel Interference Cancellation for Downlink Multirate CDMA Communications,” *In Proc. IEEE. Workshop on Signal Processing Advances for Wireless Communications (SPAWC)*. Lisboa, Portugal. July 2004.
- [6] B. Mouhouche, K. Abed-Meraim and S. Burykh, “Spreading Code Detection and Blind Interference Cancellation for DS/CDMA Downlink”, *IEEE International Symposium on Spread Spectrum Systems and Applications (ISSSTA)*). Sydney, Australia. August 2004.
- [7] B. Mouhouche, Ph. Loubaton, W. Hachem and N. Ibrahim, , “ Asymptotic Analysis of Reduced Rank Downlink CDMA Wiener Receivers”, *In Proc. European Signal Processing Conference (EUSIPCO)*, Vienna, Austria, September 2004.
- [8] B. Mouhouche, K. Abed-Meraim and N. Ibrahim, “On the Effect Of Power and Channel Estimation in Equalized Blind PIC for Downlink Multirate CDMA Communications” ,” *in Proc. the 38th- Asilomar conference on Signals, Systems and Computers*, Pacific Grove, CA, USA. November 2004.

- [9] B. Mouhouche, Ph. Loubaton, K. Abed-Meraim and N. Ibrahim, , “On the Performance of Space Time Transmit Diversity for CDMA Downlink with and without equalization,” *In Proc. International Conference on Acoustics Speech and Signal Processing (ICASSP’05)*, Philadelphia, PA, USA. March 2005.
- [10] B. Mouhouche, K. Abed-Meraim, N. Ibrahim and Ph. Loubaton, “Procédé de Réception d’un signal CDMA á annulation d’interférence et récepteur correspondant,” *French National Patent N 03-10987*. Filed Sptember 2003.
- [11] B. Mouhouche, K. Abed-Meraim, N. Ibrahim and Ph. Loubaton, “Procédé de Détermination de codes d’étalement utilisés dans un Signal CDMA et dispositif de Communication Correspondant,” *French National Patent Pending* . Filed April 2004.
- [12] B. Mouhouche, Ph. Loubaton and W. Hachem, “Asymptotic Analysis of Chip Level MMSE Equalizers in the Donwlink of CDMA Systems,” *Submitted to IEEE Trans. On Signal Processing*. June 2005.
- [13] B. Mouhouche, K. Abed-Meraim and N. Ibrahim, “ Combined MMSE Equalization and Partial Blind Interference Cancellation for W-CDMA ,” *Submitted to IEEE Communication Letters*. March 2005.
- [14] 3GPP TS 25.211 v3.0.0 (1999-10): “Physical channels and mapping of transport channels onto physical channels (FDD)” 3GPP, October 1999. UMTS Standardization.
- [15] 3GPP TS 25.213 v3.0.0 (1999-10): “ Spreading and Modulation (FDD)” 3GPP, October 1999. UMTS Standardization.
- [16] N.I. Akhiezer, *The Classical Moment Problem*, Oliver & Boyd.
- [17] S. Alamouti, ”A simple transmit diversity technique for wireless communications ”, *IEEE Journal on Selected Areas in communications* , vol. 16. No. 8, pp 1451-1458, Oct 1998.
- [18] A. Bastug and D.T.M. Slock, “Structured interference cancellation at a WCDMA terminal,” *Proc of Intl. Symp. on Signal Proc. and its Applications ISSPA, Paris, France, 1-4 july 2003*.
- [19] A. Bultheel, C. Díaz-Mendoza, P. Gonzalez-Vera, and R. Orive, ”Quadrature on the Half Line and Two-Point Pad Approximants to Stieltjes Functions. Part II : Convergence” , *J. Comput. Appl. Math.*, 65, 1996.
- [20] S. Burykh, “Multiuser detection and Blind Channel Estimation for DS/CDMA systems.”, Ph.D. Thesis report, Telecom Paris, 2003.
- [21] S. Burykh and K. Abed-Meraim, “Multi-stage reduced-rank filter with flexible structure,” *in Proc. Eusipco’2002*, September 2002.
- [22] S. Burykh and K. Abed-Meraim, “Reduced-rank adaptive filtering using Krylov subspace,” *EURASIP Journal on Applied Signal Processing (accepted for publication)*.

- [23] S. Burykh and K. Abed-Meraim, "Blind Interference Cancellation for Downlink DS/CDMA," in *Proc. SPAWC*, Jun. 2003.
- [24] J.M. Chaufray, Ph. Loubaton, P. Chevalier, "Consistent estimation of Rayleigh fading channel second order statistics in the context of the wideband CDMA mode of the UMTS", *IEEE Trans. on Signal Processing*, vol. 49, no. 12, pp. 3055-3064, December 2001.
- [25] J. M. Chaufray, W. Hachem, P. Loubaton, "Asymptotic analysis of optimum and sub-optimum CDMA downlink MMSE receivers", *IEEE Trans. on Information Theory*, vol. 50, no. 11, pp. 2620-2638, Nov. 2004.
- [26] S. Chowdhury, M. D. Zoltowski, and J. S. Goldstein, "Reduced-rank adaptive MMSE equalization for the forward link in high-speed CDMA," in *Proc. 43rd IEEE Midwest Symp. on Circuits and Systems*, 2000.
- [27] S. Chowdhury, M. D. Zoltowski, and J. S. Goldstein, "Structured MMSE equalization for synchronous CDMA with sparse multipath channels," in *Proc. ICASSP'2001*, 2001.
- [28] S. Chowdhury and M. D. Zoltowski, "Application of Conjugate Gradient Methods in MMSE Equalization for the Forward Link of DS-CDMA", *In Proc. 54th Vehicular Technology Conference*, pp. 2434-2438, October 2001.
- [29] L. Cottatellucci, R. Mller, " Asymptotic Design and Analysis of Multistage Detectors with Unequal Powers", in *Proc. of IEEE Information Theory Workshop (ITW) Bangalore, India*, October 2002, pp. 167-170.
- [30] M. Debbah, W. Hachem, P. Loubaton, M. de Courville, "MMSE Analysis of Certain Large Isometric Random Precoded Systems", *IEEE Trans. on Information Theory*, vol. 51, no. 5, pp. 1020-1034, May 2003.
- [31] G. Dietl, M. D. Zoltowski and M. Joham, "Reduced-Rank Equalization for EDGE Via Conjugate Gradient Implementation of Multi-Stage Nested Wiener Filter", *In Proc. 54th Vehicular Technology Conference*, pp. 1912-1916, October 2001.
- [32] C.D. Franck, E. Visotsky, "interference suppression for the downlink of a direct sequence cdma system with long spreading sequences", *Special Issue on Signal Processing for Wireless Communications: Algorithms, Performance, and Architecture, Journal of VLSI Signal Processing*, vol. 30, no. 1, pp. 273-291, January 2002.
- [33] V. L. Girko, *Theory of Random Determinants*. Kluwer Academic Publishers, 1990.
- [34] J.S. Goldstein, I.S. Reed, and L.L. Scharf,"A Multistage Representation of the Wiener Filter Based on Orthogonal Projections", *IEEE Trans. on Information Theory*, Vol. 44, No. 7, November 1998.
- [35] G. H. Golub and C. F. Van Loan, *Matrix Computations*, John Hopkins Univ. Press, 1989.

- [36] M. Guenach “Receiver Design For Wideband CDMA Communication Systems”, Ph.D. Thesis report, Université catholique de Louvain (UCL), April 2002.
- [37] S. Haykin, *Adaptive Filter Theory*, 3rd ed. Englewood Cliffs, NJ: Prentice Hall, 1996.
- [38] F. Hiai, D. Petz, ”The Semicircle Law, Free Random Variables and Entropy”, AMS Mathematical Surveys and Monographs, vol. 77, 2000.
- [39] J. M. Holtzman, “DS/CDMA Successive Interference Cancellation,” in *Proc. ISSTA '94*, July 1994.
- [40] M. L. Honig and J. S. Goldstein, “Adaptive reduced-rank interference suppression based on the multistage Wiener filter ”, *IEEE Trans. On Communications.*, Volume: 50 , Issue: 6 , June 2002 Pages:986-994.
- [41] M. Honig, U. Madhow, and S. Verdu, “Blind adaptive multiuser detection ,” *IEEE Trans. On Information Theory* , , vol. 41, pp.944-960, July. 1995.
- [42] M. L. Honig and M. K. Tsatsanis, “Adaptive Techniques for Multiuser CDMA Receivers”, *IEEE Signal Proc. Magazine*, pp. 49-61, May 2000.
- [43] M. L. Honig and W. Xiao, “Adaptive Reduced-Rank Interference Suppression with Adaptive Rank Selection,” in *Proc. Milcom 2000*, Los Angeles, CA, October 2000.
- [44] M. L. Honig and W. Xiao, ”Performance of Reduced-Rank Linear Interference Suppression”, *IEEE Trans.on Information Theory*, Vol. 47, No. 5, pp. 1928–1946, July 2001.
- [45] K. Hooli, M. Juntti, M. Heikkila, M. Latva-Aho, J. Lilleberg, “Chip-level channel equalization in WCDMA downlink”, *EURASIP Journal on Applied Signal Processing*, no. 8, pp. 757-770, August 2002.
- [46] W. C. Jakes, “ Microwave Mobile Communications”, *New York: Wiley* , 1974.
- [47] D. H. Johnson and D. E. Dudgeon, *Array Signal Processing: Concepts and Techniques*, Prentice-Hall, Englewood Cliffs, NJ, 1993.
- [48] A. Klein, “Data detection algorithms specially designed for the downlink of CDMA mobile radio systems,” *IEEE 47th Vehicular Technology Conference*, vol. 1, pp. 203–207, 4-7 May 1997.
- [49] T.P. Krauss, M. D. Zoltowski and G. Leus, “Simple MMSE equalizer for CDMA downlink to restore chip sequence: Comparison to Zero-Forcing and RAKE,” *ICASSP, Istanbul, Turkey*, 5-9 june 2000.
- [50] M. Lenardi, ”Advanced mobile receivers and downlink channel estimation for 3G UMTS-FDD WCDMA systems” Ph.D. Thesis report, Ecole Polytechnique Fédérale de Lausanne (EPFL), May 2002.

- [51] M. Lenardi, A. Medles, D.T.M. Slock, "A SINR maximizing RAKE receiver for DS-CDMA downlinks", in Proc. 34th Asilomar Conf., Pacific Grove, California, October 2000.
- [52] L. Li, A. M. Tulino, S. Verdu, "Design of MMSE multiuser detectors using random matrix techniques", in proc. IEEE International Conference on Communications, 2003. ICC '03., Volume: 4, 2003 Pages:2537 - 2541.
- [53] P. Loubaton, W. Hachem, "Asymptotic analysis of reduced rank Wiener filters", in Proc. of Information Theory Workshop, Paris, April 2003.
- [54] U. Madhow and M. L. Honig, "MMSE Interference Suppression for Direct-Sequence Spread-Spectrum CDMA," *IEEE Trans. On Communications*, 42(12):3178-3188, December 1994.
- [55] M.F. Madkour, S.C. Gupta and Y.E. Wang, "Successive Interference Cancellation Algorithms for Downlink W-CDMA Communications," *IEEE Trans. Wirelss Comm.*, vol. 1, N: 1, Jan. 2002.
- [56] A. R. Margetts and P. Schniter, "Adaptive Chip-Rate Equalization of Downlink Multirate Wideband CDMA," *IEEE Transactions on Signal Processing*, Vol. 53, No. 6, pp. 2205-2215, Jun. 2005.
- [57] A. Margetts "Adaptive Chip-Rate Equalization of Downlink Multirate Wideband CDMA" Master thesis report, Ohio State University, 2002
- [58] S. Moshavi, E.G. Kanterakis, and D.L.Schilling, "Multistage Linear Receivers for DS-CDMA Systems," *Int. J. of Wireless Inf. Networks*, 3(1):1-17, 1996.
- [59] R. Müller and S. Verdù, "Spectral Efficiency of Low-Complexity Multiuser Detectors," in *Proc. ISIT'2000*, p. 439, June 2000.
- [60] D. A. Pados and S. N. Batalama, "Joint Space-Time Auxiliary-Vector Filtering for DS/CDMA Systems with Antenna Arrays," *IEEE Trans. On Communications*, pp. 1406-1415, Sept. 1999.
- [61] D. A. Pados and G. N. Karystinos, "An Iterative Algorithm for the Computation of the MVDR Filter", *IEEE Trans. on Signal Proc.*, pp. 290-300, February 2001.
- [62] I. N. Psaromiligkos and S. N. Batalama, "Finite data record maximum SINR adaptive space-time processing", in *Proc. 10th IEEE Workshop on Statistical Signal and Array Processing*, pp. 677-681, 2000.
- [63] H. Poor and S. Verdù, "Probability of Error in MMSE Multiuser Detection", *IEEE Transactions on Information Theory*, vol. 43, no. 3, pp. 858-871, May 1997.
- [64] Y. Saad, "An overview of Krylov subspace methods with applications to control theory", Report MTNS89, NASA Ames Research Center, Moffet Field, CA, 1989. Available at <http://www.cs.umn.edu/~saad>.

- [65] J. W. Silverstein and Z. D. Bai, "On the empirical distribution of Eigenvalues of a class of large dimensional random matrices," *J. Multivariate Analysis*, vol. 54, no. 2, pp. 175-192, 1995.
- [66] R. Singh and L. B. Milstein, "Interference suppression for DS/CDMA," *IEEE Trans. On Communications*, vol. 47, pp. 446-453, March 1999.
- [67] H. Stahl and V. Totik, "General Orthogonal Polynomials", *Encyclopedia of Mathematics and its Applications*. Cambridge University Press, 1992.
- [68] G. Szegő, Orthogonal Polynomials, Vol. 33 of *Amer. Math. Soc. Colloq. Publ.*, AMS.
- [69] L.G. F. Trichard, J.S. Evans and I.B. Collings,"Optimal Linear Multistage Receivers for Synchronous CDMA", Proceedings of IEEE International Conference on Communications, New York City, New York, USA, Apr. 2002, pp. 1461-1465.
- [70] L.G.F. Trichard, J.S. Evans, and I.B. Collings, "Optimal Linear Multistage Receivers and the Recursive Large System SIR", *ISIT 2002*, Lausanne, Switzerland.
- [71] D.N.C Tse and S. Hanly, "Linear Multi-User Receiver: Effective Interference, Effective Bandwidth and User Capacity", *IEEE Trans. on Information Theory*, vol. 45, no. 2, pp. 641-657, February 1999.
- [72] A. M. Tulino and S. Verdu, "Random matrix theory and wireless communications", *Foundations and Trends in Communications and Information Theory*, vol. 1, no. 1, pp. 1182, 2004.
- [73] M. K. Varanasi and B. Aazhang, "Multistage Detection in Asynchronous Code-Division Multiple-Access Communications," *IEEE Trans. On Communications*, 38(4): 509-519, April 1990.
- [74] S. Verdu, *Multuser detection*, Cambridge University Press, 1998.
- [75] X. Wang and H. V. Poor, "Blind Multuser detection: A subspace approach," *IEEE-T-IT*, 44(2): 677-690, March 1998.
- [76] M. Wax and T. Kailath, "Detection of signals by information theoretic criteria," *IEEE Trans. On Acoustics, Speech and Signal processing*, ASSP-33:387-392, April 1985.
- [77] W. Xiao and M. L. Honig, "Convergence and tracking of adaptive reduced-rank interference suppression algorithms", in *Proc. 34th Asilomar Conference on Signals, Systems and Computers*, Pacific Grove, CA, pp. 1143-1147, November 2000.
- [78] J. Zhang, E.K.P. Chong, and D.N.C. Tse, "Output MAI Distributions of Linear MMSE Multiuser Receivers in DS-CDMA Systems", *IEEE Transactions on Information Theory*, vol. 47, no. 3, pp. 1128-1144, Mar. 2001.